Answers Research Journal 14 (2021): 159–254.
www.answersingenesis.org/arj/v14/petrology_tapeats_sandstone.pdf

ARJ

The Petrology of the Tapeats Sandstone, Tonto Group, Grand Canyon, Arizona

Andrew A. Snelling, Answers in Genesis, PO Box 510, Hebron, Kentucky 41048.

Abstract

Investigation of the nature of the folding of the Cambrian Tonto Group strata in the Grand Canyon necessitates first investigating the petrology of those strata. At the base of the Tonto Group the Tapeats Sandstone is the 30–100m thick cliff-forming formation that prominently outcrops through ~500km in the walls of the Grand Canyon and beyond. Erosion of the underlying Precambrian basement rocks produced the Great Unconformity on which the Tapeats Sandstone was deposited as the basal part of the fining upwards Sauk megasequence that blankets North America, and both have been traced across other continents. Tracks and traces left by trilobites and other invertebrates are fossilized in the Tapeats Sandstone, which consists of 0.3–1.0m thick non-bioturbated beds that are strongly cross laminated with shallow dips characteristic of water transport of the sand and many lens-shaped scour-and-fill "channels." The predominant paleocurrent direction is between west and southwest. Detrital zircon U-Pb ages confirm the conventional age and the source of the sandy sediment. The consensus uniformitarian interpreted depositional environments for the Tapeats Sandstone are intertidal to subtidal shallow-marine environments with local beach and fluvial deposits, yet it has been described as "one of the most dramatic global marine transgressions in Earth history." K-feldspar content ranges from 1.8–33.1%, with variously sized K-feldspar grains scattered through the rock, and occasional detrital muscovite flakes wedged between quartz and K-feldspar grains. The fabric is cemented by silica as quartz overgrowths. Being poorly to moderately well-sorted and dominated by sub-angular to sub-rounded, coarse silt to very coarse sand-sized quartz grains, with some granules and small pebbles, makes this a well-cemented sub-mature arkosic sandstone. There are no signs, either macroscopic or microscopic, that the sandstone or its constituent grains have been even slightly metamorphosed. Instead, the mineralogical content, textural features, sedimentary structures, continental-scale deposition, paleocurrent directions matching continental patterns, and even the tracks and traces of transitory invertebrates, all indicate rapid burial. Furthermore, all are consistent with the catastrophic erosion of the Great Unconformity near the initiation of the global Genesis Flood cataclysm only about 4,350 years ago, and the subsequent hurricane- and tsunami-driven rapid short-distance transport and deposition of the Tapeats Sandstone, likely in the first few days or weeks of that year-long event.

Keywords: Tapeats Sandstone, Cambrian, Tonto Group, Grand Canyon, stratigraphy, trace fossils, sedimentary structures, U-Pb detrital zircon ages, provenance, depositional environments, quartz, K-feldspar, detrital muscovite, silica cement, global Flood cataclysm

Introduction

The Cambrian Tapeats Sandstone is the 30–100m (~100–330ft) thick cliff-forming formation that prominently outcrops at the base of the Tonto Group and of the Paleozoic sequence of flat-lying sedimentary layers making up the walls of the Grand Canyon for ~500km through the Canyon and beyond. It is a poorly to moderately well-sorted, well-cemented, generally coarse-grained, sub-mature arkosic sandstone dominated by quartz but with significant amounts of K-feldspar and detrital muscovite eroded from the underlying Precambrian basement rocks, primarily granites and schists. Bedding is very clearly developed, and the 0.3–1.0m (1–3ft) thick beds are often variably cross-laminated with relatively shallow dips. The Tapeats Sandstone was deposited as the basal part of the fining upwards Sauk megasequence that blankets North America and has been traced across other continents.

Many structures in sedimentary rock layers result from the primary depositional processes, such as graded bedding and cross-bedding (Boggs 1995). On the other hand, soft-sediment deformation structures are so called because they developed at the time of deposition or shortly thereafter, during the early stages of the sediment's consolidation and before full lithification. This is because the sediments needed to be unsolidified or "liquid-like" for the deformation to occur (Boggs 1995).

However, many other structures in sedimentary rocks are caused by deformation long after lithification and diagenesis have occurred. Rocks buried deep in the earth may be under sufficient prolonged confining pressures or stress and temperatures to deform plastically. In other words, incremental strain over a long period is believed to be able to fold rock layers. This type of behavior is called ductile deformation. It is the ability of a rock to accumulate strain (folding) on a mesoscopic scale. Under the confining pressures and accompanying elevated temperatures the rock grains may recrystallize and/or the minerals undergo metamorphism, some new minerals such as micas

growing perpendicular to the stress to accommodate it. Hand and thin section analysis should be able to determine if rocks have experienced ductile deformation. The Paleozoic rocks of Grand Canyon most likely were not buried deep enough to experience this type of ductile deformation as they were well above the brittle-ductile transition zone.

On the other hand, under some near-surface conditions, rock layers may remain coherent because the grains and/or layers within them can facilitate the folding. This type of deformation is most common in near-surface rocks and is called brittle deformation. The rock layers undergo brittle fracturing and are faulted, and the rock's grains are likewise fractured. Telltale signs of this should be thus clearly evident in outcrops and from microscope examination of the rock fabric and the sediment grains.

There are several prominent locations in the Grand Canyon where the Paleozoic sedimentary rock layers are folded, sometimes in conjunction with faulting, where there apparently are unresolved questions as to whether the folding represents soft-sediment deformation folding or later tectonic folding (ductile or brittle) well after the whole strata sequence was deposited. In most instances the folding is usually claimed to be the result of ductile (plastic) behavior of the lithified sedimentary rocks under prolonged stress due to Late Mesozoic-Early Cenozoic deformation during the Laramide Orogeny, hundreds of millions of years after the whole Paleozoic strata sequence was deposited (Huntoon 2003; Karlstrom and Timmins 2012). However, the macroscopic fabric of the Tapeats Sandstone, Bright Angel Formation, and Muav Formation of the Cambrian Tonto Group sedimentary rock layers involved in these folds might suggest, and seems to be more consistent with, the folding being due to soft-sediment deformation. Any soft-sediment deformation should have occurred soon after deposition of these sedimentary units in the Cambrian (499–508 Ma) (Karlstrom et al. 2020), well before the tectonic activity associated with the Laramide Orogeny that occurred in the terminal Mesozoic and earliest Cenozoic (60–70 Ma). This poses an apparent dilemma that obviously needs resolving, and thus a focused study was designed to determine the timing and nature of this folding, beginning with a thorough investigation of the petrology of each of these rock units generally, and subsequent detailed examination of these rock units in each fold.

The prime example of the folds in question is the folding of the Cambrian Tapeats Sandstone (Middleton and Elliott 2003) where those sandstone beds were dragged upwards into, against and by the Butte Fault at the synclinal hinge of the East Kaibab Monocline in the eastern Grand Canyon during the Laramide Orogeny (Huntoon 2003; Karlstrom and Timmins 2012). The best exposed fold in this system is in Carbon Canyon at river mile 65 (figs. 1 and 2). Hill and Moshier (2009) claim that evidence from field studies and rock deformation experiments demonstrate that these solid rocks behaved in a ductile manner as the sandstone strata were deformed slowly under great stress, and that the strata thus were "bent" by microscopic reorientations of mineral grains and by changes in bedding thickness along the fold. They then reference Huntoon (2003) to state that these tight folds in beds of the Tapeats Sandstone in Carbon Canyon can be explained by mechanical crowding at the synclinal hinge of the East Kaibab Monocline during slow deformation under stress of the solid sandstone in a ductile manner.

However, Hill and Moshier (2009) offer no supporting evidence of these claims. They provide no documentation of the quoted rock deformation studies, nor any evidence from any thin section examination of the Tapeats Sandstone from these folds of the claimed microscopic reorientations of mineral grains. And the only documentation they provide of any field studies is a single photograph of the vertical beds of the Tapeats Sandstone at the Carbon Canyon location, but not of the folded beds showing the mechanical crowding. For that they refer to Huntoon (2003), but his field photograph, while showing the bent beds of the Tapeats Sandstone at the location in question, is incorrectly labeled as the south wall of Chuar Canyon, when it is in fact the south wall of Carbon Canyon. Furthermore, Huntoon (2003) did not provide any thin section evidence for any reorientation of mineral grains.

Subsequently, Tapp and Wolgemuth (2016) similarly focused on the Carbon Canyon fold. They showed a photo of the fold (their fig. 12-14, p. 125), describing it as compressional folding in the Tapeats Sandstone. On an overlay they traced some of the sandstone beds through the fold, some of the fractures, and the apparent changing direction of the fold hinges, which they claimed to be due to flexural slippage. They claimed that the bending resulted in numerous fractures in each sandstone bed that did not heal (reseal). They then illustrated what flexural slippage would look like in two hypothetical folds (in their fig. 12-14, p. 125), describing how flexural slippage creates gaps in the fold hinges that may be filled in later with weathered material or weaker rock may deform into the spaces. Either way, the layering in the fold hinges would be thicker relative to the widths of the sandstone beds along the fold limbs. They claimed that neither of these features would be present if this fold had occurred due to soft-sediment deformation. However, their photo of the fold shows no such thickening of the sandstone beds in the fold hinges, and they fail to discuss alternate explanations

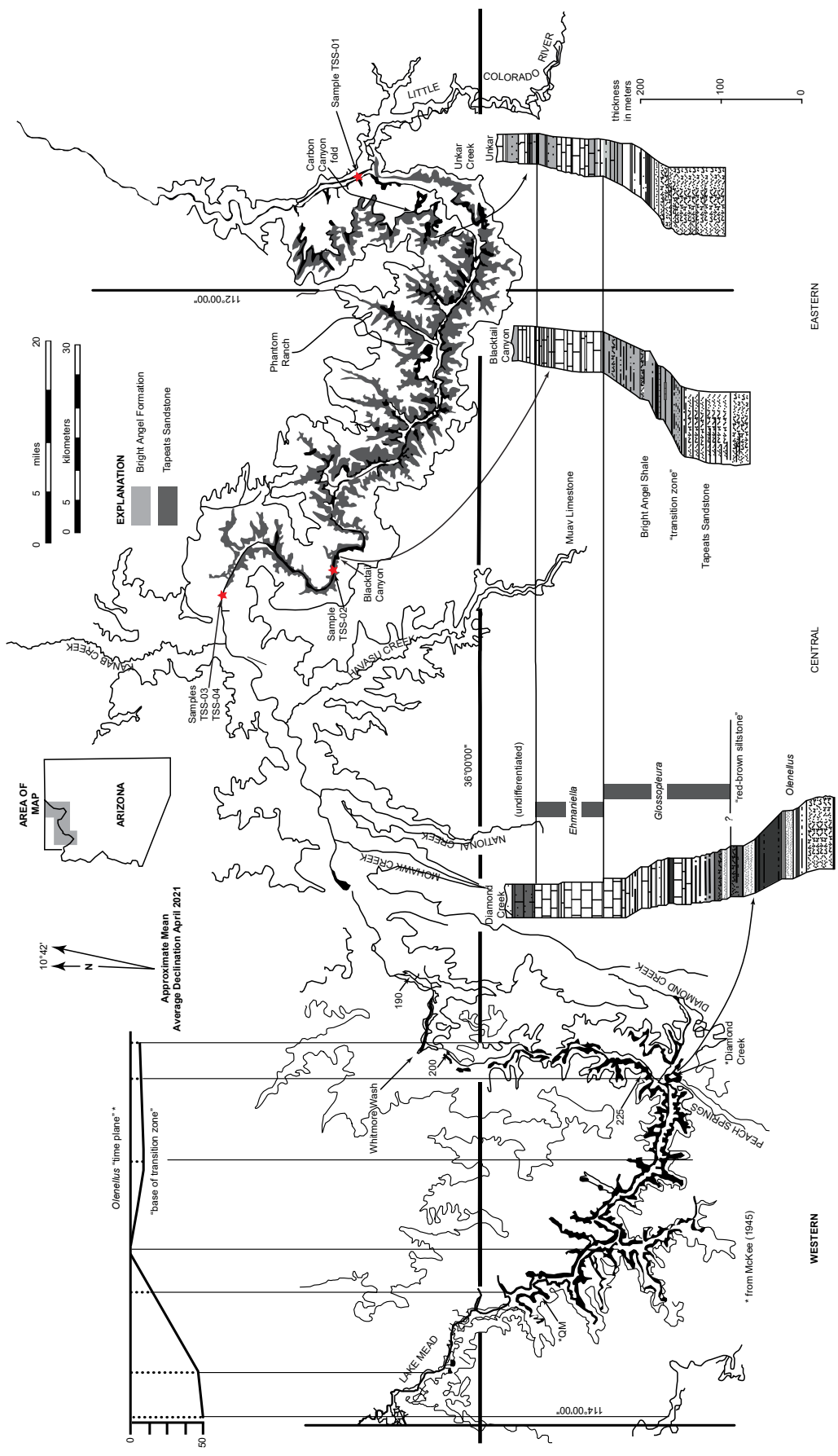

Fig. 1. Map of Grand Canyon showing the extent of exposure of the siliciclastic components of the Tonto Group, the Tapeats Sandstone and the overlying Bright Angel Formation (after Rose 2006, 225, fig. 1). Below the map are three representative stratigraphic sections shown in stylized profile of geomorphic expression. These three sections are provided in detail in Appendices A (Unkar), B (Blacktail Canyon), and C (Diamond Creek), available online in the Supplementary material. The inset in the upper left is the basis for the time-transgressive model proposed by McKee (1945). The datum was compiled from the reported height (in meters) at which McKee reported collecting *Olenellus* fossils from seven sites above the base of the "base of the transition zone" in the western Grand Canyon.

Fig. 2. The Carbon Canyon fold in which beds of the Tapeats Sandstone have been folded (bent) through 90 degrees adjacent to the Butte Fault. Carbon Canyon is a side canyon to the Colorado River corridor at river mile 65 and the fold is exposed best in the southern wall of the canyon about 2 km (about 1.2 mi) from the river. The man who is ~1.8 m (6 ft) tall standing on the fold provides the scale.

for the fractures, such as due to horizontal contraction within the beds during dewatering and lithification. Elsewhere, there is also no evidence of thickening of shale-rich beds in the Bright Angel Formation where they are folded.

There is another location in the Grand Canyon where there is similar folding of the Tapeats Sandstone, at the Monument Fault at river mile 116.4 (figs. 1 and 3). There the fold is right by the Colorado River, clearly visible, and thus easily accessible. It is a very open fold with virtually no mechanical crowding of the constituent sandstone beds in the Tapeats Sandstone. Again, the folding and faulting are claimed to have occurred during the Laramide Orogeny (Karlstrom and Timmins 2012), a very long time after the Cambrian deposition of the Tapeats Sandstone, yet the character of the sandstone beds also appear to be consistent with soft-sediment deformation soon after deposition very much earlier. Neither Hill and Moshier (2009) nor Tapp and Wolgemuth (2016) make any mention of the Monument fold.

It has been extensively documented that lithified rocks which have suffered ductile deformation will exhibit outcrop evidence of bedding plane slip and attenuation, such as flexural slippage (Ramsay 1967). However, field examination of these specific folds is insufficient to determine whether they were due to such ductile behavior of the lithified rocks under much later prolonged stress or due to soft-sediment deformation soon after deposition. Detailed microscopic examination is thus absolutely necessary to document the character of the sandstone, specifically, the textural relationships between the constituent grains and the timing of the formation of the cement (lithification). Tell-tale microscopic textures would be evident, such as grain-boundary sliding, the preferred orientation and recrystallization of the original detrital grains, as well as deformation lamellae and undulose extinction in those grains, and the original sedimentary cement between them would be absent or metamorphosed. Such textural features would be absent if the folding were due to soft-sediment deformation, as the original detrital

Fig. 3. The Monument fold in which beds of the Tapeats Sandstone have been folded (bent) in the northern wall of the Grand Canyon right near river level at Colorado River mile 116.4. The fold sits astride the Monument Fault. The vertical scale bar to the bottom left is ~10 m (~33 ft).

grains and the cement binding them together in the sandstone in the folds would be essentially identical to those in the same sandstone distant from the folds.

Yet it appears that none of these investigators have done any thin section investigations of the Tapeats Sandstone to substantiate their claims of ductile deformation of the Tapeats Sandstone in these two folds. Obviously, more detailed field and laboratory studies (especially intensive microscope examination) are needed to resolve the questions of what condition the sandstone was in when it was deformed into these folds, and thus how soon after deposition the deformation occurred, before or after lithification of the sandstone. Any field and laboratory study of the Tapeats Sandstone in the Carbon Canyon fold should thus also include a field and laboratory study of the Tapeats Sandstone in the Monument fold, as well as field and laboratory studies of the Tapeats Sandstone in other locations distant from these folds. This would enable observations and conclusions at the one location to be confirmed in the studies at the other locations, because the evidence seen in thin section examination of the Tapeats Sandstone in these folds should be different from that in the distant sandstone samples if the folding was due to ductile behavior under the stress of deformation of the lithified sandstone, whereas the microscope evidence should be nearly identical in all samples if the folding was due to soft-sediment deformation.

Therefore, on a research and sampling trip through the Grand Canyon with National Park Service approval, some 26 samples of the Tapeats Sandstone were collected from these two folds (12 samples from the Carbon Canyon fold and its vicinity, and ten samples from the Monument fold), and four samples from the Tapeats Sandstone at similar stratigraphic positions within the formation at sufficient distances away from those two folds so as to provide comparative control samples for the subsequent detailed thin section examination. Thus, the purpose of this paper is to review extensively what is already known about the petrology of the Tapeats Sandstone as the context for then reporting the detailed microscope observations made on the collected samples. From the mineralogy and textures of these samples, inferences can then be drawn about the sand source, its transport and deposition, and the sandstone's subsequent history, providing the documentation that can be referred to and built on in subsequent papers focused on the timing of lithification (cementation) of the Tapeats Sandstone in the Carbon Canyon and Monument folds before or after the folding occurred, that is, soft-sediment deformation or ductile deformation, respectively.

Past Investigations of the Tonto Group

The earliest conventional scientific explanations for deposition of the lower Paleozoic strata of the Grand Canyon region were offered by some of the most prominent North American geologists. Indeed, the Cambrian of the Grand Canyon is regarded as one of the classic sedimentary rock sequences exposed in North America. These strata crop out in the lower cliff sections of the Grand Canyon, along a prominent, essentially horizontal surface known as the Tonto Platform in the central part of the canyon, and near the banks of the Colorado River in western areas of the Canyon (figs. 1 and 4). The surface of the Tonto Platform roughly coincides with the top of the lowermost Cambrian formation, the Tapeats Sandstone. Above the Tapeats, a series of small cliffs are separated by thicker intervals of slopes composed of alternating beds of finer-grained deposits of shale, siltstone and sandstone of the Bright Angel Formation. These, in turn, are overlain by cliffs of resistant carbonates of the Muav Formation and then the Frenchman Mountain Dolostone (formerly the "unclassified dolomites"), the topmost units of the Tonto Group.

The Tonto Group forms the base of the kilometers-thick succession of generally flat-lying sedimentary strata that make up the Colorado Plateau. As described above, it straddles the conspicuous slope in the classic Grand Canyon cliff-slope profile known as the Tonto Platform (fig. 4). This geomorphic profile is consistent throughout the eastern exposures of Grand Canyon, which are much more visited, photographed, and familiar to most people. However, there is a great gap in exposed outcrops which separates the distinct eastern and western exposures of the Tonto Group (fig. 1). Only the uppermost cliff-forming carbonates of the Muav Formation are continuously traceable across the ~50 km (31 mi) gap between these exposures, and the stratigraphy of the less familiar western exposures differs in important ways from that of the eastern exposures. For one, the quality of Tonto Group exposure is poorer in the western canyon due to several faults complicating the traceability of marker beds. Secondly, it is covered by lava or rubble across several tens of kilometers. Lastly, the inaccessible sheer cliffs impede close inspection.

The Tonto Group was first defined by Gilbert (1875, his fig. 82) and Powell (1876, 60) and then recognized to be Cambrian by Walcott (1895, 317). The conventional model of shelf deposition for the Tonto Group on a passive continental margin can be traced from Powell (1891) through Gilbert (1875), Walcott (1910) and Noble (1914, 1922), to McKee (1945). It is now a textbook example of a marine transgressive sequence to which Sloss (1963) applied the term "Sauk sequence."

McKee (1945) provided the most comprehensive account of Tonto Group deposition. He proposed a time-transgressive, "deepening seas" model which has endured as the classic model of passive margin sedimentation and a landward advance of a wave-worn shoreline. His "deepening seas model" described the major threefold division of the Tonto Group as:

(1) a nearshore, high-energy regime represented by the Tapeats Sandstone,
(2) an offshore, low-energy regime represented by the Bright Angel Shale (now the Bright Angel Formation), and
(3) an even more distal low-energy carbonate buildup as "a chemical precipitate", represented by the Muav Limestone (now the Muav Formation).

Unlike his predecessors McKee (1945) claimed that all three units, including the Tapeats Sandstone, were deposited below wave base. That conclusion was necessitated by the presence of the phyllosilicate glauconite in the upper portion of the Tapeats Sandstone. Glauconite has long been accepted as a necessary indicator of low oxygen conditions in a deep marine setting, but this is no longer the case (McRae 1972). Other facies characteristics that are contrary to deep marine deposition were only minimally discussed by McKee (1945) in general terms of minor regressions or other temporarily exceptional conditions. This simple and elegant explanation for the intact layer-cake stratigraphy of the Grand Canyon's Tonto Group was thus settled on early and generally has not been revisited.

An important consideration in the development of the "deepening seas" model of time-transgressive shoreline retreat is that McKee (1945) worked his way eastward from the thicker basin-ward exposures of the western Grand Canyon, starting at Grand Wash Cliffs, to the region of central Grand Canyon reported previously by Noble (1914, 1922). Comparatively little early stratigraphic work was done on the eastern exposures, so McKee (1945) depended on the single generalized measured section of Wheeler and Kerr (1936) to characterize the stratigraphy of the eastern exposures. In so doing he applied Noble's solely lithologic facies criteria for subdividing the Tonto Group to the western exposures and as a result placed the Bright Angel Formation–Muav Formation contact some 150 m (492 ft) below what it would be if lithologic contacts were followed instead (Huntoon 1989). This quirk in nomenclature provided the impression that the Muav and Bright Angel Formations crossed time boundaries with reference to biostratigraphically defined "time planes" (fig. 5).

Conventional chronostratigraphic control within the Tonto Group is provided by sparse and poorly preserved trilobite fragments and rare

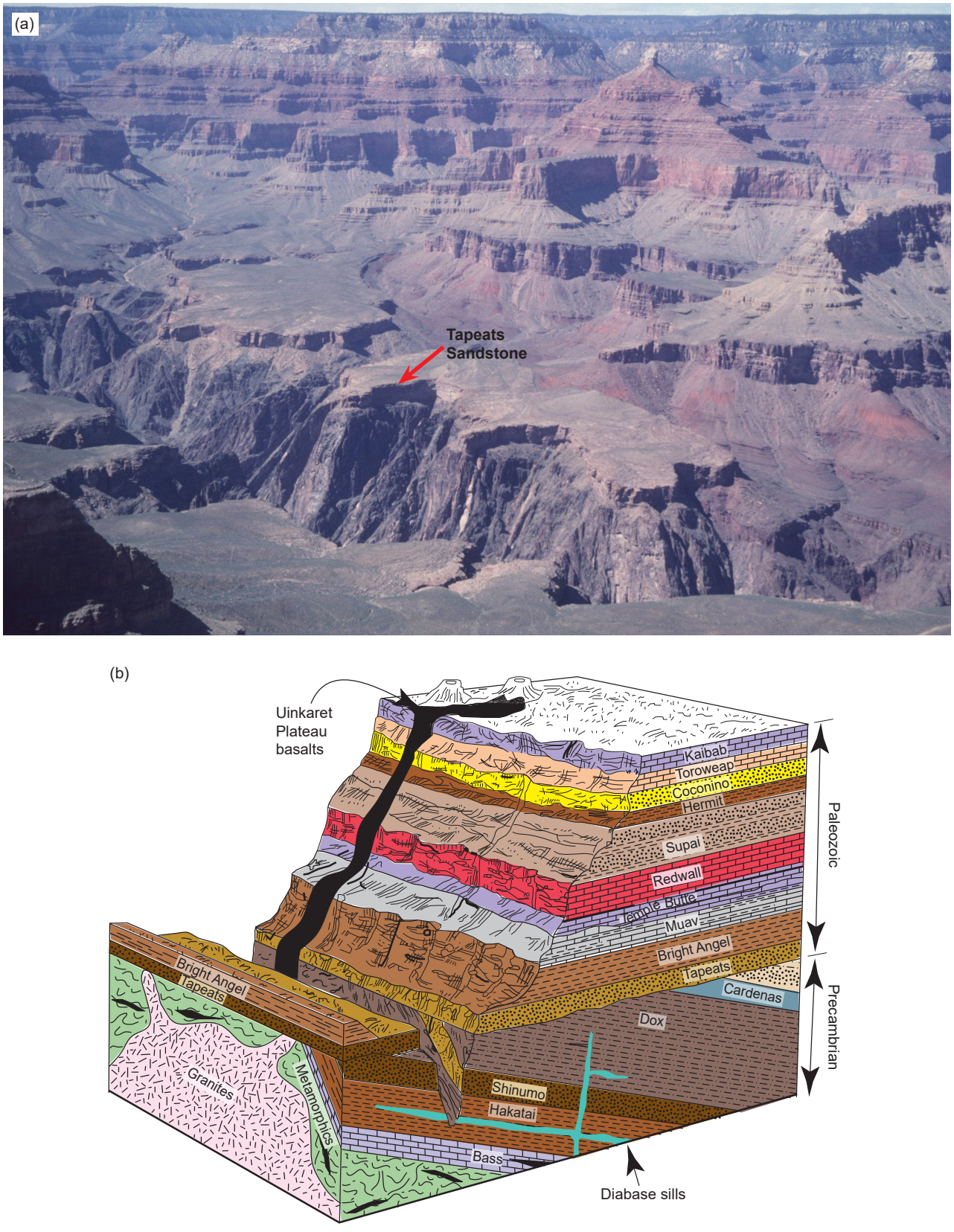

Fig. 4. The strata of the Grand Canyon. (a) The view of the Grand Canyon from the South Rim overlooks. From the skyline looking down are the horizontal sedimentary layers making up the walls of the Canyon. The Tapeats Sandstone is the lowermost layer exposed in the "small" cliff near the foreground (arrowed), below which is the inner gorge consisting of schists intruded by granites (b) A block diagram of the Grand Canyon strata corresponding to the vista seen in (a), except for the basalts that are found in the western Canyon (after Austin 1994).

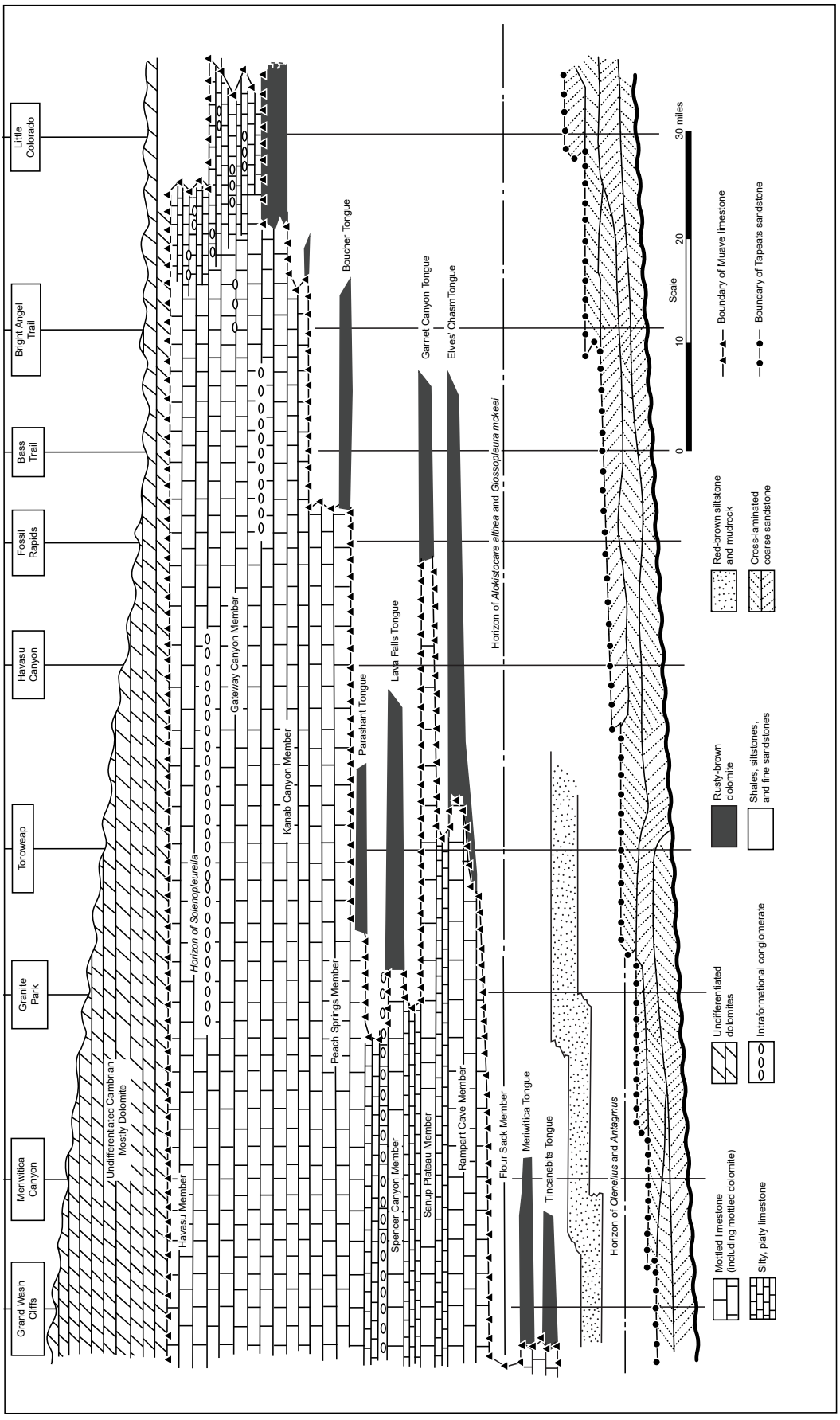

Fig. 5. The diagrammatic section of McKee (1945, 14, fig.1) of the Cambrian deposits in the Grand Canyon, showing stages in transgression and regression and distribution of facies from east to west. His time planes are horizontal, and the actual thickness varies from 1500 ft (about 460 m) in the west to 800 ft (about 245 m) in the east.

articulated trilobites but is complicated by numerous misidentifications by Resser (1945), subsequent taxonomic revisions (for example, Sundberg 1999), and the probability of mixed samples among poorly recorded collection sites. Nevertheless, McKee (1945) portrayed the biostratigraphy as thorough and precise, indicating uniform convergence of "thin fossil zones" with definite lithologic boundaries lower in the section as they are traced from west to east (fig. 5).

The classic work of McKee (1945) and Resser (1945) has endured as the most comprehensive study of the Cambrian system in the Grand Canyon. These Cambrian strata occur throughout the Rocky Mountains and have since become the classic (textbook) example of a transgressive fining-upwards sequence of sandstone, mudstone, and limestone that accumulated on the slowly subsiding Cordilleran miogeosyncline and adjacent craton (Lochman-Balk 1970, 1971; Stewart 1972; Stewart and Suczek 1977). It is thus postulated that during the early and middle Cambrian, a north-south trending strandline migrated progressively eastward across the craton. This shoreline was characterized by numerous embayments and offshore islands that affected sedimentation in nearshore areas. Shoreline migration was mostly eastward, resulting in deposition of coarse clastics in shallow water areas to the east and finer clastics and carbonates in the more offshore areas to the west. Numerous regressive phases apparently interrupted this overall eastward transgression resulting in complicated facies interactions.

However, subsequent limited research on these Tonto Group strata has not kept pace with conventional developments in the last 50 years of the dynamics of today's nearshore and shelf depositional systems (for example, Nummedal 1991) and then applied them to the uniformitarian explanation for the deposition of these rock units. Only a few studies have attempted to document carefully the lateral and vertical facies associations (Blakey and Middleton 2012; Elston 1989; Hagadorn et al. 2011; Hereford 1977; Martin 1985; Middleton 1989; Middleton and Elliott 2003; Rose 2003, 2006, 2011, Wanless 1973a). Wanless (1973a, b, 1975, 1981) presented the first challenge to the "deepening seas" model in demonstrating the petrographic similarity between modern intertidal carbonates and the Muav Formation facies that McKee (1945) interpreted as the most distal and deepest of the Tonto Group units. Wanless (1973a, b, 1981) further suggested that the whole of the Tonto Group deposition was in extremely shallow water.

Elston (1989) built on the "classic work" of McKee (1945) by taking his measured sections, and those of Noble (1922) and Wheeler and Kerr (1936) and recompiling them carefully with the same lithologies but adding some measured sections of his own in the eastern Grand Canyon. His correlations and his revised nomenclature are depicted in fig. 6. He concluded that his proposed correlations indicated that following deposition of the massive sandstone member of the Tapeats Sandstone in the western Grand Canyon, an eastward transgression of the epicontinental sea across the central and eastern Grand Canyon area occurred at or near the *Olenellus* horizon, which lies a few feet above the top of the massive sandstone member. The overlying red brown sandstone member in the west traces into the upper part of the Tapeats Sandstone in the central and eastern Grand Canyon, and the underlying shaly interval in the west passes into parallel-bedded, cross-laminated sandstone eastwards into the central Canyon.

Subsequently, Middleton and Elliott (2003) summarized the available data to describe the depositional systems of the Tonto Group presumed to have existed during the Cambrian history of northern Arizona, using both sedimentologic and ichnologic data. Then Rose (2003, 2006, 2011) provided new stratigraphic data and sedimentologic evidence from his 29 measured complete and partial sections to support Wanless' claim and explored more fully the depositional, geochemical, and biological characterization of his proposed extensive, pervasively shallow paleoenvironment responsible for the Tonto Group strata. Finally, Blakey and Middleton (2012) briefly reviewed the interpreted paleogeography and geologic history of the Cambrian system's record in the Grand Canyon area within the overall tectonic setting of southwestern North America.

Most recently, Karlstrom et al. (2018, 2020) have redefined the Tonto Group and Sauk megasequence in the Grand Canyon region. They concluded that the Sixtymile Formation is Cambrian and therefore locally the base of the Tonto Group, conformably overlain by the Tapeats Sandstone. Similarly, they concluded the Frenchman Mountain Dolostone is conformable above the Muav Formation. It extends across the Grand Canyon as the Undifferentiated Dolomite (McKee 1945) whose name it now replaces and is thus the topmost part of the Tonto Group and the Sauk megasequence transgression.

Regional Stratigraphic Relationships of the Tonto Group

As now proposed, the Tonto Group in the Grand Canyon region comprises five formations that are, in ascending order, the Sixtymile Formation, Tapeats Sandstone, Bright Angel Formation (primarily shale), Muav Formation (primarily limestone), and

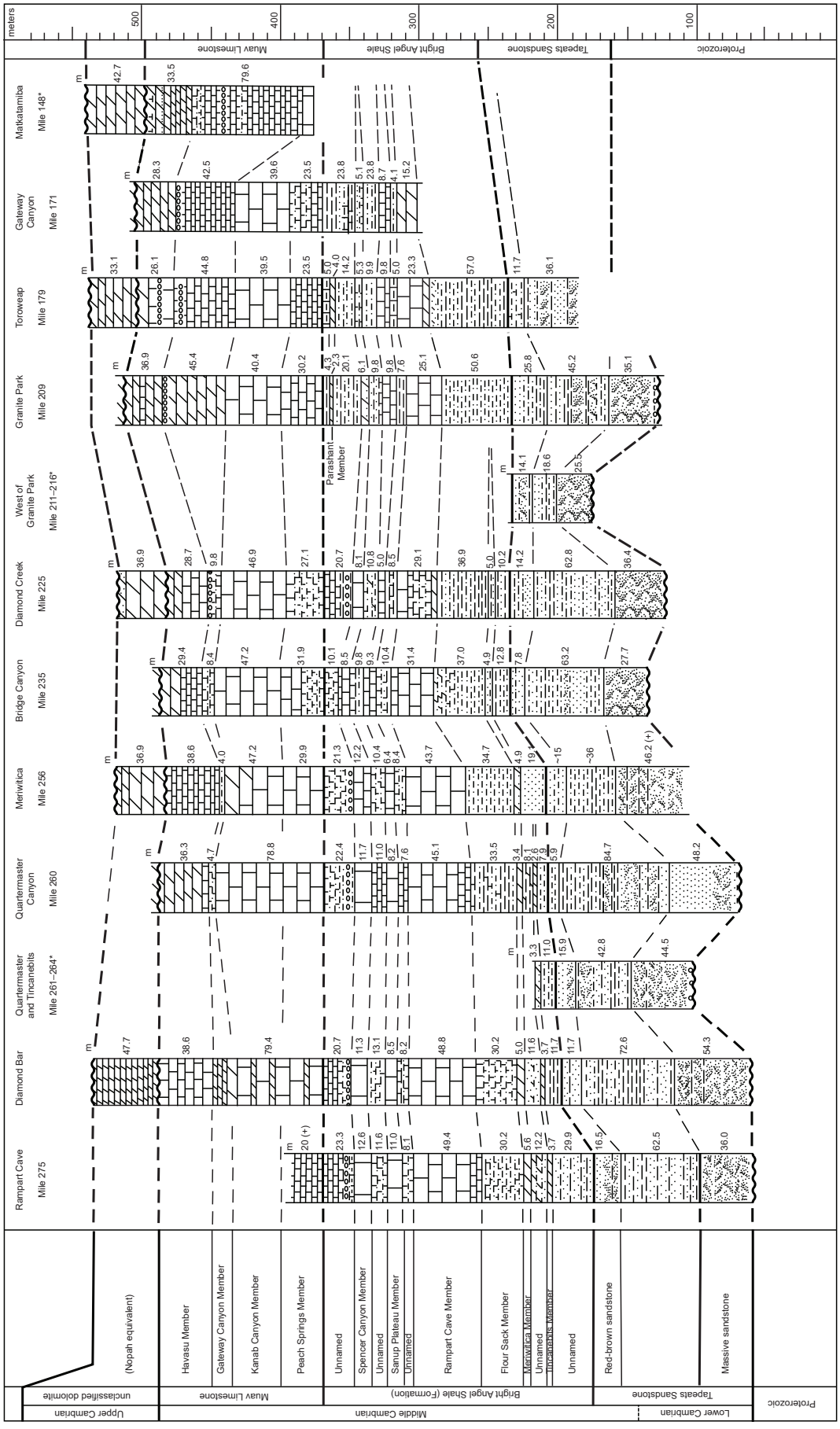
meters
500
400
300
200
100
Mojave Limestone
Bright Angel Shale
Tapeats Sandstone
Proterozoic
Rampart Cave Mile 275
Diamond Bar
Quartermaster and Tincanebils Mile 261–264*
Quartermaster Canyon Mile 260
Meriwitica Mile 256
Bridge Canyon Mile 235
Diamond Creek Mile 225
West of Granite Park Mile 211–216*
Granite Park Mile 209
Toroweap Mile 179
Gateway Canyon Mile 171
Matkatamiba Mile 148*
Parashant Member
(a)
Upper Cambrian
Middle Cambrian
Lower Cambrian
Proterozoic
unclassified dolomite
(Nopah equivalent)
Mojave Limestone
Havasu Member
Gateway Canyon Member
Kanab Canyon Member
Peach Springs Member
Bright Angel Shale (Formation)
Unnamed
Spencer Canyon Member
Unnamed
Sanup Plateau Member
Unnamed
Rampart Cave Member
Flour Sack Member
Meriwitica Member
Unnamed
Tincanebils Member
Unnamed
Tapeats Sandstone
Red-brown sandstone
Massive sandstone

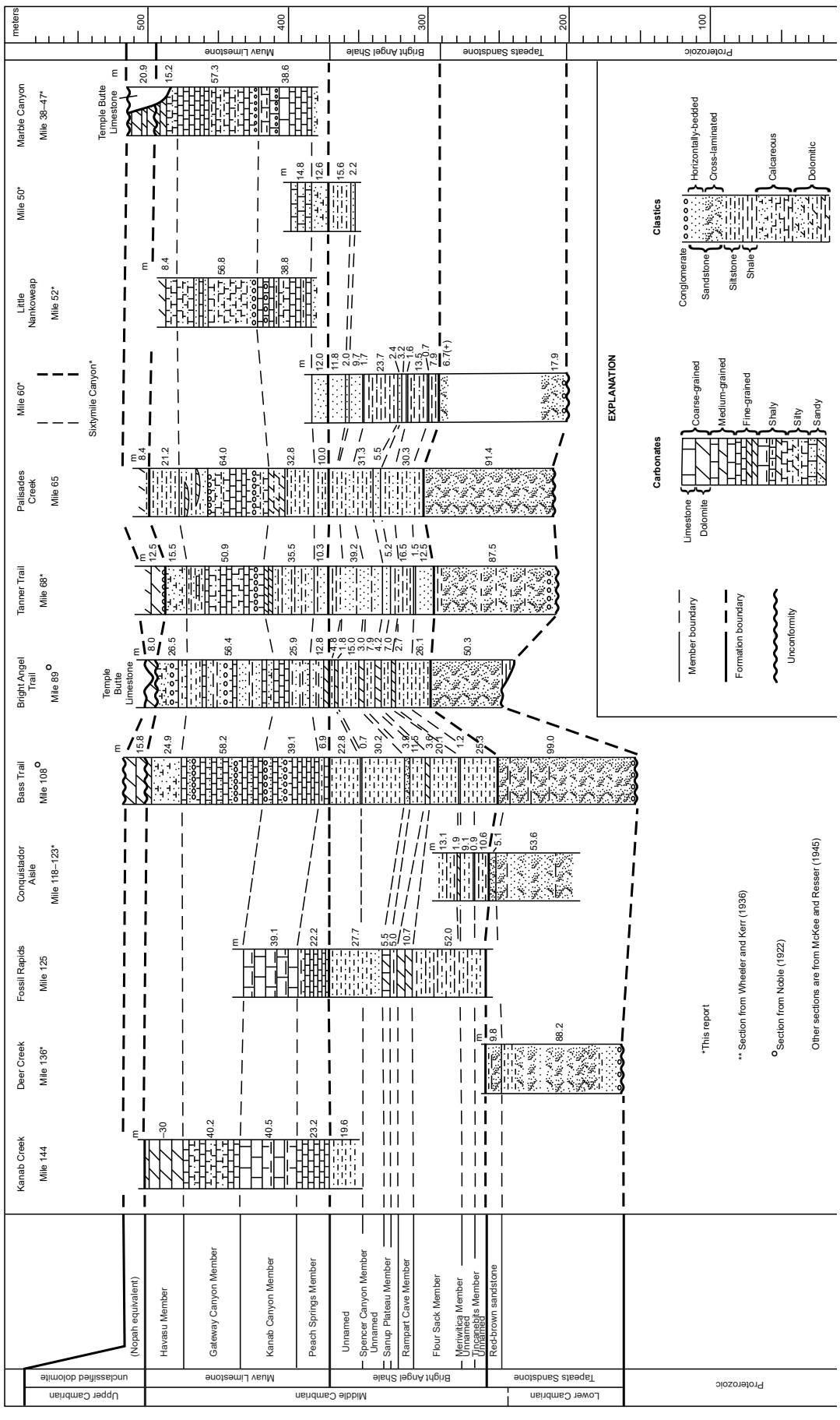

Fig. 6. The diagrammatic sections of Elston (1989, 134-135, figs. 15a,b) showing the correlation of the Cambrian Tonto Group deposits in the Grand Canyon and the facies changes based on McKee (1945), Noble (1922), and Wheeler and Kerr (1936) but with his revised nomenclature. (a) The western half of the Grand Canyon, Rampart Cave (river mile 275) to Matkatamiba Canyon (river mile 150). (b) The eastern half of the Grand Canyon, Kanab Creek (river mile 144) to Marble Canyon (river miles 38-47).

the Frenchman Mountain Dolostone (Karlstrom et al. 2020). The term "Tonto Group" was first used by Gilbert (1874, 1875) to describe the Tapeats-Bright Angel-Muav fining-upwards sandstone-shale-limestone sequence, although he considered these rock units to be Silurian. Subsequent stratigraphic and paleontologic work by Walcott (1890, 1895) established that the Tonto Group is Cambrian, and Noble (1914) introduced these three formation names during his mapping of the Shinumo Quadrangle in the Grand Canyon.

Strata of the Tonto Group also crop out along the Grand Wash Cliffs in western Arizona and further west at Frenchman Mountain just outside Las Vegas, Nevada, where the Muav Formation is overlain conformably by the Frenchman Mountain Dolostone. To the east the Tonto Group also crops out in the Juniper Mountains and Black Hills in west-central Arizona (Middleton and Elliott 2003). In those areas the Tapeats Sandstone is overlain disconformably by the Devonian Martin Formation, or the Chino Valley Formation of uncertain age designation (Hereford 1975). It is presumed that the Bright Angel and Muav Formations were removed by extensive pre-Devonian erosion (Middleton and Elliott 2003). In central Arizona scattered outcrops of the Tapeats Sandstone occur along the East Verde River and in the Sierra Ancha Range north of Young, Arizona. Tonto Group equivalents in southeastern Arizona include the Bolsa Quartzite and part of the overlying Abrigo Formation (Hayes and Cone 1975; Middleton 1989).

These Cambrian strata overlie a variety of Precambrian lithologies throughout the Grand Canyon. In the eastern canyon and in some central areas, the Tonto Group rests on tilted beds of the Precambrian Grand Canyon Supergroup, which consists of the Unkar and Chuar Groups, whereas in the western areas and other central places the Tonto Group nonconformably overlies various older Precambrian granite plutons that intrude schists of the Granite Gorge Metamorphic Suite (figs. 4 and 7). This major unconformity between the Precambrian and Tonto Group strata has been long recognized and is called the Great Unconformity due to its visual prominence and continental (and global) extent (Peters and Gaines 2012). Traditionally, it has been thought to represent either a considerable period of time during which there were episodes of slow mountain-building and extensive weathering and erosion, or a very short and intense period of catastrophic uplift and erosion. Walcott (1910) applied the name "Lipalian interval" to the period of uniformitarian time represented by this unconformity. Since the Tonto Group is Cambrian, where it sits on the crystalline basement granites and metamorphic schists (fig. 7c and 7d) that are generally dated at 1.6–1.7 Ga (Karlstrom et al. 2003) the time interval at the Great Unconformity is about 1.1 Ga. In contrast, where the Tonto Group sits on the tilted Grand Canyon Supergroup sedimentary strata (figs. 7a and 7b) it has been harder to date those sedimentary rocks, so their ages have been variously estimated based on the 1.1 Ga Rb–Sr age for the Cardenas Basalt lavas that are sandwiched between the Unkar Group and Chuar Group sedimentary strata (Elston and McKee 1982; Larson, Patterson, and Mutschler 1994). Thus, the time interval at the Great Unconformity with the Grand Canyon Supergroup sedimentary strata is <500 Ma.

However, recent radiometric dating results have further constrained the time interval represented by the Great Unconformity. A U-Pb age of 742 Ma was obtained for zircons within a thin tuff bed at the top of the Walcott Member of the Kwagunt Formation just below the Great Unconformity (Karlstrom et al. 2000). Subsequently, an Ar-Ar age of 764 Ma was obtained for authigenic K-feldspar within early diagenetic marcasite nodules in the underlying Awatubi Member of the Kwagunt Formation (Dehler et al. 2017), and a U-Pb age of 729 Ma was obtained for zircons from the same thin tuff bed at the top of the overlying Walcott member (Rooney et al. 2018), both in the upper Chuar Group of the uppermost Grand Canyon Supergroup in the eastern Grand Canyon. Furthermore, in the eastern Grand Canyon a small wedge of sedimentary strata known as the Sixtymile Formation is sandwiched between the Grand Canyon Supergroup and the Tonto Group. Hithertofore they have been regarded as Precambrian and thus below the Great Unconformity. However, Karlstrom et al. (2018, 2020) have convincingly demonstrated that the Sixtymile Formation contains detrital zircons with the youngest U-Pb ages of 505–527 Ma and is thus Cambrian. It is therefore now regarded as being above the Great Unconformity, and thus represents the onset of the transgression that deposited the rest of overlying Tonto Group. So, the time interval at the Great Unconformity could be <200 Ma.

The surface on which the Tonto Group accumulated was fairly irregular, though it is also flat at many locations. Where irregular it was characterized by a rolling topography of resistant bedrock "hills" (often Unkar Group Shinumo Quartzite) and "lowlands." The Precambrian bedrock appears to have been extensively weathered in places and eroded during the claimed prolonged period of subaerial exposure. Walcott (1880) and Noble (1914) were first to recognize that the Precambrian surface represented an apparent paleotopography and that Tonto Group sedimentation patterns were influenced by the relief and lithologies of those "hills." Others likewise

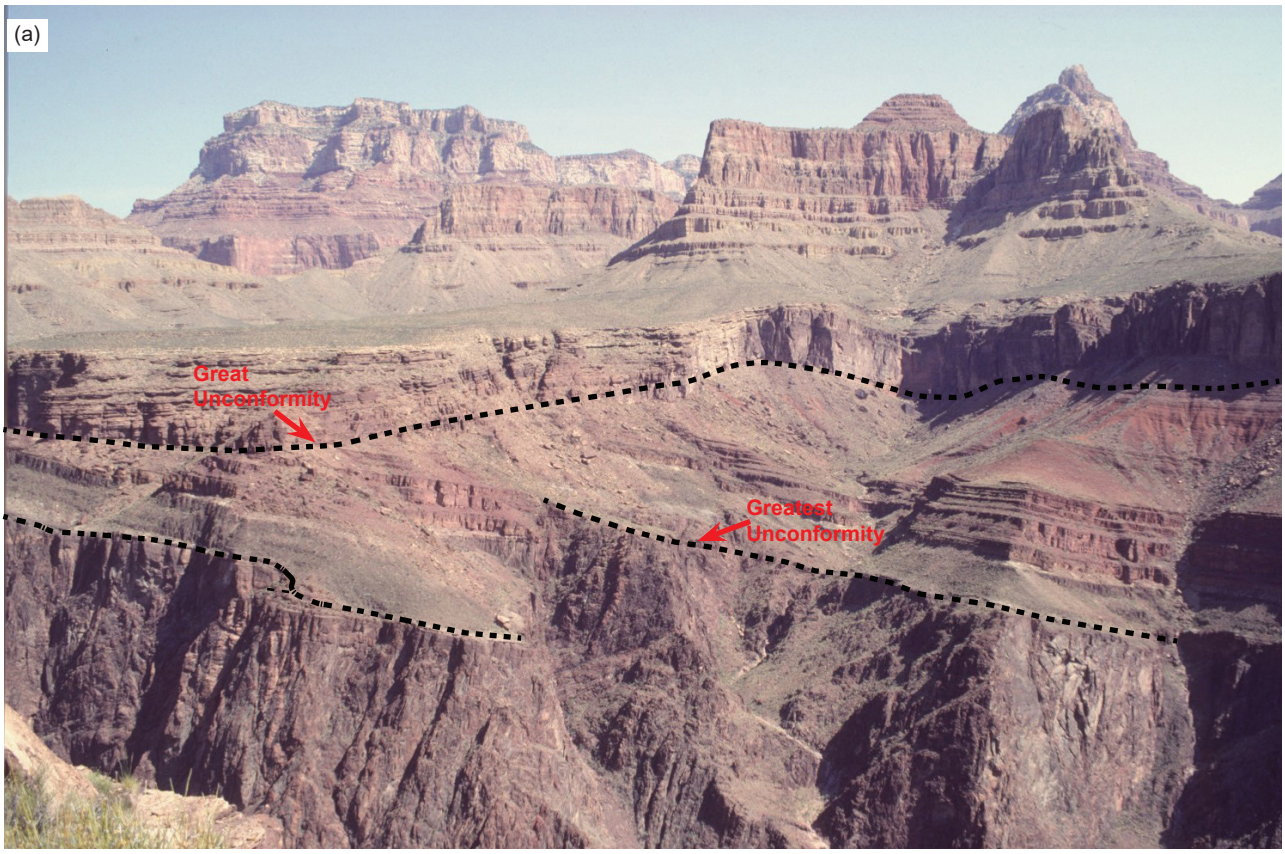
(a)
Great Unconformity
Greatest Unconformity


(b)
Great Unconformity


(c)
Great Unconformity

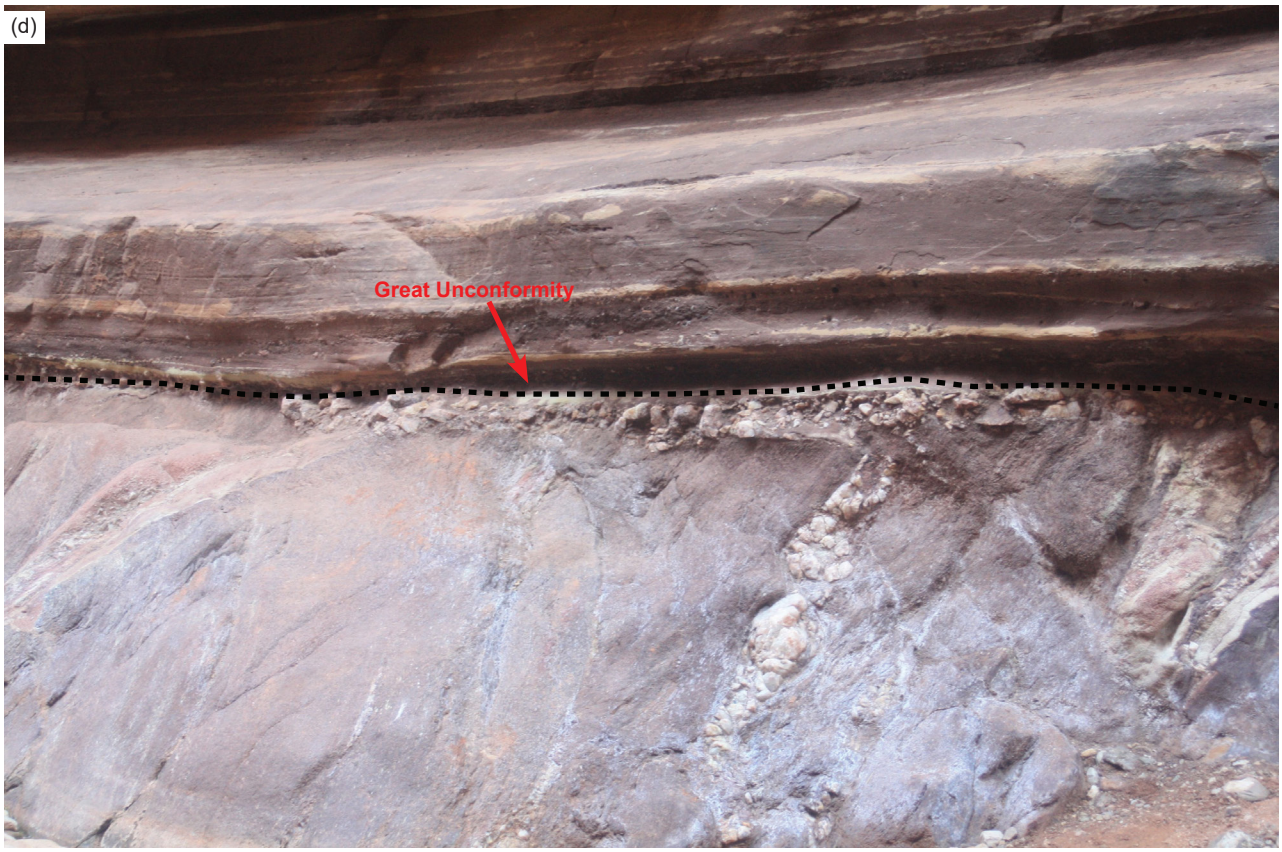
(d)
Great Unconformity

Fig. 7 (pages 171 and 172). The Great Unconformity as exposed throughout the Grand Canyon. It is marked with dashes in each image. (a) View from the edge of Horseshoe Mesa of the tilted Precambrian Unkar Group sedimentary strata within the Grand Canyon Supergroup eroded across at the Great Unconformity with the Tapeats Sandstone deposited on it. Further below is the Greatest Unconformity (marked), separating the tilted Grand Supergroup strata from the crystalline basement metamorphics and granites below it. (b) The Great Unconformity eroded across the Hakatai Shale of the Precambrian Unkar Group with the Tapeats Sandstone sitting on top of it, in the cliff face of the northern edge of Hance Canyon above river mile 79. (c) The Great Unconformity is just below the cliff of Tapeats Sandstone on the near horizon and consists of the eroded surface of the Ruby Pluton (a hornblende-biotite granodiorite intruded by later large granitic veins) at about river mile 105. (d) The Great Unconformity as seen up close in Blacktail Canyon at river mile 120.5. Here the Tapeats Sandstone is sitting on the Vishnu Schist of the Granite Gorge Metamorphic Suite.

documented the influence of the Precambrian topography on Cambrian sedimentation in other areas of the Rocky Mountains and in the midcontinent (Middleton and Elliott 2003). There are numerous places in the Canyon where the Tapeats Sandstone thins across or pinches out against those Precambrian highs. Where the Tapeats Sandstone pinches out, the Bright Angel Formation overlies the Precambrian surface.

An apparently highly weathered horizon occurs on top of the Precambrian surface in several places in the Canyon. The only effort to understand the genesis of that potentially significant horizon is that of Sharp (1940). His study suggested that extensive chemical weathering of Precambrian rocks occurred prior to deposition of Cambrian sediments. In places that apparently highly weathered surface or potential regolith is up to 15.3 m (50 ft) thick, but elsewhere is generally less than 3.1 m (10 ft) thick. Sharp (1940) speculated that where the Tapeats Sandstone sits on unaltered Precambrian basement, that regolith was probably removed by the wave erosion associated with the initial Cambrian transgression. Sharp (1940) and McKee (1945) suggested that the presence of such a thick, apparently weathered horizon indicated that dominantly humid conditions existed during the earliest Paleozoic prior to deposition of the Tonto Group. However, there have been no petrologic and geochemical studies that could substantiate that hypothesis. Furthermore, from a uniformitarian perspective during the <200 million years represented at the Great Unconformity the climate could have changed numerous times prior to deposition of the Tonto Group, and in the presumed absence of terrestrial vegetation weathering processes in soils would have been different (Basu 1981), so a humid climate interpretation is quite tenuous.

At the continental scale, Sloss (1963) recognized that the Great Unconformity and the overlying Tonto Group could be correlated across North America, the latter representing the first of six major sequences of rock-stratigraphic units which he named the Sauk megasequence. Peters and Gaines (2012) further documented that the Great Unconformity is a well-recognized, globally-occurring stratigraphic surface, which in most regions across the globe separates continental crystalline basement rocks from much younger Cambrian shallow marine sedimentary deposits, that is, the Sauk megasequence. Using stratigraphic and lithologic data for 21,521 rock units from 830 geographic locations in North America they demonstrated that the Tapeats Sandstone correlates with very similar basal Sauk sandstones right across North America (figs. 8 and 9a), such as the Flathead Sandstone in Wind River Canyon, Wyoming, the Mt. Simon Sandstone in a drill-hole in northern Illinois, and the Sawatch Formation near Manitou Springs, Colorado. Similarly, Clarey and Werner (2018) constructed over 1,500 local stratigraphic columns across North America, South America, Africa, and the Middle East recording the detailed lithologic information and the Sloss megasequence boundaries at each site. From these data they created a detailed 3-D lithology model for each continent using the local columns, and also constructed maps of the basal lithology for each megasequence. They thus demonstrated the continuity of the basal Sauk sandstone layer (the Tapeats Sandstone and its equivalents) across the North American continent, across North Africa and the Middle East (fig. 9b), and across South America where the Sauk is only found within portions of Peru, Bolivia and northern Argentina. Furthermore, in many locations the basal Sauk megasequence is also coincident with the Great Unconformity (fig. 9).

The Stratigraphy of the Tapeats Sandstone

The Tapeats Sandstone is exposed across a ~500 km (310 mi) wide swath of Nevada and Arizona. It was named after the exposures along Tapeats Creek in the western Grand Canyon (river mile 134.5). For the most part, the formation is a medium- to coarse-grained K-feldspar- and quartz-rich sandstone with a granule- and pebble-size quartz-rich conglomerate present locally near its base (Middleton and Elliott 2003) (fig. 10). The percentage of K-feldspar appears to be highest at the base and decrease upwards through the sandstone. The composition of the Tapeats Sandstone and its basal section reflects to varying degrees the mineralogy of the underlying

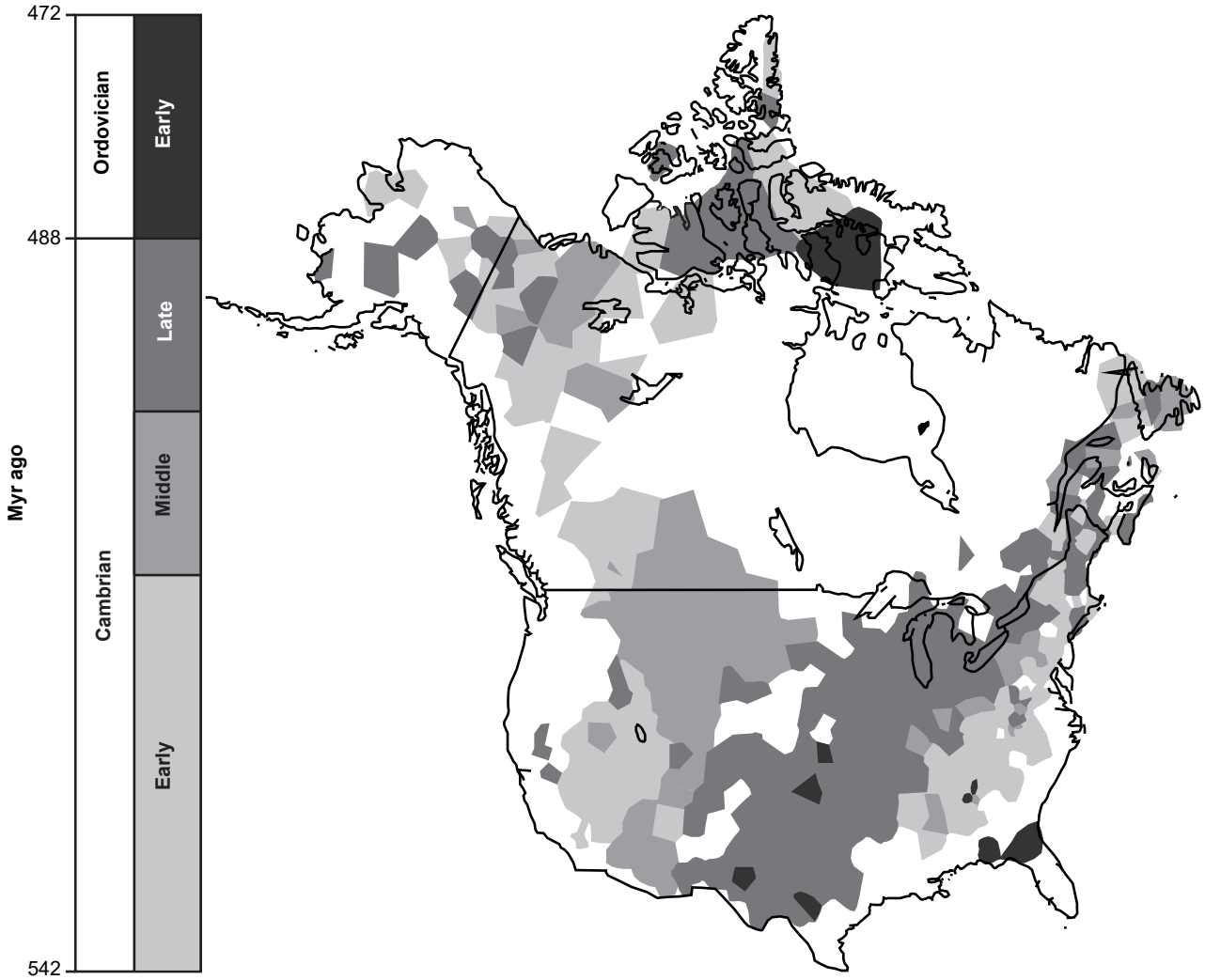

Fig. 8. The distribution and age of the Sauk megasequence, the oldest Phanerozoic sedimentary rocks of North America (after Peters and Gaines 2012, 363, fig.1). Not only were the basal Tapeats Sandstone and its equivalents deposited continent-wide, but the Great Unconformity beneath it was also eroded continent-wide and beyond (globally).

Precambrian sedimentary and crystalline rocks (Blakey and Middleton 2012). However, Middleton and Elliott (2003) opined that to-date there have been no systematic petrologic studies of the Tapeats Sandstone documenting changes in mineralogy with respect to facies changes or evaluating the influence of basement lithology and paleotopography on the composition of the Tapeats Sandstone.

The upper boundary of the Tapeats Sandstone as first recognized by Noble (1922) is marked by the highest bed of coarse-grained, cross-laminated, resistant sandstone (fig. 10). McKee (1945) noted that in some localities such as in the extreme eastern Grand Canyon this is at the top of the main cliff of coarse-grained sandstone, but elsewhere there is a weak, slope-forming unit of alternating sandstone and shale beds above the main cliff (fig. 10). Thus, the formation can be divided into two generalized packages (McKee 1945; Middleton and Elliott 2003). The majority of the Tapeats Sandstone crops out as a cliff consisting of beds typically less than 1 m (3 ft) thick (figs. 11 and 12). Sedimentary structures include planar and trough cross-stratification and crudely developed horizontal stratification (fig. 11). Both the scale of the bedding and the cross-stratification decrease upwards. Overlying the main cliff is a thinner zone of interbedded fine- to medium-grained sandstone and mudstone (fig. 10). Stratification is on a smaller scale in these beds and is largely trough and ripple cross-stratification and horizontal stratification.

The significance of the upper unit is that it marks a major facies transition into the lower Bright Angel Formation. An increase in finer-grained sediment indicates an apparent reduction in the bedload to suspension load ratio (Middleton and Elliott 2003). The consistent changes in bedding thickness and scale of sedimentary structures appear to be consistent

Fig. 9. Trans-continent and between-continent occurrences of the Tapeats Sandstone equivalents with identical diagnostic features sitting on the Great Unconformity (marked with dashes in each image), similarly-eroded into the top of Precambrian crystalline basement rocks. (a) Chippewa Falls, Wisconsin, USA, and (b) Timna, southernmost Israel.

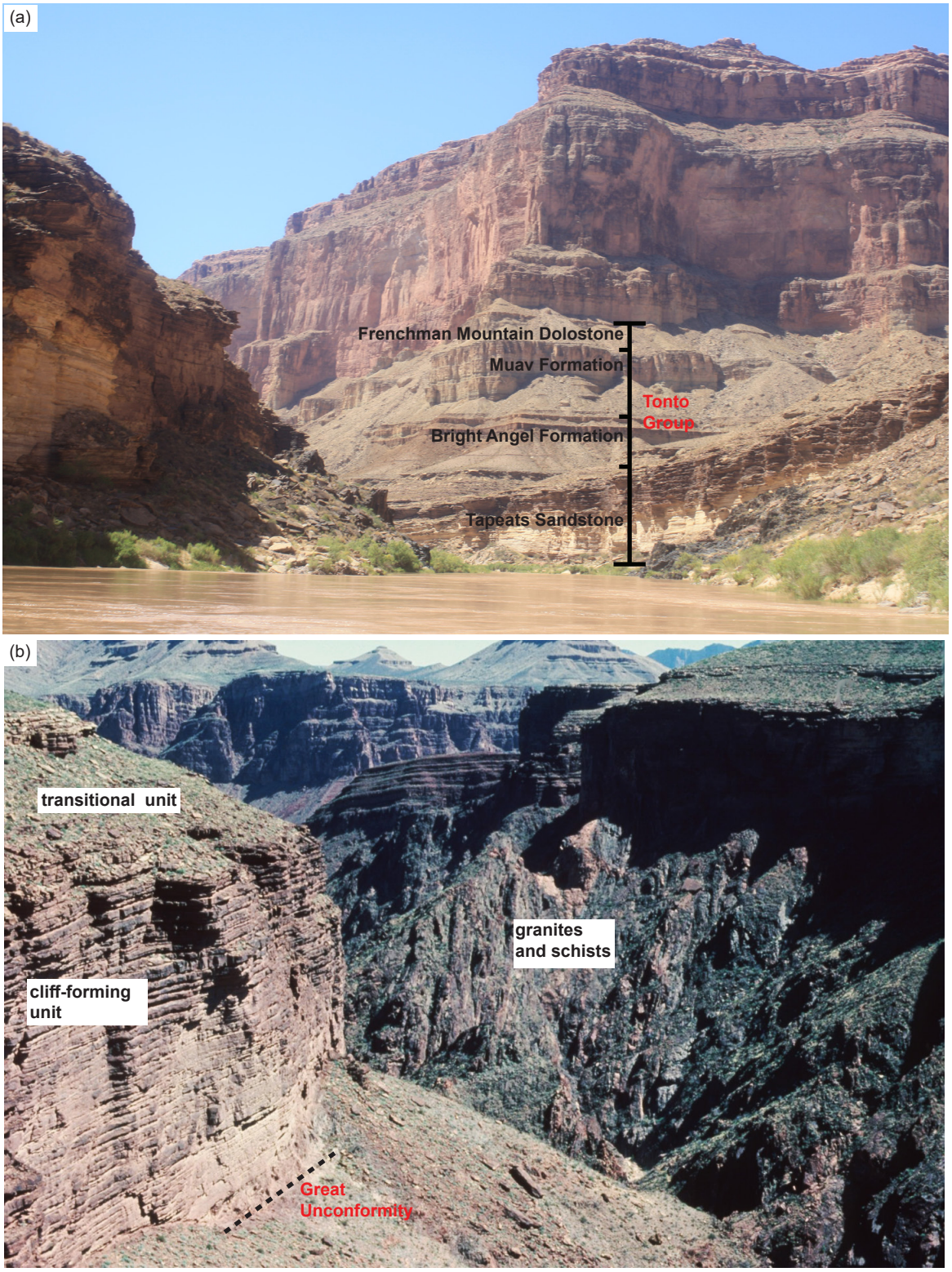

Fig. 10. (a) The full profile of the Tonto Group, except for the Sixtymile Formation, just above Blacktail Canyon and looking towards it around river mile 120, central Grand Canyon (indicated). The three formations making up the Tonto Group (as labeled) are easily distinguished by their profiles in the cliff face (see also the matching graphic stratigraphic log in Appendix B of the Supplementary materials). (b) The full profile of the Tapeats Sandstone, as seen in the eastern Grand Canyon. Above the basal section that sits on the Great Unconformity eroded into the underlying Precambrian schists intruded by pink granite veins is the dominant cliff-forming unit with its thin plain bedding. At the top of the cliff there is a slope with many more thin sandstone beds interspersed with thin siltstone and shale beds that together make up the transitional unit up to the highest resistant sandstone bed (top left), above which the overlying Bright Angel Formation here has been eroded back to produce the widespread Tonto Platform.

Fig. 11. Closer view of the cliff-forming Tapeats Sandstone at Colorado River level at about river mile 59.5. The scale bar to the right is ~2 m (~6.5 ft). The thin horizontal sandstone beds of varying thickness making up the formation are visible, along with the planar and trough cross-stratification.

Fig. 12. The cliff-forming unit of the Tapeats Sandstone behind the Science Camp opposite the confluence of the Little Colorado River. The dominant thin plain bedding is very evident due to weathering of softer levels in the sandstone producing ledges. The scale bar to the right is ~2 m (~6.5 ft).

with that interpretation. The contact between the two formations, therefore, is arbitrary and probably should be placed at the top of the thickest sandstone bed within the transitional interval. This transitional unit is especially thick and well-developed in the western Grand Canyon (McKee 1945).

The Tapeats Sandstone varies considerably in thickness throughout the Grand Canyon and also in areas to the south and west. Noble (1922) reported a thickness of 120 m (393 ft) along the South Bass Trail in the central Grand Canyon, which possibly represents the maximum thickness in the Canyon. Typically, the formation is between 30 m (100 ft) and 100 m (325 ft) thick. The thickness of the Tapeats Sandstone is clearly controlled by the relief of the underlying Precambrian surface because there are areas where it thins across and/or pinches out against Precambrian highs.

Rose (2003) collected stratigraphic data from 29 representative full and partial measured sections at sites throughout the western, central, and eastern Grand Canyon from which he developed an idealized section of the Tapeats Sandstone (Rose 2006) (fig. 13). Three of his sections, the locations of which are indicated in fig. 1, are reproduced in detail in Appendices A, B, and C (in the Supplementary material). As also described by Middleton and Elliott (2003), Rose (2006) depicted the Tapeats Sandstone as consisting of a coarse-grained, sub-arkosic ribbon sandstone with high-angle tangential cross-beds, apparent channels and lateral accretion surfaces together forming a cliff averaging about 36.5 m (120 ft) high, that sits on top of basal gravels and cobble breccias up to 4 m (13 ft) thick, with what he interpreted as occasional arkosic micaceous redbeds and saprolites. There is no sign of any bioturbation of this part of the Tapeats. Overlying this lower or cliff-forming unit of the Tapeats Sandstone is an upper unit averaging about 18 m (59 ft) that forms a slope and is the transition to the Bright Angel Formation above (figs. 10 and 13). It consists of recess-forming green fissile shale alternating with fine quartz sandstone with trace fossils *Arenicoloides* and *Arencolites*, overlain by interpreted isolated channels of sandstone and rare thin beds of bioturbated quartzite containing *Skolithos* or *Diplocraterion*, which in turn is overlain by more green fissile shale and interbedded fine quartz sandstone, the latter with *Cruziana* (see below).

Subsequently, Gehrels et al. (2011) described the Tapeats Sandstone in the Grand Canyon area as generally ranging from 0 m to 122 m (400 ft) thick, locally pebbly in the lower few meters, then grading from thick beds of cross-bedded and horizontally-stratified sandstone upward into thinly-layered sandstones interbedded with shales. Based on the original work of McKee (1945) and Resser (1945), and their use of the fossil horizons as time markers, Gehrels et al. (2011) reiterated the Middleton and Elliott (2003) claim that these strata become younger eastward from late Early to early Middle Cambrian age.

Finally, Hagadorn et al. (2011) stated that the Tapeats Sandstone is a sheet siliciclastic lithesome that contains three stratigraphically distinct, sedimentologically defined suites of lithofacies (figs. 10 and 13):

(1) Facies Suite A is typically a gravelly to boulder conglomerate or red-purple mudstone that directly overlies the basement rocks;
(2) Facies Suite B consists of a variety of ledge-forming sandstone lithofacies that may include trough cross-, ribbon-, or flaser-bedded, or planar-laminated or tabular sub-arkosic to arenitic sandstones with minor mudstone; and
(3) Facies Suite C is typically dominated by interbedded sandstones and shales and coincides with a "transition zone" that in places is variously assigned as part of the overlying Bright Angel Formation.

They added that at any given locality all or a subset of these facies suites occur, and any of them may directly mantle the Precambrian basement. But the Tapeats Sandstone is everywhere overlain by the Bright Angel Formation.

Furthermore, Rose (2011) remarked that no type section yet exists for the Tonto Group or any of its constituent units, even though the section described by Noble (1922) has served as a de facto type section. He thus proposed his (Rose 2003) measured section at Blacktail Canyon (river mile 120.5) as a suitable formal type section (fig. 1, and Appendix B in the Supplementary material), because it is accessible from the Colorado River, and because it is between two long straight stretches of the river, which provides a clear view in both directions of the continuity of marker beds and the cliff-slope profile that help define unit boundaries. Rose (2011) described the Tapeats Sandstone of eastern Grand Canyon as a traceable singular prominent cliff-forming unit (figs. 10 and 12) across many hundreds of kilometers of exposure. Its thickness ranges between 45–65 m (148–213 ft), or upwards of 90 m (295 ft) if the overlying "transition zone" with the Bright Angel Formation is mostly sandstone. It is generally a coarse to medium-coarse sub-arkose as a locally variegated mixture of clastic components that includes a mature, well-rounded milky and citrine quartz component and a locally sourced angular K-feldspar and lithic component. And the upper few meters of typical cliff-forming Tapeats is medium-grained bleached sandstone, commonly with glauconite as a minor component, or

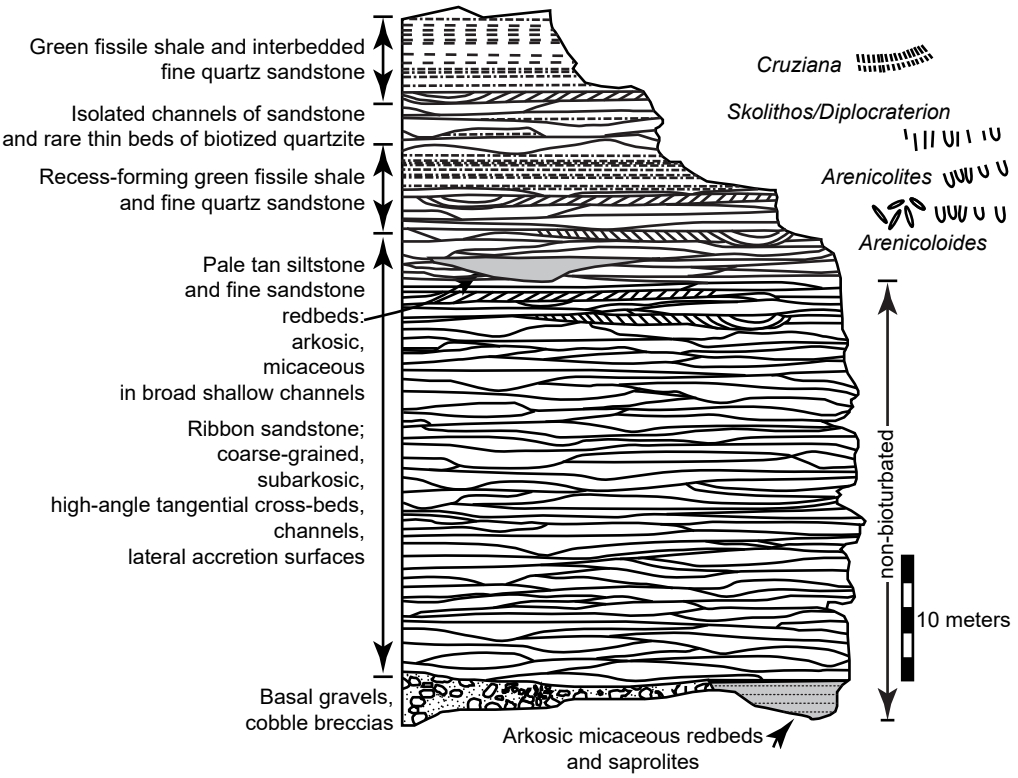

Fig. 13. The idealized section of the Tapeats Sandstone as suggested by Rose (2006, 227, fig. 3), with descriptive details of various features found at different stratigraphic levels within the formation, including the distribution of the various constituent facies, sedimentary structures, and trace fossils (as described in the text).

locally is well-sorted quartz arenite and quartzite. Furthermore, Rose (2011) observed that the base of the Tapeats Sandstone is generally grittier than higher in the unit, but local lows in the antecedent topography of the underlying eroded Precambrian strata up to several meters in depth below the lowest continuous sandstone layers can contain locally derived breccia, bedded micaceous and hematitic siltstone, or structureless micaceous and hematitic siltstone above interpreted saprolitically altered basement rock. Locally sourced breccia and isolated cobbles and boulders are also present stratigraphically higher in the Tapeats section at localities adjacent to paleotopographic highs (fig. 14).

Paleontology of the Tapeats Sandstone

Since the early work by McKee (1945) and Resser (1945) there have been very few studies of the biostratigraphy of Cambrian strata in the Grand Canyon and the taxonomy of their fossils (Middleton and Elliott 2003). Thus, the systematics of the invertebrate fauna remain the same. Middleton and Elliott (2003) state that except for trace fossils, which in places are quite common, body fossils are rare in the Tapeats Sandstone and only occur within the beds of the transition zone to the overlying Bright Angel Formation. However, Hagadorn et al. (2011) insist that nowhere does the Tapeats contain body fossils, including in subaqueously-deposited interbedded shales of the transition zone.

Despite the paucity of well-preserved invertebrate fossils, analysis of the fauna has provided information on the biostratigraphic zonation of the Tonto Group (Middleton and Elliott 2003). Trilobites and brachiopods are the most abundant fossils reported from the Bright Angel and Muav Formations, though most specimens are poorly preserved. McKee (1945) found and defined several thin fossil zones which were so restricted vertically yet so uniformly developed that they constituted excellent horizon markers or key beds indicating time planes (fig. 5). The lowest and one of the most persistent of these thin faunal zones (first reported by Wheeler and Kerr 1936) is identified by the trilobites *Olenellus* sp. and *Antagmus arizonaensis* (Resser 1945). McKee (1945) described it as a fine- and even-grained, reddish or gray sandstone, only a few feet thick (~1m), which extends from Grand Wash Cliffs (where it is apparently in the base of the Bright Angel Formation) eastward at least 35mi (~56km) (where it is in the upper Tapeats Sandstone). Impressions of trilobite fragments, especially spines, and specimens of the brachiopod *Nisusia*? sp. and the mollusk *Hyolithes* sp. are extremely common on thin, flat surfaces and were found by McKee (1945) at every location examined in the western third of the Grand Canyon. Further

Fig. 14. Boulders of various sizes of the Shinumo Quartzite of the Unkar Group included in the basal section of the Tapeats Sandstone. (a) Huge boulders, with the man for scale, in Ninetyone Mile Canyon (photo: Art Chadwick). (b) Smaller boulders, with hand for scale, in the cliff face of the northern edge of Hance Canyon above river mile 79.

eastward this horizon has not been recognized, presumably because in that direction it is within the cliff-forming coarse sandstone of the lower Tapeats Sandstone in which no body fossils are preserved.

Trace fossils are more abundant in the upper half of the Tapeats Sandstone in finer-grained lithologies, particularly in the uppermost transition interval into the Bright Angel Formation where they are common (Blakey and Middleton 2012; Middleton and Elliot 2003). These include a diverse array of tracks, trails, and burrows, and consist of single and paired vertical tubes, and several types of horizontal traces. Despite this, the ichnofauna in the Tapeats Sandstone has been described in only a few studies (Hereford 1977; McKee 1932, 1945; Resser 1945; Seilacher 1970). However, Hagadorn et al. (2011) reported that their Facies Suite B, the major or cliff-forming section of the Tapeats (fig. 13), contains abundant *Arenicolites* trace fossils and rare *Aulichnites*, *Planolites*, and *Skolithos*, while their Facies Suite C, the so-called "transition zone" with the Bright Angel Formation, contains a diverse assemblage of trace fossils including *Arenicolites*, *Aulichnites*, *Cruziana*, *Diplichnites*, ?*Diplocraterion*, *Monomorphichnus*, *Planolites*, *Rusophycus*, *Skolithos*, *Teichichnus*, and *Treptichnus*.

Single, unbranched, straight vertical cylindrical burrows assigned to the ichnogenus *Skolithos* (Alpert 1974) are common at many localities, generally in the upper few meters to 20 m (66 ft) of the cliff-forming Tapeats Sandstone (Rose 2011) and in the overlying "transition zone" (Hagadorn et al. 2011). These sand-filled burrows tend to occur near the tops of beds of fine-to-medium quartz arenites (Hagadorn et al. 2011). They are visible in cross-section and on bed tops where they are found in high abundance as monotaxic occurrences. McKee (1945, 46, Pl. 8, figs. a, c) described such vertical burrows at or near the top of the transition beds of the Tapeats in the western Grand Canyon, including some that were annulated or ringed up to several inches (~10 cm) in length and ⅜ in (~1 cm) wide. Burrows of this type probably functioned as dwellings and/or temporary resting structures for suspension feeding organisms, such as either annelids (worms) or phoronids (sometimes called marine horseshoe worms) (Alpert 1974; McKee 1945). These abundant occurrences of *Skolithos* in this fine- to coarse-grained sandstone suggests a shallow marine environment characterized by currents capable of active bedload transport (Middleton and Elliott 2003). This is further substantiated by their occurrence also in cross-bedded sandstone. Similar structures are common in many modern nearshore marine settings.

U-shaped burrows perpendicular to bedding also occur in the fine- to coarse-grained Tapeats Sandstone (fig. 15a). These tubes appear as paired holes on bedding planes or as concave-upward scours, where they have been eroded to the base of the burrow (Middleton and Elliott 2003) (fig. 15b). These U-shaped burrows are sparsely present in planar horizons throughout much of the Tapeats Sandstone but are common in the upper part of typical Tapeats sections, where they occur on steep tangential foresets (Rose 2006). On bedding planes where these U-shaped burrows have been eroded to the bottom end of the U-shape they appear as harrowed out "trails" on the rock surface (Hereford 1977; McKee 1945) (fig. 15b). These abundant traces were assigned to the ichnogenus *Corophioides* by Hereford (1977) and to *Arenicolites* and *Diplocraterion* by Rose (2006). Hagadorn et al. (2011) observed that in Grand Canyon their Tapeats Facies Suite B is dominated by *Arenicolites*, these burrows typically occurring in fine-to-granular sandstone, at bed tops of thin-to-massive quartz arenites. Furthermore, such burrows extend from just centimeters (an inch or two) above the basal contact of the unit to the top of the unit and exhibit a similar size range, preservation, degree of truncation abundance, and depth of penetration in the Tapeats throughout the Canyon. These traces probably represent dwelling structures of suspension-feeding organisms that occur in shallow-water marine deposits, such as certain groups of annelids (worms), and are common in many modern nearshore deposits (Middleton and Elliott 2003).

Horizontal traces were first reported in the transition beds of the upper Tapeats Sandstone by Walcott (1918), and then McKee (1932, 1945, 46, Pl 6, Pl. 9, fig. c). These traces he called "fucoides." They are smooth-sided curving horizontal casts several inches (up to 10 cm) in length and up to an inch (2–3 cm) thick that typically occur in large numbers often overlapping one another covering entire bedding surfaces, both in the interbedded thin green shales and thicker fine-grained sandstones (fig. 16). Presumably, they were formed by detritus-ingesting annelids (worms) moving through the sediment (Middleton and Elliott 2003). Rose (2006) reported rare *Treptichnus pedum* in the lowermost Tapeats Sandstone. They are horizontal burrows with a fairly complicated and distinctive pattern. Along a central, sometimes sinuous, or looping burrow there are successive probes upward through the sediment, generating a trace pattern reminiscent of a fan or twisted rope. Vannier et al. (2010) demonstrated that these horizontal trails are likely the result of burrowing priapulid worms along the sediment surface underwater. Hagadorn et al. (2011) observed that these *Treptichnus*, and also *Teichichnus*, traces occur in their Facies Suite C throughout the Canyon on bed soles in convex hyporelief, or on bed tops in convex or concave epirelief, always at interfaces between greenish shales and sandstones (fig. 16).

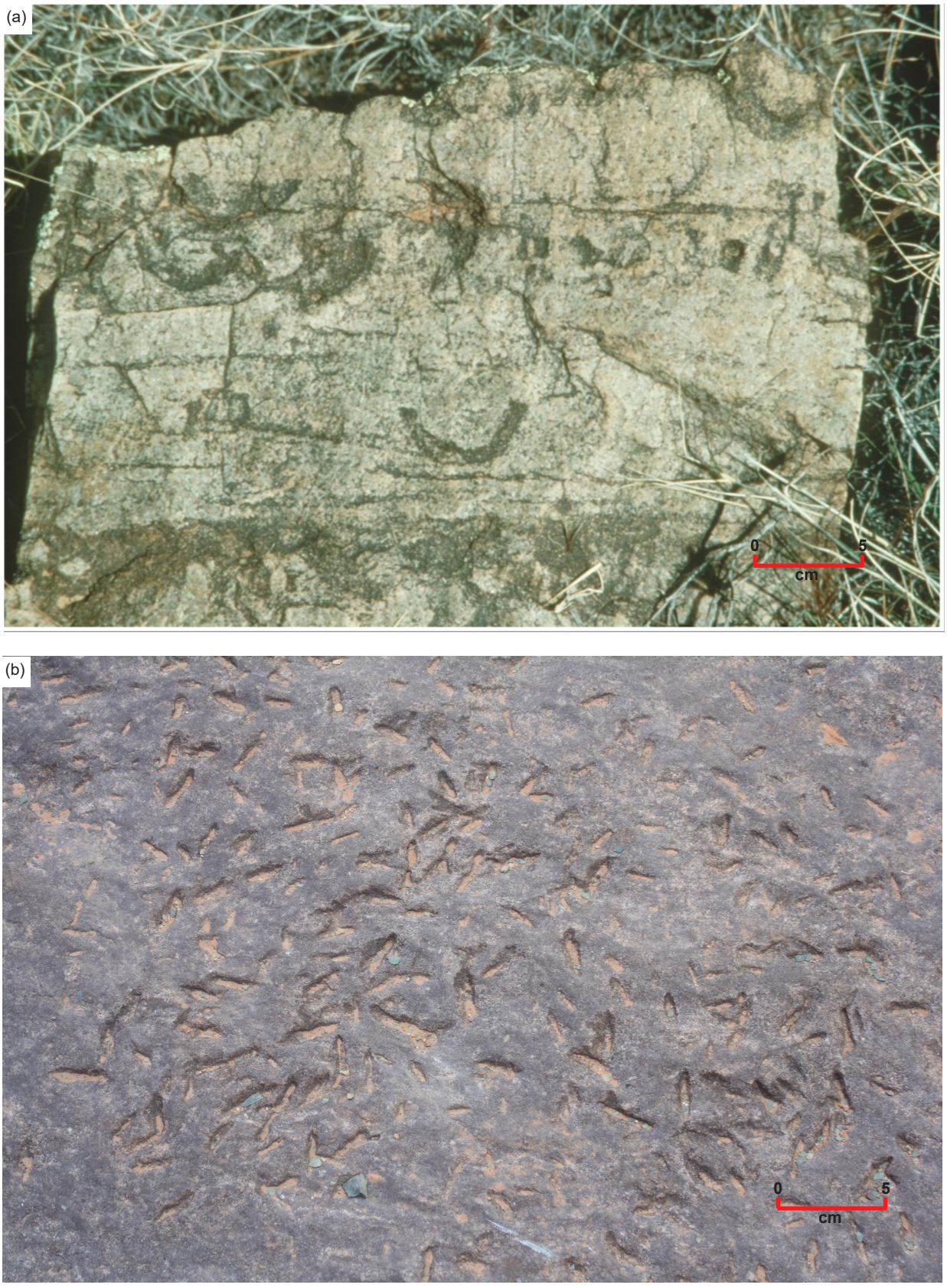

Fig. 15. U-shaped burrows designated as *Arenicolites* perpendicular to the bedding in the Tapeats Sandstone (scale as indicated). (a) Some as seen in cross-section in outcrop at the top of the cliff-forming unit at the edge of Horseshoe Mesa above river mile 80. (b) Many seen eroded to their bases on a bedding plane surface at the top of the cliff-forming unit at "The Patio" above Deer Creek Falls near river mile 137.

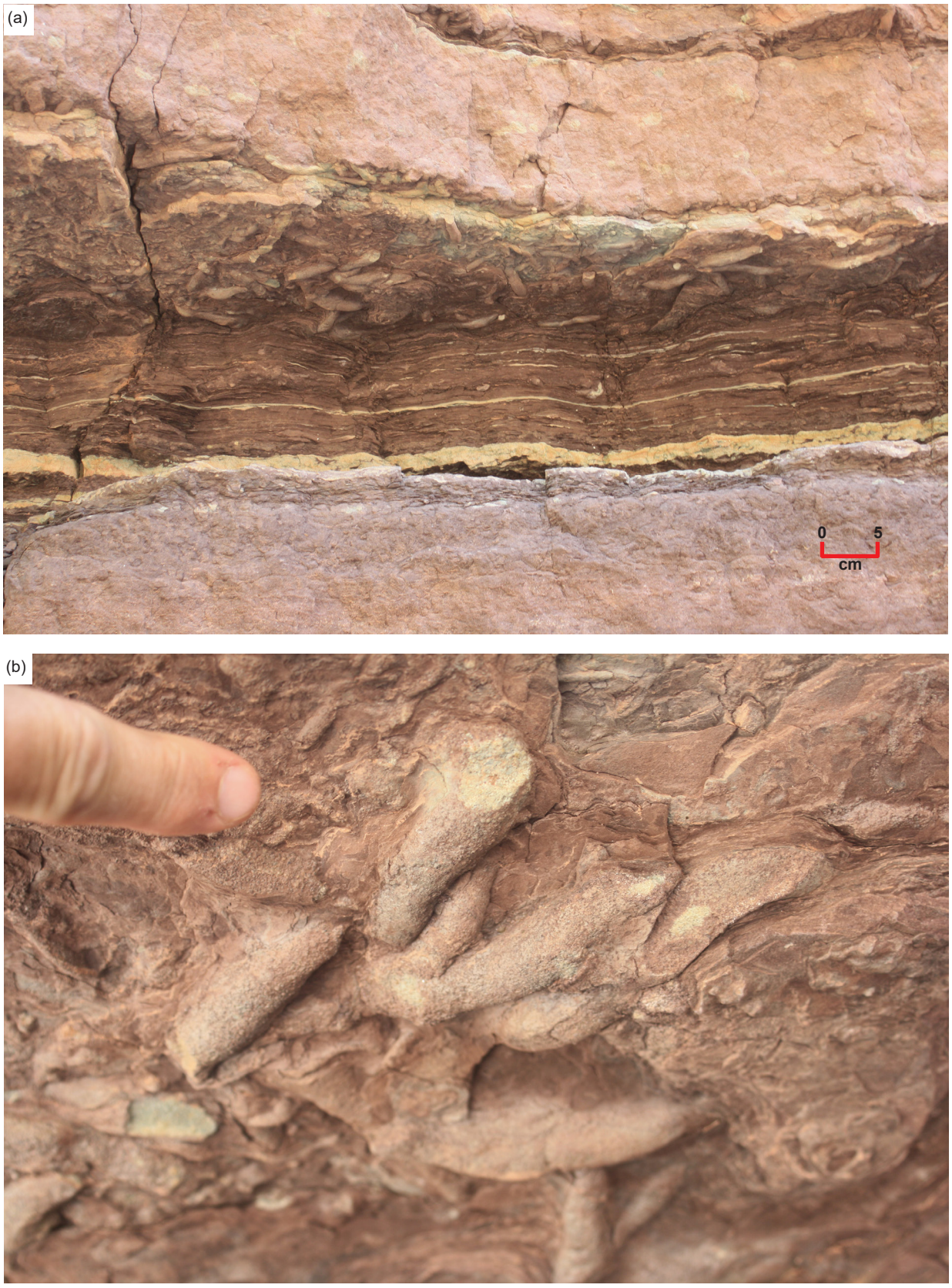

Fig. 16. The horizontal trace fossils called "fucoides" by McKee (1932, 1945) and designated as *Treptichnus* by Rose (2006) and Hagadorn et al. (2011) as found in the transition zone at the top of the Tapeats Sandstone or Facies C, where there are interbedded thin shale and thicker sandstone beds. (a) As seen here at "The Patio" above Deer Creek Falls near river mile 137 (scale as indicated). (b) A closer view of these trace fossils on the sole of the overhanging bed seen in (a) (finger for scale).

Trilobite crawling (*Cruziana*) and resting (*Rusophycus*) traces occur in the Tapeats Sandstone, almost exclusively in the transition interval into the Bright Angel Formation, Facies Suite C (Hagadorn et al. 2011). They were first reported by Walcott (1918) and Gilmore (1928), and then by McKee (1945). Seilacher (1970) provided the first detailed description of *Cruziana arizonensis* traces from the Tapeats Sandstone (fig. 17). They are thought to result from the digging action of the trilobite's underbody claws sweeping aside the sediment surface underneath the trilobite, creating two adjoining parallel lines of scooped-out burrows or double troughs along the mid-line of the trilobite's underside, as illustrated in Seilacher (1970, fig. 7). What is preserved are molds of the infilled troughs of these burrowing trails (fig. 17). Elliott and Martin (1987) suggested that these *Cruziana* traces were formed during fair-weather periods as these arthropods moved across the shelf sediments, whereas the related *Rusophycus* marks formed during storms.

Sedimentary Structures Within the Tapeats Sandstone

McKee (1945) described in some detail the sedimentary structures within the Tapeats Sandstone, in particular what he called the coarse-grained sandstone facies. That dominant facies constitutes the principal part of the Tapeats Sandstone due to its lateral distribution and vertical extent. This is the same major cliff-forming, non-bioturbated, lower unit described by Rose (2006), Facies Suite B of Hagadorn et al. (2011) (figs. 10–13). Bedding is very clearly developed in it because in most places it is conspicuous due to erosion accentuating the parting planes (fig. 12). Furthermore, contrasts in the degree of cementation within beds locally has caused them to weather into alternations of resistant ledges and shallow recesses (fig. 12). Most of these beds are 1–3 ft (0.3–1.0 m) thick and show prominent cross-lamination etched out on their faces (fig. 11). Gritty sand forming individual thin layers and laminae stands out in relief on weathered surfaces.

The Tapeats Sandstone is characteristically cross-laminated, with lamination structures that are extremely variable in detail but similar in general type. McKee (1945) grouped them into three main classes, differing more in degree than in manner of development. His class #1 is composed of small-scale scour-and-fill structures (fig. 18d, e, h), which have been developed most commonly where the sandstone flanks Precambrian hills or monadnocks of the hard Unkar Group Shinumo Quartzite. In his class #2 the cross-laminations are similar in form, but are on a larger scale, with wider and fewer channels. They are found chiefly at short distances from the bases of the Precambrian monadnocks (fig. 18b, g, i). His class #3 comprises a type of cross-lamination common throughout the Tapeats Sandstone, especially characteristic of the sandstone well away from those monadnocks. It consists of extensive, uninterrupted series of laminae dipping in one direction (figs. 11 and 18c, f, j).

McKee (1945) found that his three classes of lamination structures do not appear so distinctive as they are frequently observed only in two dimensions. He described two typical cases in three dimensions (fig. 19). In his section cut parallel to a trough of a small channel (fig. 19a), the pattern of cross-laminations resembles any section of corresponding extent cut through the more extensive succession of laminae (fig. 19b). McKee (1945) maintained that a transition in form is represented by this cross-lamination. It ranges between the extremes found in cut-and-fill channels where the depositional currents were confined and concentrated on the one hand, and in broad, gentle depressions filled under comparatively stable or constant conditions of deposition on the other. The breadth and length of these channels and the numbers of scours involved appeared to McKee (1945) to be the principal factors responsible for the final sedimentary pattern developed within any particular bed.

McKee (1940) reported the results of a preliminary statistical study of the cross-laminations in the Tapeats Sandstone. He recorded the dip angle and direction of about 30 sloping lamination surfaces selected at random at each of thirteen localities and plotted the individual readings on polar coordinates for each location (for example, six locations in fig. 20). From the 400 dip measurements at the thirteen locations, he estimated that the majority of the sloping laminations or foreset planes dip at between 20° and 25°, with the maximum dips being 27° or 28°. He also found that the sloping foreset planes or laminae in general are very uniform in character, but they vary in length according to the thickness of the bed containing them, rarely exceeding 3–4 ft (~1 m) and in places being only a few inches (5–10 cm). When his 183 dip measurements at the six locations plotted in fig. 20 were tabulated in dip angle ranges, the resulting histogram in fig. 21 demonstrated that almost 67% of the dip angles were in the 16°–25° range, with a median dip angle of 21°–22°. This is consistent with strong water currents depositing the sands (discussed below). Furthermore, McKee (1945) determined that the average direction of the dip slopes of the laminations or foreset planes, based on more than 540 readings (about 30 readings at eighteen locations), is between west and southwest, indicating there was a dominant current movement from east-northeast to west-southwest across the

Fig. 17. Trilobite crawling *Cruziana arizonensis* (Seilacher 1970) traces, as seen on an upturned fallen block of Tapeats Sandstone from the transition interval or Facies C at "The Patio" above Deer Creek Falls near river mile 137 (scale as indicated).

area during the period of the Tapeats coarse-sand deposition. This paleocurrent direction fits the continental-scale paleocurrent current direction documented by Brand, Wang, and Chadwick (2015)

Rose (2011) described the internal architecture at meter-scale of the cliff-forming part of the Tapeats Sandstone as a distinctively lumpy "pancake layering" of multi-storied amalgamated channels. Tangential cross-beds are common within individual layers, and *en-echelon* cross-beds can extend laterally for tens of meters, frequently terminating in a lens-shaped channel. Foresets dipping in the opposite direction may resume on the other side of channels and extend for additional tens of meters. Some of these apparent channels are isolated and large, up to 3–5 m (10–16 ft) in height, indicating to Rose (2011) active stream avulsion, and fine-grained inter-channel deposits are widely interspersed between channel-bound sandstone layers. The foreset dips indicate a polydisperse water flow direction with a northerly component of flow in the lower part and a southwesterly component of flow in the upper part of the Tapeats Sandstone. The southwesterly component is consistent with the southwesterly paleocurrent directions McKee (1940) measured in the Tapeats, and with the dominant southwesterly paleocurrent orientations of lithesome equivalents to the west, including the Wood Canyon Formation and the Zabriskie Quartzite (Fedo and Prave 1991). The northerly paleocurrent trend in the lower Tapeats may be a deflection of the regional flow by the northwest-southeast paleotopographic ridge of Proterozoic Shinumo Quartzite which partitioned the depositional landscape into two sub-basins that roughly correspond to the separation of the eastern and western exposures of the Tapeats Sandstone (Rose 2003, 2011). That initial northerly deflection of the regionally dominant southwesterly flow makes sense because it would have become less prominent as that barrier became buried and breeched.

Rose (2006, 2011) also claimed that in the upper portion of the Tapeats and in the "transition zone" are what he interpreted as desiccation cracks and aeolian dunes. Rose (2006) and Hagedorn et al. (2011) also identified ripple marks with these interpreted desiccation (mud) cracks in the thin fine-grained sandstone to siltstone beds within the upper Tapeats Sandstone. Hill and Moshier (2009, 2016) also reported ripple marks and supposed mud cracks in the Tapeats Sandstone and documented them with photographs. And according to Hill and Moshier (2009) supposed fossilized raindrop prints have been

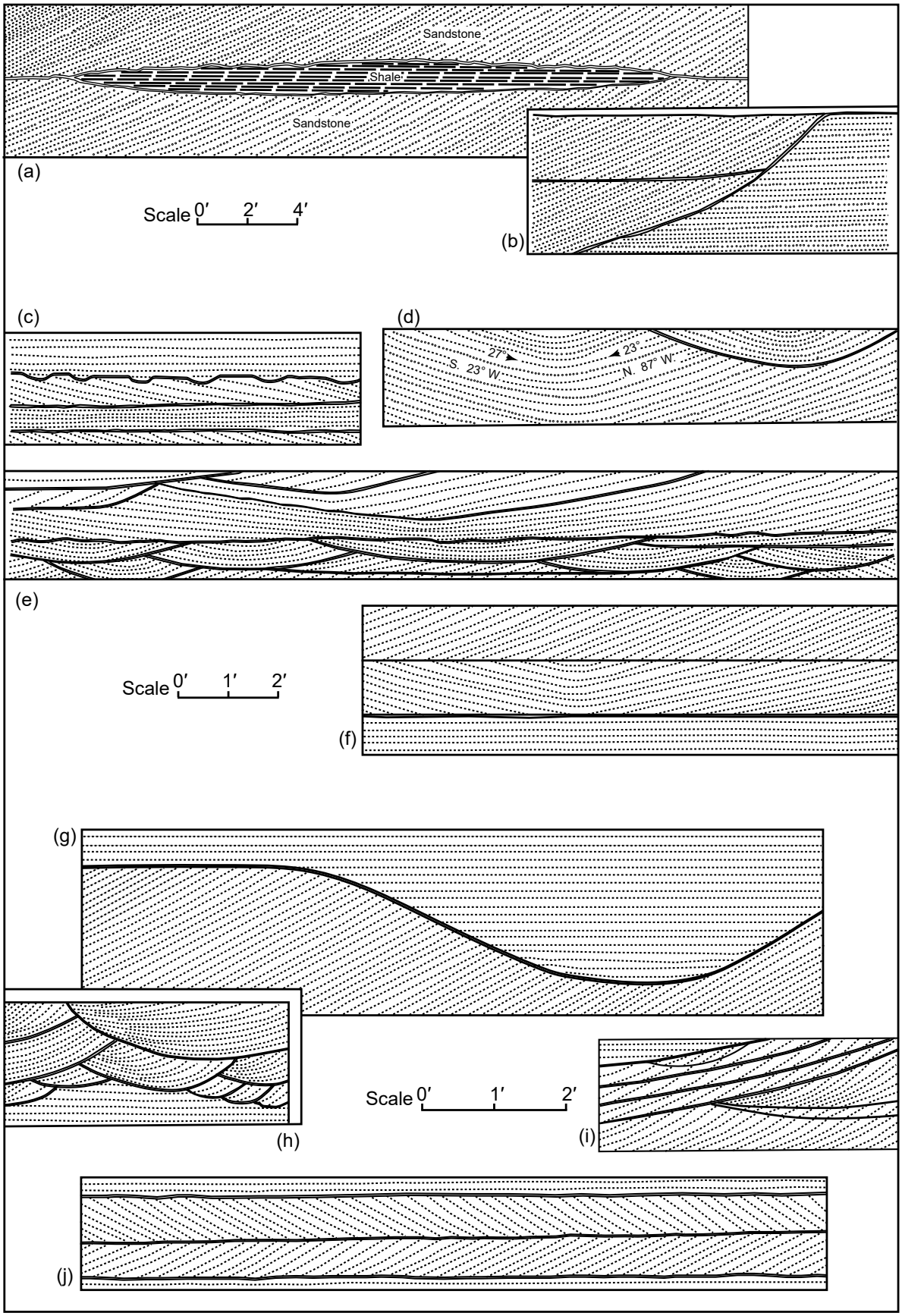

Fig. 18. Lamination patterns in the Tapeats Sandstone beds as depicted by McKee (1945, 44, fig.5). (a) 120 Mile Rapids, (b) Colorado River mile 214.5, (c) Colorado River mile 214.5, (d) East fork, Pipe Creek, (e) East of Pipe Creek, (f) 127 Mile Rapids, (g) 213 Mile Canyon, (h) Near Yaki trail, (i) West fork, Pipe Creek, and (j) 215 Mile Rapids.

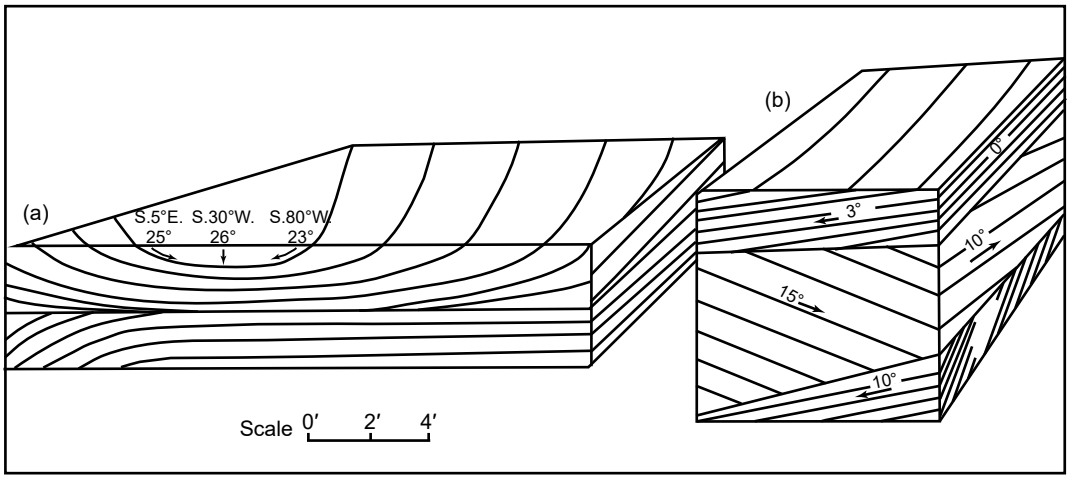

Fig. 19. Types of cross-lamination in the Tapeats Sandstone shown in three dimensions, as depicted by McKee (1945, 44, fig.6). (a) Base on monadnock, Cremation Creek. (b) Middle of formation, Colorado River mile 214.5.

reported as occurring in the Tapeats Sandstone, but they provided no documentation to support that claim.

Conventional Age of the Tapeats Sandstone

The body fossils found within the transition zone of the Tapeats Sandstone with the overlying Bright Angel Formation establish a conventional late Early Cambrian age for the upper parts of the Tapeats Sandstone in the Grand Wash Cliffs at the western end of the canyon and an early Middle Cambrian age for the formation in the eastern canyon (Middleton and Elliott 2003). These ages are based on trilobite assemblages (*Ollenellus-Antagmus*) in the overlying Bright Angel Formation (McKee 1945) (fig. 5). This supposed diachroneity is claimed to be due to the west-to-east sense of the depositional strandline migration.

Naeser et al. (1989) fission-track dated a suite of zircon grains separated from a green bentonite horizon (a former volcanic ash or tuff bed) in the Tapeats Sandstone at river mile 205.7, river right, facing downstream (Billingsley and Elston 1989). This bentonite horizon is in the upper part of the massive sandstone unit of the Tapeats, closely overlain by the early Middle Cambrian *Olenellus* horizon, which is overlain by a slope-forming interval containing shale and sandstone of Tapeats lithology, and then by the cliff-forming sandstone of Tapeats lithology called the "red-brown sandstone" that transitions in the slope above into overlying Bright Angel Formation (figs. 5 and 6a). This bentonite horizon appeared to McKee (1945) to correlate with the *Zacanthoides cf. walpai* horizon in the Toroweap section to the east (see fig. 5 and 6a), which he considered to be of early Middle Cambrian age. Naesar et al. (1989) determined a fission-track age of 563 ± 49Ma [2σ] for twelve zircon grains from this prominent green tuff bed.

Snelling (2005b) sampled the same green tuff horizon in the Tapeats Sandstone and had zircons grains separated from it for fission-track dating. Some typical Tapeats zircons and the fission tracks in them are shown in fig. 22. Because these zircon grains showed a sufficiently large range of U contents and there were enough grains with spontaneous track densities suitable for track counting (10.31×10^6 tracks per cm^2), the reported fission-track age determinations were regarded as extremely reliable. These zircon grains were characterized by a central age of 127.4 ± 30.5Ma. However, the individual zircon grains had fission-track ages from 12.3 ± 1.2Ma to 914.3 ± 414.8Ma, so the numerical value of the central age had no significance. A statistical analysis of the remaining single-grain fission-track ages suggested the presence of three prominent populations characterized by ages of 75 ± 7Ma, 158 ± 15Ma, and 408 ± 35Ma (fig. 23). It was suggested that the discrepancy between these fission-track ages and that determined by Naesar et al. (1989) could be the differences in the etching conditions used in the respective laboratories, the laboratory used by Snelling (2005b) only using a short etching time, whereas Naeser et al. (1989) already knew the target age and etched their grains longer and chose only the fission-track ages that matched the target age. Of interest though was the variety of grain morphologies present in both samples, from euhedral to rounded as well as intermediate forms.

Snelling (2005b) also reported U-Th-Pb radioisotope determinations on zircon grains from the same Tapeats tuff sample. Six grains were chemically abraded in order to totally eliminate any discordance caused by Pb loss, and isotopic analyses were performed by a thermal ionization mass spectrometer (TIMS). Three grains (z1, z6, and z7 in fig. 24) yielded concordant ages of 86.2 ±

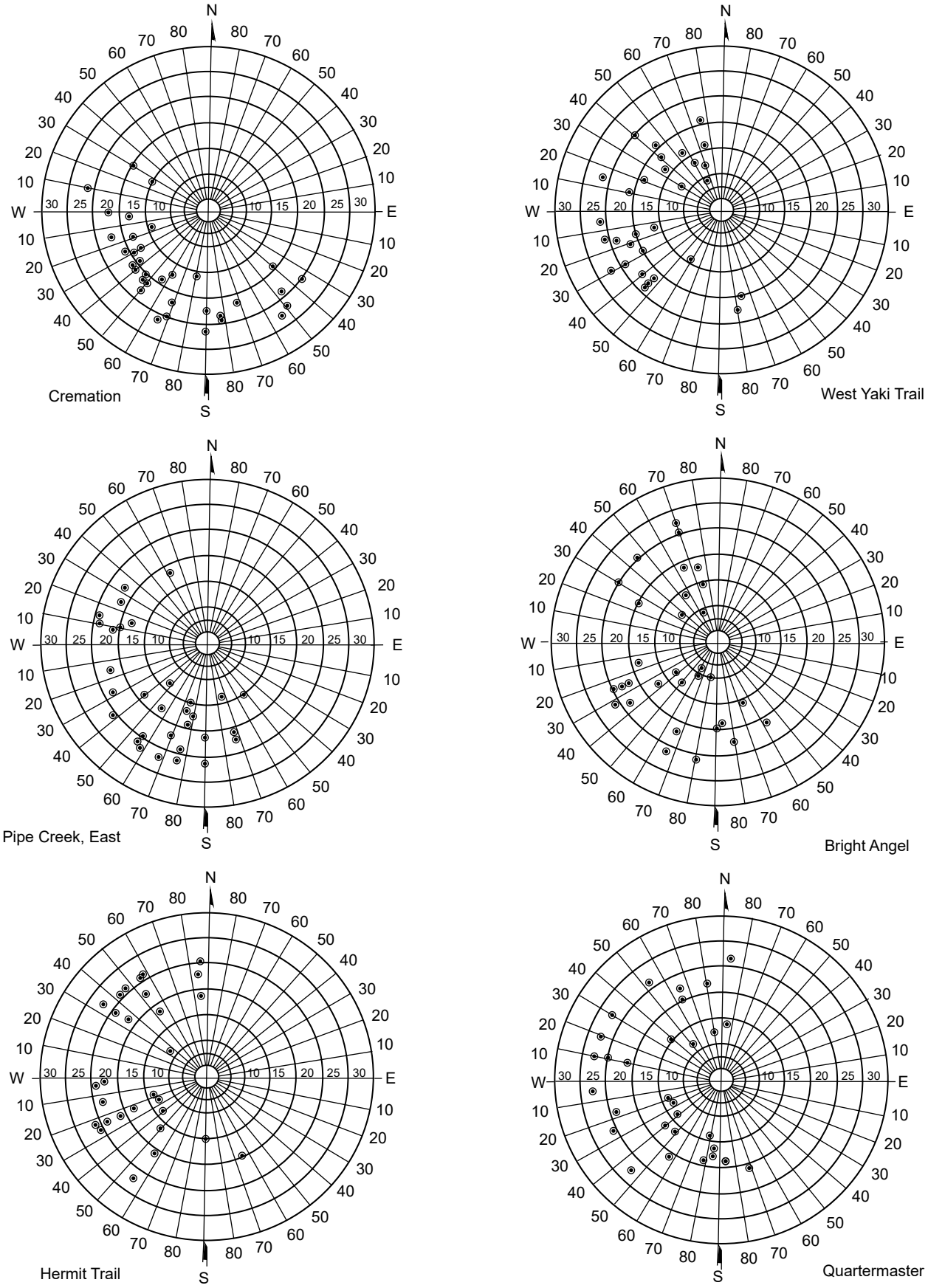

Fig. 20. Plots of dip measurements of typical samples of Tapeats Sandstone cross-laminations from six locations (McKee 1940, 813, fig.1).

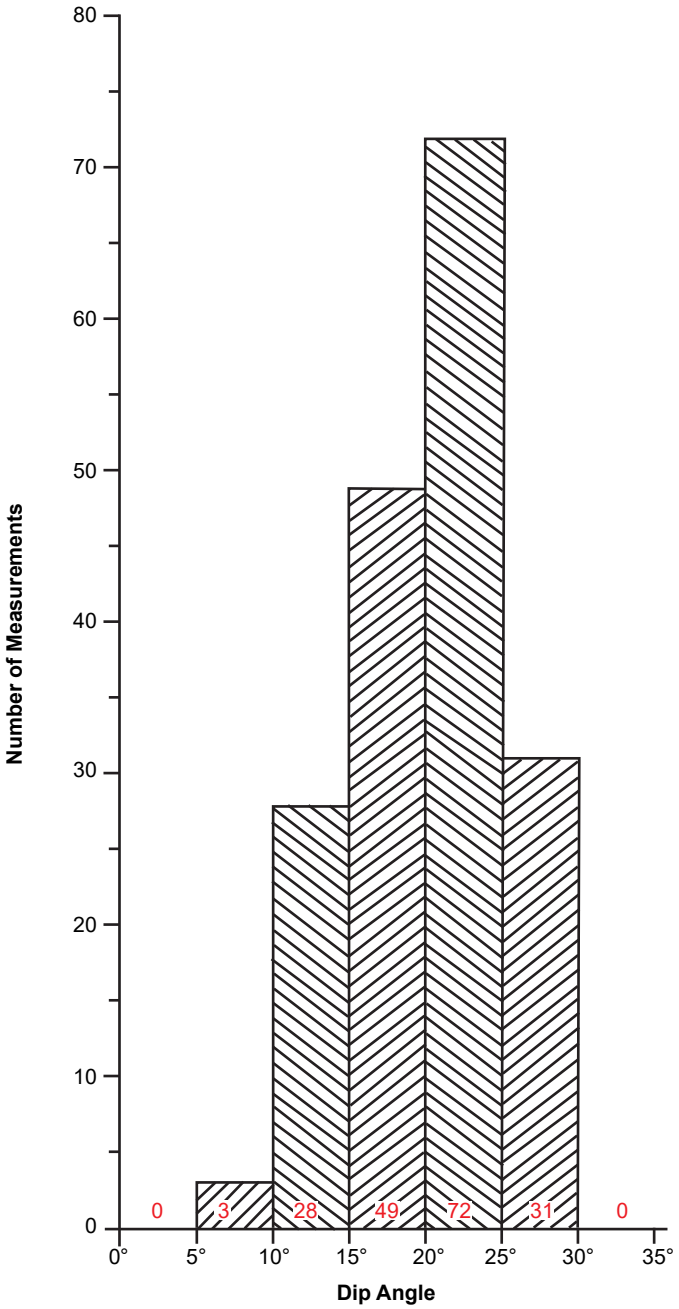

Fig. 21. Histogram of dip measurements derived by tabulating 183 dip measurements made by McKee (1940) at six locations, as per fig.20.

0.3Ma, 98.2 ± 1.3Ma, and 90.1 ± 0.2Ma (2σ errors) respectively, while the three other grains (z2, z4, and z5 in fig. 24) yielded older essentially concordant ages of approximately 319Ma, 1681Ma, and 1662Ma respectively. Otherwise, the individual grain model ages ranged from a $^{207}Pb/^{206}Pb$ age of 73.2Ma for grain z6 to a $^{206}Pb/^{238}U$ age of 1682.0Ma for grain z4. On a $^{206}Pb/^{207}Pb$ diagram two isochrons were plotted from selected data, one corresponding to an age of 437 ± 100Ma (2σ errors) and the other corresponding to an age of 1774 ± 200Ma. The oldest ages were consistent with zircon U-Pb ages of the granitic basement rocks in the western Grand Canyon (Karlstrom et al. 2003), which suggests that this tuff has a very small component of contamination by older igneous material.

Matthews, Guest, and Madronich (2018) analyzed samples of the Tapeats Sandstone from East Verde River, central Arizona and Frenchman Mountain, southern Nevada and found they contained abundant middle Cambrian detrital zircons. Eight measurements from the central Arizona sample and seven measurements from the southern Nevada sample yielded concordant $^{206}Pb/^{238}U$ ages of 502.8 ± 8.1Ma and 504.8 ± 8.2Ma, respectively (2σ including all sources of random and systematic uncertainty).

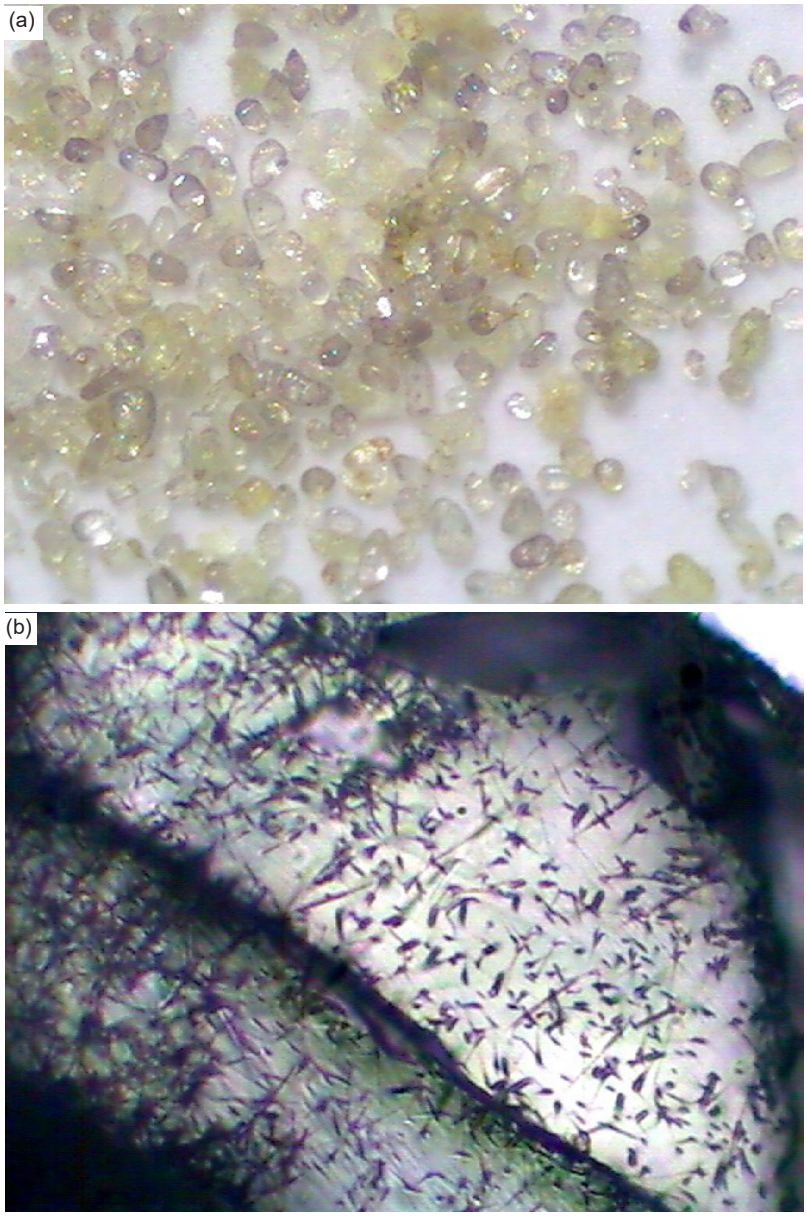

Fig. 22. Fission-track dating of a thin green tuff bed in the upper Tapeats Sandstone samples at river mile 205.7. (a) Zircon grains extracted from the tuff bed as seen under a binocular microscope (from Snelling, 2005b, 234, fig.9). (b) The spontaneous fission tracks in the polished and etched surface of a mounted zircon grain under high magnification (from Snelling, 2005b, 236, fig.10).

Similarly, Karlstrom et al. (2018) U-Pb dated zircon grains from three Tapeats Sandstone samples, two of the three being from those same locations sampled by Matthews, Guest, and Madronich (2018). The youngest zircon grains in a coarse sandstone sample from 2m (6.6ft) above the base of the Tapeats Sandstone in Hermit Creek in the Grand Canyon yielded a weighted mean LA-ICP-MS (laser-ablation–inductively coupled plasma–mass spectrometry) maximum age of 505.4 ± 8.0Ma (n=12). The youngest zircon grain population in a sample from the coarse-grained cross-bedded sandstone 30m (98ft) above the base of the unit in the westernmost limit of Tapeats exposures at Frenchman Mountain near Las Vegas, Nevada, yielded an age of 504.7 ± 2.1Ma (n=28). And the youngest grains in a sample from the coarse-grained, pebbly cross-bedded sandstone ~19m (62ft) above the unconformity with the granitic basement at the southeastern limit of Tapeats exposures along the East Verde River in central Arizona yielded a weighted mean maximum depositional age of 501.4 ± 3.8Ma (n=19).

In interpreting all these ages, Karlstrom et al. (2018) noted that the Tapeats and Bright Angel sections of western Grand Canyon that contain '*Olenellus* Zone' trilobites are thus probably older than 509Ma (Peng, Babcock, and Cooper 2012). Yet these western Grand Canyon and Lake Mead region trilobites correspond to the upper half of Stage 4 of Cambrian

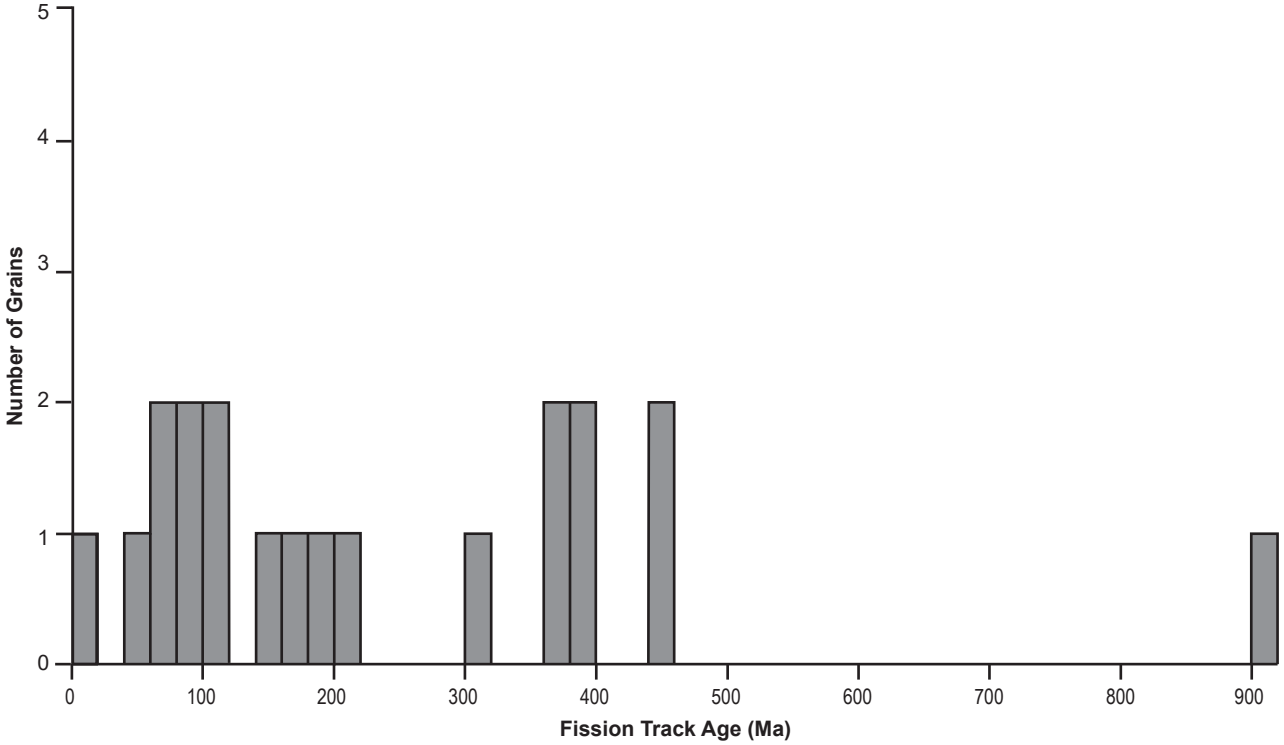

Fig. 23. Histogram of the individual zircon grain fission-track ages in a sample from the thin tuff bed in the upper Tapeats Sandstone at river mile 205.7 (from Snelling, 2005b, 243, fig.13c).

Series 2 (Sundberg 2011), whereas *Glossopleura walcotti* Zone trilobites of the overlying Bright Angel Formation in eastern Grand Canyon (Foster 2011) correlate with Stage 5 of Cambrian Series 3. While a numerical age for the boundary between Cambrian Stages 4 and 5 has not yet been firmly established by the International Union of Geological Sciences, the International Commission on Stratigraphy (2020) has designated an age of ~509Ma. Furthermore, the ages of fossils from these successions have been constrained by correlation of North American trilobite zones to trilobite provinces from other continents and by integrating recalibrated ages of Stages 3–5 ashes globally (Schmitz 2012) with revised fossil zonation (Sundberg et al. 2016) and chemostratigraphic and magnetostratigraphic correlation (Peng, Babcock, and Cooper 2012). Similarly, the *Peachella iddingsi* to *Bolbolenellus euparyia* Zone trilobites from upper Tapeats exposures near Las Vegas are probably 508.1–503.8Ma. Thus, it can be concluded that conventionally the Tapeats Sandstone must have been deposited between 510Ma and 500Ma, with younging of the formation from west to east.

Finally, Karlstrom et al. (2020) tandem U-Pb dated detrital zircons from the same samples of the Tapeats Sandstone and the locally underlying Sixtymile Formation (in the eastern Grand Canyon) as used in the Karlstrom et al. (2018) study. That involved both LA-ICP-MS analyses followed by CA-ID-TIMS (chemical abrasion–isotope dilution–thermal ionization mass spectrometry) analyses of the youngest grains plucked from the LA-ICP-MS epoxy mounts in order to obtain precise maximum depositional ages for those two units based on the youngest zircon grains. For the Tapeats Sandstone the resultant depositional ages were ≤508.19 ± 0.39Ma in the eastern Grand Canyon, ≤507.68 ± 0.36Ma in Nevada, and ≤506.64 ± 0.32Ma in central Arizona. And because the locally conformable underlying Sixtymile Formation had a similar maximum depositional age of ≤508.6 ± 0.8Ma they added it to the Tonto Group, as well as adding the Frenchman Mountain Dolostone, which conformably overlies the Muav Formation (fig. 25). They then combined these depositional ages with the biostratigraphy of trilobite biozones in the Tonto Group based on available precisely-dated regional and global sections (Schmitz 2012; Sundberg et al. 2016, 2020), tied to U-Pb zircon dated Cambrian marker beds elsewhere (Landing et al. 2015; Peng, Babcock, and Cooper 2012), to conclude that the Tapeats Sandstone is ~507–508Ma.

Karlstrom et al. (2020) also confirmed that the long-proposed time transgressive nature of the Tonto Group is supported because the trilobite *Olenellus* is found in the western, but not the eastern, Grand Canyon (fig. 25). Since they determined that the Bright Angel Formation which contains the *Olenellus*, *Glossopleura* and *Ehmaniella* biozones is ~502–507Ma, the conventional timeframe for

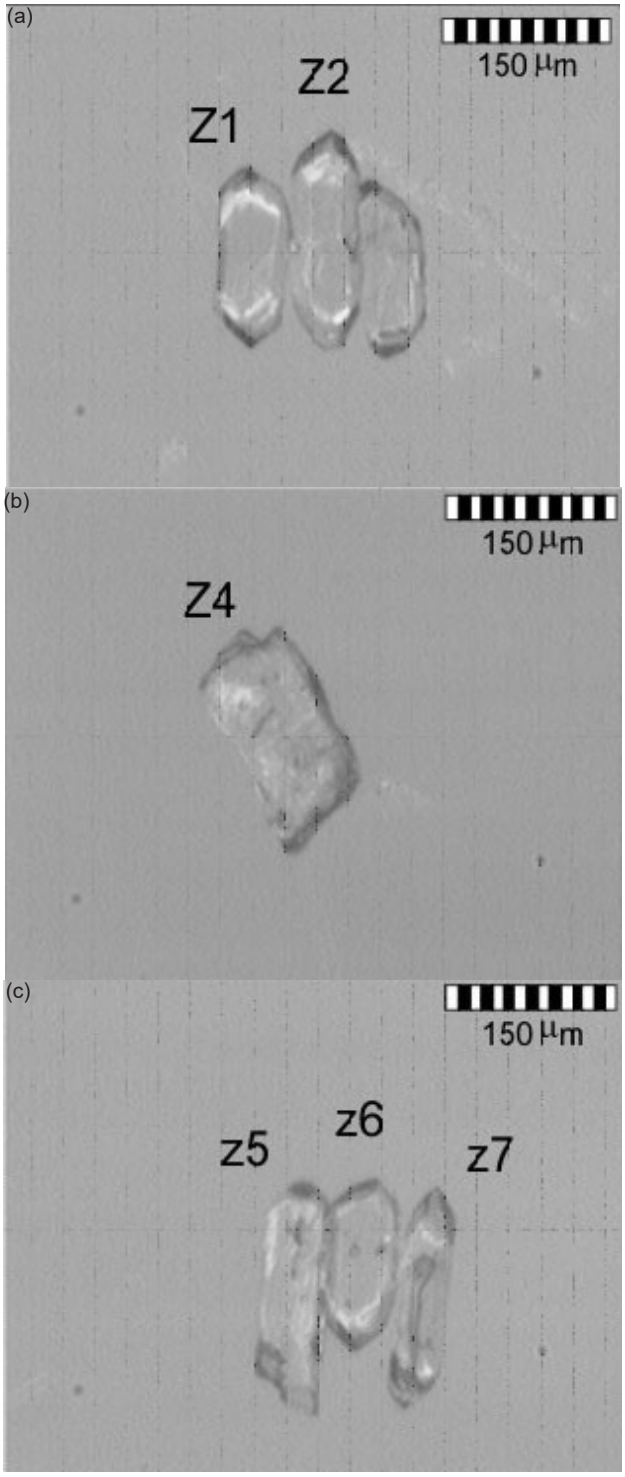

Fig. 24. Seven zircon grains from the thin tuff bed in the upper Tapeats Sandstone at river mile 205.7 after being chemically abraded before of six them were U-Pb dated (from Snelling, 2005b, 270, fig.19).

deposition of the initial sheet Tapeats sands and Bright Angel muds of the Tonto Group transgression likely took place in less than ~4Ma (~504–508Ma) rather than the 40–60Ma proposed by McKee (1945) and Resser (1945).

Provenance of the Tapeats Sandstone

Several recent studies have U-Pb dated detrital zircons recovered from the Tapeats Sandstone to determine the provenance of the sand.

Gehrels et al. (2011) analyzed two samples from the Tapeats Sandstone, one from 2m (6.6ft) above the base of the formation in Hermit Creek near Phantom Ranch, and one from near the top of the formation opposite the confluence of the Little Colorado River. Their lower Tapeats Sandstone sample was coarse-grained and feldspathic, with pebbles of schist and granite, whereas their upper Tapeats sample consisted of well-sorted, medium-grained, quartz-rich sandstone. Zircons in both samples were mainly colorless to light pinkish, with low degrees of rounding and sphericity. Grain size was variable, with zircons up to ~250µm in length in the lower unit but only up to ~150µm in length in the upper unit.

Their two Tapeats samples yielded very similar age distributions. To Gehrels et al. (2011) this was somewhat surprising given that the lower sample was from part of the basal conglomerate, resting directly on the Precambrian crystalline basement, whereas it has been postulated the upper part of the unit formed in a more integrated tidal flats drainage system (see below). These very similar U-Pb age distributions consisted of two main age groups of ~1.45Ga and ~1.70–1.75Ga (age peaks of 1455Ma and 1711Ma for the lower Tapeats sample and 1450Ma and 1736Ma for the upper Tapeats sample). That means the zircon grains in these Tapeats samples are very similar to conventional ages of crystalline basement

Fig. 25 (page 193). Diagrammatic cross-section of the Tonto Group redefining it across Arizona and through the Grand Canyon, from Karlstrom et al. (2020, 428, fig.3) but modified from McKee (1945, 14, fig.1). The vertical scale is time and the red scale bars show approximate thicknesses at each margin of the cross-section. The biochronology shown to the left is their working hypothesis, that could be refined with additional precise U-Pb detrital zircon (DZ) bracketing dates. The lower Tonto Group is in the subsurface in the central part of the transect, making correlations tentative. The sub–Tonto Group angular Great Unconformity has a variety of different-age Precambrian rocks beneath it, and hence a variable hiatus. Above the unconformity in the eastern part of the transect, islands (monadnocks) of tilted Unkar Group strata (resistant Shinumo Sandstone) created up to 200m (~656ft) of relief and were only covered by the Bright Angel Formation. Tonto Group biozones mentioned are: OL—*Olenellus*; Pd—*Poliela denticulata*; M—*Mexicella mexicana*; G—*Glossopleura walcotti*; Eh—*Ehmaniella*; Bo—*Bolaspidella*; Ce—*Cedaria*; Cr—*Crepicephalus*. GSSP—global stratotype section and point; CA-IDTIMS—chemical abrasion–isotope dilution thermal ionization mass spectrometry; LAD—last appearance datum; Terr.—Terreneuvian; Delam.—Delamaran; and Top.—Topazan.

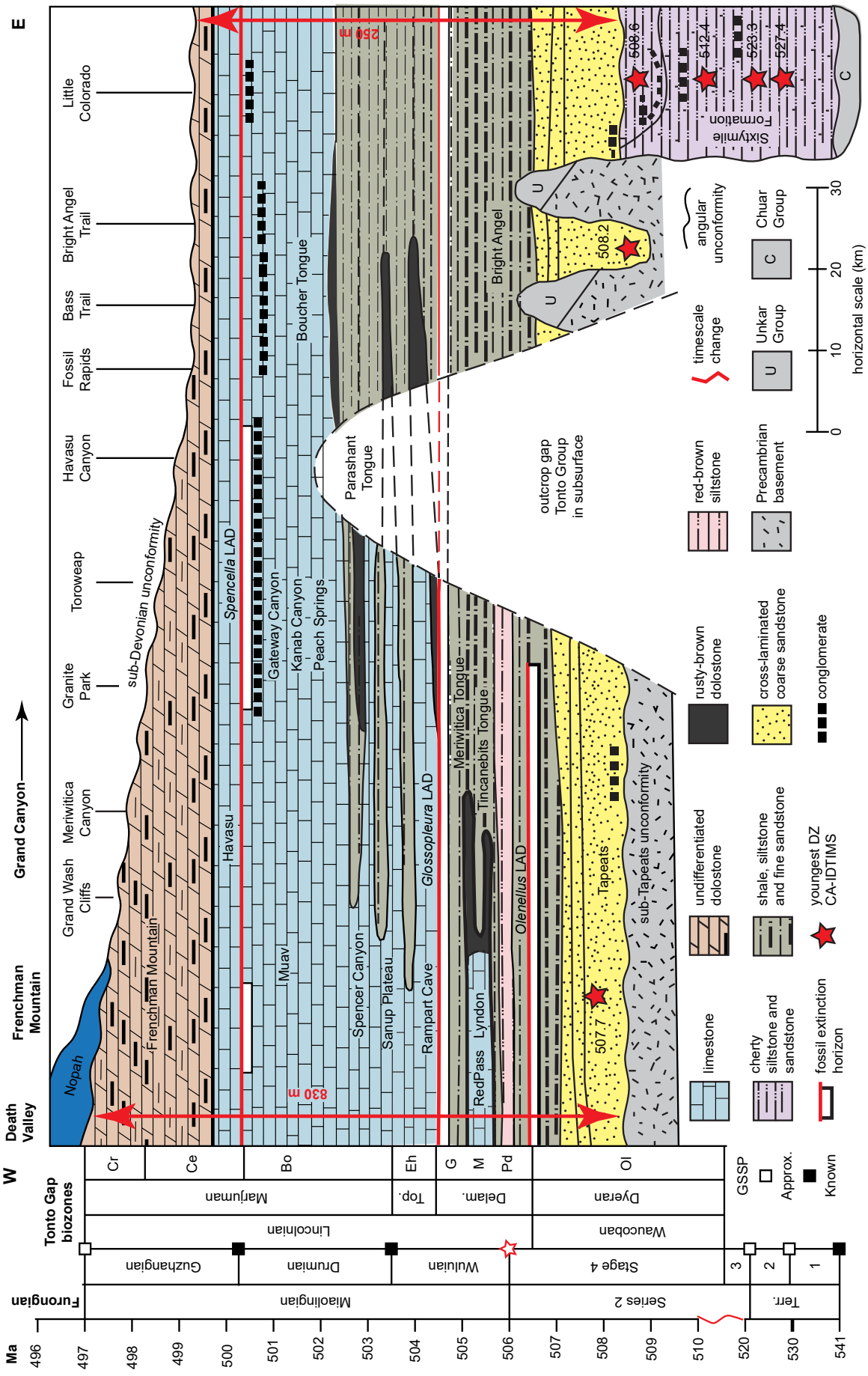
W
E
Death Valley
Frenchman Mountain
Grand Canyon
Grand Wash Cliffs
Meriwitica Canyon
Granite Park
Toroweap
Havasu Canyon
Fossil Rapids
Bass Trail
Bright Angel Trail
Little Colorado
sub-Devonian unconformity
Nopah
Frenchman Mountain
Havasu
Muav
Spencer Canyon
Sanup Plateau
Rampart Cave
Glossopleura LAD
Spencella LAD
Gateway Canyon
Kanab Canyon
Peach Springs
Boucher Tongue
Parashant Tongue
Meriwitica Tongue
Tincanebits Tongue
RedPass
Lyndon
Olenellus LAD
Tapeats
sub-Tapeats unconformity
Bright Angel
Sixtymile Formation
outcrop gap Tonto Group in subsurface
830 m
250 m
507.7
508.2
508.6
512.4
523.3
527.4
U
C
limestone
cherty siltstone and sandstone
fossil extinction horizon
undifferentiated dolostone
shale, siltstone and fine sandstone
youngest DZ CA-IDTIMS
rusty-brown dolostone
cross-laminated coarse sandstone
conglomerate
red-brown siltstone
Precambrian basement
angular unconformity
timescale change
Unkar Group
Chuar Group
horizontal scale (km)
0
10
20
30
Tonto Gap biozones
Cr
Ce
Bo
Eh
G
M
Pd
Ol
Marjuman
Top.
Delam.
Dyeran
Lincolnian
Waucobian
Guzhangian
Drumian
Wuliuan
Stage 4
3
2
1
GSSP
Approx.
Known
Furongian
Miaolingian
Series 2
Terr.
Ma
496
497
498
499
500
501
502
503
504
505
506
507
508
509
510
520
530
541

rocks throughout the southwestern United States, with dominantly Paleoproterozoic grains (peak age=1728Ma; n=102) and a lower proportion of 1.4–1.5Ga grains (peak age=1452Ma; n=65). In fact, Gehrels et al. (2011) concluded that 69% of the Paleoproterozoic grains had been shed from the local 1.68–1.80Ga (Yavapai) province, with 31% derived from the local 1.60–1.72Ga (Mazatzal) province, both provinces being local to the Grand Canyon region (Karlstrom et al., 2003). There were also a few Grenville-age (1.0–1.2Ga) grains, with an age peak at 1064Ma (n=8). These grains were presumably shed from the Grenville orogen further to the south and/or east.

Gehrels et al. (2011) also compared these Tapeats Sandstone detrital zircon ages with the detrital ages of zircons in Proterozoic strata of the locally underlying Grand Canyon Supergroup (Unkar and Chuar Groups) and found that little detritus was recycled from those underlying units. They concluded that these relationships supported the facies and paleocurrent patterns reported by McKee (1945) and summarized by Middleton and Elliott (2003). A major source of the sand for the Tapeats Sandstone was thus derived locally from the Paleoproterozoic crystalline basement exposed along the western flank of the Transcontinental Arch, to the east of Grand Canyon, with the sediment accumulating in a transgressional setting on a west-facing shelf, with deposition grading eastward from subtidal to intertidal to beach and eventually fluvial environments (see below).

As part of their study of detrital zircons from latest Neoproterozoic to middle Cambrian sandstones of western North America, Matthews, Guest, and Madronich (2018) collected two Tapeats Sandstone samples, one from Frenchman Mountain, Nevada and the other from East Verde River, Arizona for U-Pb dating. They added to their study the results of U-Pb dating of detrital zircons obtained by Gehrels et al. (2011) from the two Tapeats Sandstone samples collected in the Grand Canyon. Matthews, Guest, and Madronich (2018) concurred with Gehrels et al. (2011) that the detrital zircons in their two Tapeats samples from the Grand Canyon were derived from relatively local crystalline sources within the Paleoproterozoic Yavapai (1.68–1.8Ga) and Mazatzal (1.60–1.72Ga) provinces. The lack of Archean and >1.8Ga zircons in all the Tapeats Sandstone samples suggested that little sand detritus was derived from the Wyoming craton to the north, consistent with paleoflow measurements that indicate transport was dominantly from the east to the west (Brand, Wang, and Chadwick 2015; Stewart et al. 2001). Furthermore, the two Tapeats samples from southern Nevada and central Arizona (105 zircon grains U-Pb dated in each) were dominated by younger Paleoproterozoic ages (mode <1.7Ga), reflecting increased input of detritus from the nearby Mazatzal province relative to the two Gehrels et al. (2011) Grand Canyon samples. And as already reported above, the two Matthews, Guest, and Madronich (2018) samples also contained abundant middle Cambrian detrital zircons.

Similarly, as reported above, Karlstrom et al. (2018) collected their own three samples, the first from the coarse sandstone 2m (6.6ft) above the base of the Tapeats Sandstone in Hermit Creek, eastern Grand Canyon, the second from a coarse-grained cross-bedded quartzite 30m (98ft) above the base of the unit from the westernmost limit of Tapeats exposures at Frenchman Mountain near Las Vegas, Nevada, and the third from a coarse-grained, pebbly cross-bedded sandstone ~19m (62ft) above the unconformity with granitic basement from the southeastern limit of Tapeats exposures along the East Verde River in central Arizona. The Grand Canyon sample had zircons with U-Pb modes at 1,680Ma and 1,412Ma (430 out of 453 grains), the detrital zircon spectrum of the Nevada sample contained prominent U-Pb modes at 1,692Ma and 1,444Ma, and smaller modes at 1,239Ma and 1,078Ma (703 out of 764 grains), and the detrital zircon spectrum of the central Arizona sample contained U-Pb modes at 1,669Ma, 1,420Ma and 1,222Ma (657 out of 726 grains). The other grains in these three samples yielded middle Cambrian U-Pb modes of 501–505Ma, although it should be noted that a small minority of grains (at least 59, 45, and 51 grains respectively) yielded U-Pb ages of <500Ma (with one as low as 407.2Ma). Karlstrom et al. (2018) concluded that deposition of the Tapeats Sandstone had been rapid (in conventional terms) across a width of 300km (~185mi) as documented by the 501–505Ma detrital zircon maximum depositional ages for it (revised to 507–508Ma by Karlstrom et al. 2020). They also noted that this is a much shorter duration than previously envisioned conventionally, which they said challenges traditional models for the very slow time-transgressive eastward shoreline migration in a deepening sea for deposition of the Tonto Group over 40–60Ma as proposed by McKee (1945).

Interpreted Depositional Setting of the Tapeats Sandstone

The uniformitarian interpreted depositional environments for the accumulation of the Tapeats Sandstone range widely to include beach and intertidal flats, to shallow, subtidal sand wave complexes (Middleton and Elliott 2003). Deposition of the Tapeats Sandstone was certainly influenced by a variety of geomorphic factors, as well as processes

inherent in the presumed fluvial and shallow marine depositional environments. The basal sediments were deposited on a Precambrian surface that had been exposed for possibly long periods of time. There was considerable relief on that surface. The "hills" have a relief as great as 244 m (800 ft) (McKee 1945). Generally, however, the relief is considerably less. Large blocks of the Precambrian Unkar Group Shinumo Quartzite occur in the basal deposits of the Tapeats Sandstone, for example, in Ninetyone Mile Canyon (fig. 14a) (Chadwick 1978). Walcott (1883) reported large basement blocks mantling the sides of areas of high relief.

McKee (1945) attempted to reconstruct the depositional environments of the Tapeats Sandstone based on texture of the sediments, paleocurrent trends, and to some degree, the types of sedimentary structures. He concluded that most sedimentation occurred below the beach zone and seawards for tens of miles from the coast in water depths up to 33 m (100 ft). The prevalent west-to-southwest dip of the cross-bedding indicated to him that net transport of the sediment was offshore. He also believed that the wide channels filled with cross-stratification and other large-scale scour-and-fill structures represented rip channels oriented perpendicular to the coast.

McKee (1945) also concluded that the monadnocks, or islands, in the relief of the Precambrian surface had relatively little impact on sedimentation, other than serving as a local source of coarse clastic sediment. He based his conclusions on the relatively consistent dip directions of the cross-stratification. According to him, the major influence of these islands was in modifying sedimentation patterns in the inter-island embayments. He reported southeast-directed current trends in the major embayment that developed between the Shinumo Quartzite islands in Bright Angel Canyon.

The earliest proposal that the Tapeats Sandstone represented a fluvio-deltaic depositional setting was that of Schuchert (1918), who judged the "poor assorting" and apparent presence of paleosols as ample criteria for assigning it a non-marine origin. However, it was Wanless (1973a, b, 1975, 1981) who presented the first challenge to the subtidal transgressive-regressive ("deepening seas") model of deepening offshore accumulations of marine sandstone, shale, and limestone by attempting to demonstrate the stratigraphic similarity between modern intertidal carbonates and the Muav Formation limestone facies that McKee (1945) had interpreted as the most distal and deepest of the Tonto Group deposits. Wanless reinterpreted the Tonto Group as a record of shallow-marine, tidal-flat, and fluvial sedimentation on the landward part of a vast cratonic platform and thus suggested that the whole of the Tonto Group deposition was in extremely shallow water. He described the Tapeats Sandstone as dominantly trough cross-bedded, well- to moderately-sorted, medium- to coarse-grained sands containing no record of organic activity or marine-tracer grains and buried regolith in bedrock depressions, and displaying a low-variance unimodal paleocurrent trend down the paleoslope. He maintained that the Tapeats was the result of bedload fluvial sedimentation in which the bedload transported sands (>200 µm) matured from arkosic to orthoquartizitic within 5–10 m (16–33 ft) of the base. Furthermore, he claimed that the finer, suspension-transported sands remained sub-arkosic the entire 250–500 m (820–1,640 ft) of the Cambrian Tonto group section, which implied their rapid dispersal.

Hereford (1977) provided a far more detailed uniformitarian facies analysis of the Tapeats Sandstone, although his study was concentrated in Chino Valley and the Black Hills of north-central Arizona. He recognized six postulated environmentally specific lithofacies that he related to physical and biological processes operative on modern tidal flats, beaches, and braided river systems.

Hereford (1977) further documented a continuum of postulated tidal flat deposits ranging from lower tidal flats to upper tidal flats dissected by channels. The postulated lower tidal flat sandstones are characterized by complex cross-stratification, reactivation surfaces and herringbone cross-stratification. The complex cross-stratification appears to reflect the passage of smaller bedforms across the surfaces of larger dunes or sand waves. Reactivation surfaces are common in today's tidal systems where reversals of water flow and/or erosion during bedform immobility result in the scouring of lee-side avalanche deposits. The herringbone cross-stratification appears to reflect the bimodal-bipolar flow of the tidal currents. Despite the polymodality of the apparent current directions indicated in the Hereford (1977) study, there is a dominantly southwestern component in the direction of sediment transport that agrees with the data of McKee (1945). Tidal systems today are typically characterized by asymmetry in flow velocities and durations. In the case for the Tapeats Sandstone it is apparent that the ebb phase was the strongest and that it resulted in a preservational bias toward the structures produced during offshore flow.

Deposits of the postulated high intertidal flats are characterized by interbedded sandstones and mudstones exhibiting a variety of features that appear to attest to exposure and late-stage emergent runoff. Additionally, Hereford (1977) documented the presence of apparent tidal channels that drained the

postulated tidal flats. Large channels occur near the top of the Tapeats Sandstone at several localities in the central and western Grand Canyon. The channels are up to 4m (13ft) deep and 18m (60ft) wide. At several localities up to three contiguous channels form a complex of southwest-oriented channel systems. Channel fill is variable and consists of thick sets of planar-tabular cross-stratification, co-sets of planar tabular and trough cross-stratification, and/or simple vertical fills that conform to the shape of the channel. Flow would have paralleled the southwestern strike of the channel axes, and in some instances, there is a well-developed bimodal-bipolar orientation to the cross-bed dip directions. Vertical trace fossils occur in the upper parts of the channel fills.

Although the geometry of these channels appears to be similar to that of both fluvial and tidal flat channels today, the internal stratification differs from that found in supposed fluvial sequences in the Tapeats Sandstone (Middleton and Hereford 1981). The presence of trace fossils and bimodal-bipolar foreset dips, along with the absence of exposure features, may instead suggest a subtidal channel complex dominated by offshore flow, with minor preservation of flood-oriented structures. Although subtidal channels occur on modern tide-dominated coasts, comparatively little is known of their sedimentologic characteristics. In the lower intertidal and shallow subtidal zones, bedload transport and erosion can be intense, particularly along meso- and macro-tidal coasts, because of the concentration of flow in these areas. Not enough data would seem to have been gathered to identify definitively the sandstone bodies that surround these channels as subtidal ridges or sand-waves. Nor has the fair-weather or storm-generated origin of these channels been established. Nummedal (1991), however, has documented some of the features of current shallow marine storm sedimentation which produces sand deposits not dissimilar to those in the Tapeats Sandstone.

Two other facies reported by Hereford (1977) were not documented by McKee (1945). One comprises low-angle, cross-laminated sandstone that might have formed on beaches. These tend to occur most frequently around Precambrian highs, where beach and upper foreshore sediments would supposedly have been common. The other facies association supposedly represents braided stream deposits that grade into the marine units. Supposed fluvial deposits in the Tapeats Sandstone occur in the basal portions of the formation. Typically, they are less mature texturally and mineralogically than the marine deposits, which reflects a lack of reworking that is common in today's high-energy nearshore. These deposits are characterized by broad, shallow channels that are filled with horizontally-stratified, coarse-grained sandstone and conglomerate that alternate with thick sets of planar-tabular and trough cross-stratified sandstone (Middleton and Hereford 1981). This sequence of structures would appear to be consistent with processes operative in modern coarse-grained fluvial systems. Deposition would have apparently occurred in wide, shallow streams where in-channel transport of sediment was accomplished by movement of sheets of coarse-grained sediment along the bed and by migration of dunes and slightly sinuous transverse bars.

The most recent in-depth field study of the Tonto Group is that of Rose (2003, 2006), who provided new stratigraphic data and sedimentologic evidence which he claimed supported Wanless' shallow-marine, tidal-flat, and fluvial sedimentation model. Rose (2003) collected stratigraphic data from 29 full and partial measured sections at sites throughout the western, central, and eastern Grand Canyon from which he developed his interpretation of the depositional environments. In presenting his evidence for non-marine deposition of the Tapeats Sandstone, Rose (2006) maintained that the Tapeats Sandstone varies considerably in grain size, sorting, and composition, but is dominated by what he regarded as amalgamated channels of tangentially cross-bedded arkosic to sub-arkosic coarse to very coarse to gravelly sandstone. High-angle tangential cross-beds (15–60° foreset dips) can be traced along crude bedding planes a few to a few tens of meters into apparent nested channels. Commonly only the gravelly bases of those purported channels are preserved, but what he claimed are apparent mud-cracked overbank deposits and even what he interpreted as eolian dunes are also preserved high in the Tapeats Sandstone sections near the transition to shale of the Bright Angel Formation.

Rose (2006) also highlighted the pervasive red–brown coloration within the Tapeats Sandstone, concluding that it may be depositional due to co-occurring with early hematite crystallization that was identified as syndepositional by Elston and Bressler (1977) through their paleomagnetic analysis. Indeed, the most robust paleomagnetic data from that study were obtained from a subordinate facies of bimodally fine-grained micaceous and argillaceous sandstone with a diffuse or diffusely planar-bedded component of subrounded coarse-grained sand. Rose (2006) maintained that such finer-grained supposed redbed facies are common in the Tapeats Sandstone, occurring in sharply-bounded horizons of limited lateral extent within or between the apparent channels, and may in some instances contain random cobble, boulder, or gravel stringers. Furthermore, U-shaped burrows (*Arenicolites*) are

sparsely present in planar horizons throughout much of the Tapeats Sandstone but are common in the upper part of typical Tapeats sections (fig. 15a), where they occur on steep tangential foresets. Yet these tangential foresets are not obviously bundled wherever they occur, nor do they occur *en echelon*, so he admitted that they do not contribute to his interpretation of tidal origin. On the other hand, he maintained that the common occurrence of isolated apparent channels provided evidence for avulsion, a process that is dependent on high bedload and that is incompatible with a low-slope subaqueous setting.

In summary, Rose (2006) stated that the key empirical observations contributing to his non-marine characterization of the Tapeats Sandstone included the isolated apparent channels which to him indicated channel-constrained fluid energy and avulsion, the presence of apparent mud cracks in the finer-grained deposits between what he interpreted as channels, and the presence of what he claimed are eolian dunes with characteristic frosted grains and flaggy cross-beds. He claimed that these apparently non-marine features of the Tapeats Sandstone fitted a model for a new depositional system which he called an expansive epicratonic estuary.

Hagadorn et al. (2011) reiterated that parts of the Tapeats Sandstone have been interpreted to be of non-marine origin for nearly a century, beginning with Schuchert (1918), and then Sharp (1940) who invoked sedimentologic and geochemical evidence to account for interpreted basement weathering, alluvial gravels and boulder conglomerates, and apparent paleosols in Facies Suite A (basal Tapeats). Additionally, they noted the interpreted overbank and fluvial avulsion facies documented by Rose (2006) within Facies Suite B (the cliff-forming Tapeats), together with settings that have internal bedding and primary structures interpreted as consistent with shallow aquatic deposition. Finally, they agreed with the apparent eolian and alluvial facies that have been claimed in Facies Suite C (the "transition zone") in the Tapeats of the eastern Grand Canyon (McKee 1945; Rose 2003; Wanless 1981), and the claimed paleosols (Wanless 1973a, b).

Given the context of coeval apparently marine sandstones to the north, west and south that contain a diverse and abundant array of horizontally- and vertically-oriented trace fossils, Hagadorn et al. (2011) questioned why there is an absence of a diverse suite of the marine trace fossils one would thus expect to find in the lithologically similar, subaqueously deposited Facies Suite B (cliff-forming) Tapeats Sandstone strata. They argued that clearly such trace fossils can be readily preserved in such strata, as is indicated by their presence in a range of lithologies, grains sizes, and apparent hydraulic flow conditions representing fully aquatic and intermittently aquatic environments. Thus Hagadorn et al. (2011) were puzzled that although *Skolithos* and other traces occur rarely in Facies Suite B, there are abundant U-shaped *Arenicolites* burrows in various facies not typically conducive to preservation of many delicate trace fossils, such as in purple mudstones, green shale flasers, gravelly-pebbly conglomerates, and arkosic sandstones of Facies Suite B. They noted that such a ubiquitous monotaxic concentration of *Arenicolites*, coupled with the near exclusion of other trace or body fossils, is present in other basement-mantling epicratonic sheet sandstones that correlate with the Tapeats Sandstone and also sit on the Great Unconformity in Colorado, Quebec-Ontario-New York, and even in Jordan and Saudi Arabia (Hagadorn et al. 2011, 73).

In modern aquatic settings where extant metazoan species diversity is lowest in brackish or euryhaline settings, and where only animals adapted to fluctuating salinities can survive, there are non-overlapping trace fossil occurrences. Therefore, Hagadorn et al (2011) interpreted the monotaxic concentration of *Arenicolites* in the range of sizes, depth, and shallow tiering of the Tapeats Sandstone beds as pointing to multiple healthy generations of biological activity of a single taxon temporarily colonizing the accumulating sediments in a brackish continental setting during saltwater wedging. They maintained that these repeated and persistent conditions must have excluded "normal marine" trackmakers and permitted only *Arenicolites* trackmakers to live there, and perhaps even excluded any competitors. They also pointed out that sedimentologic, clay mineral and palynological data from Tapeats exposures of the eastern Grand Canyon suggest that many of the sandstones and shales of Facies Suite C (the transition zone) may have been deposited under estuarine conditions (Baldwin et al. 2004; Rose 2006). Additionally, some of these *Arenicolites*-dominated glauconitic sandstones are characterized by an altered, hematitic, oolitic zone that has been interpreted as an oxidized ferricrete paleosol formed during subaerial exposure of burrowed surfaces, perhaps representing exposure of flooded marine sediments or supposed paleosol-generating conditions (Wanless 1973a, b).

Nevertheless, Gehrels et al. (2011) maintained the long-established view that the facies patterns in the Tapeats Sandstone suggested deposition in intertidal to subtidal shallow-marine environments, with local beach and fluvial deposits. And as summarized by McKee (1945), Hereford (1977), Middleton and Hereford (1981), and Middleton and Elliott (2003), the paleocurrent indicators and apparent channel patterns indicate overall westward (offshore)

transport of the detritus, with local derivation from isolated basement highs. Similarly, Blakey and Middleton (2012) stated that deposition for the most part was within intertidal and shallow subtidal zones, although adjacent to Precambrian highs wave processes were more dominant. Furthermore, in conceding to Hereford (1977), they added that locally, deposits of supposed braided streams occur near the base of the Tapeats and were deposited on interpreted floodplains that merged into nearshore marine areas. Nevertheless, Karlstrom et al. (2018) emphasized that the Sauk transgression, represented by the Tonto Group, "was one of the most dramatic global marine transgressions in Earth history."

However, the McKee (1945) deepening seas model for Tapeats Sandstone deposition has also had its supporters. Austin (1994) described the model in detail, while Kennedy, Kablanow, and Chadwick (1996, 1997) and Chadwick and Kennedy (1998) provided evidence of more catastrophic deposition of the Tapeats as a deep-water, submarine fan complex. They recorded paleoslope measurements and sedimentological features at 21 localities in the Grand Canyon where significant topographic relief occurred. At 24 of these sites, they found that debris flows were evident, apparently having been initiated by some catastrophic event that simultaneously broke and transported Shinumo Quartzite clasts (up to large boulder size, fig. 13) in a matrix of Tapeats sand. These brecciated flows were clearly deposited along the Precambrian surface topography from the cliff faces basinward. Furthermore, they noted that the widespread preservation of these breccias along the topographic relief during deposition of the entire thickness of the Tapeats Sandstone plus much of the overlying Bright Angel Formation indicated sediment deposition of even the shallowest material had been below storm wave base. Additionally, they obtained thorium/uranium ratios from the breccia matrix in Ninetyone Mile Canyon that indicated deposition in a reducing environment. They concluded that such conditions were unlikely in a high-energy nearshore facies, and that because these submarine debris flows had been deposited on a surface with over 140 m (460 ft) of vertical relief, deposition would have required water depths in excess of 200 m (656 ft) below storm wave base. Thus, this evidence for the more catastrophic deposition of the Tapeats Sandstone suggested to them that features such as sedimentary structures interpreted as pertaining to slower deposition as shallow marine and intertidal facies need to be re-evaluated.

Petrography of the Tapeats Sandstone

Previous Studies

McKee (1945) described the Tapeats Sandstone as remarkably uniform in general character throughout the region and as a clean, vitreous quartz sandstone which is locally arkosic. He determined that a majority of the grains are angular or subangular, coarse to medium, and moderately well-sorted. The cement is largely silica but locally iron oxide and varies so greatly in amount that some beds are crumbly, whereas others are quartzitic and hard. He studied at least one thin-section of the Tapeats Sandstone as he published one black-and-white photomicrograph.

McKee's (1945) designation of the Tapeats Sandstone as coarse-grained was based on mechanical analyses of 24 samples from the upper half of the formation (table 1). Results of these analyses are presented in histograms in fig. 26, which show that in 15 of the 24 samples the maximum grouping falls in the coarse grain size between 0.50 mm and 1.00 mm on the grain-size scale of Udden (1914) and Wentworth (1922). In the other nine samples the maximum is within the medium size range of between 0.25 mm and 0.50 mm. McKee (1945) then determined the median grain sizes of the samples and found they range between 0.34 mm and 0.94 mm, but the majority were within the limits 0.40 mm to 0.60 mm (table 1), or near the boundary between medium and coarse grain sizes. He also found no evidence of any size gradation upwards within the Tapeats Sandstone, due to high median grain-size values being found in samples both from the top of the formation and in other samples from well below (see table 1). However, the two samples with low median grain sizes were from near the top of the formation.

McKee (1945) also reported that his 24 coarse-grained sandstone samples all fell within the "well-sorted" grade in the classification of Trask (1930), since their coefficients of sorting (S_0) varied between 1.20 and 1.94. Indeed, a majority of his samples had sorting coefficients ranging between 1.40 and 1.50. However, Folk (1966) noted that the Trask S_0 scale is woefully inadequate for characterizing most sands because almost all dune, beach, marine and river sands fall in his "well-sorted" category with S_0 under 2.50. Thus, in table 1 McKee (1945) expressed the amount of spread in grain sizes which represents the degree of sorting in terms of phi (ϕ) units (after Krumbein 1934, 1938), in which negative logarithms of the grain diameters are used so an arithmetic grade-scale results. However, Krumbein's coefficient of sorting ($QD\phi$) as used by McKee (1945) is a measure of grain sizes within ±25% of the mean ϕ value (the central 50% of ϕ values). Thus, Folk and Ward (1957) and Folk (1966) introduced the standard deviation around the mean grain size as a more accurate determination of the degree of sorting. One standard deviation encompasses the

Table 1. Medians, coefficients of sorting, and skewness in terms of phi (ϕ) from typical samples of the coarse-grained facies of the cliff-forming unit as analyzed by McKee (1945, 42, table 5).

Specimen	Locality	Horizon	Mdϕ	QDϕ	Skqϕ
a	Diamond Bar Ranch, Grand Wash	50 ft below transition beds	0.8	0.75	0.05
b	Peach Springs Wash, near mouth	Upper part, transition beds	0.9	0.25	–0.05
c	Peach Springs Wash, near mouth	Upper part, transition beds	0.95	0.50	0.00
d	Foot of Toroweap Valley	10 ft below transition beds	1.1	0.55	0.35
e	Foot of Toroweap Balley	20 ft below tranisition beds	1.45	0.82	–0.975
f	Tip-off, ½ mi. W of Kaibab trail	10 ft below top	1.02	0.44	0.02
g	West fork, Pipe Creek Canyon	70 ft below top	1.1	0.60	–0.10
h	West fork, Pipe Creek Banyon	50 ft below top	0.7	0.40	0.05
i	East fork, Pipe Creek Canyon	100 ft below top	1.6	0.57	0.02
j	SE side of monadnock, Yake Pt	50 ft below top	0.1	0.67	–0.05
k	NE side of monadnock, Yaki Pt	75 ft below top	0.5	0.52	0.02
l	NE side of monadnock, Yaki Pt	50 ft below top	0.25	0.80	0.10
m	Plateau Pt, near Indian Gardens	Top of Tapeats	0.75	0.65	0.10
n	Plateau Pt, near Indian Gardens	30 ft below top	1.2	0.72	0.02
o	Clear Creek trail	20 ft below top	0.45	0.51	0.08
p	Clear Creek trail	50 ft below top	1.6	0.56	–0.15
q	W. end of bay, W. of Phantom	Cross-bedded s.s., lower part	0.8	0.57	0.12
r	W. end of bay, W. of Phantom	Cross-bedded s.s., lower part	0.7	0.50	0.10
s	E. end of bay, W. of Phantom	Flat-bedded s.s., 30 ft up	1.35	0.50	0.05
t	E. end of bay, W. of Phantom	Flat-bedded s.s., middle	1.4	0.52	0.05
u	E. end of bay, W. of Phantom	Flat-bedded s.s., top	0.55	0.32	0.07
v	E. end of bay, W. of Phantom	Flat-bedded s.s., 25 ft below top	1.2	0.57	0.07
w	E. end of bay, W. of Phantom	Cross-bedded s.s., near base	1.12	0.60	0.06
x	E. end of bay, W. of Phantom	Cross-bedded s.s., base	0.95	0.95	0.20

central 68% of the area under the frequency curve, which means 68% of the grain-size values lie within plus or minus one standard deviation of the mean grain size (Boggs 1995). However, Folk and Ward (1957) and Folk (1966) calculated the standard deviation using ϕ values, so strictly speaking it is the ϕ standard deviation. Thus, since McKee's *QDϕ* values in table 1 range from 0.25 to 0.95, with most values between 0.50 and 0.71, even though there is not a direct correlation with Folk's scale for sorting it would appear that McKee's samples were mostly only "moderately well-sorted".

McKee (1945) noted that although sorting was moderately good in most parts of the coarse-grained sandstone, his examination of hand specimens showed that in many locations there is excellent sorting within an individual lamina but considerable contrast in the average grain size of adjoining laminae. For example, he cited the sample b in fig. 26 from the upper part of the transition zone (near the top of the Tapeats Sandstone). In this uniform, coarse- to very coarse-grained sandstone, laminae are ¼ in (~6 mm) to ½ in (~13 mm) thick and are separated by other laminae ½ in (~13 mm) to 1 in or more (>~25 mm) in thickness composed of medium- to fine-grained sand grains.

McKee (1945) also determined the skewness or degree of asymmetry in the frequency curves developed from his mechanical analyses of his 24 samples. He used the ϕ unit method of Krumbein (1934, 1938) in which the curve is symmetrical when *Skqϕ* equals zero. The results are in table 1 (last column) and indicate that the grain-size frequency distributions in almost all the sandstone samples are skewed relatively little and mostly on the positive side, which indicates the peaks of the frequency distributions are on the fine side of the medians. However, Folk (1966) raised a concern that Krumbein's method of calculating the skewness was unsatisfactory because the resulting skewness measure was not geometrically independent of sorting. Thus, Folk and Ward (1957) had developed a more sensitive measure of skewness. Nevertheless, McKee's values for his 24 Tapeats Sandstone samples (table 1) do correlate with their grain-size frequency histograms in fig. 26.

Apart from the one photomicrograph published by McKee (1945), there are apparently no other

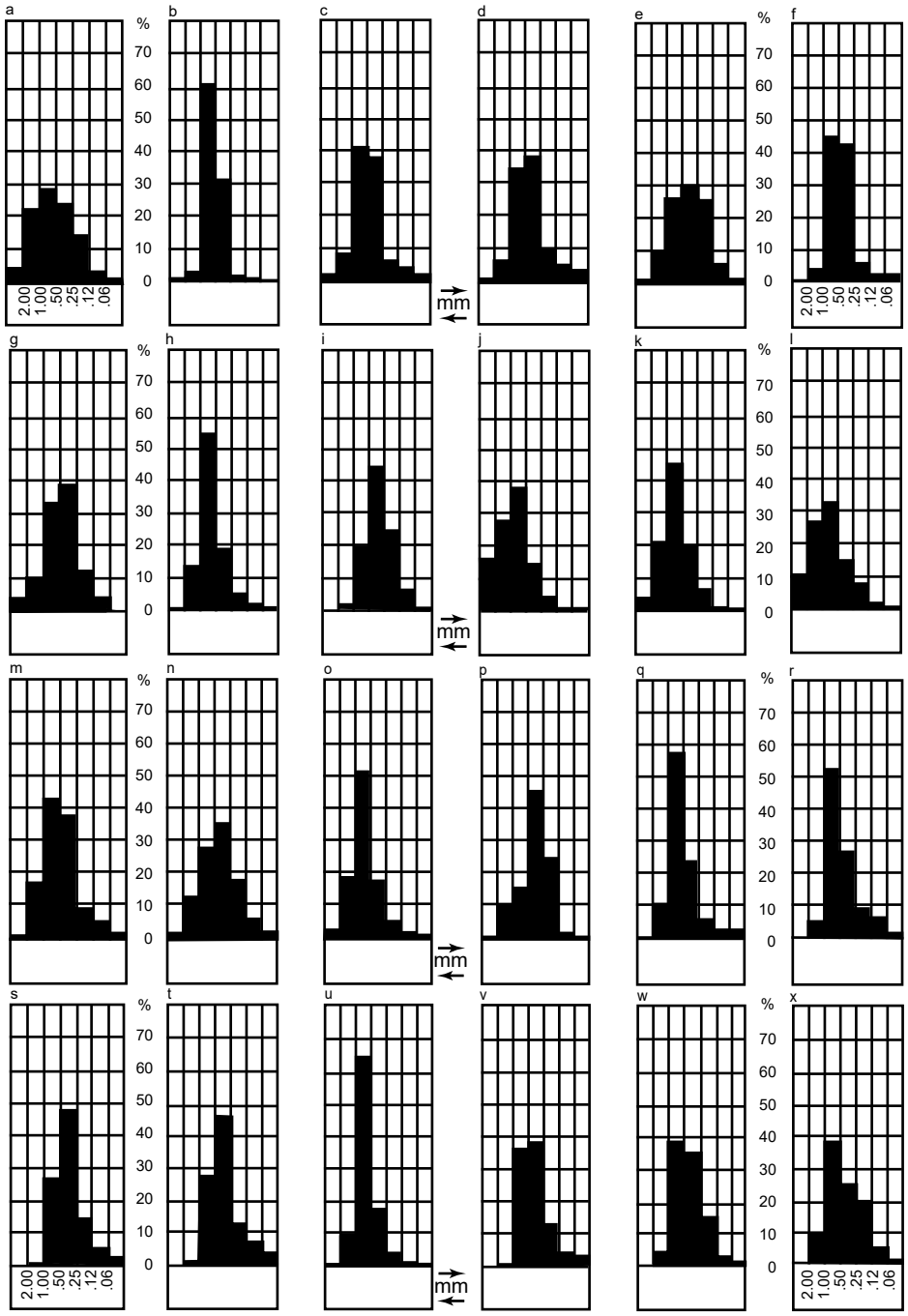

Fig. 26. Grain size distribution histograms in 24 typical samples of the Tapeats Sandstone as presented by McKee (1945, 40, fig.4). The localities and horizons his samples represent are listed in table 1.

photomicrographs of the Tapeats Sandstone in the published literature. So, it is unclear whether those who have previously investigated the Tapeats Sandstone have studied thin sections of samples under the microscope. Rose (2003) did not provide any photomicrographs of the Tapeats Sandstone and it appears that for its petrography he largely relied on the earlier unpublished work of Burgert (1972), yet it is unclear how many thin sections the latter examined. A recompiled diagrammatic summary of the latter's results was provided by Rose (2003, 48, fig. 21). Burgert (1972) reported the stratigraphic trends in grain size, sorting and feldspar abundance of the coarse-grained sandstone facies (the cliff-forming unit) from six measured and sampled sections in the eastern Grand Canyon. Rose (2003) described this major coarse-grained sandstone facies unit as including dominantly rounded to sub-angular medium-coarse to barley- or pea-sized grains of white or yellow quartz, with lesser smoky quartz, quartzite, chert, jasper, feldspar, and locally-derived clasts of schist, granite

and basalt. He also commented that Burgert's (1972) data showed considerable variability in grain size and sorting, though in some localities grain size actually increased up-section, but decreasing relative feldspar was the only reasonably consistent up-section trend among five of his sections. The exception was the Hermit Creek section in which both grain size and relative K-feldspar content increases at the top of the section. Burgert (1972) reported total feldspar concentrations from his six sections ranging from 3% to 5.5%, with orthoclase dominant over microcline and plagioclase, and altered orthoclase constituting between 50% and 96% of the total feldspar content. Furthermore, his heavy mineral analyses revealed an abundance of well-rounded grains in an assemblage dominated by zircon, tourmaline and anatase.

To support his intertidal-fluvial environment model for deposition of the Tapeats Sandstone, Rose (2003) relied on x-ray diffraction (XRD) analyses of the clay minerals in samples of fine-grained sandstone and shale mostly taken from the transition zone, or the upper Tapeats Facies C of Hagadorn et al. (2011), which is not the major component of the Tapeats Sandstone. He found that in some of his samples from two locations kaolinite predominated over illite, and sometimes smectite, and thus argued for freshwater influence during deposition, though in other samples illite was predominant. However, he assumed that these clay minerals were primary depositional features, yet in the sandstone some or all could be post-depositional due to diagenesis. Only petrographic microscope and scanning electron microscope (SEM) examinations would be definitive. Thus, thin-section study is fundamental to describing the grains in the sandstone and its cement, and to interpreting its mode of formation and subsequent history.

Finally, it should be noted that in none of these detailed studies of the petrology of the Tapeats Sandstone (Burgert 1972; McKee 1945; Rose 2003) is any mention made of either macroscopic or microscope evidence of any metamorphic effects on the sandstone or its constituent mineral grains. Even the slightly elevated temperatures of low-grade metamorphism would have substantially affected the quartz grains, which are the dominant mineral in the sandstone, and the textures in the rock fabric. All are thus agreed that the Tapeats Sandstone is unmetamorphosed in all places where it was examined in the Grand Canyon by these previous workers.

Results of the Present Mineralogic Study

During an investigation of four folds in the Grand Canyon, 26 samples of the Tapeats Sandstone were collected from the Carbon Canyon and Monument folds, and from outcrops along the Colorado River corridor distant from those folds (table 2). The purpose was to compare the samples from the two folds with the distal samples to ascertain what effects the folding had on the sandstone and thus determine the conditions during, and the timing of, the folding relative to the conditions and timing of the deposition and subsequent lithification (cementation) of the sandstone. Details of the locations of those samples are provided in fig. 1 and table 2, as well as in Appendix D (in the Supplementary material). All samples were sent to Calgary Rock and Materials Services, Inc. (Calgary, Canada) for thin sectioning and for x-ray diffraction (XRD) analyses.

XRD Results

At Calgary Rock and Materials Services, Inc., after being dried overnight at 60°C, a representative 5–10 grams of each sample was selected and ground for ten minutes in a pulverizing mill to obtain homogeneous powders. These powders were then packed in powder mounts against a glass surface before being mounted in the goniometer of a Rigaku Miniflex II x-ray diffractometer in which a copper source tube is used to provide the incident beam of monochromatic x-rays with a wavelength of 1.541874Å. Samples were typically scanned from 4 to 60° 2θ (two theta) to obtain the XRD spectra. The raw data provided in a specific form by the x-ray computer were imported into the x-ray analysis software (Jade 2010), where peak positions, areas and heights were calculated. The software then provided the most likely matches of minerals for each spectrum generated, from a database of over 100,000 compounds. The Rietveld Refinement Method was then used to determine the percentages of the minerals in the samples.

The results of the bulk rock XRD analyses are in table 3. Quartz is, of course, the dominant mineral in the Tapeats Sandstone, but it varies between 33.9% and 100% in these samples. K-feldspar features prominently in most samples, and where present ranges from 1.8% to 33.1%. Plagioclase is even present in one sample (3.1%). About a third of the samples (nine) contain significant amounts of calcite, varying from 1.1% to a dominant 34.8%, while one sample containing 3.8% calcite also contains 1.2% dolomite. Other minor minerals include anhydrite (5.1% in one sample) and halite (in four samples ranging from 0.8% to 6.9%, though three of those samples are from the Monument fold). Minor clay minerals are always present, but only reach significant quantities in two samples, one containing 1.2% kaolinite and another containing 0.5% illite.

The results of the clay fraction XRD analyses are in table 4. In most samples clay minerals are only present in trace amounts. The dominant clay mineral in all but two samples is illite (varying from 20.7% to 100%), with subordinate illite/smectite in all but two

Table 2. Locations and stratigraphic details of all the Tapeats Sandstone samples examined in this study.

Sample	Location	Location Coordinates	Stratigraphic Position	Notes
TSS-01	River Mile 60.1	N 36° 12.784' W 111° 48.411'	12 m below top of cliff-forming unit	Just below Sixtymile Rapid, river left, upstream end of the beach
TSS-02	River Mile 120.8	N 36° 14.419' W 112° 28.825'	Halfway down the cliff-forming unit	Just beyond Blacktail Canyon, river left
TSS-03	River Mile 138	N 36° 23.859' W 112° 31.896'	Close to Great Unconformity	Opposite just below Doris Rapid, river right
TSS-04	River Mile 138	N 36° 23.859' W 112° 31.896'	7.5 m stratigraphically higher than TSS-04	Opposite just below Doris Rapid, river right
CCF-01	Carbon Canyon fold River Mile 65	N 36° 09.268' W 111° 49.806'	10–12 m below top of cliff-forming unit	1.4 m above the hinge of the fold
CCF-02	Carbon Canyon fold River Mile 65	N 36° 09.268' W111° 49.806'	10–12 m below top of cliff-forming unit	Same bed, from the hinge of the fold
CCF-03	Carbon Canyon fold River Mile 65	N 36° 09.263' W 111° 49.797'	10–12 m below top of cliff-forming unit	Same bed, 2.3 m from sample CCF-02
CCF-04	Carbon Canyon fold River Mile 65	N 36° 09.264' W111° 49.794'	10–12 m below top of cliff-forming unit	Same bed, 3.5 m from sample CCF-03
CCF-05	Carbon Canyon fold River Mile 65	N 36° 09.258' W 111° 49.789'	10–12 m below top of cliff-forming unit	Same bed, 8 m from sample CCF-04
CCF-06	Carbon Canyon fold River Mile 65	N 36° 09.256' W 111° 49.784'	10–12 m below top of cliff-forming unit	Same bed, 5 m from sample CCF-05
CCF-07	Carbon Canyon fold River Mile 65	N 36° 09.260' W 111° 49.782'	10–12 m below top of cliff-forming unit	Same bed, 4 m from sample CCF-06
CCF-08	Carbon Canyon fold River Mile 65	N 36° 09.264' W 111° 49.780'	10–12 m below top of cliff-forming unit	Same bed, 6 m from sample CCF-07
CCF-09	Carbon Canyon fold River Mile 65	N 36° 09.279' W 111° 49.800'	14–16 m below top of cliff-forming unit	Another bed, ~4 m stratigraphically lower, 1.5 m above hinge of the fold
CCF-10	Carbon Canyon fold River Mile 65	N 36° 09.261' W 111° 49.797'	14–16 m below top of cliff-forming unit	Same second bed, from the hinge of the fold
CCF-11	Carbon Canyon fold River Mile 65	N 36° 09.258' W 111° 49.794'	14–16 m below top of cliff-forming unit	Same second bed, 2.3 m from sample CCF-10
CCF-12	Carbon Canyon fold River Mile 65	N 36° 09.258' W 111° 49.792'	10-12 m below top of cliff-forming unit	Around the corner about 40 m from sample CCF-11
MF-01	Monument fold River Mile 116.4	N 36° 12.225' W 112° 26.441'	3–4 m above Great Unconformity	Furthest down-river sample
MF-02	Monument fold River Mile 116.4	N 36° 12.107' W 112° 26.312'	3–4 m above Great Unconformity	In bed above, 6 m from sample MF-01
MF-03	Monument fold River Mile 116.4	N 36° 11.875' W 112° 26.218'	3-4 m above Great Unconformity	Same bed, 11.5 m from sample MF-02
MF-04	Monument fold River Mile 116.4	N 36˚ 11.832' W 112˚ 26.126'	3–4 m above Great Unconformity	Same bed, ~14 m laterally from sample MF-03
MF-05	Monument fold River Mile 116.4	N 36° 11.650' W 112° 26.168'	3–4 m above Great Unconformity	Same bed as sample MF-01, at the hinge of the fold ~5–6 m from sample MF-04
MF-06	Monument fold River Mile 116.4	N 36° 11.640' W 112° 26.151'	3–4 m above Great Unconformity	Same bed and 1.8 m further from sample MF-05
MF-07	Monument fold River Mile 116.4	N 36° 11.539' W 112° 25.941'	3–4 m above Great Unconformity	Same bed and 8 m further from sample MF-06
MF-08	Monument fold River Mile 116.4	N 36° 11.591' W 112° 26.032'	3–4 m above Great Unconformity	Same bed and 4 m further from sample MF-07
MF-09	Monument Fold River Mile 116.4	N 36° 12.925' W 112° 26.468'	3–4 m above Great Unconformity	Same bed and 4.8 m further from sample MF-08
MF-10	Monument Fold River Mile 116.4	N 36° 11.865' W 112° 26.150'	3–4 m above Great Unconformity	Same bed but lower and ~1.5 m from sample MF-05 in the hinge of the fold

Table 3. Mineral compositions of the Tapeats Sandstone samples from X-ray diffraction (XRD) analyses, courtesy of Ray Strom, Calgary Rock and Materials Services, Inc., Canada.

Sample	Stratigraphic Position	Quartz	K-Feldspar	Plagioclase	Calcite	Dolomite	Anydrite	Illite	Halite	Kaolinite	Total
TSS-01	12 m below top of cliff-forming unit	68.4%	31.6%	-	-	-	-	-	-	-	100.0%
TSS-02	Halfway down the cliff-forming unit	87.7%	6.4%	-	5.9%	-	-	-	-	-	100.0%
TSS-03	Close to Great Unconformity	83.3%	8.6%	-	8.1%	-	-	-	-	-	100.0%
TSS-04	7.5 m higher than TSS-04	98.8%	-	-	-	-	-	-	-	1.2%	100.0%
CCF-01	10–12 m below top of cliff-forming unit	92.7%	7.3%	-	-	-	-	-	-	-	100.0%
CCF-02	10–12 m below top of cliff-forming unit	67.6%	32.4%	-	-	-	-	-	-	-	100.0%
CCF-03	10–12 m below top of cliff-forming unit	92.0%	6.9%	-	1.1%	-	-	-	-	-	100.0%
CCF-04	10–12 m below top of cliff-forming unit	95.6%	4.4%	-	-	-	-	-	-	-	100.0%
CCF-05	10–12 m below top of cliff-forming unit	67.4%	29.5%	3.1%	-	-	-	-	-	-	100.0%
CCF-06	10–12 m below top of cliff-forming unit	88.5%	11.5%	-	-	-	-	-	-	-	100.0%
CCF-07	10–12 m below top of cliff-forming unit	90.2%	9.8%	-	-	-	-	-	-	-	100.0%
CCF-08	10–12 m below top of cliff-forming unit	100.0%	-	-	-	-	-	-	-	-	100.0%
CCF-09	14–16 m below top of cliff-forming unit	92.1%	7.9%	-	-	-	-	-	-	-	100.0%
CCF-10	14–16 m below top of cliff-forming unit	79.3%	19.2%	-	1.5%	-	-	-	-	-	100.0%
CCF-11	14–16 m below top of cliff-forming unit	90.4%	9.6%	-	-	-	-	-	-	-	100.0%
CCF-12	10–12 m below top of cliff-forming unit	89.1%	10.1%	-	-	-	-	-	0.8%	-	100.0%
MF-01	3–4 m above Great Unconformity	36.3%	30.0%	-	33.2%	-	-	0.5%	-	-	100.0%
MF-02	3–4 m above Great Unconformity	61.9%	33.1%	-	3.8%	1.2%	-	-	-	-	100.0%
MF-03	3–4 m above Great Unconformity	33.9%	24.4%	-	34.8%	-	-	-	6.9%	-	100.0%
MF-04	3–4 m above Great Unconformity	47.7%	22.7%	-	24.5%	-	5.1%	-	-	-	100.0%
MF-05	3–4 m above Great Unconformity	88.8%	11.2%	-	-	-	-	-	-	-	100.0%
MF-06	3–4 m above Great Unconformity	92.2%	1.8%	-	3.9%	-	-	-	2.1%	-	100.0%
MF-07	3–4 m above Great Unconformity	91.9%	8.1%	-	-	-	-	-	-	-	100.0%
MF-08	3–4 m above Great Unconformity	89.8%	5.9%	-	-	-	-	-	4.3%	-	100.0%
MF-09	3–4 m above Great Unconformity	90.2%	9.8%	-	-	-	-	-	-	-	100.0%
MF-10	3–4 m above Great Unconformity	100.0%	-	-	-	-	-	-	-	-	100.0%

Table 4. Clay mineral fraction compositions of the Tapeats Sandstone samples from X-ray diffraction (XRD) analyses, courtesy of Ray Strom, Calgary Rock and Materials Services, Inc., Canada.

Sample	Stratigraphic Position	Illite	Illite/Smectite	Kaolinite	Smectite	Total
TSS-01	12 m below top of cliff-forming unit	72.9%	27.1%	-	-	100.0%
TSS-02	Halfway down the cliff-forming unit	54.9%	45.1%	-	-	100.0%
TSS-03	Close to Great Unconformity	75.1%	24.9%	-	-	100.0%
TSS-04	7.5 m higher than TSS-04	32.6%	23.6%	43.8%	-	100.0%
CCF-01	10–12 m below top of cliff-forming unit	72.2%	22.9%	4.9%	-	100.0%
CCF-02	10–12 m below top of cliff-forming unit	70.6%	21.9%	7.5%	-	100.0%
CCF-03	10–12 m below top of cliff-forming unit	70.5%	24.8%	4.6%	-	100.0%
CCF-04	10–12 m below top of cliff-forming unit	88.4%	4.3%	7.3%	-	100.0%
CCF-05	10–12 m below top of cliff-forming unit	82.4%	14.3%	3.4%	-	100.0%
CCF-06	10–12 m below top of cliff-forming unit	66.3%	19.9%	13.8%	-	100.0%
CCF-07	10–12 m below top of cliff-forming unit	91.9%	-	8.1%	-	100.0%
CCF-08	10–12 m below top of cliff-forming unit	59.6%	17.5%	22.9%	-	100.0%
CCF-09	14–16 m below top of cliff-forming unit	84.4%	15.6%	-	-	100.0%
CCF-10	14–16 m below top of cliff-forming unit	60.3%	21.0%	18.7%	-	100.0%
CCF-11	14–16 m below top of cliff-forming unit	78.2%	21.8%	-	-	100.0%
CCF-12	10–12 m below top of cliff-forming unit	86.5%	13.5%	-	-	100.0%
MF-01	3–4 m above Great Unconformity	61.1%	20.8%	5.6%	12.6%	100.0%
MF-02	3–4 m above Great Unconformity	66.7%	27.1%	6.2%	-	100.0%
MF-03	3–4 m above Great Unconformity	58.9%	24.8%	16.3%	-	100.0%
MF-04	3–4 m above Great Unconformity	54.6%	13.1%	15.6%	16.7%	100.0%
MF-05	3–4 m above Great Unconformity	82.3%	17.7%	-	-	100.0%
MF-06	3–4 m above Great Unconformity	100.0%	-	-	-	100.0%
MF-07	3–4 m above Great Unconformity	20.7%	25.4%	8.7%	45.3%	100.0%
MF-08	3–4 m above Great Unconformity	86.9%	13.1%	-	-	100.0%
MF-09	3–4 m above Great Unconformity	60.4%	15.5%	6.7%	17.4%	100.0%
MF-10	3–4 m above Great Unconformity	85.0%	15.0%	-	-	100.0%

samples (where present varying from 4.3% to 45.1%). Many samples (16) also contain kaolinite (ranging from 3.4% to 43.8%), and four samples (from the Monument fold) contain smectite as a separate phase (ranging from 12.6% to 45.3%).

Thin Section Examination

The thin sections for this study were all mounted on standard glass microscope slides. Before the slices were cut from the rock samples using a diamond saw, the rock samples were impregnated under confining pressure with epoxy resin that contained a blue dye. This ensured that grains did not get dislocated or the rock fabrics get distorted during the sawing of the slices. However, this process left the thin sections with a blue dye staining as the surrounding background and in any holes or pores within the rock fabrics. Before cover slips were added, the thin sections were stained so as to make the K-feldspar and calcite in the rock fabrics more easily distinguished. Thus, the K-feldspar grains have a distinctive yellow color and the calcite is pinkish in plane polarized light.

Petrographic descriptions of all samples from extensive thin section examination are provided in Appendix D (in the Supplementary material), along with photomicrographs of the whole thin sections from which the descriptions were derived. The locations and stratigraphic details of all samples are provided in table 2. All samples were collected from the major cliff-forming unit (Facies B) of the Tapeats Sandstone.

In the thin sections, the sandstone is generally massive and poorly to moderately well-sorted, dominated by sub-angular to sub-rounded quartz grains ranging in size from coarse silt to very coarse sand and sometimes granules (plus occasionally some small pebbles), using the standard definitions and terminologies for sorting of Folk (1966, 1980) and Pettijohn, Potter, and Siever (1973), for shape of Powers (1953) and Folk (1955), and for size of Udden (1914) and Wentworth (1922). Thin sections of a representative set of samples are shown in fig. 27, while a representative set of photomicrographs in fig. 28 show typical textures within this sandstone. It should

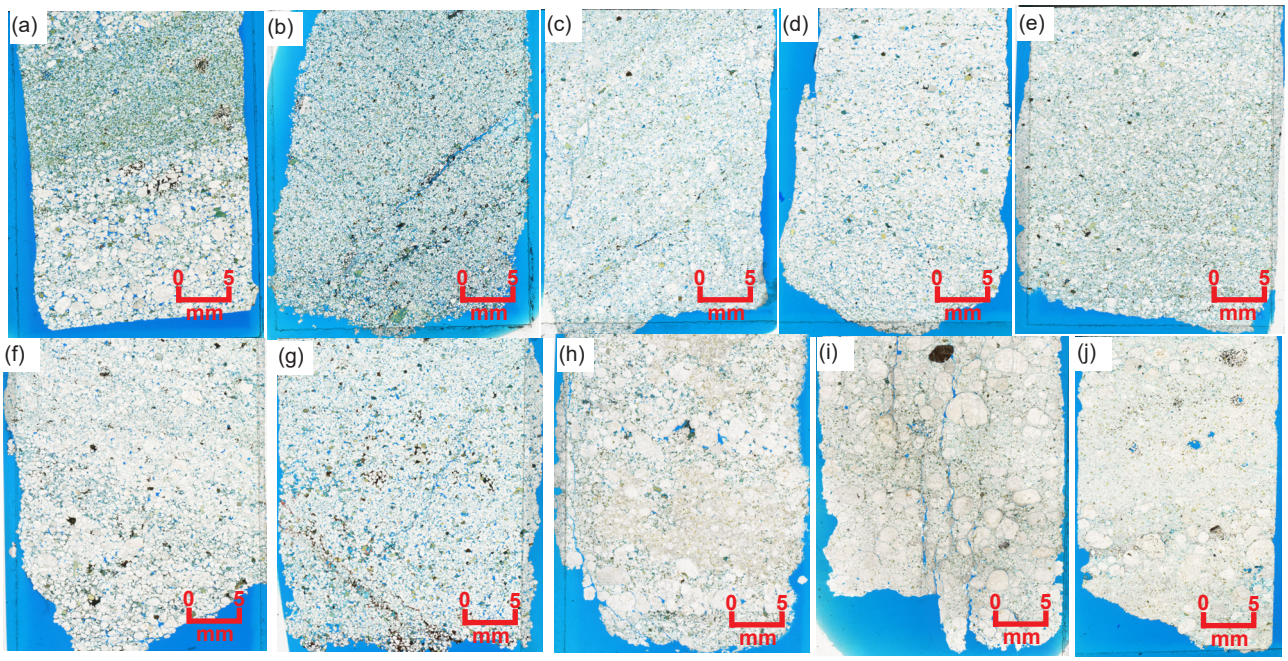

Fig. 27. Representative Tapeats Sandstone sample thin sections at normal hand specimen scale (scale bars indicate ~5 mm), showing the textures including laminations, cross-laminations, and varying degrees of sorting, as well as the variations in grain sizes, including granules and small pebbles, primarily of quartz (location details provided in table 2). The darker grains are K-feldspar grains of varying sizes, including one altered granule. These thin sections were cut perpendicular to the bedding, so in each of these shown here the top of the thin section is equivalent to the top of the bed sampled. (a) TSS-01, (b) TSS-03, (c) CCF-01, (d) CCF-03, (e) CCF-05, (f) CCF-07, (g) CCF-10, (h) CCF-12, (i) MF-08, and (j) MF-09.

be noted that in these thin sections there is often a blue dye staining between the grains, and sometimes encroaching on the grain edges or even across grain surfaces. This blue dye is associated with the epoxy that the samples were impregnated with prior to the preparation of the thin sections. Thus, some patches of blue dye mark the occasional pore spaces.

Some samples are laminated with thin (1–2 cm) coarse-grained and finer-grained laminae, even with low-angle cross-bedding in some of the laminae (for example, fig. 27a and f). But generally, the quartz grain sizes are randomly mixed and invariably occasional K-feldspar grains of various sizes are scattered through the poorly to moderately well-sorted rock fabric. Indeed, all samples contain numerous K-feldspar grains and at least a few thin edge-on muscovite flakes, while a few samples contain possible plagioclase grains which are evident from their multiple twinning under crossed polars. Generally, there are very few pore spaces remaining, most pores having been filled by quartz (silica) cement, often as a result of the quartz growing as overgrowths around the original detrital grains (sometimes still outlined by the original iron oxide coatings), with the overgrowths meeting at triple points. Occasional former pores have been filled with later secondary iron oxides, and sometimes also with calcite or clay minerals. Minimal diagenetic alteration has occurred, primarily alteration or dissolution of some K-feldspar grains and laths, the formation of clay minerals, and the sporadic introduction of occasional calcite, and in only a few samples also halite and/or anhydrite. In summary, this is a submature arkosic sandstone or sub-arkose that is well-cemented, predominantly by silica (quartz) but with trivial secondary calcite and iron oxides in a few samples. This classification is based on the predominance of quartz, and the K-feldspar content, which averages much less than 25% (Dott 1964; Folk 1980; McBride 1963; Pettijohn 1954, 1957; Pettijohn, Potter, and Siever 1972; Scholle 1979; Ulmer-Scholle et al 2015).

Quartz

As seen under the microscope the quartz grains are invariably in a tightly-packed interlocking mosaic with some samples having virtually no pore spaces and many samples having very few remaining pores (figs. 28 and 29). The quartz grains are of variable sizes randomly mixed in some parts of the rock fabric but are of similar sizes in other parts (for example, see fig. 28a and b). The grain sizes range from small (0.06-0.24 mm, ϕ=+4.05–+2.06, coarse silt size and very fine to fine sand size), to medium (0.26-0.50 mm, ϕ=+1.95–+1.00, medium sand size), to large (0.52-1.98 mm, ϕ=+0.95–-0.98, coarse to very coarse sand size), and to extremely large (2.14-3.85 mm,

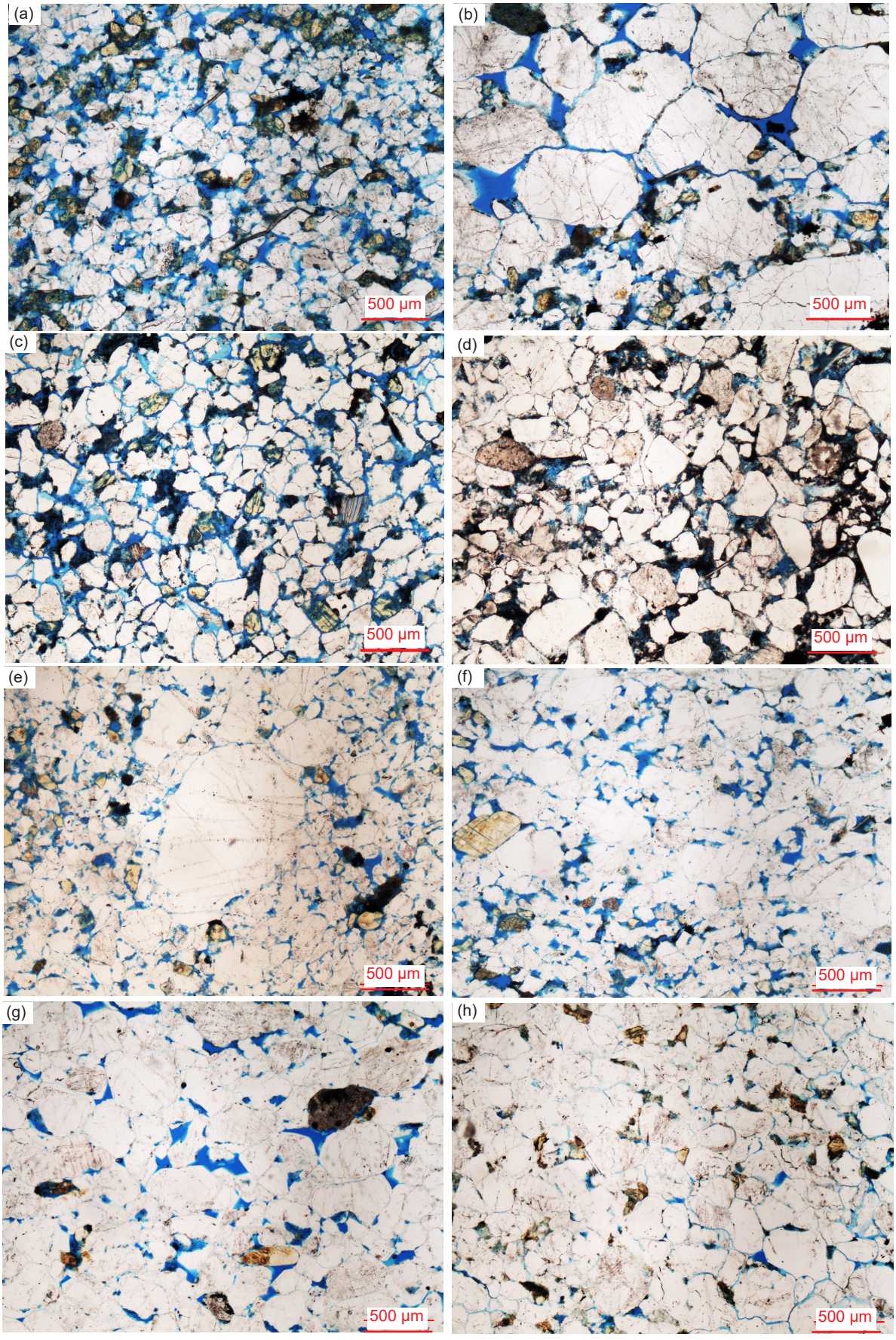
(a)
500 μm
(b)
500 μm
(c)
500 μm
(d)
500 μm
(e)
500 μm
(f)
500 μm
(g)
500 μm
(h)
500 μm

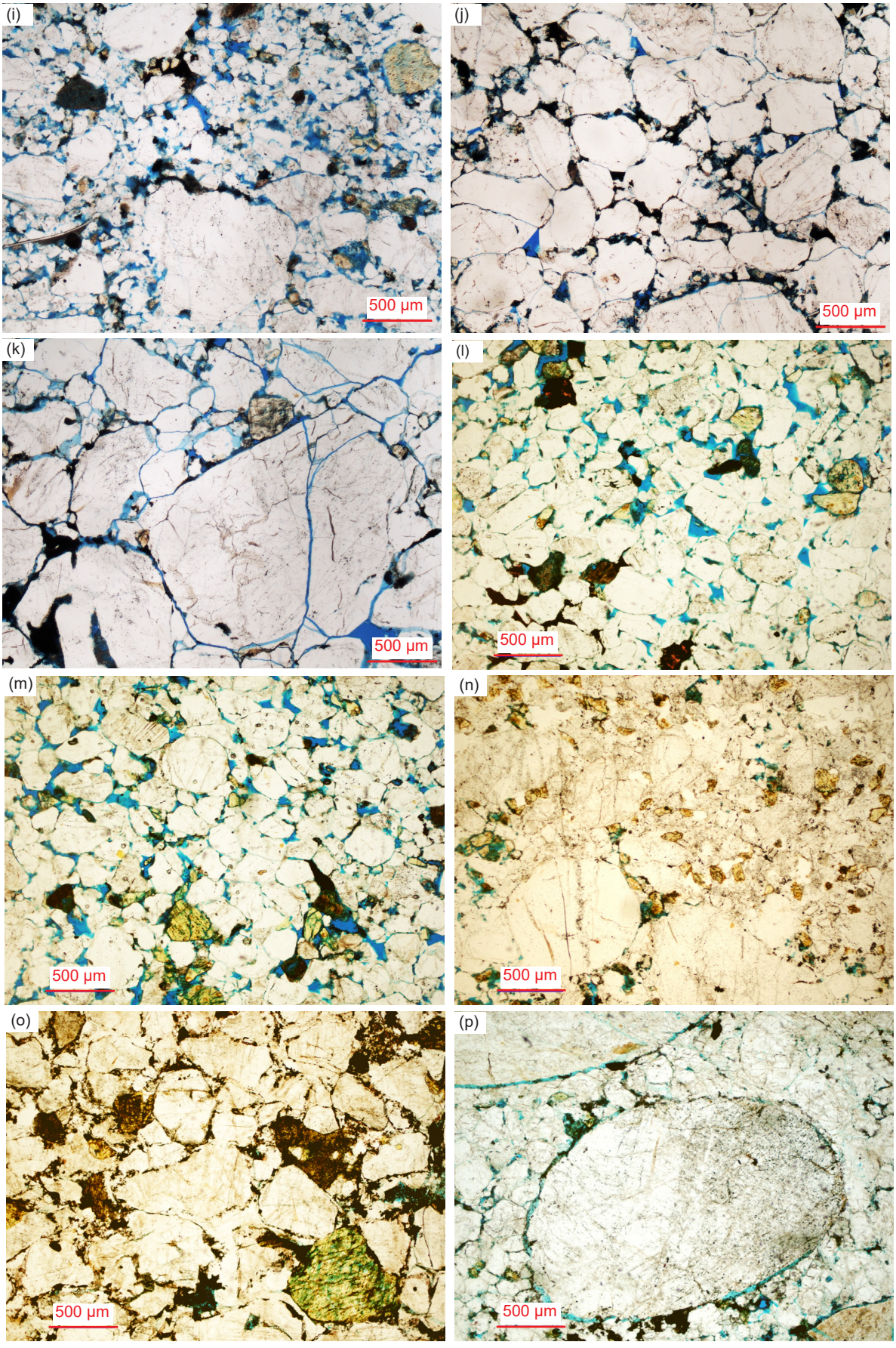
(i)
500 µm
(j)
500 µm
(k)
500 µm
(l)
500 µm
(m)
500 µm
(n)
500 µm
(o)
500 µm
(p)
500 µm

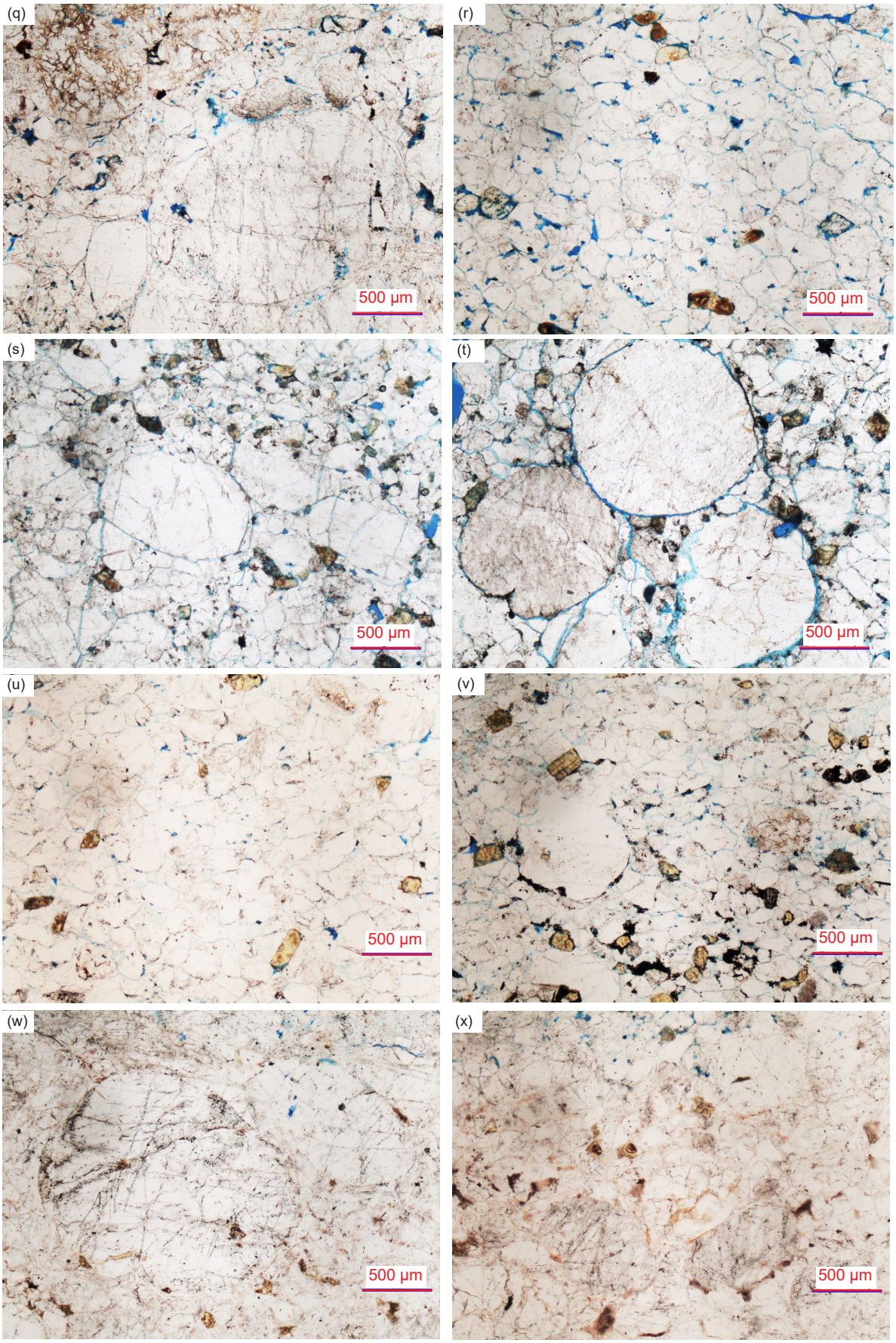
(q)
500 µm
(r)
500 µm
(s)
500 µm
(t)
500 µm
(u)
500 µm
(v)
500 µm
(w)
500 µm
(x)
500 µm

Fig. 28 (pages 206, 207, 208). A representative set of photomicrographs at the same scale (as indicated) showing the variations in textures in the Tapeats Sandstone samples (location details provided in table 2). The thin sections were stained for ease of distinguishing K-feldspar and calcite. Note the variations in grain sizes, shapes and sorting, and the almost universal presence of K-feldspar grains. Most samples have some residual pore spaces (usually highlighted by the blue dye), but most pores have been infilled with quartz cement (as overgrowths), or in a few places by calcite and/or iron oxides. (a) TSS-01, (b) TSS-01, (c) TSS-03 (d) TSS-04, (e) CCF-01, (f) CCF-02, (g) CCF-03, (h) CCF-04, (i) CCF-05, (j) CCF-07, (k) CCF-08, (l) CCF-10, (m) CCF-11 (n) CCF-12, (o) MF-04, (p) MF-05, (q) MF-06, (r) MF-07, (s) MF-08, (t) MF-08, (u) MF-09, (v) MF-09, (w) MF-10, and (x) MF-10.

ϕ=−-1.09—1.94, small granules), plus occasional small pebbles (4.03-7.58mm wide, ϕ=-2.01—-2.56). The grains often appear "molded" so they fit together tightly, mainly due to the silica cement overgrown on the original detrital quartz sand grains. They are occasionally rounded, but predominantly sub-rounded to sub-angular, and sometimes sub-euhedral to euhedral (fig. 29), usually with straight or curved defined edges, but sometimes with irregular or diffuse edges that give the impression of having been resorbed (possibly representing solution of the quartz into the original pore water that then precipitated as the infilling overgrowths of quartz cement), or rarely some apparently broken edges. Internal spotted and linear markings of iron oxide within some medium to large grains often define original rounded and sub-rounded detrital grains (as "ghost" outlines), with clear sub-euhedral overgrowths in optical continuity that infill the original inter-grain pores and usually meet at tightly-fitting triple points due to the quartz cement crystal terminations (figs. 28 and 29). In some parts of the mosaic the quartz grains thus display "lock and key" meetings at triple points or irregular interlocking.

Some sub-angular to rounded, large and huge quartz grains have patchworks of sub-domains (with irregular or "ameboid" edges, irregularly-shaped, and various sizes) or sometimes sub-grains with different crystallographic orientations and thus extinction angles, surrounded and molded around them by tightly-packed mosaics of sub-angular to rounded, medium and small quartz grains. Sometimes it is hard to discern whether such huge quartz grains are single grains with internal patchworks (and thus may be quartzite or even metamorphic quartz grains), or are many smaller grains cemented together in a closely-knit mosaic (somewhat like glomerocrysts). In other places, there are either lots of very small to small interlocking quartz grains or very small and medium to large irregularly-shaped sub-angular to sub-rounded quartz grains mixed or clustered together. Some quartz grains exhibit undulose extinction and some appear to have internal crack traces. Occasional quartz grains or overgrowths appear "dirty," perhaps from included iron oxide stippling or markings consistent with them being detrital, while other grains are speckled (some heavily making them look "dirty") with streaks of iron oxide. Such "dirty" quartz grains may likely be chert clasts.

In many places the mosaic is so well overgrown and/or totally cemented in such a tight fit that the boundaries between the small-medium quartz grains are faint and have almost disappeared, resulting in one apparent solid mass of quartz in optical continuity. However, some faint or heavy streaks of iron oxide still outline the original detrital quartz grain shapes, which sometimes are also evident with different extinction angles under crossed polars. Otherwise generally there is a clear infilling quartz cement between the quartz grains. Some patches of the mosaic in some samples appear to be recrystallized as they consist of small quartz grains with sharp euhedral contacts meeting at triple points. In other samples there are some large angular fractured quartz grains that display evidence of healing along the thin fracture zones, which consist of many tiny quartz sub-grains with different extinction angles, while these large grains are themselves in triple point contacts with surrounding smaller quartz grains.

In some portions of these mosaics the quartz grains, whether large or small, can appear to be tabular or slightly elongated and subtly parallel to the bedding, or sometimes at various angles to the bedding. Some embayed large rounded and euhedral grains have other grains protruding into them. One huge quartz grain impinges into an adjoining quartz grain and consists of an internal original sub-angular detrital grain covered in wavy dirty lines and speckles of iron oxide as well as the iron oxide outline, with its overgrowths in optical continuity. Sometimes the matrix mosaic consists of a mixture of large and small quartz grains with irregular to polygonal shapes still meeting at triple points. In other samples some matrix mosaic quartz grains and their overgrowths (cement) are in optical continuity with the very large and huge grains they surround. One medium sub-angular to sub-rounded matrix mosaic quartz grain has internal thin needles of rutile (?), while one medium sub-angular irregularly-shaped mosaic quartz grain contains a fluid inclusion (?).

K-Feldspar

Scattered throughout the mosaic of cemented quartz grains, wedged in as a part of the mosaic, are numerous subordinate K-feldspar grains and former laths, and some broken fragments. They vary in size from very small to large and a few huge (0.04-4.03mm,

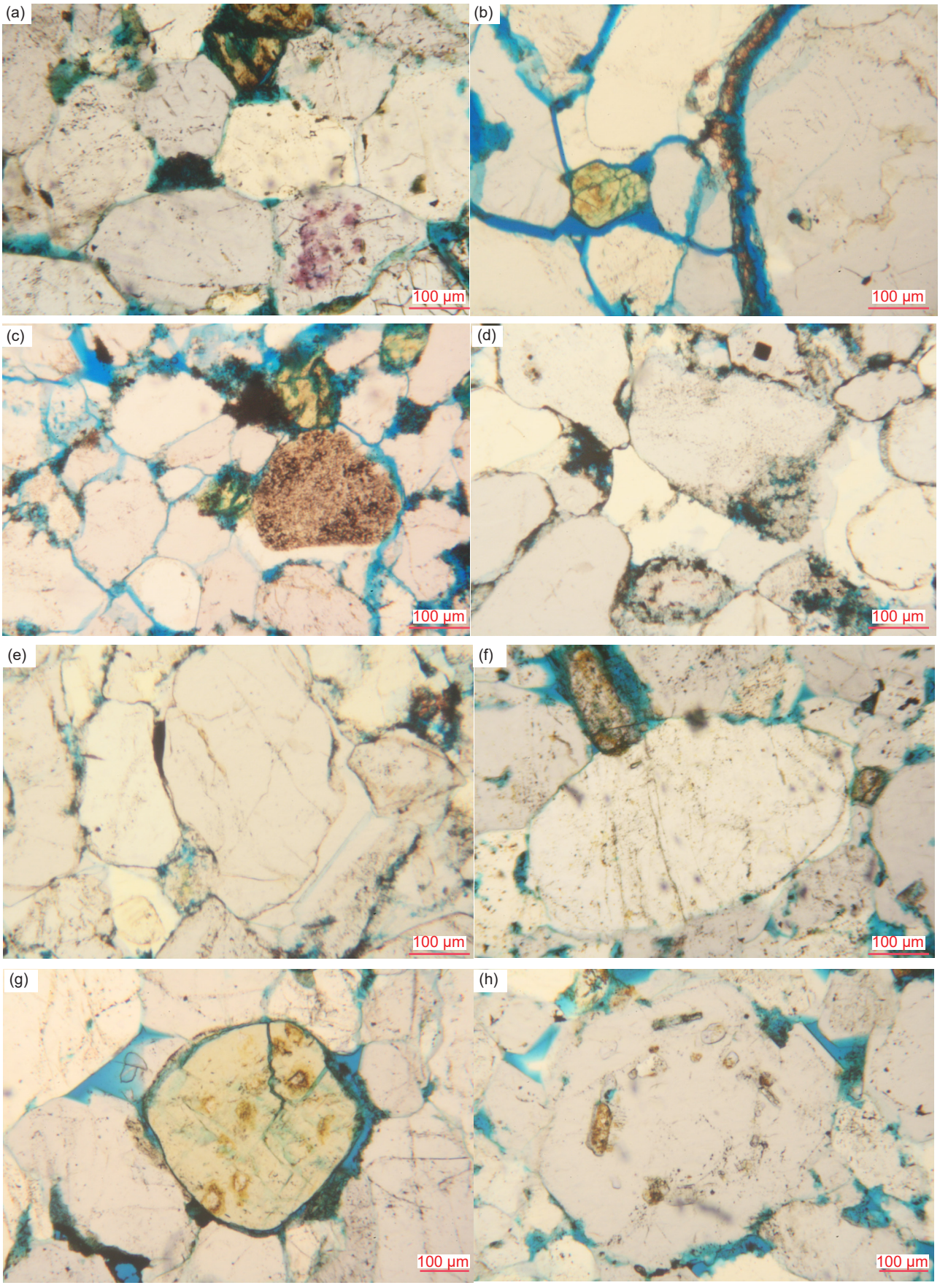
(a)
100 μm
(b)
100 μm
(c)
100 μm
(d)
100 μm
(e)
100 μm
(f)
100 μm
(g)
100 μm
(h)
100 μm

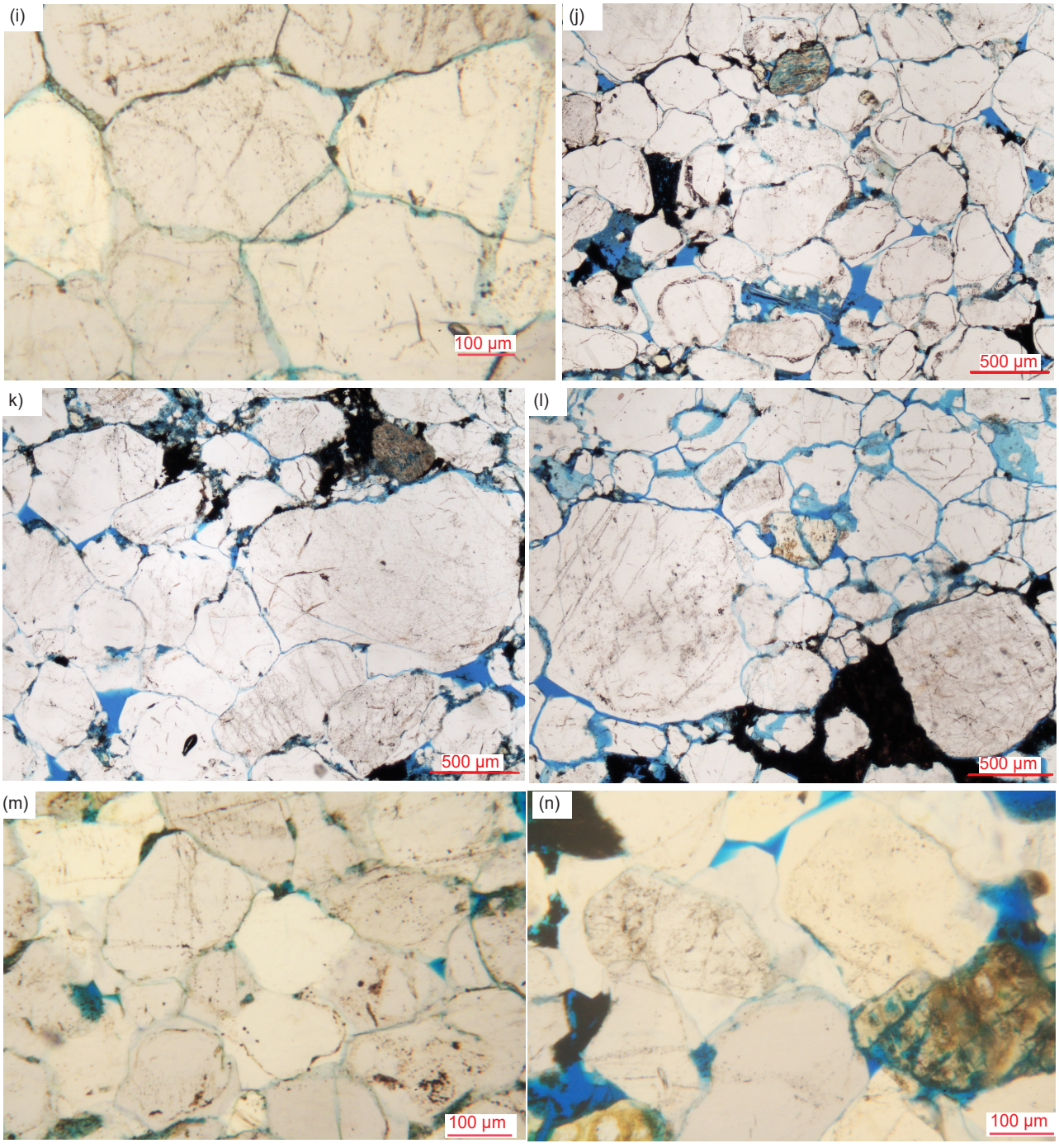
(i)
100 µm
(j)
500 µm
k)
500 µm
(l)
500 µm
(m)
100 µm
(n)
100 µm

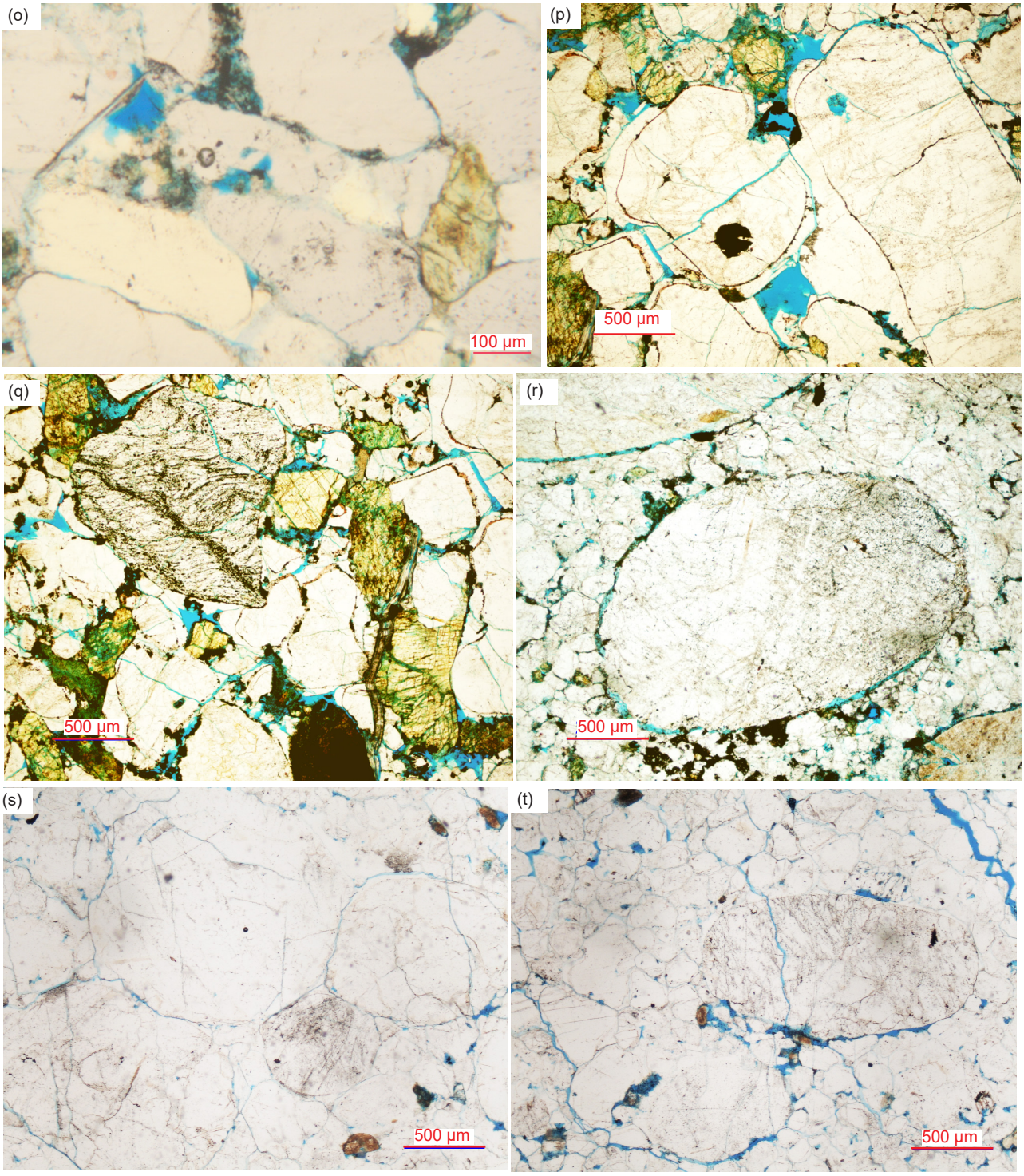
(o)
100 µm
(p)
500 µm
(q)
500 µm
(r)
500 µm
(s)
500 µm
(t)
500 µm

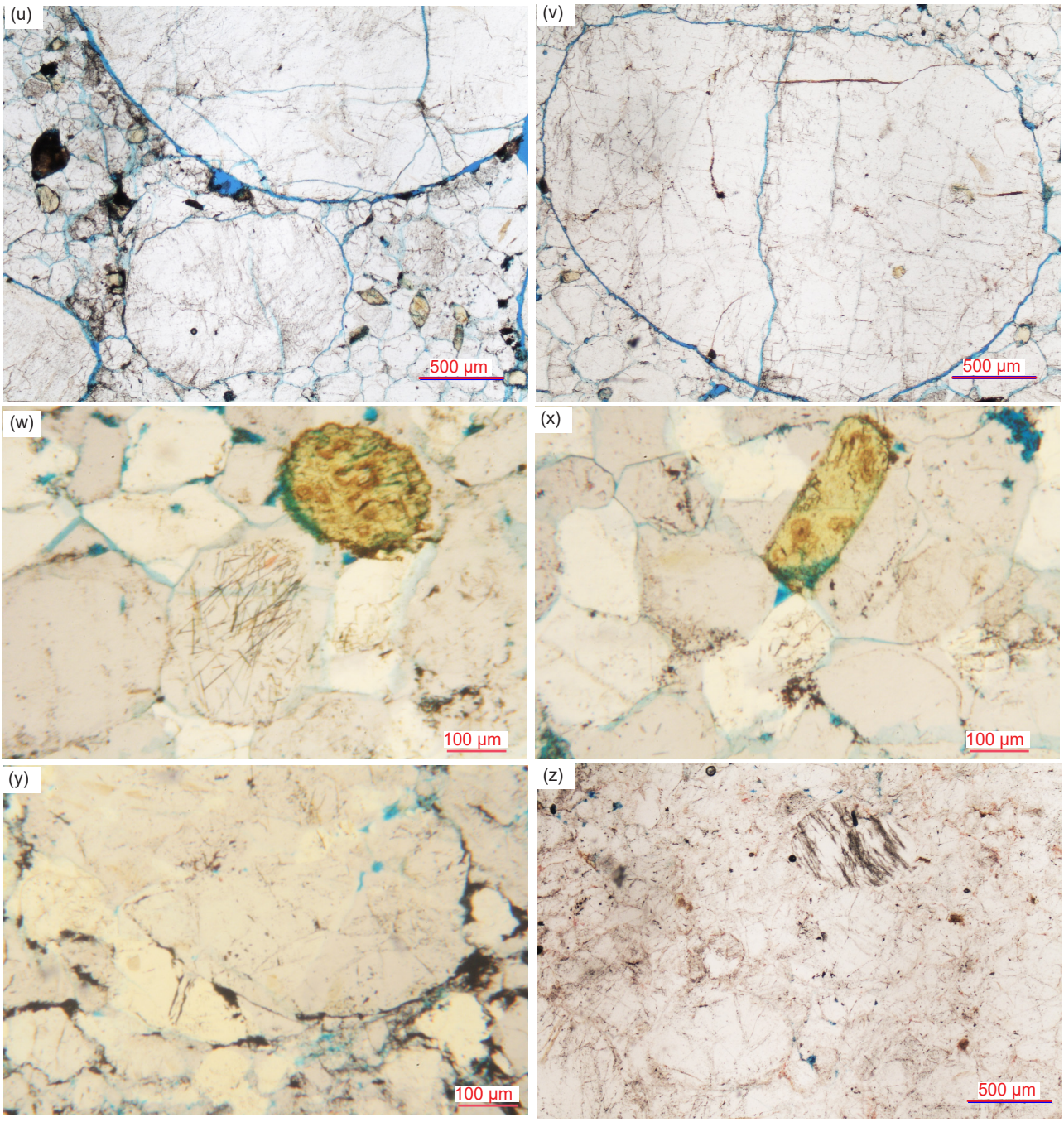

Fig. 29 (pages 210, 211, 212, and 213). A representative set of photomicrographs at various scales (as indicated) showing the quartz grains and quartz cement in the Tapeats Sandstone samples (location details provided in table 2). The thin sections were stained for ease of distinguishing K-feldspar and calcite. Note the variations in grain sizes, shapes, inclusions, and sorting. Most samples have some residual pore spaces (usually highlighted by the blue dye), but most pores have been infilled with quartz cement (as overgrowths), or in a few places by calcite and/or iron oxides, which gives the appearance of close packing, whereas the continued presence of many pores indicates only moderate compaction of the sandy sediment. (a) TSS-01, (b) TSS-02 (c) TSS-03, (d) TSS-04, (e) TSS-04, (f) CCF-01, (g) CCF-02, (h) CCF-03, (i) CCF-04, (j) CCF-06, (k) CCF-07, (l) CCF-08, (m) CCF-09, (n) CCF-10, (o) CCF-11, (p) MF-02, (q) MF-02, (r) MF-05, (s) MF-07, (t) MF-07, (u) MF-08, (v) MF-08, (w) MF-09, (x) MF-09, (y) MF-10, and (z) MF-10.

ϕ=+4.64–-2.01, coarse silt to very coarse sand and small granule size), are often rounded but sometimes euhedral or sub-euhedral (some partially), are usually fully altered (some highly) or altered around their edges with some iron oxide staining, and some are even cracked (fig. 30). Several larger rounded and cracked K-feldspar grains have angular K-feldspar fragments nearby. The K-feldspar grains occur in three distinct size groupings—many small grains and fragments, a few medium-sized grains, and many larger, some huge, grains and former laths, some of which have been rounded or have corroded or ragged edges and are usually surrounded by the molded mosaic of small and medium quartz grains (some of which are euhedral), between which they are wedged (likely by quartz grain overgrowths as quartz cement in optical continuity). A few K-feldspar grains retain part of their normal tabular euhedral habit, while several are half-moon shaped, most likely due to abrasion during transport and deposition. Some medium and large K-feldspar grains exhibit cross-hatched twinning under crossed polars, characteristic of microcline.

Most K-feldspar grains are altered, especially some large and very large laths. Some also have calcite veins or linings, patches of calcite alteration on them, large portions or wholly replaced by calcite, or ends with a thin calcite coating. Iron oxides occur especially in cracks (often along cleavage planes) and often coat the grains as speckles or stains. Several altered former K-feldspar grains and laths or broken portions of them, and a medium angular heavily-altered K-feldspar lath, are included within and surrounded by large and huge quartz grains, while several huge, altered K-feldspar laths have small rounded quartz inclusions, which may represent silica produced by the alteration or be due to original exsolution. A large angular altered K-feldspar grain is included in a large quartz grain with sub-domains, while several small, rounded, altered K-feldspar grains are included with tiny-small edge-on altered muscovite flakes within similar huge quartz grains. Several huge (2.83-4.03 mm, ϕ=-1.50–-2.01, granule-size) euhedral K-feldspar laths with sub-angular to sub-rounded corners, and many medium-large rounded K-feldspar grains (often former laths), are not only cracked but some display warped and stressed cross-hatched twinning extinction under crossed polars. Some large irregular grains and very large euhedral laths of K-feldspar have small-medium rounded inclusions of quartz cement, the laths being fractured and bent between adjoining very large quartz grains. One ragged remnant of a former large K-feldspar lath has been partially replaced by calcite and iron oxides but beyond its ragged edge and around its other perimeter is halite, all wedged between quartz grains.

Plagioclase

Within the molded matrix are quite a few large rounded and sometimes elongated grains, or smaller angular or rounded grains or fragments, variably altered to clay(?) minerals and iron oxides, that exhibit remnants of definite or possible multiple twinning under crossed polars characteristic of plagioclase (fig. 31). These surviving plagioclase grains are found in approximately half the samples, with generally two-five such grains per sample. They range in size from small (0.07-0.22 mm, ϕ=+3.77–+2.19) through medium (0.26-0.50 mm, ϕ=+1.95–+1.00) to a few larger (0.53-0.61 mm, ϕ=+0.92 –+0.70) grains. Some have retained their original tabular lath shape, but many others have been abraded to be sub-angular to sub-rounded. Some are still fresh, but most have been altered to varying degrees, yet they all retain the multiple twinning under crossed polars characteristic of plagioclase. Some grains are broken remnants of former laths, while many grains have been rounded by abrasion during transport and deposition.

Muscovite

There are numerous muscovite flakes in every sample, in spite of muscovite not being recorded in the XRD analyses (table 3). This is likely due to the XRD registering the muscovite as illite because the muscovite has been degraded, as is evident in some of the samples. Most muscovite flakes occur edge-on in the thin sections, which were cut perpendicular to the bedding in the sandstone (fig. 32). This suggests the flakes were generally deposited parallel and subparallel to the bedding, though some are at various angles to the bedding, and a few even perpendicular to the bedding. The flakes range in size from tiny (0.03-0.05 mm long, ϕ=+5.01–+4.23) through small (0.07-0.23 mm long, ϕ=+3.77–+2.13) and medium (0.25-0.42 mm long, ϕ=+2.00–+1.25) to large (0.50-0.76 mm long, ϕ=+1.00–+0.40) and very large (1.30-2.20 mm long, ϕ=-0.37–-1.13). They are invariably thin and wedged at different angles between and bent (sometimes even contorted) around the quartz and K-feldspar grains (and in one instance a zircon grain) in the tightly packed mosaic, in two instances bending around or jutting into iron-oxide-filled former pores (?). Thus, these muscovite flakes appear to be detrital.

Some edge-on flakes are thick and fresh, some with pronounced bends, and/or frayed and split-apart/frayed or bent ends (fig. 32d, g and m). Thick edge-on flakes are generally 0.09–0.16 mm thick, but one is very thick at 0.47 mm. There are even pairs of offset splayed edge-on flakes, which occasionally are thick and sometimes bent. One long moderately thick edge-on muscovite flake has one broken end

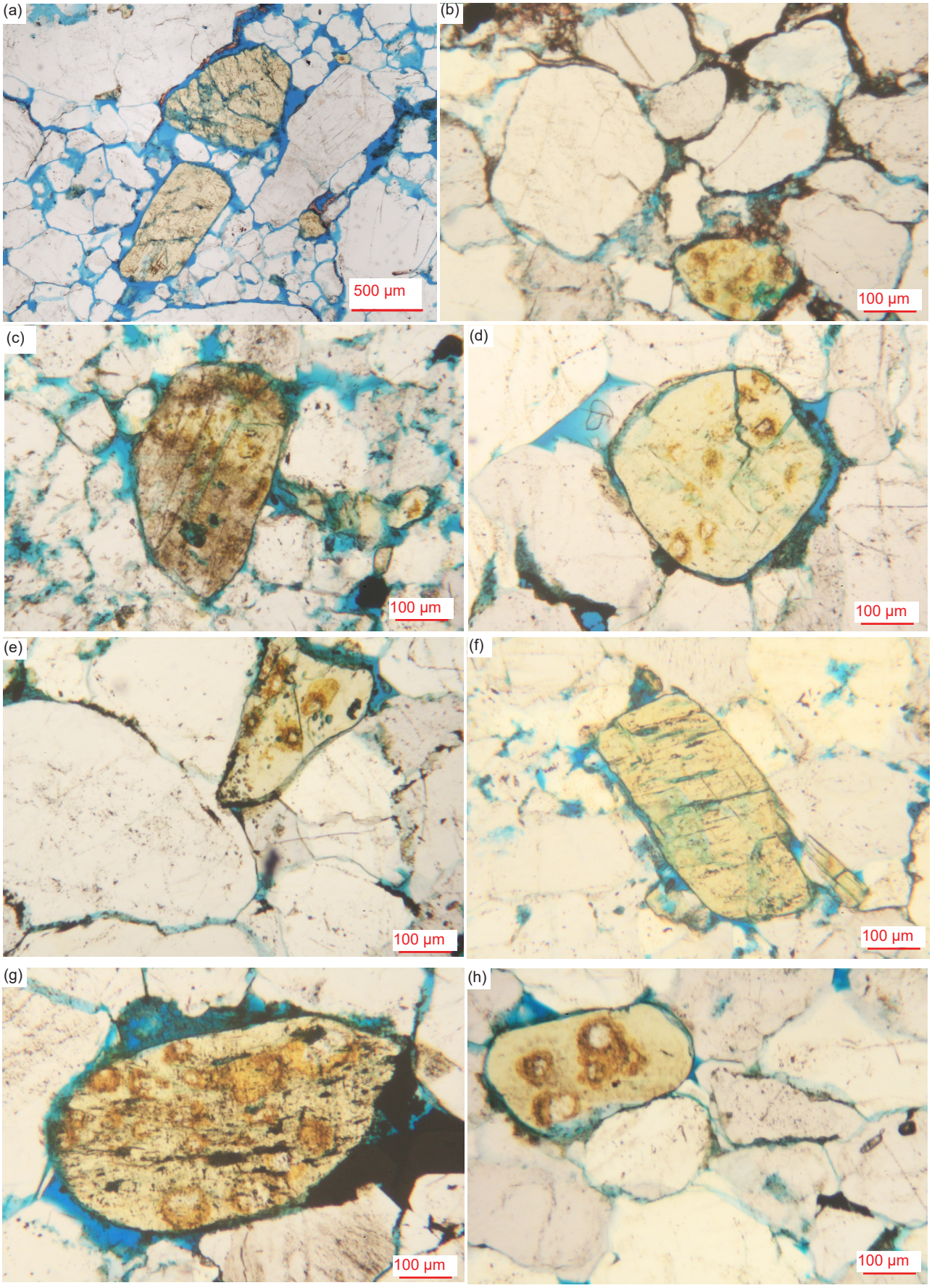
(a)
500 µm
(b)
100 µm
(c)
100 µm
(d)
100 µm
(e)
100 µm
(f)
100 µm
(g)
100 µm
(h)
100 µm

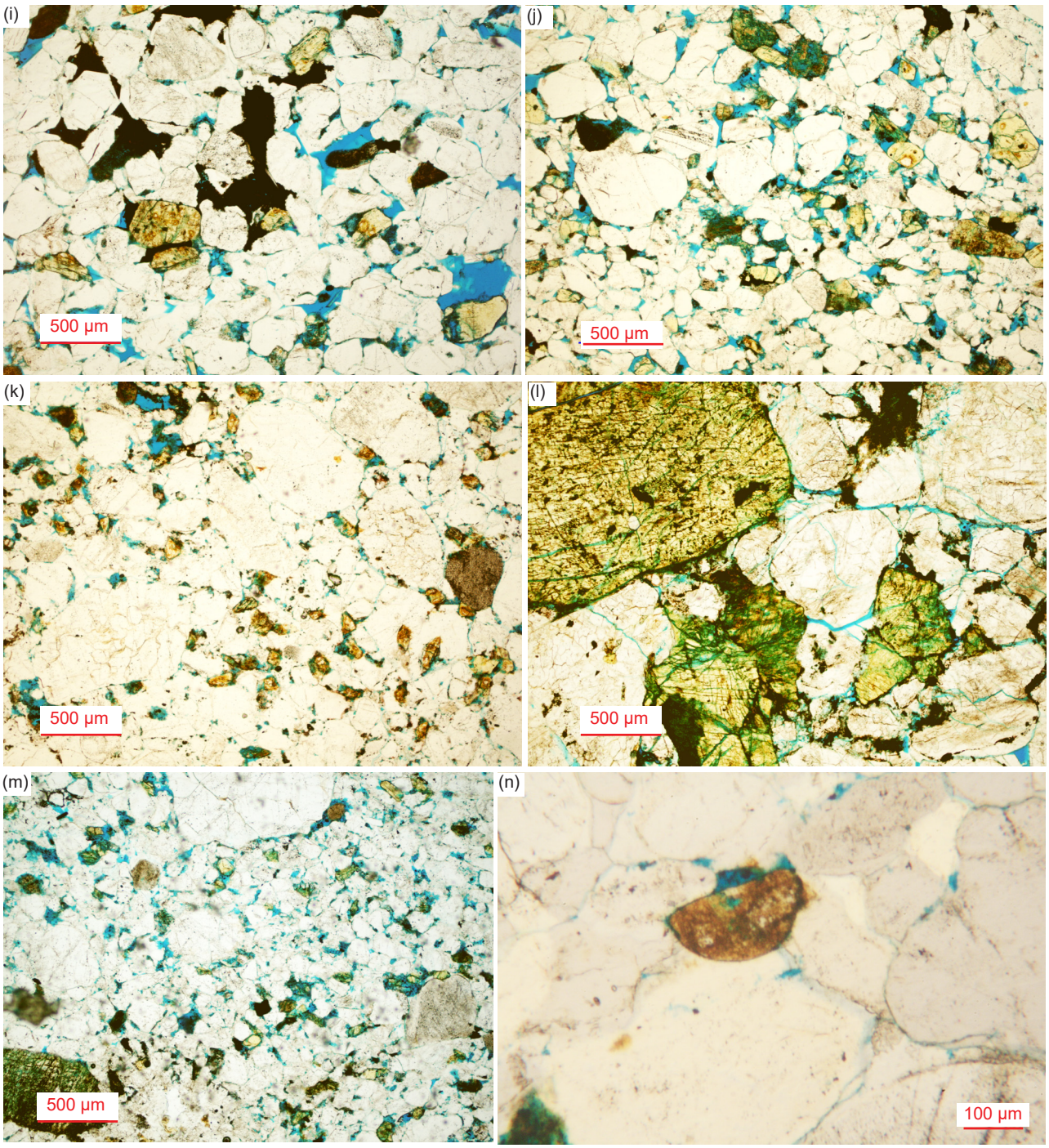
(i)
500 µm
(j)
500 µm
(k)
500 µm
(l)
500 µm
(m)
500 µm
(n)
100 µm

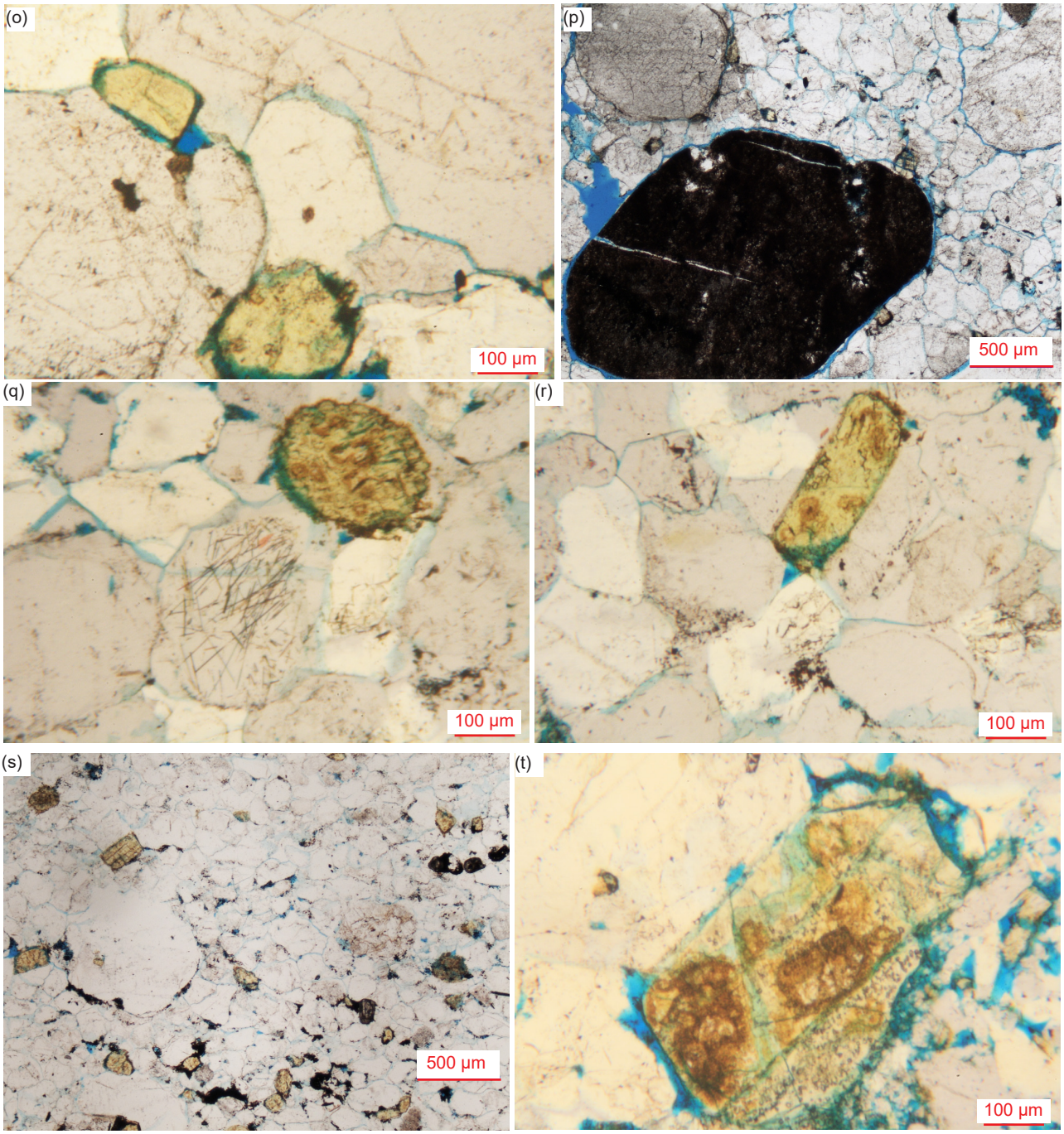

Fig. 30 (pages 215, 216, and 217). A representative set of photomicrographs at various scales (as indicated) showing the K-feldspar grains of various sizes, shapes and states of alteration in the Tapeats Sandstone samples (location details provided in table 2). The thin sections were stained for ease of distinguishing K-feldspar and calcite. While most K-feldspar grains are rounded, many have retained their original lath shape, also with the cleavage still evident. (a) TSS-2, (b) TSS-04, (c) CCF-01, (d) CCF-02, (e) CCF-04, (f) CCF-05, (g) CCF-08, (h) CCF-09, (i) CCF-10, (j) CCF-11, (k) CCF-12, (l) MF-02, (m) MF-05, (n) MF-07, (o) MF-08, (p) MF-08, (q) MF-09, (r) MF-09, (s) MF-09, and (t) MF-10.

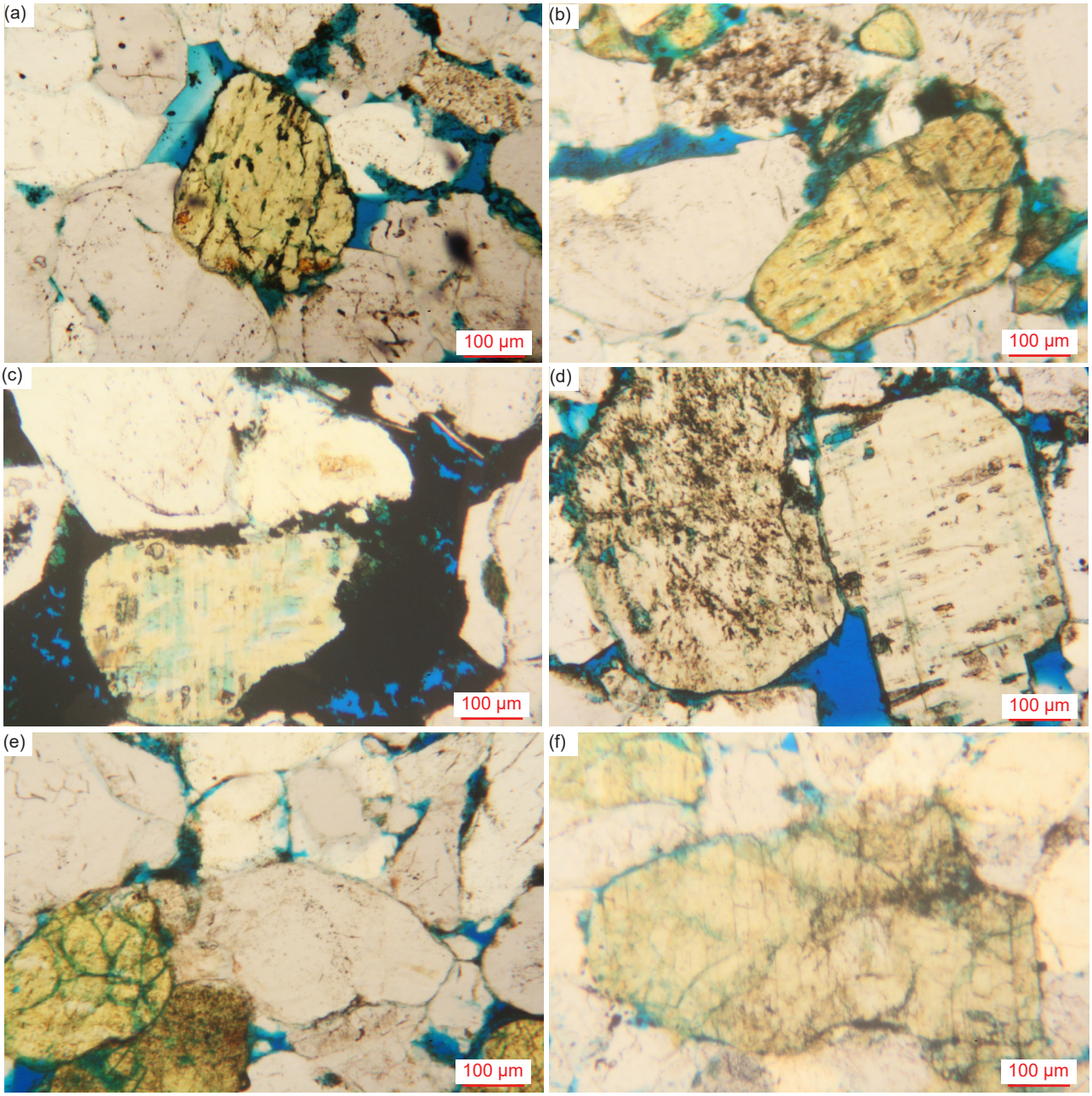

Fig. 31. A representative set of photomicrographs at the same scale (as indicated) showing the plagioclase grains, evident from the multiple twinning under crossed polars, and distinguished from K-feldspar grains alongside them in some samples. Most are rounded, but a few have retained their original lath shape. The thin sections were stained for ease of distinguishing K-feldspar and calcite. (a) CCF-03, (b) CCF-05, (c) CCF-06, (d) CCF-07, (e) CCF-11, and (f) MF-05.

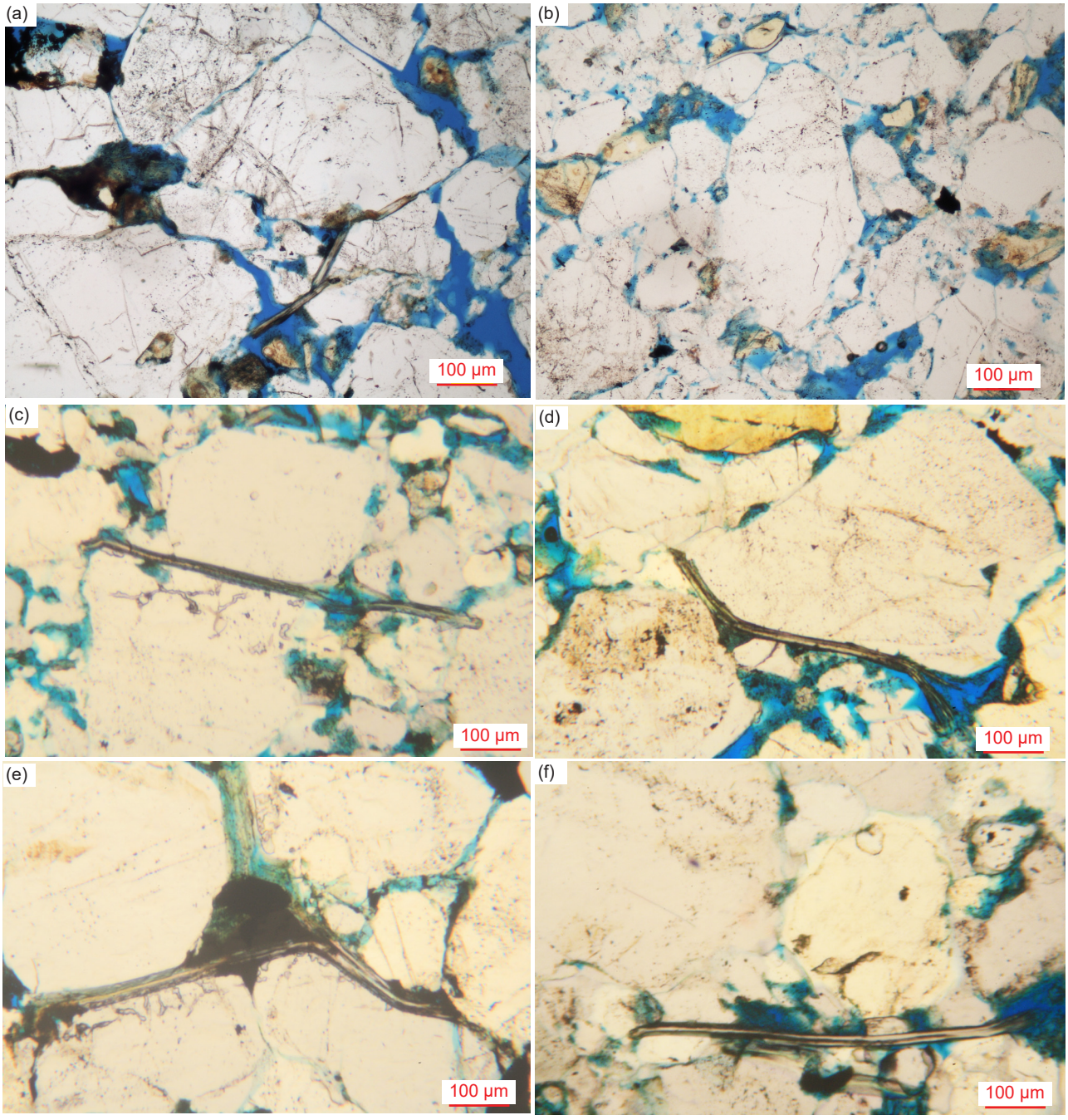
(a)
100 µm
(b)
100 µm
(c)
100 µm
(d)
100 µm
(e)
100 µm
(f)
100 µm

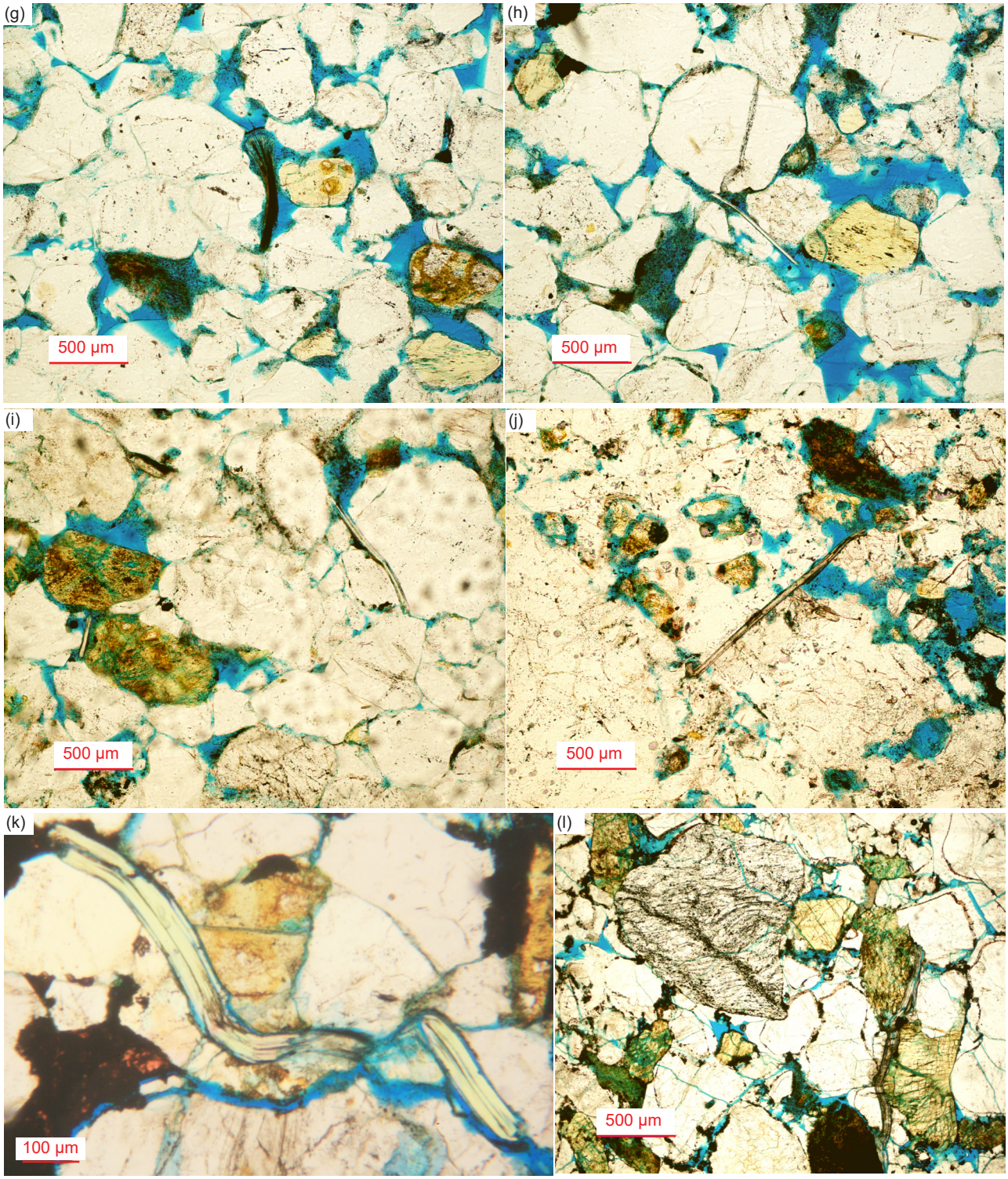
(g)
500 μm
(h)
500 μm
(i)
500 μm
(j)
500 μm
(k)
100 μm
(l)
500 μm

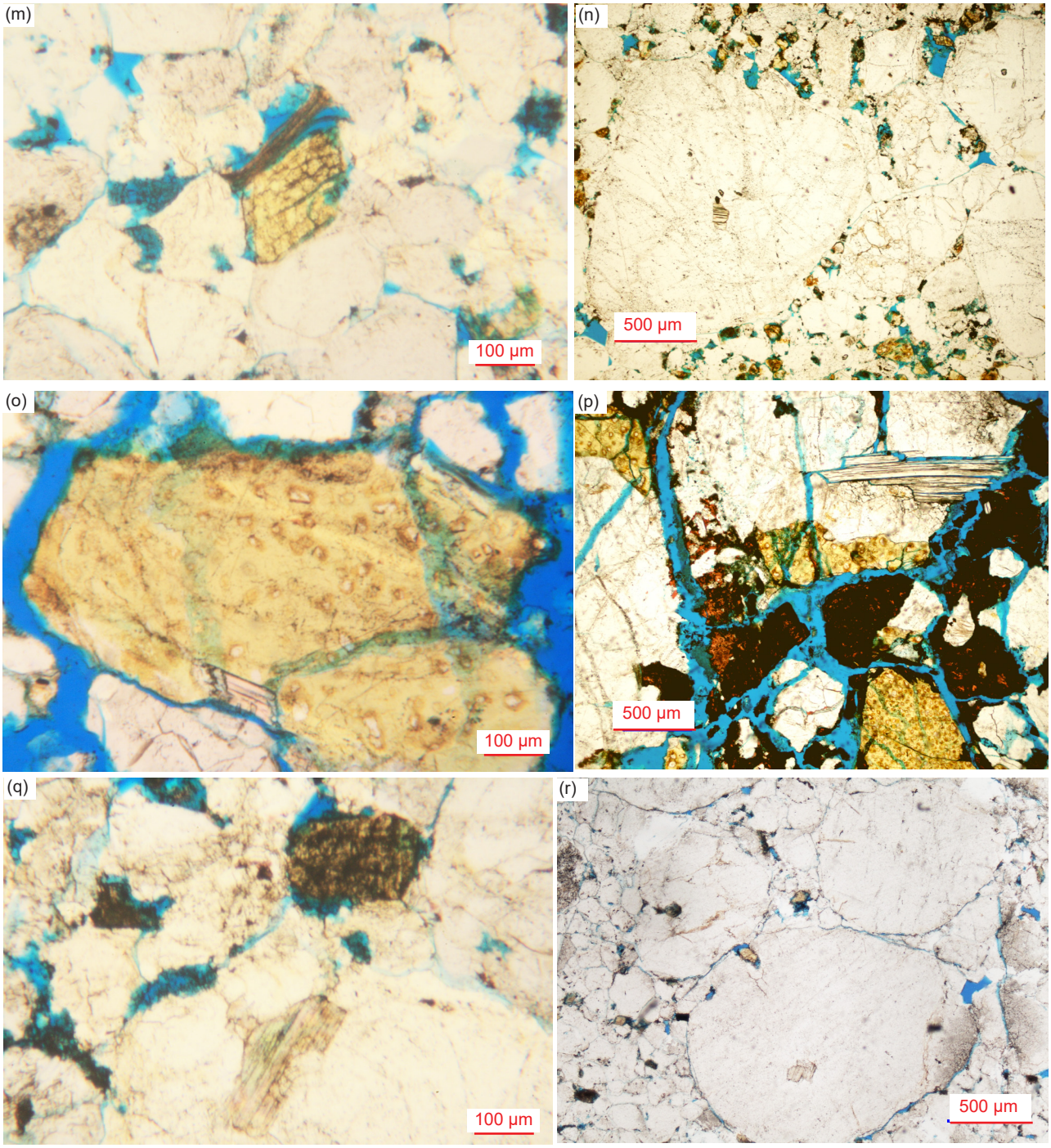

Fig. 32. A representative set of photomicrographs at various scales (as indicated) showing typical muscovite flakes in the Tapeats Sandstone samples with features such as frayed or flayed ends and/or bent around quartz and K-feldspar grains indicating they are detrital grains. The thin sections were stained for ease of distinguishing K-feldspar and calcite. Edge-on flakes predominant and some have expanded due to alteration: (a) TSS-01, (b) CCF-01, (c) CCF-05, (d) CCF-05, (e) CCF-06, (f) CCF-07, (g) CCF-10, (h) CCF-10, (i) CCF-11, (j) CCF-12, (k) MF-01, (l) MF-02, and (m) MF-06. Face-on inclusions within quartz and K-feldspar: (n) CCF-12, (o) MF-01, (p) MF-01, (q) MF-06, and (r) MF-08.

with a broken piece twisted back, and the other end bent and frayed, and is wedged tightly at an angle between mosaic quartz grains. Other edge-on muscovite flakes are thick and degraded (expanded by alteration), sometimes iron-oxide-stained, and even partially replaced by iron-oxide-stained calcite. Thick "books" of edge-on muscovite flakes also occur, one narrow (0.20 mm) but incredibly thick (0.16 mm) "book" being wedged between two large quartz grains. Some edge-on muscovite flakes are very long and/or thick (up to 2.20 mm long and 0.30 mm thick), often expanded between sheets with the ingress of alteration and have frayed ends. Other very long altered (and expanded) edge-on muscovite flakes with some frayed ends are broken into thick pieces, and altered with accompanying calcite, quartz and iron oxides. In one instance the remnants of a totally frayed and pulled-apart thick altered edge-on muscovite flake are between mosaic quartz grains.

Other edge-on muscovite flakes are embedded in or even appear to cross-cut quartz grains. Furthermore, numerous tiny-very small (0.03-0.12 mm long, ϕ=+5.01–+3.06), and a few small-medium (0.14-0.25 mm, ϕ=+2.84–+2.00), thin and thick, occasionally curved, fresh, or altered, edge-on muscovite flakes are totally included within mosaic small and medium quartz grains and their overgrowths. Sometimes the ends of the included edge-on muscovite flakes are frayed. One medium (0.23 mm long, ϕ=+2.13), thick edge-on muscovite flake is at an angle included within and beyond the edge of a large quartz grain. Three large altered/degraded muscovite flakes with iron oxides along cleavages, and in part broken, are embedded in huge quartz grains which are now fractured and surrounded by smaller mosaic quartz grains. Several small (0.12-0.14 mm, ϕ=+3.06 –+2.84) edge-on altered muscovite flakes are included within the sub-domains of very large, rounded quartz grains. One small (0.10 mm, ϕ=+3.32) edge-on thick (0.04 mm) muscovite flake is even included in the edge of a very large altered and broken K-feldspar lath.

There are also many tiny-very small (0.03-0.10 mm wide, ϕ=+5.01–+3.32) and small-medium (0.12-0.22 mm wide, ϕ=+3.06–+2.19) face-on muscovite flakes included in medium, large, very large and huge, rounded, sub-euhedral and part-euhedral quartz grains, and even a K-feldspar grain, one accompanied by a small tabular iron oxide grain (fig. 32n-r). Three tiny-very small (0.03-0.12 mm, ϕ=+5.01–+3.06) face-on muscovite flakes (one altered) are wedged between mosaic quartz grains, while two tiny-very small (0.03-0.09 mm, ϕ=+5.01–+3.47) face-on muscovite flakes are wedged between sub-domains within the edges of two huge, rounded quartz grains. Two irregularly-shaped, one medium (0.22 mm wide, ϕ=+2.19) and one small, partially face-on/edge-on muscovite flakes are included within very large quartz grains.

Biotite

At least five samples each contain one medium to very large, sub-angular or rounded, quartz grain with one-two face-on biotite flakes included in it (fig. 33). These biotite flakes range in size from 0.08 mm to 0.20 mm wide (ϕ=+3.64–+2.33). In two instances these face-on biotite flakes are altered, one having one end partly altered to calcite.

Zircon

Half the samples (13) each contain at least one-two high relief, high birefringent, zircon grains (fig. 34). They are invariably very small (0.03-0.10 mm long, ϕ=+5.01–+3.32), but several are slightly larger (0.12-0.15 mm long, ϕ=+3.06–+2.75). Most are thin and tabular, but sub-rounded to rounded oval-shaped, are partially coated with iron oxides, and are tightly wedged between quartz grains in the mosaic fabric. One medium-large quartz grain contains several very small (0.03 mm, ϕ=+5.01) rounded zircon inclusions, while two small (0.07-0.08 mm, ϕ=+3.77–+3.64) prismatic zircon grains are included within a very large rounded but broken quartz grain.

Sphene (Titanite)

In two samples, in each there is a single small (0.13-0.18 mm diameter, ϕ=+2.95–+2.48), high relief, high birefringent grain of sphene (fig. 35). One is sub-rounded and gray, and the other is lozenge-shaped with rounded ends, and olive-gray. Both are embedded within quartz grains.

Rock Fragments

There are several rock fragments in almost every sample (fig. 36). Generally, they are small (0.09-0.23 mm, ϕ=+3.47–+2.13) and medium (0.28-0.47 mm wide, ϕ=+1.85–+1.09), but there are occasional large (0.50-0.91 mm, ϕ=+1.00–+0.14) and several very large (1.13-2.66 mm wide, ϕ=-0.17–-1.41) grains. Most of these rock fragments are rounded or sub-rounded, and some are elongated, though two are squarish with rounded corners, one large (0.91 mm, ϕ=+0.14) grain is half-moon-shaped, and one is a large granule size (2.66 mm wide, ϕ=-1.41), angular breccia fragment. Most fragments are altered, heavily-altered or weathered, and often stained with iron oxides, and a few have partially resorbed edges. Many of these rock fragments appear to be schist and/or fine-grained siltstone, though the iron oxide staining makes further identification difficult, while several rounded to sub-angular unaltered rock fragments may be siltstone. Some fragments

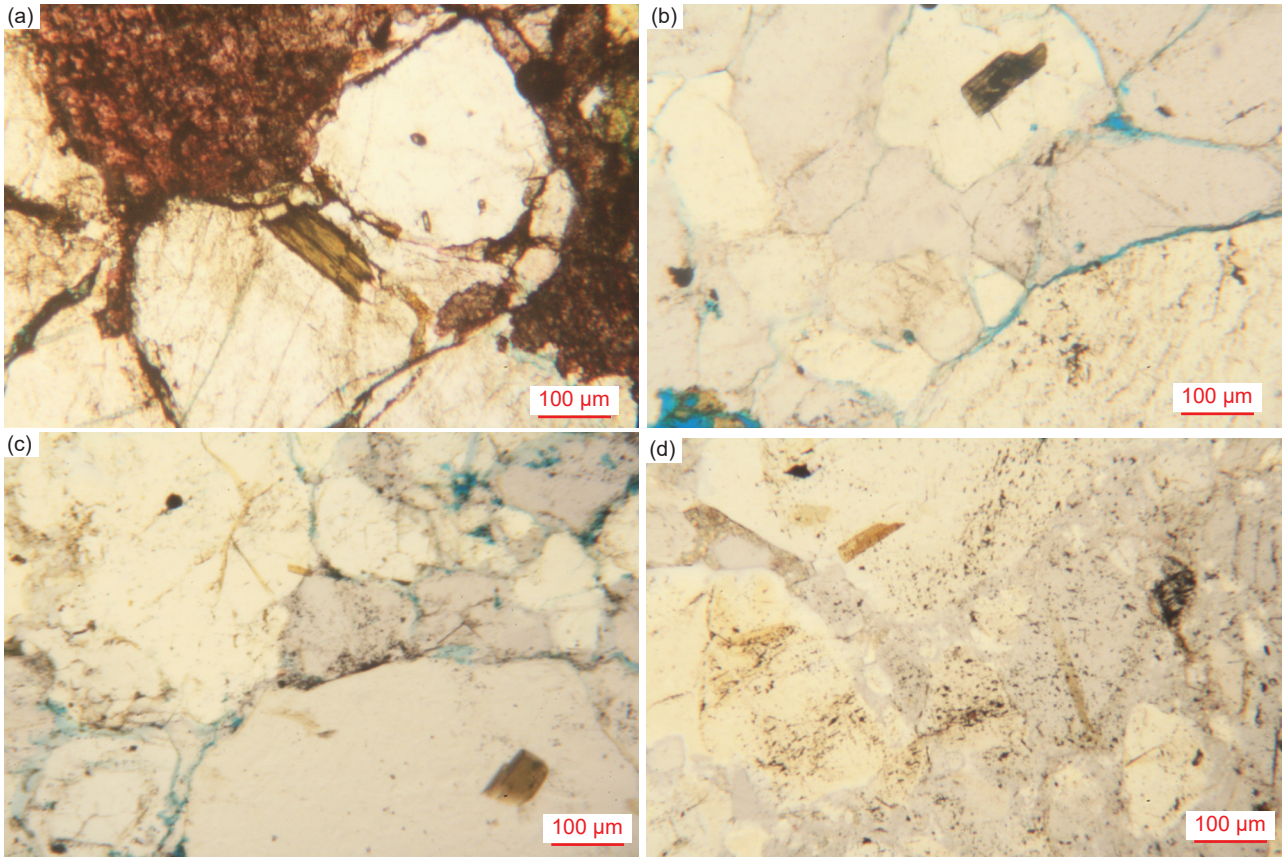

Fig. 33. A representative set of photomicrographs at the same scale (as indicated) showing face-on biotite flakes included in quartz grains. The thin sections were stained for ease of distinguishing K-feldspar and calcite. (a) MF-03, (b) MF-08, (c) MF-09, and (d) MF-10.

consist of patchworks of tiny irregularly-shaped, approximately equal-sized quartz sub-grains with different extinction angles under crossed polars giving the rock a "sugary" texture, or of small iron-oxide-stained polygonal quartz grains. These thus likely represent quartzite fragments. Other "dirty" quartz grains may be chert. Several other possible rock fragments consist of small bladed tabular grains or flakes with some relief and iron oxides between them (covering some other mineral?) or consist of many scattered iron oxide grains and blades between tiny quartz grains, with internal layering marked by iron oxides. Most of these rock fragments are wedged tightly in the mosaic of quartz grains of various sizes, including large rounded and smaller matrix quartz grains, "molded" around them, and include later quartz cement attached to them like overgrowths in apparent optical continuity. And a few rock fragments have their ends impinging on adjoining mosaic quartz grains, while others are within iron oxides filling a medium-sized pore in the precise shape needed between euhedral ends of medium and large quartz grains.

Calcite

The XRD analyses (table 3) indicate nine samples contain significant quantities of calcite, but it was observed in thin sections of ten samples (fig. 37). Calcite (with or without iron oxides) is often abundant locally between and lining the edges of quartz and K-feldspar grains, thus having penetrated between them to act as a late secondary trivial cement. Calcite also occurs as veins in cracks and fractures cross-cutting a few quartz or K-feldspar grains or laths. Sometimes calcite coats some K-feldspar grains in spots or as total replacements as alteration of them, with or without iron oxides, sometimes engulfing them. Calcite also occurs in scattered small, medium, and large totally-altered patches (with or without iron oxides, and rarely kaolinite or illite) that possibly are infilled pores, thus acting as a late secondary trivial cement. In one sample there is a linear area or band of very small-small calcite patches and small quartz grains, both with irregular edges with some iron oxides, and areas of calcite with iron oxides. Sometimes very small quartz fragments are cemented together with calcite and possibly infill pores or infill between partially resorbed larger quartz grains, the calcite clearly having been introduced to the rock fabric after its fracturing. In another sample wide vein-like patches and outright veins (sometimes thick)

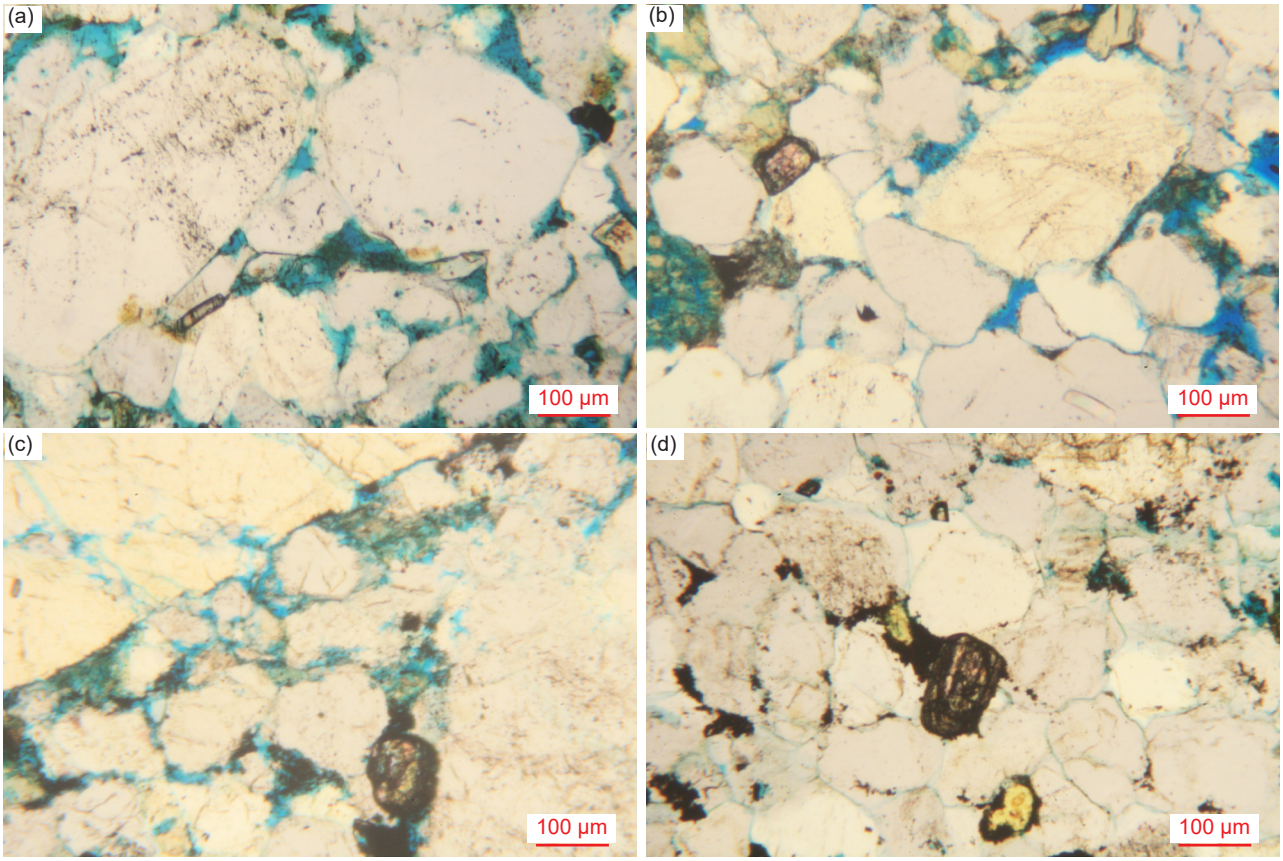

Fig. 34. Representative zircon crystals, evident from their high relief and high birefringence, as well as their tabular habit, found in many samples of the Tapeats Sandstone (scale as indicated). The thin sections were stained for ease of distinguishing K-feldspar and calcite. (a) CCF-02, (b) CCF-11, (c) MF-05, and (d) MF-09.

of calcite (with or without iron oxide staining) occur between (and sometimes across) overgrown very large quartz grains and altered K-feldspar ex-laths, in places appearing to replace the quartz and K-feldspar grain edges, as evidenced by their ragged edges. Sometimes the calcite entrains tiny quartz remnants. Elsewhere calcite patches infill between adjoining grains or displace angular quartz fragments, sometimes accompanied by patches of iron oxides. Calcite veining is also within and on the edge of a crushed quartz "mylonite" zone and around quartz "remnants." In yet another sample a thin vein of calcite ± quartz ± iron oxides cuts across earlier calcite between quartz grains.

Halite

While the XRD analyses in table 3 indicate four samples contain halite, it was only recognizable in two samples (fig. 38). In sample MF-03 (6.9% halite in table 3), there are many low relief (and

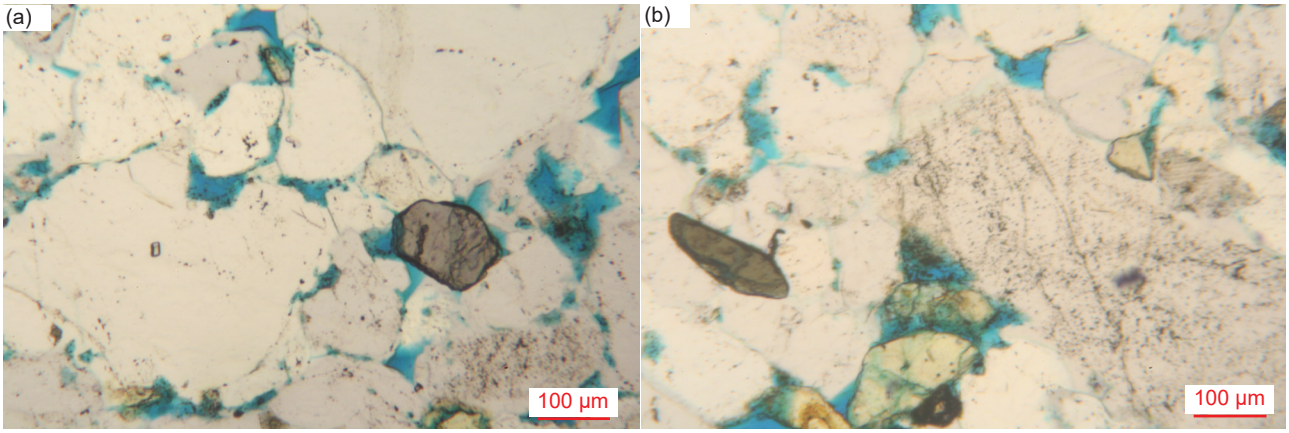

Fig. 35. Two sphene (titanite) crystals, evident from their lozenge-shape, color and high relief, found in two samples of the Tapeats Sandstone (scale as indicated). (a) CCF-01, and (b) CCF-03.

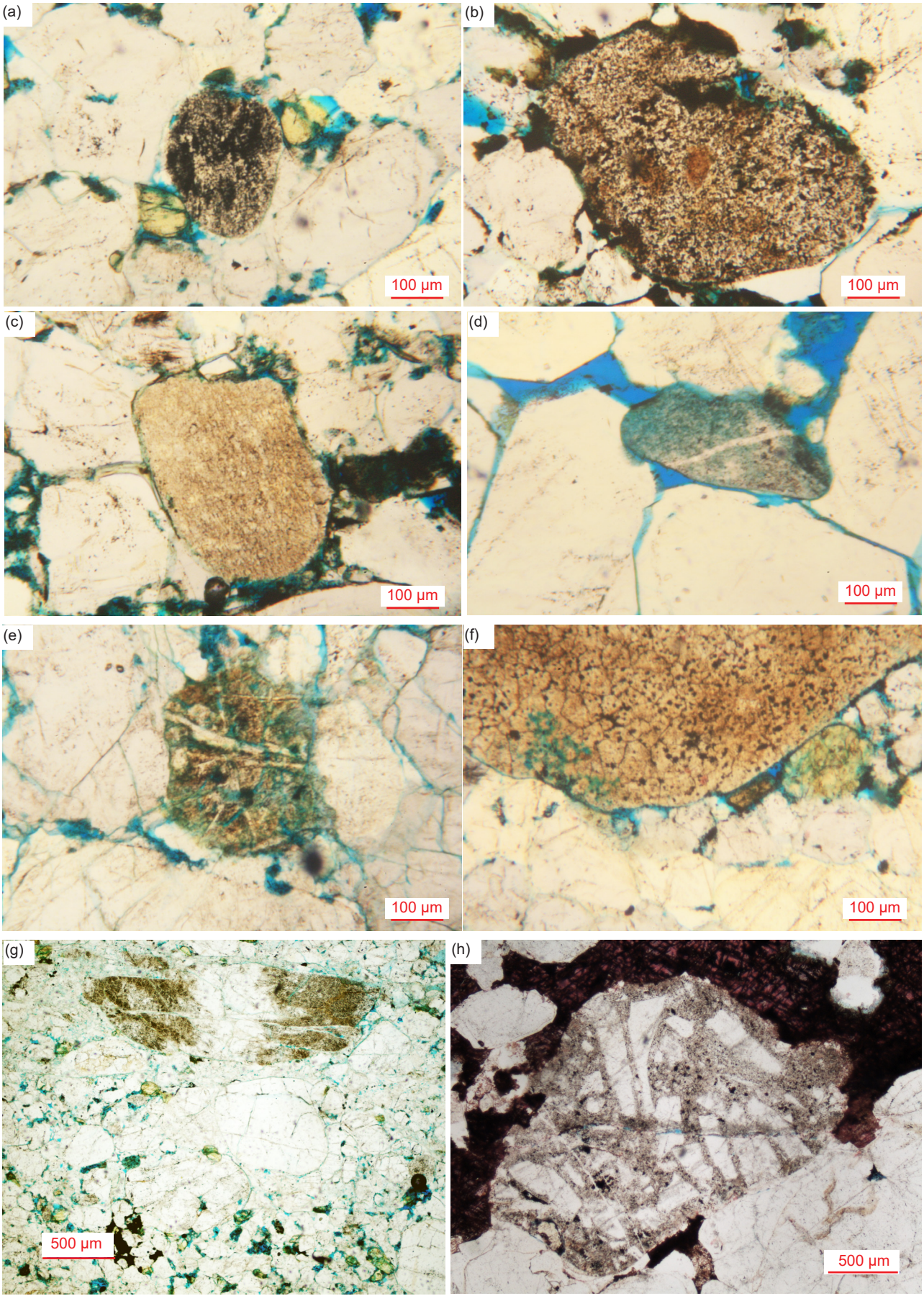
(a)
100 µm
(b)
100 µm
(c)
100 µm
(d)
100 µm
(e)
100 µm
(f)
100 µm
(g)
500 µm
(h)
500 µm

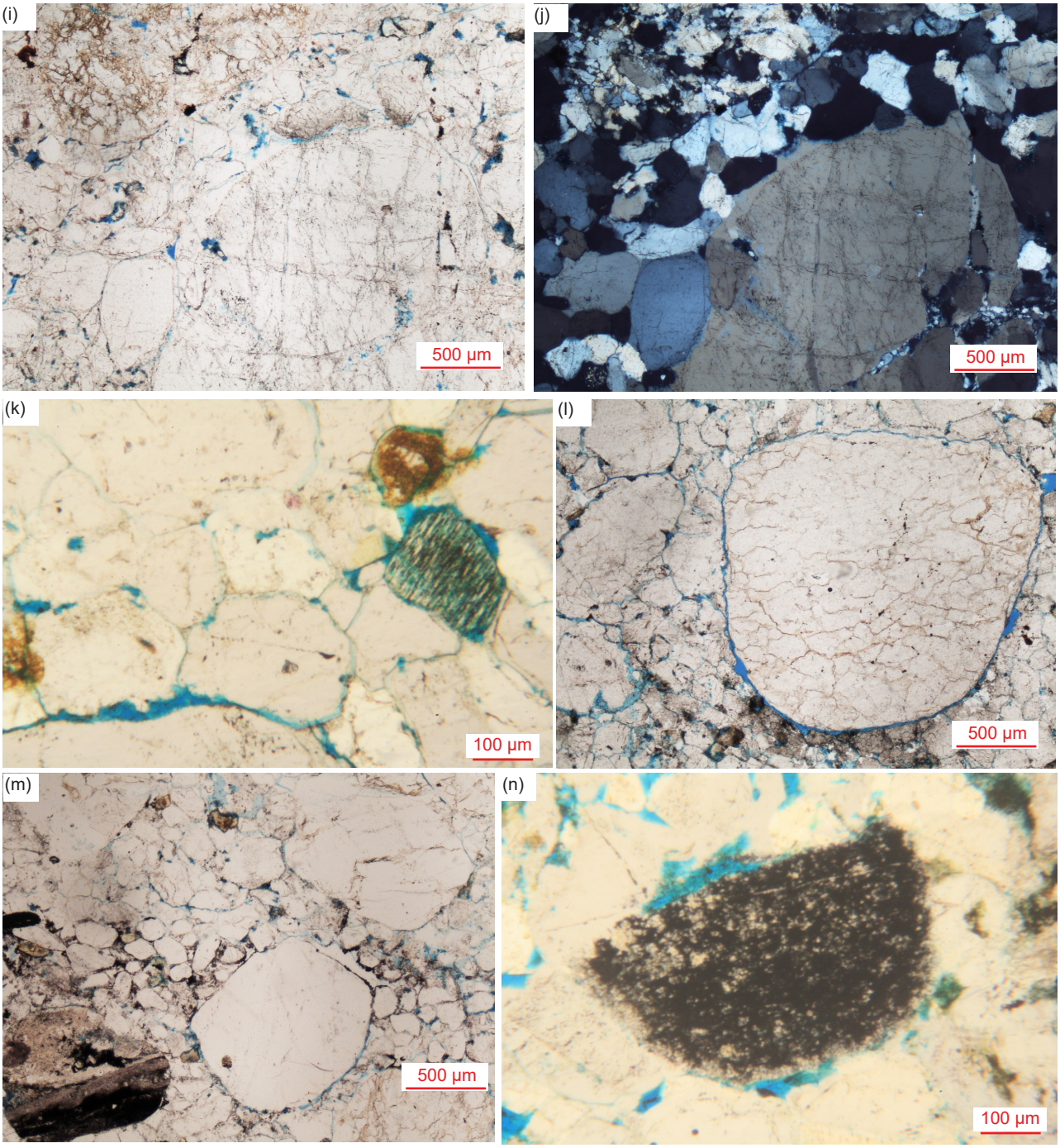

Fig. 36 (pages 225 and 226). A representative set of photomicrographs at various scales (as indicated) showing the rock fragments in the Tapeats Sandstone samples, often broken and/or rounded to sub-angular, tentatively identified as indicated. (a) CCF-05 siltstone, (b) CCF-06 siltstone, (c) CCF-07 quartzite, (d) CCF-08 quartzite, (e) MF-02 basalt, (f) MF-05 quartzite, (g) MF-05 siltstone, (h) MF-06 breccia, (i) MF-06 quartzite (plain polarized light) (j) MF-06 quartzite (crossed polars) (k) MF-07 schist, (l) MF-08 quartzite, (m) MF-09 breccia, and (n) MF-10 schist or siltstone.

isotropic) clear (cream) irregular, small and large, areas of halite sometimes with fuzzy edges or with fine "prominences" reaching out into adjoining quartz grains along fractures. Sometimes the halite is within, maybe replacing, huge quartz grains and large altered K-feldspar laths, and elsewhere occurs as veins across iron-oxide-stained calcite infilling between mosaic grains, indicating the halite was the latest alteration. There is also an area of small-medium (0.23-0.28mm, ϕ=+2.13–+1.85) polygonal clean grains of halite in association with calcite infilling between quartz and K-feldspar grains. In a second sample a large patch of low relief, isotropic halite adjoins iron-oxide-stained anhydrite alteration

between two large, rounded quartz grains next to a K-feldspar lath.

Anhydrite

The XRD analyses in table 3 indicate only one sample contains anhydrite (sample MF-04). In it, some veins of anhydrite (tiny, high birefringent grains and flakes) are along fractures in some quartz grains and between quartz grains, and some anhydrite patches replace the ends of K-feldspar laths and are between quartz grains. Small and large patches of partially iron-oxide-stained anhydrite alteration are between and draped around quartz grains, some potentially being infilled former pores. One patch of small anhydrite grains infills between broken pieces of overgrowths from adjacent quartz grains and abuts a patch of calcite against a K-feldspar grain, suggesting the anhydrite was the last alteration. There is also a thin anhydrite vein filling a fracture parallel to the bedding.

Iron Oxides

Iron oxides are always present in varying amounts in all samples (fig. 39). Occasional scattered iron oxides stain around and between, line, and/or heavily coat, quartz and K-feldspar grain edges (often making them irregular), or stain K-feldspar grains, and even coat or infill some former very small or small pore spaces, sometimes with calcite, illite or kaolinite, all of which added trivially to the secondary late cementing of the sandstone. There are occasional

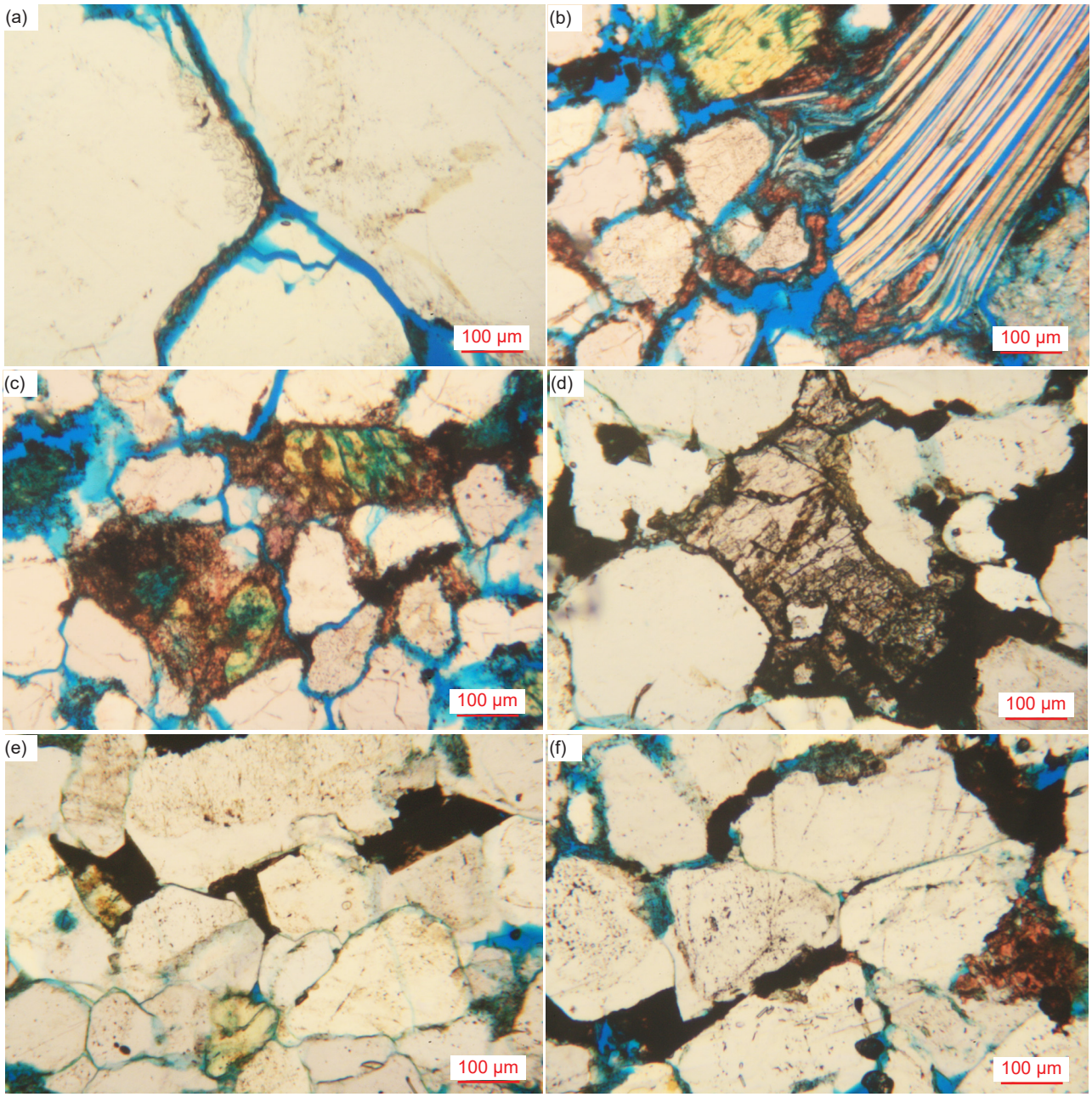

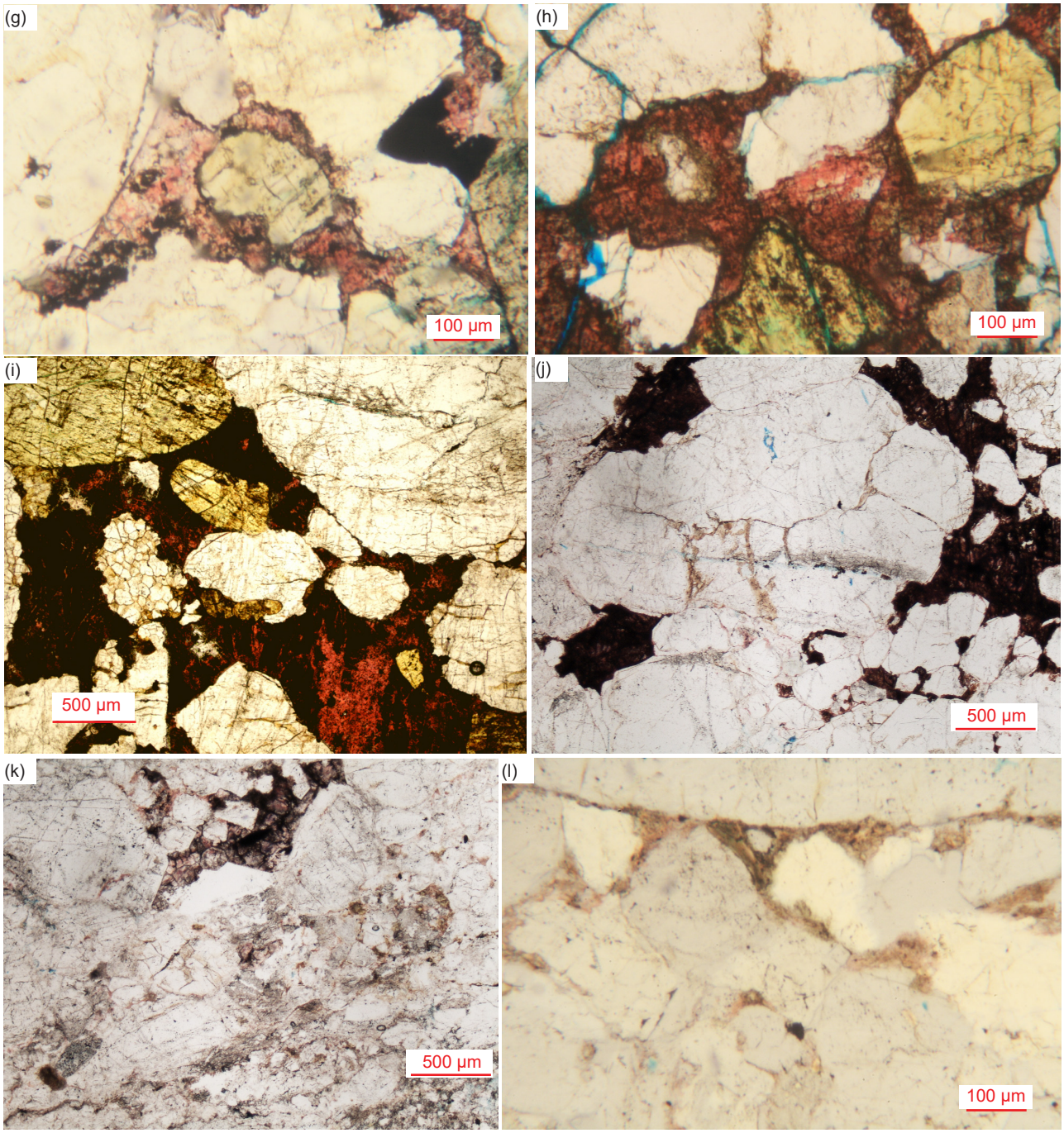

Fig. 37 (pages 227 and 228). A representative set of photomicrographs at various scales (as indicated) showing the calcite alteration (sometimes accompanied by iron oxides) as cement between or lining grains, or between edge-on muscovite sheets in the Tapeats Sandstone samples. The thin sections were stained for ease of distinguishing K-feldspar and calcite. (a) TSS-2, (c) TSS-03, (c) TSS-03, (d) CCF-06, (e) CCF-09, (f) CCF-10, (g) MF-02, (h) MF-03, (i) MF-04, (j) MF-06, (k) MF-10 and (l) MF-10.

small, medium, large, and very large iron oxide patches, blotches and streaks (possibly sometimes with illite alteration?) between and around some quartz and K-feldspar grains. Occasionally iron oxides fill in spaces shaped like former (resorbed) sub-euhedral quartz grains with straight edges or meet quartz grains at triple points suggesting they accompanied late kaolinite and/or illite alteration and/or infilling. In one sample, an area of iron-oxide-covered alteration with fuzzy edges adjoins a large K-feldspar lath with rounded corners, and in another sample, there are tiny illite/muscovite flakes after multiple K-feldspar laths that fill probable former pores. Iron oxides are also in some cracks and fractures within a few grains, or in one case a large streaky swath of iron oxides is over part of a large, altered K-feldspar lath. In all samples, iron oxides are in spots and streaks on many quartz grains and

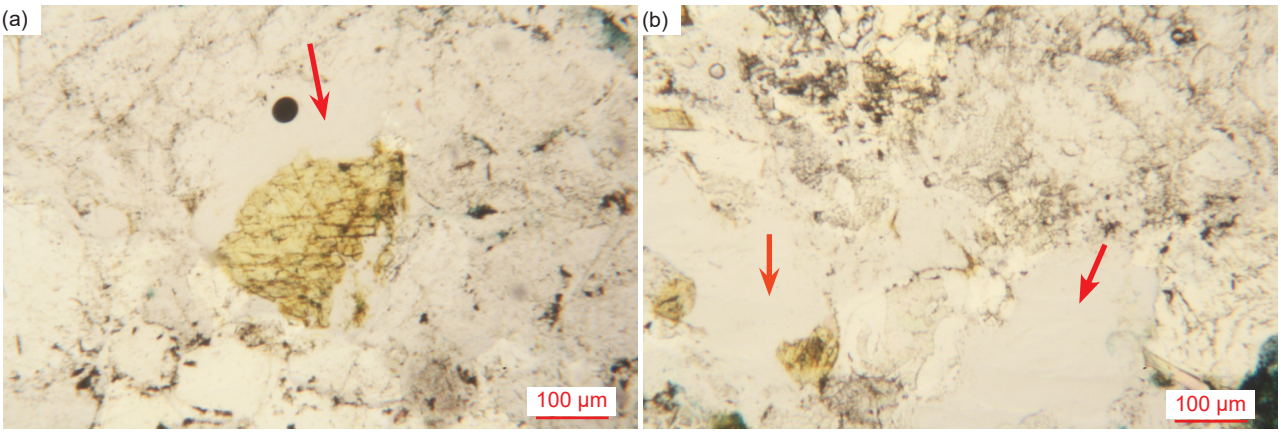

Fig. 38. Halite (as indicated by arrows) found in several Tapeats Sandstone samples (primarily from the Monument fold), evident from its low relief and clear, clean color in this sample (scale as indicated). (a) CCF-12, and (b) CCF-12.

as "ghost" outlines that delineate the original detrital grains. Iron oxides stain the "mylonite" zone cutting through one sample. Occasional calcite infilling or veining is also accompanied by iron-oxide staining, which clearly occurred after the cementing quartz overgrowths and often appears to be replacing the quartz grains. In one sample, a thin vein of calcite ± quartz ± iron oxides even cuts across earlier calcite between quartz grains.

Illite and Kaolinite

Even though illite and kaolinite are significant enough in only one sample each to register in the XRD analyses (samples MF-01 and TSS-04 respectively in table 3), the muscovite in some samples has been degraded and likely altered to illite. Additionally, the iron-oxide-stained patches of various sizes between quartz and other grains in some samples are likely former pores (or may potentially be after K-feldspar grains or laths) and are sometimes accompanied by alteration consisting of kaolinite and/or tiny illite flakes (and maybe other clay minerals) and occasionally with tiny quartz grains. Some of these patches are in the precise shapes needed between euhedral ends (likely cementing overgrowths) of medium and large quartz grains and so represent a later addition to the rock fabric after the quartz cementation, while other infilling patches encroach on the quartz and K-feldspar grains, perhaps with some resorption. Thus, these clay minerals would appear to be minor and secondary due to diagenesis after deposition of the sandstone. One large patch of alteration consists of a fan of radiating iron-oxide-stained bladed flakes of possible illite/smectite which replaces or covers a large oval quartz grain with remnants showing around the periphery, all between other quartz grains. In another sample a linear patch of alteration between quartz grains consists of tiny and small illite flakes with some iron oxides. Illite sometimes totally replaces former K-feldspar grains and laths, and some minor illite alteration accompanies the tiny quartz grains in parts of healed fracture zones.

Pores

As already noted, there are very few pore spaces remaining, since most pores have been filled by quartz (silica) cement as a result of quartz growing as overgrowths on the original detrital quartz grains. Furthermore, a few former pores have occasionally been filled with later secondary iron oxides, sometimes accompanying calcite or clay minerals. Nevertheless, there are some samples with significant remaining pore spaces, the amount varying within them, but sometimes averaging overall 5–6.5% of the rock volume. Most other samples have remaining pore spaces that overall average 0.5–3% or even 4% of the rock volume (see each sample's thin section description in Appendix D of the Supplementary material), while a few have few remaining pores, their porosity averaging ~0.1–0.3%. In places within some samples, the quartz and K-feldspar grains have been fully cemented together into a tight mass, whereas other portions of the same samples have remaining pore spaces.

Finally, during this extensive petrographic examination of these 26 samples of the Tapeats Sandstone no macroscopic or microscopic evidence was found of any metamorphic effects on the sandstone or its constituent mineral grains. This includes the many samples from the two folds, as well as those samples distant from the folds selected for comparison. Not only have the quartz grains maintained their detrital characteristics, but the ubiquitous K-feldspar grains and the muscovite flakes have also, some of the latter having been bent around the quartz grains they are wedged between and some having frayed or split ends caused by abrasion during deposition. Even the slightly elevated temperatures of low-grade metamorphism

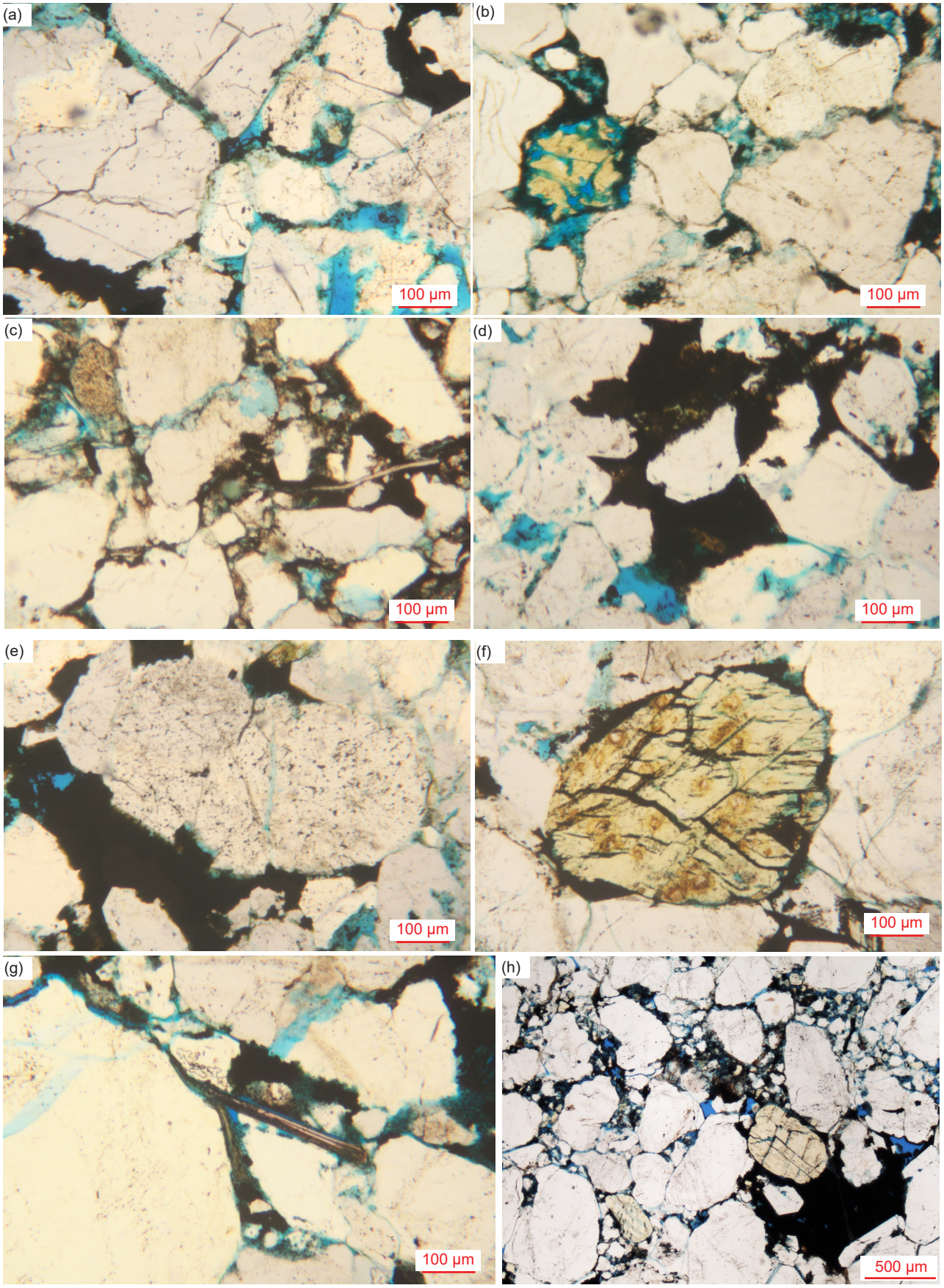
(a)
100 μm
(b)
100 μm
(c)
100 μm
(d)
100 μm
(e)
100 μm
(f)
100 μm
(g)
100 μm
(h)
500 μm

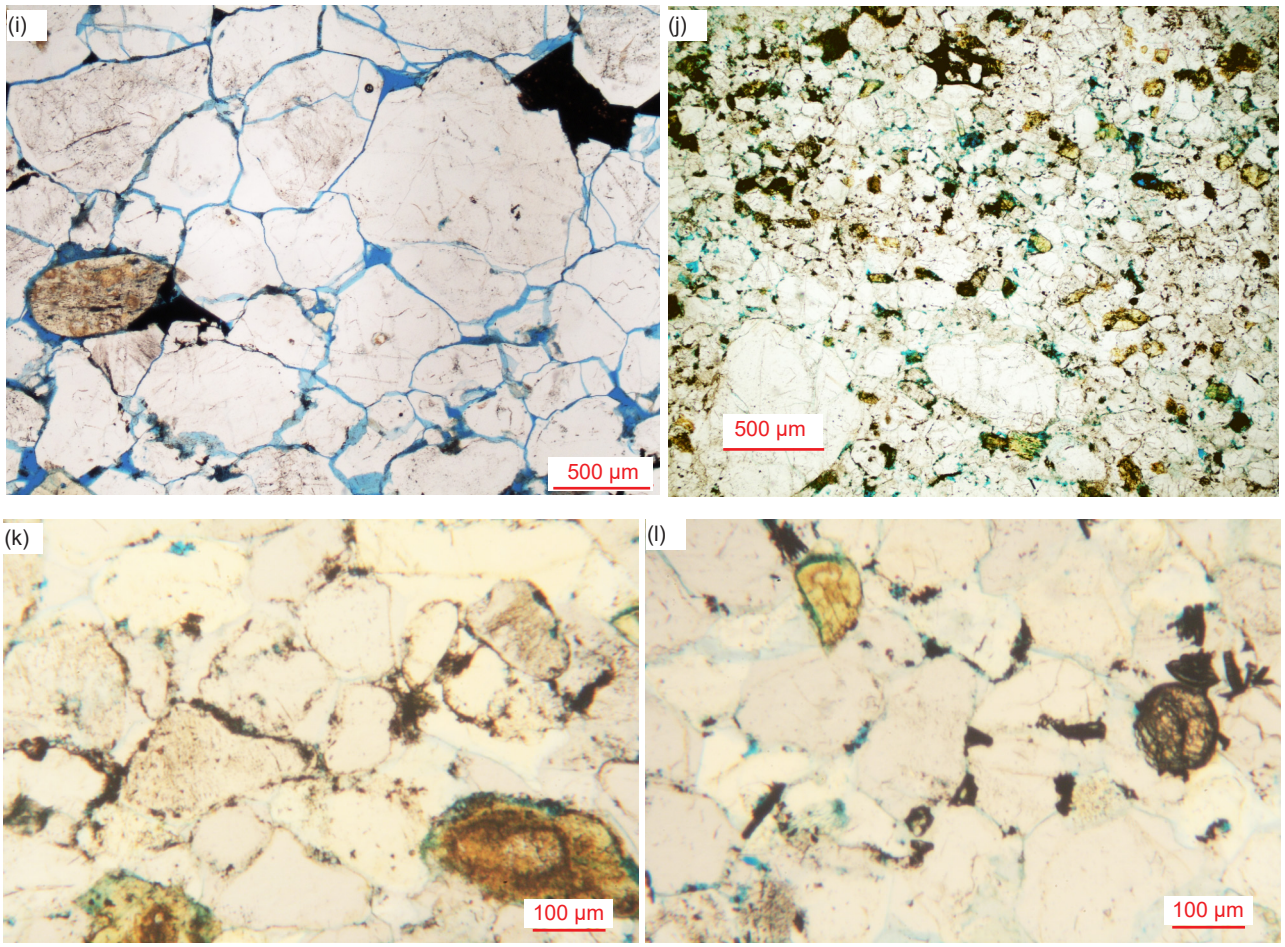

Fig. 39 (pages 230 and 231). A representative set of photomicrographs at various scales (as indicated) showing the iron oxides in parts of some Tapeats Sandstone samples as cement and alteration in patches and between grains (sometimes filling pore spaces) and sometimes on grain edges, coating grains, or within grains in cracks or cleavages. (a) TSS-01, (b) TSS-04 (c) TSS-04, (d) CCF-01, (e) CCF-02, (f) CCF-04, (g) CCF-06, (h) CCF-07, (i) CCF-08, (j) MF-05, (k) MF-09, and (l) MF-09.

would have substantially affected the quartz grains, the quartz being the dominant mineral in the sandstone, as well as affecting the textures in the rock fabric. The clay minerals still present due to post-depositional diagenesis would not have survived such metamorphism but would have been transformed into other minerals, such as metamorphic muscovite. Thus, it is likewise concluded that the Tapeats Sandstone is unmetamorphosed in all places where it was examined in the Grand Canyon.

Discussion

Details gleaned from this intensive petrographic examination of these Tapeats Sandstone samples in conjunction with previous field and other studies enable various relevant conclusions to be drawn.

Mineralogical Composition Indicates Nearby Sediment Provenance

Quartz is obviously the most abundant mineral in terrigenous sedimentary rocks, especially sandstones like the Tapeats Sandstone, being exceedingly durable due to often surviving multiple generations of weathering and deposition (Ulmer-Scholle et al. 2015). Quartz can occur as single crystals or polycrystalline aggregates that may provide clues to the provenance of the grains, but quartz is common to most rock types, though rare in basalts. Semi-composite and polycrystalline quartz can be found in metamorphic and plutonic rocks as well as hydrothermal vein deposits and fractures. For metamorphic quartz, the size of the crystals may represent increasing metamorphic grade, larger crystals forming under higher temperatures and pressures.

Grain size can make provenance determination more difficult (Ulmer-Scholle et al. 2015). With decreasing grain size, the ability to see undulatory quartz or polycrystalline/composite grains becomes more difficult. Since crystal sizes within polycrystalline grains may be large, grains formed from their breakdown may not exhibit polycrystallinity or undulatory extinction. According to Krynine (1946) and Folk (1980) straight to slightly undulose extinction in quartz is characteristic of

plutonic igneous and schistose metamorphic rocks. They also noted that whereas plutonic igneous rocks generally have sub-equant to xenomorphic quartz grains (that is, they did not develop their otherwise typical external form because of late crystallization as the matrix between earlier formed crystals), schistose metamorphic rocks generally have elongated composite quartz grains with straight borders and commonly have mica inclusions.

Feldspars are far less resistant than quartz to chemical and physical destruction, although they can survive some aqueous transport with only a relatively small reduction in grain size, but not angularity (Garzanti et al. 2012, 2015). However, they are often altered or removed by weathering, transport and diagenesis yielding secondary pores or alteration products such as illite, white mica/sericite, albite or kaolinite (Ulmer-Scholle et al. 2015). Almost all detrital feldspars are igneous or metamorphic in origin, with the K-feldspars orthoclase and microcline being the most common. Na-rich plagioclase, the next most common feldspar, is usually from volcanic rocks. Sanidine, from high-temperature felsic volcanic rocks, and Ca-rich plagioclase, from mafic to intermediate igneous rocks, are relatively uncommon.

Detrital micas are rarely mentioned or discussed as being present in any sandstones, except when they are present in rock fragments (Ulmer-Scholle et al. 2015). However, standard petrography textbooks suggest that detrital micas should be found in subaqueous sediments, but not eolian ones (Hallam 1981, 20; Moorhouse 1959, 343; Tucker 1981, 45). This notion is so entrenched in the minds of some geologists that they proclaim the absence of mica in certain sandstones based only on their assumption that a particular sandstone is eolian, without even doing any petrographic work, for example, the Permian Coconino Sandstone of Grand Canyon region (Young and Stearley 2008, 305). As they claim, the less resistant (softer) mica grains and ultra-fine clay particles have been abraded to oblivion and / or wafted off site by the wind. Yet sandstones like the Coconino contain abundant detrital mica flakes (Whitmore et al. 2014), as does the Tapeats, so both are water-deposited.

Rock fragments (also called lithic fragments or composite grains) can be derived from a wide variety of lithotypes and commonly have source-specific textures and compositions that can be recognized in thin section. Because of their multi-crystalline or granular nature, rock fragments obviously tend to be more common in the coarser grain-size modes of clastic terrigenous rocks, primarily sandstones and conglomerates. Rock fragments should be very common in sediments, but many succumb to the effects of weathering, abrasion or later mechanical or chemical diagenesis. Nevertheless, the surviving rock fragments yield some of the most direct evidence of contributions from igneous, metamorphic, or sedimentary terranes, so it is especially important that such grains be accurately identified.

Among sedimentary rock fragments are eroded and transported clasts of siliciclastic rocks (sandstone, siltstone, and claystone), which consist of a variety of mineral particles, but are dominated by quartz, feldspars, heavy minerals, micas, and clays (Ulmer-Scholle et al. 2015). Textures within the clasts sometimes can give clues to their origin. Argillaceous/micaceous metamorphic rock fragments cover a wide spectrum of grain types derived from high- to low-grade metamorphic rocks, which is a function of texture and sheet silicate mineralogy. Common grain types include schist, gneiss, and quartzite clasts, dominated by quartz and sheet silicates (muscovite, biotite, and chlorite), while gneiss fragments also contain feldspar. Metamorphic grains commonly display some foliation or schistosity, and may be composed of polygonal equant crystals, depending on whether they have been annealed. Quartz crystals may display sutured contacts if highly strained. Cemented and compacted sandstones grade into metamorphic quartzite. Quartzite consists of polycrystalline elongated quartz crystals that have undulatory extinction of the individual sub-crystals as well as sutured boundaries.

Because igneous rock fragments can be composed of a number of minerals with a range of sizes, determinations of their mineralogic composition, crystallinity and texture are key to identifying them. Plutonic grains must contain two or more crystals to qualify as a rock fragment, and they are composed of phaneritic crystals (that is, large enough to be seen with the naked eye). The most common are granitic clasts composed of quartz, feldspar, iron-titanium oxides and mica or hornblende. Component crystals tend to be roughly the same size and commonly are anhedral to subhedral. As with other rock fragments, they are more common in coarser-grained clastic sedimentary rocks.

In the Tapeats Sandstone, quartz grains are overwhelmingly the dominant clasts. However, subordinate K-feldspar grains and former laths are common, as well as occasional detrital muscovite flakes. The presence of a few plagioclase grains and former laths is somewhat surprising, as well as the rare sphene crystals. Together with the occasional zircon crystals, this combination of mineral grains is clearly indicative of the sediment source area(s) consisting of granitic plutons and metamorphic rocks, which are of course locally present, exposed in the inner gorges of the Grand Canyon, where

often the Tapeats Sandstone directly overlies them, separated by the Great Unconformity erosion surface. Consistent with this conclusion are the quartz grains which have undulose extinction and the quartz grains with inclusions of muscovite and/or biotite flakes, occasional K-feldspar grains or laths, some plagioclase grains, and a few zircon grains. Also, there are the occasional K-feldspar grains and former laths with inclusions of quartz or muscovite.

Furthermore, among the identified rock fragments are possible pieces of altered (weathered) schist. Additionally, some of the quartz and K-feldspar grains with muscovite or biotite inclusions would likely be derived from granitic rocks. Otherwise, the other identified rock fragments are primarily altered (weathered) siltstone and quartzite, which are consistent with rock types in the Grand Canyon Supergroup strata that in some locations within the Grand Canyon corridor unconformably overlie the granitic plutons and metamorphic rocks and on which locally the Tapeats Sandstone sits separated by the Great Unconformity. Furthermore, some of the large quartz grains that consist of many sub-grains (sometimes as patchworks) with different extinction angles may also be quartzite grains. These are likely from the Shinumo Quartzite in the Grand Canyon Supergroup, which is very hard and resistant to erosion, and of which many of the large boulders are composed that are in the base of the Tapeats Sandstone near resistant "hills" or monadnocks of Shinumo Quartzite in the paleotopography of the Great Unconformity surface (see fig. 13a) (Chadwick 1978; McKee 1945; Middleton and Elliott 2003; Noble 1914; Walcott 1880).

Strong confirmation of this interpretation of the provenance of the sand grains for the Tapeats Sandstone comes from the U-Pb ages of the detrital zircon grains extracted from it in studies by Gehrels et al. (2011), Matthews, Guest, and Madronich (2018), and Karlstrom et al. (2018, 2020), already discussed in detail above. All their Tapeats Sandstone samples yielded detrital zircons overwhelmingly dominated by U-Pb ages of around 1.45 Ga, 1.60–1.72 Ga and 1.68–1.80 Ga, the former age consistent with the Quartermaster pluton in the far western Grand Canyon, and the latter two age ranges consistent with the Mazatzal and Yavapai provinces respectively, some of whose granites and schists crop out in the Grand Canyon's inner gorges locally underneath the Tapeats Sandstone (Karlstrom et al. 2003). Thus, while not definitive, this combined evidence is certainly consistent with the provenance of the sand being local and quite close to where the Tapeats Sandstone was deposited and sampled.

It is somewhat puzzling though that the Tapeats Sandstone, at least in the Grand Canyon area, seems to contain very few zircon grains from the underlying Grand Canyon Supergroup (Unkar and Chuar Groups). After all, large boulders of Shinumo Quartzite are clearly evident locally in the base of the Tapeats Sandstone. Gehrels et al. (2011) determined the detrital ages of zircons in these locally underlying Grand Canyon Supergroup sedimentary strata and found that little detritus had been recycled from them. Thus, it may well be that the extent of the Grand Canyon Supergroup is limited, because elsewhere across North America underlying the Tapeats equivalents and the Great Unconformity are invariably Precambrian granites and metamorphics (fig. 9a and Peters and Gaines 2012). Yet this widespread occurrence of underlying Precambrian basement granites and metamorphics with similar zircon and crystalline signatures might suggest at least some detrital grains in the Tapeats Sandstone could have been transported longer distances from outside the Grand Canyon area. This would make sense in a global Flood cataclysm model (see below), especially as Gehrels et al. (2011) found that the detrital zircons in higher layers in the Grand Canyon Paleozoic sequence had been transported longer distances.

Mineralogical and Textural Indicators of Short-Distance Transport and Deposition

Petrographic examination of the Tapeats Sandstone samples in this study overwhelmingly revealed the sandstone is poorly to moderately well-sorted and dominated by a wide range of sizes of sub-angular to sub-rounded quartz grains, with subordinate K-feldspar grains and former laths of various sizes that are generally smaller than the surrounding quartz grains and are often rounded, though sometimes are still euhedral or sub-euhedral, or even occur as angular fragments. It is also noteworthy that the K-feldspar contents of the samples were independent of their stratigraphic positions in the Tapeats Sandstone (see table 3). Samples in this study collected from the bottom, middle and near the top of the main cliff-forming unit contained variable small to large subordinate amounts of K-feldspar, as did samples collected only meters apart at the same stratigraphic level within the two folds.

There have been several explanations for how sand grains, especially more resistant quartz grains, become rounded (Chandler 1988; Dott 2003; Goudie and Watson 1981):

(1) abrasion of sand grains by wind,
(2) selective transport of better-rounded grains (to the dune) with the more angular ones being left behind in aqueous environments,
(3) recycling of older deposits containing rounded grains, and
(4) intense chemical activity causing sharp corners of grains to be removed.

Of these four suggested mechanisms for how sand grains become rounded, the current consensus appears to be *only* eolian transport, especially for the more mechanically and chemically resistant quartz grains (Chandler 1988; Dott 2003), even though there have been several other explanations for how quartz grains become rounded. Thus, it is inferred that textural and compositional maturity is inherited and usually the result of several sedimentary cycles, with eolian abrasion having happened in at least one of the cycles in the history of the sand grains (Dott 2003; Folk 1978). Chemical activity can also make a sandstone appear more "mature" by removing or altering more soluble grains such as feldspars, especially in wet tropical environments, thus leaving quartz behind. McBride (1985) referred to these as "diagenetic quartz arenites."

In stark contrast, it has been well-known for some time that aqueous transport does not appreciably round quartz or K-feldspar sand grains (Kuenen 1960; Russell and Taylor 1937; Twenhofel 1945). Indeed, it is now undisputed that even energetic aqueous conditions (such as longshore currents and daily tidal currents) are insufficient to round any minerals. It is believed that this is because the differences in rounding between eolian and aqueous environments are due to the ability of water to cushion impacts between grains. A noteworthy study is that of Garzanti et al. (2012, 2015), who investigated sand from the Orange River and Orange River Delta that empties into the Atlantic Ocean in southwestern Africa. Sand from these locations is carried northward along the African coast by continuous longshore currents and tidal activity, some of it for over 1,400 km. After this great distance of transport and mechanical activity, all of the sand grains are still angular. The angular beach sand grains are then blown inland by southwesterly winds where they are deposited in the dunes of the Namibian Erg. They found that aqueous transport of beach sand grains, along the entire transport distance, fails to make them appreciably rounded compared to the original river and delta sand grains. It is not until the wind picks up the sand grains and blows them into the erg does any appreciable rounding take place. Thus, from that study it can be concluded that rounding appears to happen *only* by eolian transport and not by any other mechanisms. This has been confirmed by Whitmore and Strom (2017a, b, 2018), whose studies demonstrated that feldspar grains can show rounding with as little as a few hundred meters of eolian transport from a beach to a nearby eolian setting.

Thus far, this discussion on rounding has mainly focused on quartz, which is the most common component of most sandstones. However, Pye and Tsoar (2009, 72) claim that K-feldspar rounds faster than quartz because of its lower hardness (6.0 on Mohs scale of hardness, compared to 7.0 for quartz). Therefore, it is to be expected that during erosion and transport the softer K-feldspar grains would deteriorate more quickly and, depending on the distance of transport, would likely be totally eliminated by the abrasive action on them by the harder quartz grains. Some theoretical, experimental, and observational rounding data has been collected on K-feldspar grains. Marsland and Woodruff (1937) demonstrated experimentally that K-feldspar rounds slightly faster than quartz. Yet the lack of consensus is probably because the movement of various shapes, sphericities and sizes of grains is a complex process and is highly dependent on various velocity conditions (Morris 1957).

Despite these studies, some have suggested K-feldspar grains can be successfully abraded in aqueous environments. Odom (1975) and Odom, Doe and Dott (1976) studied a variety of quartz arenites. They observed that K-feldspar content increases with decreasing grain size. In many sandstones with mean grain sizes greater than about 0.177 mm (ϕ=+2.50), K-feldspar is often less than 10% of the rock volume (which defines a quartz arenite or quartz sandstone). With grain sizes less than about 0.125 mm (ϕ=+3.00), K-feldspar is often more abundant (10–25%), a rock which is called a feldspathic arenite (or arkosic sandstone or subarkose). Those authors suggested that this trend occurs because K-feldspar grains are abraded more easily in aqueous high energy environments (forming the larger-grained quartz arenites) and conserved in lower energy aqueous environments (forming the smaller-grained feldspathic arenites). However, this inverse relationship between K-feldspar grain size and the K-feldspar percentage of the rock volume does not match the Tapeats Sandstone, as some of the largest K-feldspar clasts (2.00-4.00 mm, ϕ=-1.00 —-2.00, granule size) occur in samples with K-feldspar amounting to 22–33% of the rock volume.

As already noted, Garzanti et al. (2015) found that angular sand grains of all mineral species changed little from marine and fluvial transport but were only significantly rounded by eolian abrasion. Most detrital mineral grains were still angular to sub-angular after ~2,000 km (~1,240 mi) of transport along the Orange River, confirming that fluvial environments are ineffective in rounding sand grains. Roundness changed little in the marine environment even after 300 to 350 km of high-energy littoral transport along the Atlantic shores of the Sperrgebiet. This condition demonstrated that beach action, as any transport in aqueous media, does not have much influence either (Pettijohn 1957) and disproves the long-held idea that beach sand grains are rounded faster than river sand

grains because the former grains are rolled back and forth repeatedly on beaches (Folk 1980).

From their observations Garzanti et al. (2015) also concluded the "relative toughness" or susceptibility of various minerals to rounding. Based on the observed compositional trends and differential rates of increased roundness with transport distance, the following sequence of relative toughness and mechanical durability was established:

> garnet > quartz > epidote ≥ volcanic rock fragments ≥ feldspars > opaques ≥ pyroxene > amphibole > sedimentary/metasedimentary rock fragments.

However, K-feldspar also cleaves relatively easily compared to the conchoidal fracture of quartz. This perhaps explains why angular K-feldspar grains were found in virtually every Tapeats Sandstone thin section examined (see Appendix D in the Supplementary material). Similarly, Whitmore et al. (2014), Whitmore and Garner (2018) and Whitmore and Strom (2018) found angular K-feldspar grains in virtually every sample they examined of the Permian Coconino Sandstone and many other related or correlated sandstones in the western USA, England and Scotland. Indeed, they reported that the angular K-feldspar sand grains were sometimes more angular than the similar-sized quartz grains that surrounded them. Yet many of those same sandstones that have angular K-feldspars also contain angular grains of quartz and mica flakes (mostly muscovite), and are moderately to poorly sorted (Borsch et al. 2018; Maithel, Garner, and Whitmore 2015; Whitmore et al. 2014). In other words, under the microscope these sandstones are not as texturally mature as they might appear to be at the outcrop scale. They thus concluded that the presence of angular K-feldspar grains in ancient sandstones should be a reliable indicator of

(1) a first-order cycle of at least some of the sediment, and
(2) aqueous transport and depositional processes of the sandstone.

This is consistent with the claim of Wanless (1973a, b, 1981) that the water suspension transported sands remained sub-arkosic throughout the entire Tonto Group section (defined at that time as just the Tapeats, Bright Angel, and Muav), implying the rapid transport and dispersal of the Group's constituent sandy formations. Similarly, as reported by Rose (2003), the results of systematic sampling of the Tapeats Sandstone through six stratigraphic sections by Burgert (1972) confirms that K-feldspar grains are scattered in significant amounts throughout the entire unit, consistent with the rapid transport and deposition of all its sand grains.

Furthermore, micas are much softer on the Mohs scale of hardness (muscovite 2.0–2.5 and biotite 2.5–3.0) and consist of fragile sheets that easily cleave. Therefore, in a sediment dominated by quartz and K-feldspar grains with hardnesses of 7.0 and 6.0 respectively, the micas should be rapidly abraded. Standard petrography textbooks thus suggest micas should only be found in subaqueously transported and deposited sediments (Hallam 1981, 20; Moorhouse 1959, 343; Tucker 1981, 45).

In their studies of sand transport along the southwestern coast of Africa, Garzanti et al. (2012, 2015) found that the composition of the sand transported for hundreds of kilometers along the coastline (which contained micas) did not appreciably change. However, when the beach sand was picked up by wind and transported to the Namib dunes, all mineral grains became quickly rounded and the mica flakes either disappeared or possibly were never transported to the dunes.

Similarly, Whitmore (2017) and Whitmore and Strom (2017a, b) collected sand samples from beaches along the California and Oregon coastline and compared those samples with coastal dune samples from the same locations. They found that mica flakes were conspicuously absent from dune samples, unless those dunes were in close proximity (less than tens of kilometers) from mica-bearing bedrock, stream (fluvial) sediments or beach sands.

To investigate the durability of mica flakes in eolian and subaqueous environments, Anderson et al. (2013) and Anderson, Struble, and Whitmore (2017) devised a series of experiments. To simulate a subaqueous transport environment, a small amount of muscovite-rich sand was placed in a one-gallon glass jar with an RC airplane propeller attached on the inside of the lid and laid on a rock tumbler assembly, so that the rotation of the jar sustained a lateral dune. The velocity of the propeller was adjusted so that a small "dune" slowly migrated around the bottom of the jar. Surprisingly, after one year of continuous operation (roughly 7,500 km or 4,660 mi), not only did the sand still contain an appreciable number of muscovite grains, but they were still large enough to be seen with the naked eye. This is potentially explained by the cushioning effect of the water, which has a much higher viscosity than air and reduces the kinetic energy of grain-grain collisions, thereby preventing the rapid degradation of mica flakes and other softer minerals. The experiments of Marsland and Woodruff (1937) further confirm these observations. Despite the simplicity of these experiments, they confirm field and experimental observations that mica flakes are rare in modern eolian deposits and commonly present in subaqueously deposited sands.

Borsch et al. (2018) emphasized it is important to note that the mica flakes they found in cross-bedded sandstones are detrital (transported) rather

than diagenetic (altered from other minerals post-deposition) in character. For example, muscovite can be formed via the following chemical alteration of K-feldspar (orthoclase) in the presence of an acid (H^+):

$3KAlSi_3O_8$ (orthoclase) + $2H^+$
→ $KAl_3Si_3O_{10}(OH)_2$ (muscovite) + $6SiO_2$ + $2K^+$

The mica produced in this conversion is sericite, which most often occurs entirely within the host grain, and is visible in thin section as fibrous bundles. Consequently, sericite is generally much smaller than the host grain and randomly oriented. By contrast, many of the mica flakes observed in their study were longer than the matrix grains (size inversion), and the characteristic fibrous textures were not present. Furthermore, in their samples they observed:

(1) thin books of mica bent around other grains (often quartz),
(2) thin contorted mica books with splayed ends,
(3) the mica flakes did not often occupy the fairly common empty spaces of dissolved K-feldspar grains, and
(4) significant amounts of orthoclase (as much as ~8–15%) were often found in the thin sections along with the mica flakes (that is, orthoclase had not been diagenetically altered).

Together, these clearly indicated that the mica flakes they observed are detrital, and thus are part of the original depositional fabric.

The micas observed in every thin section of the Tapeats Sandstone in this study are muscovite flakes and have exactly the same characteristics as listed by Borsch et al. (2018). Most of the muscovite flakes are visible as edge-on stacked sheets in thin books. Because the thin sections were cut perpendicular to the bedding this means those muscovite flakes are parallel, and when at an angle are subparallel, to the bedding, a pattern consistent with aqueous deposition of detrital flakes. Furthermore, while the lengths of the flakes are variable, they are often longer than the widths of the surrounding quartz and K-feldspar grains and thus wedged between the quartz and K-feldspar grains (fig. 32). Sometimes they are also bent around the quartz and K-feldspar grains, and occasionally with their ends frayed, split, splayed and even in one or two examples, bent back, or segments of the long flakes have broken off. In other instances, the long thin books of muscovite have been altered after deposition, probably to illite or illite/smectite, the sheets expanding to be thicker, but still disposed in the positions in which they were originally deposited as detrital flakes. Furthermore, the muscovite flakes do not occupy empty spaces due to dissolved K-feldspar grains. To the contrary, all but four of the 26 samples contain very significant amounts of K-feldspar, primarily orthoclase (5–33%), along with the muscovite flakes. Some K-feldspar grains and former laths still display cross-hatched twinning under crossed polars characteristic of microcline and any diagenetic alteration of them is partial and in situ. Therefore, there can be no doubt these muscovite flakes are detrital, and thus were transported and deposited subaqueously.

Finally, there are the occasional grains consisting of rock fragments observed in the Tapeats Sandstone. Those that are quartzite are hard enough (with the 7.0 hardness of quartz) to have easily survived subaqueous transport and deposition. In contrast, Ulmer-Scholle et al. (2015) noted that schist fragments tend not to survive extensive transport. During more extensive transport, they reasoned, such grains would probably break down into silt-size fragments or their individual constituent quartz crystals. Thus, they suggested that mica-rich schist grains would rarely survive significant transport unless carried in suspension with muddy sediments. Therefore, Ulmer-Scholle et al. (2015) concluded that any surviving mica schist clast was probably deposited in relatively close proximity to its source.

At least one possible mica schist grain was observed in the Tapeats Sandstone in this study, plus several other rock fragments that were tentatively identified as weathered siltstone or mica schist. Thus, the observations and conclusions of Ulmer-Scholle et al. (2015) would seem to apply to the Tapeats Sandstone. Indeed, weathered mica schist fragments and even weathered siltstone fragments would seem to be very vulnerable to mechanical breakdown into their constituent grains during sediment transport and deposition unless that transport and deposition was extremely rapid and the transport distance was extremely short. Transport in suspension with muddy sediments can be ruled out as there are so few mud-sized particles in the Tapeats Sandstone and virtually no clay mineral grains, unless the sand grains were transported mixed in with the mud-sized particles of the Bright Angel Formation and then separated during deposition.

In conclusion, the collective evidence suggests a short-distance transport of the sandy and partially gravelly sediment followed by deposition of the Tapeats Sandstone. The transport distance had to be very short, since the source of the sediment has been clearly identified as the underlying Precambrian granitic plutons and schists of the Granite Gorge Metamorphic Suite, with some contributions from the stratigraphically intervening Grand Canyon Supergroup sedimentary strata. Indeed, some huge blocks of Shinumo Quartzite were deposited within the basal Tapeats Sandstone in very close proximity to (within meters of) paleotopographic hills of Shinumo Quartzite (fig. 13a). And the

transport and deposition had to be over only a very short distance for detrital muscovite flakes and mica shist fragments to have survived, and for K-feldspar grains and former laths to be so widely distributed within the full thickness of the Tapeats Sandstone. The fact that the Tapeats Sandstone is only poorly to moderately well-sorted with predominantly sub-angular to sub-rounded quartz grains ranging in size from coarse silt to granules and small pebbles is also further confirmation of short-distance transport and deposition.

Sedimentary Structures and the Depositional Environment

The above observations suggest the Tapeats Sandstone was not the product of a comparatively tranquil marine transgression lasting several million years involving shallow marine, beach, intertidal and fluvial sedimentary environments. Indeed, Kennedy, Kablanow, and Chadwick (1996, 1997) and Chadwick and Kennedy (1998) provided compelling evidence of more catastrophic deep-water deposition of at least some of the Tapeats Sandstone, and thus called for reevaluation of the sedimentary structures used to identify the Tapeats Sandstone as a shallow marine to intertidal facies. If the Tapeats Sandstone were thus deposited under the catastrophic conditions of a massive flood event in which the sea level rose rapidly and thus the resulting "dramatic global marine transgression" (Karlstrom et al. 2018) was exceedingly rapid, then we know of no such processes operating today. Therefore, the slavish commitment to the uniformitarian dogma that "the present is the key to the past" by most past workers researching the Tapeats Sandstone is totally unwarranted. Such researchers have tried to interpret the sedimentary structures in the Tapeats Sandstone on the basis of those produced in today's relatively slow-and-tranquil shallow marine, intertidal and even fluvial sedimentary environments. Garzanti (2017) has commented that sedimentologists "often resort to mythical thinking in the face of natural phenomena that we hardly understand" and that myths are ideas that owe their popularity to plausible reasoning rather than to observational evidence. It is no wonder that no unified consensus has been reached after over 150 years of investigations. Indeed, since the focus of uniformitarian-thinking investigators has been only on the Tapeats Sandstone primarily in the Grand Canyon region, they have ignored the global context of this "dramatic global marine transgression" which catastrophically eroded the underlying Precambrian basement rocks and rapidly deposited the Tapeats Sandstone and its correlated sandstones on a global scale.

Therefore, in reevaluating the sedimentary structures in the Tapeats Sandstone, the only sedimentary environment today that might be used as a guide to the more catastrophic environmental conditions under which it was deposited would be that produced by severe storms and hurricanes. Yet even that comparison would be deficient, as today severe storms and hurricanes are seasonally intermittent, whereas under the likely catastrophic flooding conditions of a dramatic global marine transgression severe storms and hurricanes would be happening continuously. Thorne et al. (1991) have endeavored to quantify how much of the thicknesses of the beds produced by intermittent storms would be preserved based on the periodicity of the storms and the sediment accumulation rate. Obviously, they found that the more frequent the severe storms and the more rapid the rate of sediment accumulation the greater the potential preservation of thicker beds. Also, the greater the water depths the greater is the preservation potential. In their modeling such storm event beds would be up to a meter (~3.3 ft) or so thick, though typically 25–50 cm (~10–20 in) or less, not unlike the 0.3–1.0 m (~1–3.3 ft) thick beds preserved within the Tapeats Sandstone (figs. 10–12).

Seilacher and Aigner (1991) and Walker and Plint (1992) identified what would be the distinguishing features of storm deposits, and hummocky cross-stratification was concluded to be a primary feature. As originally defined by Harms et al. (1975), hummocky cross-stratification is low-relief surfaces with overlying parallel to subparallel laminae of slightly variable thickness and scattered dip directions. More recently, Boggs (1995) defined hummocky cross-stratification as characterized by amalgamated undulating sets of cross-laminae that are both concave-up (swales) and convex-up (hummocks), the cross-bed sets being commonly 15–50 cm (~0.5–1.6 ft) thick and cutting gently into each other with curved or wavy basal erosion surfaces. The spacing of the hummocks and swales are typically from 50 cm to several meters (~1.6–13 or so ft). Dott and Bourgeois (1982) noted that hummocky cross-stratification has been identified in the geologic record in transgressive strata up to 175 m (~575 ft) thick and may be interstratified (between storm events) with mudstone, siltstone, sandstone and conglomerate. They also calculated the formation of hummocky beds (storm beds or tempestites) occurred in the upper sheet flow regime with water flow velocities at 80–200 cm/sec (0.8–2 m/sec), with intense oscillatory flow in shallow water depths. Prave and Duke (1990) also argued for upper flow regime sediment transport, but with unidirectional flow. In contrast, Duke (1985) after examining the paleogeographic distribution of 107 occurrences of

hummocky cross-stratification in the geologic record spanning the Proterozoic to Recent concluded that most occurrences were generated by hurricanes and that hurricane-generated bottom flows tend to be oscillatory- or multi-directionally-dominant.

Ironically, Rose (2003) claimed that hummocky cross-stratification structures widely regarded in the literature as produced by storm-accentuated oscillatory flows have neither been successfully reproduced in controlled laboratory conditions nor observed directly forming from oscillatory flows. Yet when Duke, Arnott, and Cheel (1991) proposed a depositional model for hummocky cross-stratification formation from storm transport of coastal sand to the inner shelf under dominantly oscillatory flow controlled by a very minor component of unidirectional flow, they based it in part on controlled laboratory experiments by Arnott and Southard (1990) and Southard et al. (1990). Those experiments had successfully reproduced hummocky cross-stratification and symmetrical 3D mega-ripples in a long-period purely oscillatory flow and very strong oscillatory-dominant combined flow. Duke, Arnott, and Cheel (1991) also commented that the grain fabric in hummocky sandstones indicates rapid reversals of bed shear stress consistent with deposition due to shore-normal transport of coarse bedload on the inner shelf during storms caused by the interactions of high-speed oscillatory bottom motions and a relatively slow bottom current. DeCelles and Cavazza (1992) likewise invoked high-energy oscillatory flow as the primary entrainment and bedform sculpturing mechanism, followed by a high sediment fallout rate resulting from rapid decay of storm-wave energy. Furthermore, Swift et al. (1983) had concluded that hummocky cross-strata sets are due to the action of strong storm-wave surges involving combined-flow currents with sediment deposition throughout much of the storm's duration, while Swift and Thorne (1991) argued that the depositional hydraulic conditions during storms meant sediment accumulation only occurred below storm wave base, which Walker and Plint (1992) estimated was at greater than ~25 m (~82 ft) water depth.

Rose (2003) also claimed that no hummocky cross-stratification had been reported from the Tapeats Sandstone, although Martin (1985) had reported it in a sandstone horizon within the Bright Angel Formation and Prave (1991) had reported it in the Zabriskie Quartzite, the lithosomatic and age equivalent of the Tapeats Sandstone to the west of the Grand Canyon in the Death Valley region of California and Nevada. Instead, Rose (2003, 2006) focused on the apparent channels throughout the Tapeats Sandstone and on the siltstones and mudstones associated with the flanks of such channels up in the transition zone (in his idealized section in fig. 13 to postulate a fluvial and intertidal depositional environment). Yet as noted above, Dott and Bourgeois (1982) had reported that hummocky cross-stratification identified in the geologic record may be interstratified (between storm events or surges) with mudstone, siltstone, sandstone and conglomerate. However, Rose (2003) admitted that the meter-scale high-angle tangential cross-beds in the Tapeats are clearly the product of high-energy transport. And Middleton and Elliot (2003) had suggested the apparent channels in the Tapeats Sandstone were subtidal in origin and due to strong offshore flow, rather than intertidal and/or fluvial processes.

Therefore, it is abundantly obvious that the same observed sedimentary structures in the Tapeats Sandstone are subject to different interpretations based on the bias and experience of the investigators. Yet the sedimentary structures within the Tapeats Sandstone are entirely compatible with the generalized definitions and descriptions of hummocky cross-stratification and similar bedforms produced by storm events such as hurricanes (Boggs 1995; Harms et al. 1975). The apparent channels are then simply where successive hurricane-driven storm surges eroded into the sands deposited by preceding storm surges (Swift et al. 1983). The basal section of the Tapeats Sandstone is of course dominated by gravel, pebble and boulder conglomeratic sandstone (figs. 13 and 14) that testifies to the destructive erosion at the Great Unconformity and its catastrophically rapid deposition. Above it is the thick cliff-forming unit that dominates the Tapeats Sandstone (figs. 10–13) in which there are the eroded channels but no interstratified siltstones and mudstones indicative of pauses or quieter conditions between the storm surges (that is, high-energy oscillatory flow) that deposited the sand rapidly. It would appear that only as the transition zone above is reached that there is such evidence of easing of the stormy conditions. And because these successive storm beds are well-preserved, the water depths in which this sand deposition occurred must likely have been below the storm wave base.

The greatest measured thickness of the Tapeats Sandstone is at the Unkar locality (fig. 1 and Appendix A in the Supplementary material) at 105 m (~345 ft), and 74 m (~243 ft) of this thickness is the basal and cliff-forming units which are devoid of evidence of burrowing activity (fig. 13) (Rose 2003). Bioturbation requires time for creatures to recolonize bed surfaces after deposition and commence their burrowing activity. So, the non-bioturbated state of the basal and cliff-forming units within the Tapeats Sandstone is consistent with the above scenario of deposition of the sands by rapid

successive hurricane-driven storm surges. Yet even though Hagadorn et al. (2011) observed that there are some *Arenicolites* burrows in the major cliff-forming Tapeats unit, the fact that they are in gravelly-pebbly conglomerates and arkosic sandstones and virtually no other trace fossils forced them to concede such burrows (assuming that is what they are) can be made in such a high-energy depositional environment. Indeed, Droser and Bottjer (1989) reported dense concentrations of parallel vertical *Skolithos* burrows in discrete meter-scale horizons within the correlative Wood Canyon Formation and Zabriskie Quartzite to the west of the Grand Canyon region, which they interpreted to represent high-energy littoral environments and amalgamated storm deposits due to the associated hummocky cross-stratification. Furthermore, the observation that the *Cruziana* trails are only found in the overlying transition zone associated with interstratified siltstones and mudstones is further evidence of the easing of the stormy conditions. And Pemberton, MacEachern, and Frey (1992) state such trails would only be preserved below the minimum wave base, that is, in deeper water. However, Bromley and Asgaard (1991) warned that such zones of trace fossils (ichnofacies) could be preservational (where they are buried or taphofacies) rather than behavioral (where they lived or biofaces). Therefore, in conclusion, the sedimentary structures and fossil content within the Tapeats Sandstone are entirely compatible with its catastrophically rapid deposition by successive hurricane-like storm surges.

"Age" Indicators

Karlstrom et al. (2018, 2020) have established the conventional age of the Tapeats Sandstone at ca. 507–508 Ma based on U-Pb dating of detrital zircons. Earlier studies by Gehrels et al. (2011) and Matthews, Guest, and Madronich (2018) also used the U-Pb dating of detrital zircons to establish the provenance of the Tapeats Sandstone. But the methodology they all used raises numerous issues and questions, including how reliable is the U-Pb dating method.

In the supplemental data of the Karlstrom et al. (2018) study, they tabulated all the U-Pb dating results of the detrital zircon grains they analyzed, plus all the U-Pb dating results of the detrital zircon grains analyzed by Gehrels et al. (2011) and Matthews, Guest, and Madronich (2018). Karlstrom et al. (2018) obtained from these data a wide spectrum of U-Pb ages, with peaks corresponding to the published ages of the source rocks from which they concluded the zircon grains had been eroded. They, and Karlstrom et al. (2020), then established the age of the Tapeats Sandstone by statistically determining from the spectrum of the lowest detrital zircon U-Pb ages the peak of the "bell-shaped" curve, which at 507–508 Ma they called the maximum depositional age. Yet the supplemental data tables listed that many of the detrital zircons yielded U-Pb ages less than that 507–508 Ma age for the Tapeats Sandstone—at least 59 spot analyses of zircons from their Hermit Creek sample with the lowest U-Pb age of 407.2 Ma, at least 45 spot analyses of zircons from their Frenchman Mountain sample with the lowest U-Pb age of 481.8 Ma, and at least 51 spot analyses of zircons from their East Verde River sample with the lowest U-Pb age of 468.0 Ma. Karlstrom et al. (2018) do not explain how the supposedly 507–508 million years old Tapeats Sandstone can have included within it so many detrital zircons with U-Pb ages less than its supposed depositional age, including one as "young" as only 407.2 million years old. Nor do they explain from where these "younger" detrital zircons within the Tapeats Sandstone originated. Indeed, how could even the 507–508 Ma detrital zircons be incorporated in the Tapeats Sandstone if the underlying rocks that were eroded to provide the sand grains, including the zircon grains, are older than 507–508 Ma? This question alone raises serious doubts as to the applicability and reliability of this technique for supposedly quantifying the apparent depositional ages of sedimentary rock units.

Yet not only is their methodology questionable, so must be the U-Pb dating method they used if it produced such illogical ages. Snelling (2000, 2009) has already provided details of numerous problems with the U-Pb dating method that are well-documented in the scientific literature. Furthermore, Snelling (2017a) reviewed all the determinations of the U-Pb decay rates (half-lives) and demonstrated that these crucial parameters are not yet precisely known, while Snelling (2017b, 2018, 2019) highlighted in detail the problems of common Pb, U and Pb mobility, and mass fractionation respectively that plague all efforts to obtain accurate U-Pb age determinations. Nevertheless, Karlstrom et al. (2018, 2020) championed the tandem U-Pb dating procedure they used, that is, LA-ICP-MS (laser-ablation–inductively coupled plasma–mass spectrometry) analyses followed by CA-ID-TIMS (chemical abrasion–isotope dilution–thermal ionization mass spectrometry) analyses. Although it often produced apparently concordant U-Pb dates (essentially matching ^{206}Pb-^{207}Pb, ^{238}U-^{206}Pb, and ^{235}U-^{207}Pb ages), there were still many detrital zircon grains that yielded illogically younger ages than the supposed depositional age of the Tapeats Sandstone. Recall that Snelling (2005b) reported CA-ID-TIMS analyses of three zircon grains recovered from a thin tuff bed in the Tapeats Sandstone in the western Grand Canyon that yielded

concordant ages of 86.2Ma, 98.2Ma, and 90.1Ma. Snelling (2005b) also obtained single zircon grain fission-track ages of 75Ma, 158Ma, and 408Ma that are very much younger than the Karlstrom et al. (2018, 2020) tandem U-Pb ages for deposition of the Tapeats Sandstone. Yet fission tracks are the physical evidence of the quantity of nuclear decay that has actually occurred. These considerations and highly inconsistent results from what is touted as a superior analytical procedure only highlight the unreliability and fallibility of the U-Pb dating method.

However, it could be argued that the accepted radiometric ages of the various Grand Canyon strata, including the basement granites and schists, date those rocks and strata in the correct relative order, and consistently in hundreds of millions to almost two billion years, except for the recent lava flows in the western Grand Canyon (Wiens 2016). However, Vardiman, Snelling, and Chaffin (2005) have demonstrated from six lines of evidence, supported by experimental results, that the reason for this systematic consistency of radiometric ages in the Grand Canyon stratigraphic sequence is because during some catastrophic event in the past there was a systematic acceleration of nuclear decay rates, potentially by six orders of magnitude. Three of those six lines of evidence involved experimental results obtained on Grand Canyon samples, namely, discordant radiometric ages obtained from four Precambrian units (the Cardenas Basalt, the Bass Rapids diabase sill, the Elves Chasm Granodiorite and the Brahma Schist amphibolites) (Snelling 2005c), coexisting uranium and polonium radiohalos (Snelling 2005a) and fission tracks in zircons (Snelling 2005b). Critics have pointed to the enormous quantities of heat that apparently would be released by such accelerated nuclear decay (Wiens 2016), yet Vardiman, Snelling, and Chaffin (2005) had already anticipated this criticism and provided plausible possible explanations, including the experimental fact that the radiohalos (which only form below 150°C) would have been annealed if such an enormous heat release had occurred (Snelling 2005a).

In conclusion, there is sufficient overwhelming evidence, also documented in the scientific literature, to question the reliability, and even the validity, of the U-Pb dating method. This is highly evident from so many zircon U-Pb dates for zircons within the Tapeats Sandstone that are markedly younger than the claimed depositional age of the sandstone. Thus, the U-Pb dating of detrital zircons from the Tapeats Sandstone (Karlstrom et al. 2018, 2020), coupled with the claimed biostratigraphic age of the Tapeats Sandstone (Karlstrom et al. 2020; Sundberg et al. 2020), is not an impediment to explaining the deposition of the Tapeats Sandstone in a much more recent catastrophic event, namely, the global Genesis Flood cataclysm. That would be more consistent with the textural and mineralogical evidence for the rapid local erosion and short-distance rapid transport and rapid deposition of its constituent sand.

Furthermore, the continued existence of so many pore spaces (~5%) within the Tapeats Sandstone after being subjected to the confining pressures of the ~15,000ft (~4570m) of overlying sedimentary rock layers for more than 500 million years begs the question as to the Tapeats Sandstone's true age. Would not such confining pressures have "squeezed out" the formation water, compacted the sand grains and then diagenetic processes infilled almost all the sandstone's remaining pore spaces after such a long time? On the other hand, if deposition were rapid and recent in the global Genesis Flood cataclysm, water would be trapped between the sand grains and then confined by the rapidly accumulating overlying sediment layers. That water would have held most of the pore spaces in place supporting them and resisting compaction until subsequent drying out, silica cementation and minor diagenetic alteration occurred over only a few thousand years to infill many of them but leave some still open.

Initial Flood Catastrophic Erosion and Deposition

Austin (1994) provided a detailed comprehensive description and account of the geological development of the Grand Canyon strata in the context of the global Genesis Flood cataclysm and the canyon's erosion in the Flood's aftermath. In particular, he described the Tapeats Sandstone as being deposited by the Flood waters advancing eastwards onto the western edge of the North American portion of the pre-Flood supercontinent at the initiation of the Flood event with the breaking up of the "fountains of the great deep" (Genesis 7:11) and the triggering of catastrophic plate tectonics (Austin et al. 1994; Baumgardner 2003). However, before the Tapeats Sandstone was deposited there had to be a prolonged period (days or more) in which there was a significant amount of continental-scale erosion to bevel the Precambrian (pre-Flood) land surface to produce the Great Unconformity. In the Grand Canyon region this involved intensive catastrophic erosion to remove several thousand meters of Grand Canyon Supergroup strata (which appear to only have survived in several down-faulted blocks) and then to bevel the underlying metamorphic schists and granite plutons. Then after this period of destructive erosion, and subsequent to the localized deposition of the Sixtymile Formation, the Tapeats Sandstone represents the first widespread (continental-scale) deposit of the Tonto Group.

Austin (1994) diagrammatically envisaged a fining upwards model for the time transgressive rapid deposition of the Tonto Group strata as the powerful westward back under-flow of the advancing Flood waters at a water flow speed of >2 m/sec intensely scoured and catastrophically eroded all pre-Flood rocks to produce the Great Unconformity before sequentially depositing their load of sediments as horizontally segregated facies in the vertically stacked Tonto Group strata (fig. 40). In the adjacent shallow-water area the westwards-flowing, intense bottom-surging current deposited coarse pebbles and sand with lag boulders up to 9 m (30 ft) diameter in flat beds or cross-beds to form the base of the Tapeats Sandstone at a water flow speed of 1.5 m/sec. Further westwards in deeper water the central portion (cliff-forming unit) of the Tapeats Sandstone composed of sand waves of coarse sand in thin cross-beds with westerly and south-westerly dips was deposited at a water velocity of about 1 m/sec. And simultaneously even further westwards the top of the formation composed of thinner, fine-grained sand and silt beds dominated by plane beds with ripples was deposited by deeper and slower moving waters at 0.5 m/sec, forming a gradational transition into the overlying shales of the Bright Angel Formation. It is in this uppermost Tapeats transition zone that the fossilized *Cruziana* trackways of trilobites are found.

This sedimentation model is consistent with the conventional, classical time-transgressive deepening seas model first advocated by McKee (1945) and the deep-water deposition of the Tapeats Sandstone proposed by Kennedy, Kablanow, and Chadwick (1997), except that the timeframe for deposition of the Tapeats Sandstone is a mere few days as part of the initial catastrophic erosion and deposition of the global Genesis Flood cataclysm only about 4,350 years ago. This is in stark contrast to the conventional 1 million years of slow deposition of the Tapeats Sandstone about 507–508 million years ago (Karlstrom et al. 2020). Karlstrom et al. (2018) admitted though that the Sauk transgression represented by the Tonto Group "was one of the most dramatic global marine transgressions in Earth history." And even Rose (2003) admitted that these lower Paleozoic strata were deposited during higher rates of tectonism and of the accompanying inertial true polar wander which generated an historic high sea-level rise and abnormally high-frequency sea-level fluctuations. The fact that the Great Unconformity is well recognized and documented as a globally-occurring stratigraphic surface (Peters and Gaines 2012) which in most regions across the globe separates continental crystalline basements rocks from the overlying Cambrian Sauk megasequence shallow marine sedimentary deposits, coincident with the Tapeats Sandstone. This surface and sandstone unit have been correlated with similar basal Sauk sandstones across North America, North Africa, the Middle East, and parts of South America

Fig. 40 (page 242). A model for the formation of the Tonto Group sedimentary deposits beneath advancing floodwaters across Nevada, Arizona, and New Mexico (after Austin 1994, 69. fig. 4.12). This likely occurred well after the onset of the Flood, as much of the Grand Canyon Supergroup had to first be planed off down to the crystalline basement granites and metamorphics. The water mass advancing eastward over Arizona has been "lifted" off the surface of the earth to reveal, underneath, the erosion and sedimentation that was occurring. The Flood model explains the erosion of the Great Unconformity, and subsequent deposition of the Tapeats Sandstone, Bright Angel Formation (shale), and Muav Formation (limestone). The waters of the Flood advanced eastward through Nevada (lower left of diagram), finally reaching the more elevated area in Arizona and New Mexico (upper right of diagram). As the Flood advanced eastward, it produced horizontally segregated deposits (facies) and vertically stacked sediments (strata).
Zone 1 is the highest elevation area of the continent, where shallow, fast floodwaters are causing intense scouring and erosion of the pre-Flood rocks.
Zone 2 is the adjacent shallow-water area, where coarse pebbles and lag boulders are accumulating at the base of the Tapeats Sandstone. All the finer sand, silt, and mud are being winnowed from Zone 2, and moved westward into Zones 3 and 4 by the intense bottom-surging current (velocity about 1.5 m/sec).
Zone 3 is composed of sand waves forming thinly cross-bedded sands, which compose the middle section of the Tapeats Sandstone (the cliff-forming unit). Here, the water velocity is about 1.0 m/sec.
Zone 4 is plane beds of sand and some silt, with ripples representing the deepest and lowest-velocity waters depositing the uppermost Tapeats Sandstone (the "transitional" unit).
Zone 5 is located in still deeper and slower-moving waters. The silicate clay- and silt-sized particles are accumulating as graded silt and clay beds. These deposits are the residue winnowed from Zones 1 through 4 and compose the Bright Angel Formation (principally shale and siltstone but with some sandstone beds). Here, the water velocity is about 0.5 m/sec.
Zone 6 is farthest to the west, in the deepest and slowest-moving water, where there is a deficiency of silicate clay and silt-sized particles. Lime mud, apparently the dominant type of pre-Flood sediment to the west, is accumulating in Zone 6 as rhythmically laminated and bedded flat strata, where the water current velocity is less than 0.5 m/sec.
The continuous advance of the Flood over Arizona caused deeper-water, slower-velocity sediment facies to be stacked above the shallower-water, faster-velocity sediment facies. The result is the vertical sequence, consisting of the Great Unconformity, and the Tapeats Sandstone, Bright Angel Formation, and Muav Formation comprising the Tonto Group. Each has enormous horizontal extent, which can be measured in hundreds of kilometers.

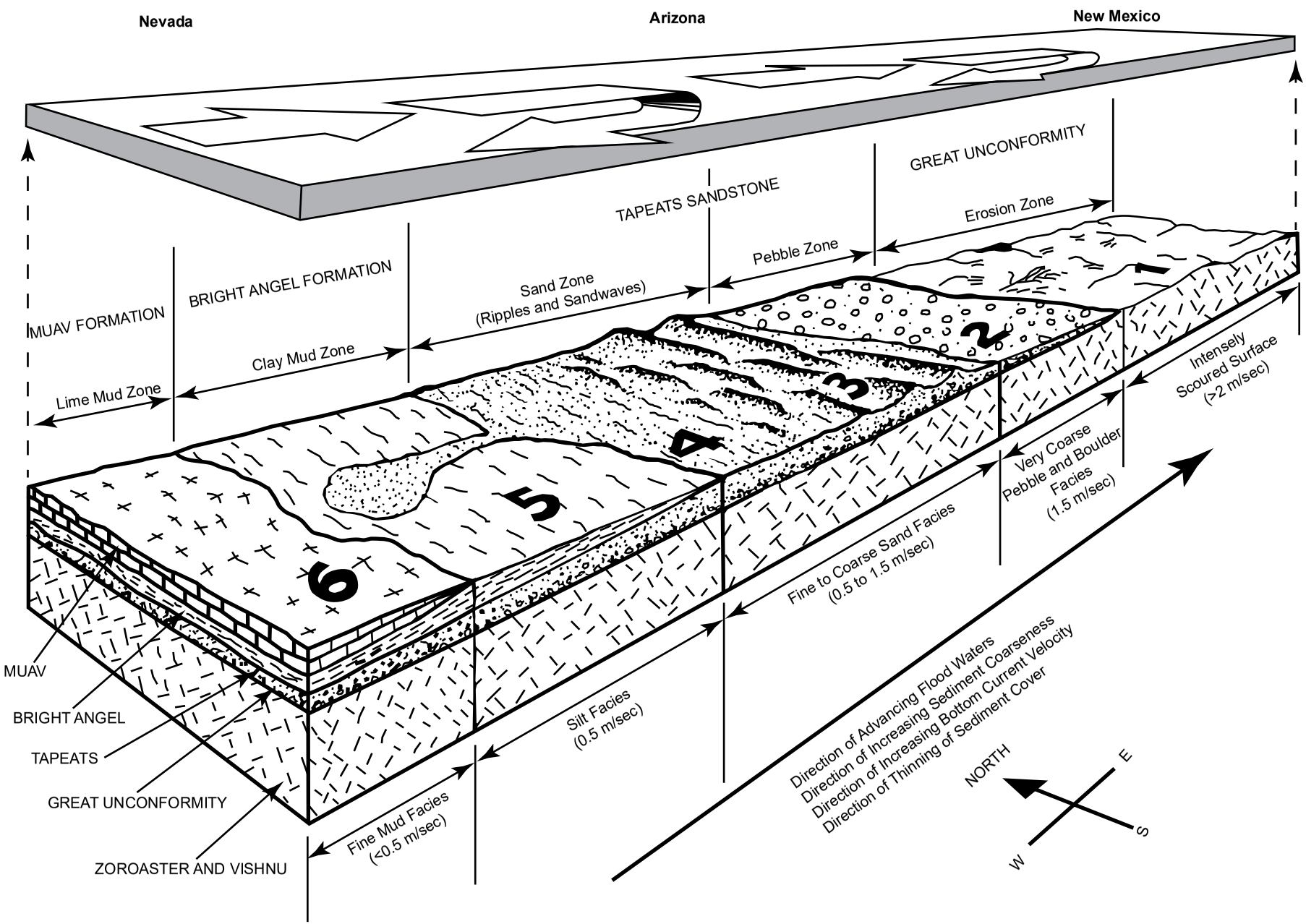
Nevada
Arizona
New Mexico
GREAT UNCONFORMITY
TAPEATS SANDSTONE
Erosion Zone
Pebble Zone
MUAV FORMATION
BRIGHT ANGEL FORMATION
Sand Zone
(Ripples and Sandwaves)
Clay Mud Zone
Lime Mud Zone
Intensely
Scoured Surface
(>2 m/sec)
Very Coarse
Pebble and Boulder
Facies
(1.5 m/sec)
Fine to Coarse Sand Facies
(0.5 to 1.5 m/sec)
Silt Facies
(0.5 m/sec)
Fine Mud Facies
(<0.5 m/sec)
1
2
3
4
5
6
MUAV
BRIGHT ANGEL
TAPEATS
GREAT UNCONFORMITY
ZOROASTER AND VISHNU
Direction of Advancing Flood Waters
Direction of Increasing Sediment Coarseness
Direction of Increasing Bottom Current Velocity
Direction of Thinning of Sediment Cover
NORTH
E
S
W

(Clarey and Werner 2018). Furthermore, it is totally consistent with initial catastrophic erosion of locally underlying basement rocks and rapid, short-distance transport and deposition at the onset of the global Genesis Flood cataclysm, which would have been accompanied by continuous intensive high-energy storms and tsunamis due to the hot waters erupting from the fountains of the great deep.

Furthermore, the westward transport of the detritus has been confirmed by the documentation of continental-wide paleocurrent direction indicators by Brand, Wang, and Chadwick (2015), who have demonstrated this was a global phenomenon consistent with the direction of the global tidal movements in the global Flood cataclysm. And Baumgardner (2013, 2018a, b) has made considerable progress with numerical simulations of the catastrophic erosion of bedrock via cavitation to produce the sediments that were rapidly deposited on the continental plates as shallow waters moved rapidly around the surface of the rotating globe. His modeling posits that the dominant means for sediment transport during the Flood was by rapidly flowing turbulent water, and that water motion was driven by large-amplitude tsunamis that were generated along subduction zone segments as the subducting plate and overriding plate, in a cyclic manner, locked and then suddenly released and slipped rapidly past one another. His calculations show that with plausible parameter choices average erosion and sedimentation rates on the order of 9 m/day (0.38 m/hr) occurred with tsunami-driven pulses of turbulent water that transported the generated sediments vast distances across the continental plate surfaces, sufficient to deposit the Tapeats Sandstone within 3–10 days and during the initial 150-day rising and prevailing waters phase of the Flood (Genesis 7:18–24) to account for some 70% of the Phanerozoic sediments that blanket the earth's continental surfaces today.

Austin and Wise (1994) described in detail five robust criteria for defining the pre-Flood/Flood boundary and then applied them to the Grand Canyon region. They concluded that the Great Unconformity under the Tapeats Sandstone and occasionally under the locally underlying Sixtymile Formation in the eastern Grand Canyon matched all five criteria. Thus, they included the Sixtymile Formation in the Sauk megasequence, which has recently been confirmed by Karlstrom et al (2018, 2020) who have proposed the formation be added to the base of the Tonto Group. Within the Sixtymile Formation Wise and Snelling (2005) reported large megaclasts of the underlying Kwagunt Formation of the Chuar Group piled up at least three deep and separated by meter-thick pebble to boulder breccia layers, which were first recognized by Elston (1979) and subsequently documented by Karlstrom et al. (2018). Elston (1979) and Elston and McKee (1982) argued that these megaclasts were emplaced by sliding as the Sixtymile Formation was rapidly deposited as a result of more than 2 km of displacement of the adjacent Butte Fault in a sudden tectonic disturbance. Austin and Wise (1994) also correlated these megaclasts and breccias in the Sixtymile Formation with the gigantic breccia clasts, some more than a mile wide, in the Kingston Peak Formation in the eastern Mohave Desert of California with the tectonic upheaval that marked the initiation of the Flood cataclysm (the breaking up of the fountains of the great deep). They suggested those gigantic breccia clasts in the Kingston Peak Formation resulted from the collapse of the continental margin as the sequence dramatically thickened westward towards what was the pre-Flood ocean basin. Additionally, Austin (1994) had suggested the Chuar Group underlying the Sixtymile Formation was deposited in latest pre-Flood time, which was confirmed by the identification by Wise and Snelling (2005) of in situ grown stromatolites in an apparent reef structure in the Kwagunt Formation of the Chuar Group, an example of the pre-Flood hydrothermal biome proposed by Wise (2003).

This overall scenario and model for the tectonic upheaval at pre-Flood/Flood boundary and the initial catastrophic Flood deposition of the Tapeats Sandstone have also been summarized by Snelling (2009). However, critics have countered with the claimed evidences for slow-and-gradual deposition of the Tapeats Sandstone in non-marine, subaerial eolian and fluvial, and intertidal to shallow-marine environments as suggested by Wanless (1973a, 1975), Hereford (1977), Middleton and Hereford (1981), Rose (2003, 2006), and Hagadorn et al. (2011). In particular, Hill and Moshier (2009, 2016) have pointed to the marine invertebrate tracks and burrows found throughout most of the Tapeats Sandstone, suggesting such delicate trace fossils require relatively gentle conditions for preservation. However, as already explained above, both the sedimentary structures and fossil content within the Tapeats Sandstone are entirely compatible with its catastrophically rapid deposition by hurricane-driven storm surges.

Hagadorn et al. (2011) admitted they were puzzled by the trace fossil *Skolithos* and other traces occurring rarely in Facies B (the medium-to-coarse-grained cliff-forming unit), whereas there are abundant *Arenicolites* burrows in facies not typically conducive to preservation of delicate trace fossils, such as in purple mudstones, green shale flasers, gravelly-pebbly conglomerates and arkosic sandstones of Facies B. They also noted that the same ubiquitous

monotaxic concentration of *Arenicolites* burrows, coupled with the near exclusion of other trace or body fossils, is present in other sandstones that correlate with the Tapeats Sandstone sitting on the Great Unconformity in other places across North America and in the Middle East. In other words, Hagadorn et al. (2011) admitted that these *Arenicolites* burrows can be made in such a high energy environment as that required to deposit a gravelly-pebbly conglomerate, which totally demolishes the claim of Hill and Moshier (2009, 2016) that such delicate trace fossils require relatively gentle conditions for preservation. Rather, once the tracks and burrows have been made, they need to be buried rapidly to be preserved. And this was happening on a global scale. Thus, the prevalence of these trace fossils in the Tapeats Sandstone instead indicates that these invertebrate track and burrow makers were highly active as they tried to survive during the rapid deposition of the Tapeats Sandstone at the beginning of the global Flood cataclysm, and not in the postulated slow-and-gradual, gentle conditions of the postulated uniformitarian sedimentary environments.

In reality, however, these trace fossils pose an insurmountable problem for these uniformitarians. Why are only these tracks and burrows made by these invertebrates preserved and fossilized in the Tapeats Sandstone, and not the bodies of these invertebrates? For example, trilobite crawling (*Cruziana*) and resting (*Rusophycus*) traces occur almost exclusively in the Tapeats Sandstone Facies C, the transition interval to the overlying Bright Angel Formation (Hagadorn et al. 2011), and yet the bodies of the trilobites that made the traces are only found buried and fossilized much higher stratigraphically in the Bright Angel Formation, which conventionally was deposited a million or more years after the Tapeats Sandstone (Karlstrom et al. 2020). If the delicate traces of these invertebrates could be fossilized in the high-energy depositional environment of rapid deposition of the Tapeats Sandstone, then the more robust bodies of these trace-makers should likewise have been buried and fossilized along with these tracks and traces they made. This conventional, millions-of-years "offset" between fossilized tracks and the body fossils of the track-makers has been documented by Brand and Florence (1982) and Brand (1997) as a ubiquitous occurrence throughout the fossil record, among both invertebrates and vertebrates. It does not make any rational sense that over the supposed millions of years the bodies of the track-makers were not even sometimes buried with or near the tracks they made. Instead, this is evidence of rapid burial and preservation of the tracks just before (hours to days) the track-makers themselves were also rapidly buried and fossilized in the ongoing rapid accumulation of the sedimentary strata during the global Flood cataclysm.

Hill and Moshier (2009) claimed that fossilized raindrop prints are found in the Tapeats Sandstone and thus those sandstone surfaces had to be subaerially exposed during a rainstorm, and then gently buried to be preserved, all of which is evidence against the Flood cataclysm. However, Hill and Moshier (2009) provided no proof of their claim, not even a reference or photograph. Furthermore, Hill and Moshier (2016) did not repeat this claim in their updated descriptions of sedimentary structures in Grand Canyon sedimentary strata. Yet McKee (1945) provides a photo (plate 7d) of what he describes as "gas pits" in sandstone, which are small and circular like craters that could be interpreted as possible raindrop prints by those wanting such to exist. Nevertheless, Hill and Moshier (2009, 2016) do claim fossilized rain prints are found in the Coconino Sandstone and provided photographs. In response Whitmore and Garner (2018) noted that the crater-like features claimed to be fossilized "raindrop" prints in the Coconino have different characteristics than raindrop prints found in modern settings. In particular, raindrop prints in sandy substrates do not typically form well-defined crater-like depressions. Instead, the surface becomes rather mottled and the prints do not form distinct craters. And since these claimed raindrop prints often form in "zones," Whitmore and Garner (2018) suggested that perhaps they are related to some type of water or gas escape process (as suggested by Lowe [1975] and McKee [1945]) occurring between the vortices that form current lineation (Allen 1985, 111). Others may be related to burrowing activity.

Hill and Moshier (2009, 2016) provided a photograph of ancient ripple marks in the Tapeats Sandstone and a photograph for comparison of ripple marks on a sandy sea bottom under about 20ft (6m) of water and formed by a current of about 0.5–1.0mph (0.2–0.4m/sec), thus again implying these were incompatible with the hurricane- and tsunami-driven, rapid sediment transport and deposition during the global Flood cataclysm. However, their comparison photograph clearly acknowledges these Tapeats ripple marks were formed subaqueously, as seen by both the ancient and modern ripple marks having sharp crests and being asymmetrical, the steeper lee slopes indicating the direction of the current flow. Furthermore, it has been demonstrated that the cross-bedding within the Tapeats Sandstone may have resulted from large subaqueous sand waves. Although much is not known about the fine-scale structures associated with large subaqueous sand waves, some observations have been made using radar and video. Thus, it has been found that

small ripples are present on the backs of megaripples which occur on the backs of larger sand waves in Long Island Sound, near New York City (Poppe et al. 2006). Currents flowing over the tops of sand waves should produce lee vortices in much the same way as they are produced in eolian settings, so this could possibly produce subaqueous ripples, depending on current velocity. Houbolt (1968) suggested currents could flow perpendicular to the flanks of large sand ridges on steep foreset slopes.

Hill and Moshier (2009, 2016) also provided a photograph of polygonal crack-like patterns on the top of a bounding surface in the Tapeats Sandstone infilled with calcite and claimed they were mud or desiccation cracks. For comparison, they included a photograph of recently formed mud cracks in wet mud along the Little Colorado River. They argued that such mud cracks in the Tapeats Sandstone indicate dry subaerial conditions at that bounding surface, which are incompatible with the global Flood cataclysm. However, these cannot possibly be "mud" cracks because these features are in a clay-poor sandstone, not mud. And as seen in their photograph of modern mud cracks, when the mud dries the polygonal shapes become concavely arched, whereas the claimed fossilized "mud" cracks are flat. In order for any sediment to crack by desiccation it must be dominated by clay-sized particles and must have certain clay minerals. Sand grains are usually too large and insufficiently cohesive to form cracks during desiccation (Lowe 1975). In the XRD analyses of the Tapeats Sandstone (table 3) there are no clay minerals in 21 of the 26 samples, and four of the other five contain between 0.8% and 6.9% illite, which could largely be muscovite, as evidenced under the microscope, while the remaining sample contained 1.2% kaolinite. Then in the clay fraction XRD analyses (table 4), the clay contents are dominated by illite and illite/smectite and sometimes kaolinite. So, the most common clays in the Tapeats are illite and kaolinite, but in insignificant amounts. By comparison, modern soils that crack due to desiccation have significant amounts of clay. Basma et al. (1996), Harianto et al. (2008), Yassoglou et al. (1994), and Yesiller et al. (2000) report cracking in soils with clay contents ranging from 13 to 58.3% and silt contents ranging from 21 to 52%. The medium- to coarse-grained Tapeats Sandstone simply does not have the clay minerals necessary for any kind of desiccation to occur. The origin of these rare polygonal structures in the Tapeats is not known and is still a mystery, though Peters and Brand (1999) have offered a possible explanation.

Thus, none of these apparent objections are counter evidence as claimed. All such occurrences can be reconciled with the rapid transport and deposition of the Tapeats Sandstone very soon after the initiation of the global Flood cataclysm. The fact that the Tapeats Sandstone, and its equivalents, was deposited on top of the very source rocks its sand grains were eroded from indicates a very short transport distance. And the ubiquitous presence of K-feldspar grains and former laths, as well as soft and fragile detrital muscovite flakes, found throughout the thickness of the sandstone is indicative of rapid transport and deposition of the sand. The sedimentary structures within the Tapeats Sandstone, particularly the hummocky cross-stratification, the cross-bedding, the lack of significant bioturbation, the lack of erosion of the tops of most of the successive beds and the erosion of some channels and rapid cross-bedded deposition of sand within them without interstratified siltstones and mudstones, are consistent with this rapid transport and deposition. The invertebrates caught up in the eroded sand left their traces on transient surfaces on the tops of beds immediately after their deposition as they tried to survive before eventually being overwhelmed. Robust simulations of the catastrophic erosion of the underlying basement rocks and rapid deposition of the Tapeats Sandstone is consistent with this occurring early in the global Flood cataclysm. Once deposited, silica dissolved in the connate water trapped between the sand grains, along with additional dissolved silica in ground water, precipitated to lithify the sandstone towards the end of the Flood event year, or shortly thereafter.

Summary and Conclusions

The Tapeats Sandstone is the generally 30–100 m thick cliff-forming unit that prominently crops out through ~500 km in the walls of the Grand Canyon, Arizona, and beyond. Up to 120 m thick, it is usually the basal formation within the fining upwards lithologies of the Cambrian Tonto Group, which has been touted conventionally as the classic example of the time-transgressive "deepening seas" sedimentation model. The Tapeats Sandstone mostly sits directly on a pronounced erosion surface known as the Great Unconformity, but locally uncomformably overlies the breccias of the Sixtymile Formation, which has now been included in the Tonto Group. The underlying rocks eroded at the Great Unconformity include granitic plutons intruded into the Granite Gorge Metamorphic Suite schists unconformably overlain by the tilted sedimentary strata and basalt layers of the Grand Canyon Supergroup, all dated as Precambrian. Both the correlated equivalents of the Tapeats Sandstone and the Great Unconformity have been traced across several continents and around the globe, respectively.

Within the Tapeats Sandstone are found numerous trace fossils, primarily burrows and trails likely

left by various worms and other invertebrates, and trails left by trilobites. These are mostly found in the uppermost thin alternating sandstone and shale beds of the transition interval with the overlying Bright Angel Formation. The prominent coarse-grained sandstone cliff-forming unit within the Tapeats Sandstone consists of 0.3–1.0 m thick non-bioturbated beds that are strongly cross-laminated with shallow dips characteristic of water transport of the sand and many lens-shaped scour-and-fill "channels." The predominant paleocurrent direction is between west and southwest. Detrital zircon grains extracted from the Tapeats Sandstone have been U-Pb dated to determine both the maximum depositional age of the formation, as well as the potential provenance of its sand. Coupled with biostratigraphic trilobite faunal zones correlated globally, the Tapeats Sandstone has been dated at 507–508 Ma (early Middle Cambrian). U-Pb age peaks among the detrital zircons match the nearby Paleoproterozoic Yavapai and Mazatzal provinces, indicating the primary source of the sand grains was the locally underlying granitic plutons and schists, plus a very small portion from the underlying Grand Canyon Supergroup strata (though a long-distance transport of some grains cannot be entirely ruled out). The consensus uniformitarian-interpreted depositional environments for accumulation of the Tapeats Sandstone are intertidal to subtidal shallow-marine environments with local beach and fluvial deposits, yet it has been described as "one of the most dramatic global marine transgressions in Earth history."

Quartz sand grains are the dominant component of the Tapeats Sandstone, but bulk rock XRD analyses of 26 samples collected from bottom to top of its main cliff-forming unit confirmed K-feldspar contents ranging from 1.8–33.1%. In thin sections, the sandstone is poorly to moderately well-sorted and dominated by sub-angular to sub-rounded, coarse silt to very coarse sand-sized quartz grains, with some granules and small pebbles. Many variously sized K-feldspar grains are scattered through the rock fabric, with occasional thin edge-on detrital muscovite flakes wedged between quartz and K-feldspar grains. Some samples contain a few plagioclase, rounded tabular zircon, and rare sphene grains. With very few pores remaining and the porosity generally 2–5%, the rock fabric is cemented by silica as quartz overgrowths. There is no evidence, macroscopic or microscopic, of any metamorphic changes to the detrital mineral grains or textures. This is a well-cemented, unmetamorphosed, sub-mature arkosic sandstone.

These mineral constituents of the Tapeats Sandstone are consistent with the underlying local basement rocks being the sediment provenance, as indicated by the detrital zircon U-Pb ages. The rare presence of mica schist and siltstone fragments within the sandstone underscores the conclusion that transport was over a short distance and likely rapid. Indeed, due to the very short-distance transport and deposition of the sandstone, K-feldspar grains and former laths are scattered randomly through the entire unit and are not always rounded, while the extremely soft detrital muscovite flakes have survived, sometimes bent with frayed ends. The thin, non-bioturbated, strongly cross-laminated beds, and eroded "channels" filled with cross-laminated sand, both including likely hummocky cross-stratification, are consistent with rapid sequential deposition by high-energy storm-like surges. Numerous detrital zircon grain U-Pb ages are considerably less than the designated depositional age of the Tapeats Sandstone. These coupled with the well-documented problems with the many assumptions undergirding the U-Pb dating method, and the impeccable evidence of past grossly accelerated nuclear decay rates, totally undermine the validity of the conventional age for the Tapeats Sandstone. Instead, when combined, the mineralogical content, textural features, sedimentary structures, the continental-scale deposition, paleocurrent directions identical to the same continental pattern, and even the tracks and traces of transitory invertebrates that had to be buried and fossilized rapidly, are all consistent with the catastrophic erosion of the Great Unconformity near the onset of the global Genesis Flood cataclysm about 4,350 years ago and the hurricane- and tsunami-driven rapid short-distance transport and deposition of the Tapeats Sandstone at the base of the fining upwards Sauk megasequence in the first few days or weeks of that year-long event.

Future Work

As indicated at the outset, the purpose of this study of the petrology of the Tapeats Sandstone was to thoroughly describe this rock unit in preparation for detailed studies to determine the nature and timing of the folding of this sandstone unit in the Carbon Canyon and Monument folds in the Grand Canyon. Future work will thus involve closer attention to comparing the petrography of the samples from the folds with those samples distant from the folds, especially with respect to grain boundary relationships and textures, the frequency of remaining pores, the compaction of the sandstone, and the nature and timing of the cement between the detrital grains that produced the rock's lithification. This will require scanning electron microscope (SEM) imaging of selected samples to closely examine the cement crystals which would show evidence of brittle fracturing and healing if the folding occurred after

lithification, but would be still pristine if cementation occurred after soft-sediment deformation and before lithification.

Acknowledgements

All samples were collected under the authority of National Park Service Scientific Research and Sampling Permit #GRCA-2017-SCI-0052 dated June 23, 2017, issued by the Grand Canyon National Park's Research Office, and Permit #032767 issued by the Hualapai Department of Natural Resources dated July 27, 2017. The Alliance Defending Freedom (ADF) team led by then Senior Counsel Gary McCaleb is especially thanked for their legal work that led to a successful lawsuit against viewpoint discrimination in the permit application and granting process. Tom Vail, founder of Canyon Ministries who encouraged this research from its start, is also thanked for organizing with Terry Vallely, and assisted by their wives Paula and Kathy, respectively, the August 6–12, 2017 research raft trip down the Colorado River through Grand Canyon to collect the samples, facilitated by Grand Canyon National Park Special Use Permit #GRCA-3701 issued June 26, 2017. Special thanks go to Tom Vail and Dr. John H. Whitmore, Senior Professor of Geology at Cedarville University, OH for their invaluable field assistance, without which the samples would not have been collected, especially after I was injured early in the trip. Ray Strom of Calgary Rock and Materials Services, Inc. is thanked for the thin sections he prepared, and for the XRD analyses, as well as for the use of his research microscope for photography. Cedarville University is also thanked for use of their geologic research microscope and Dr. John H. Whitmore for his advice, support, and encouragement. The helpful comments and edits from three kind reviewers were much appreciated. This research was fully funded by many generous donors to Answers in Genesis and has had the full support of the Answers in Genesis leadership team under Ken Ham. Our production assistant Laurel Hemmings is also thanked for her work in preparing this paper for publication. Nevertheless, I take full responsibility for the content of this paper.

References

Allen, John R.L. 1985. *Principles of Physical Sedimentology*. London, United Kingdom: George Allen and Unwin Publishers Ltd.

Alpert, Stephen P. 1974. "Systematic Review of the Genus *Skolithos*". *Journal of Paleontology* 48, no. 4 (1 July): 661–669.

Anderson, Calvin J., Matthew S. Cheney, Alex Struble, and John H. Whitmore. 2013. "Muscovite Survival in Simulated (Turbulent) Eolian and Subaqueous Conditions." *Journal of Creation Theology and Science Series C: Earth Sciences* 3: 1.

Anderson, Calvin J., Alex Struble, and John H. Whitmore. 2017. "Abrasion Resistance of Muscovite in Aeolian and Subaqueous Transport Experiments." *Aeolian Research* 24 (February): 33–37.

Arnott, R. William, and John B. Southard. 1990. "Exploratory Flow-duct Experiments on Combined-flow Bed configurations, and Some Implications for Interpreting Storm-event Stratification." *Journal of Sedimentary Petrology* 60, no. 2 (1 March): 211–219.

Austin, Steven A., Editor. 1994. *Grand Canyon: Monument to Catastrophe*. Santee, California: Institute for Creation Research.

Austin, Steven A., and Kurt P. Wise. 1994. "The Pre-Flood/Flood Boundary: As Defined in Grand Canyon and Eastern Mojave Desert, California." In *Proceedings of the Third international Conference on Creationism*. Edited by Robert E. Walsh, 37–47. Pittsburgh, Pennsylvania: Creation Science Fellowship.

Austin, Steven A., John R. Baumgardner, D. Russell Humphreys, Andrew A. Snelling, Larry Vardiman, and Kurt P. Wise. 1994. "Catastrophic Plate Tectonics: A Global Flood Model of Earth History." In *Proceedings of the Third International Conference on Creationism*. Edited by Robert E. Walsh, 609–621. Pittsburgh, Pennsylvania: Creation Science Fellowship.

Baldwin, Christopher T., Paul K. Strother, John H. Beck, and Eben Rose. 2004. "Palaeoecology of the Bright Angel Shale in the Eastern Grand Canyon, Arizona, USA, Incorporating Sedimentological, Ichnological and Palynological Data." In *Application of Ichnology to Palaeoenvironmental and Stratigraphic Analysis*. Edited by Duncan McIlroy, 213–236. London, United Kingdom: Geological Society of London, *Special Publication 228*.

Basma, Adnan A., Azm S. Al-Homoud, Abdallah I.H. Malkawi, and Mohamed A. Al-Bashabsheh. 1996. "Swelling-Shrinkage Behavior of Natural Expansive Clays." *Applied Clay Science* 11, nos. 2–4 (December): 211–227.

Basu, Abhijit. 1981 "Weathering Before the Advent of Land Plants: Evidence from Unaltered Detrital K-Feldspars in Cambrian-Ordovician Arenites." *Geology* 9, no. 3 (March): 132–133.

Baumgardner, John R. 2003. "Catastrophic Plate Tectonics: The Physics Behind the Genesis Flood." In *Proceedings of the Fifth International Conference on Creationism*. Edited by Robert L. Ivey, Jr., 113–126. Pittsburgh, Pennsylvania: Creation Science Fellowship.

Baumgardner, John R. 2013. "Explaining the Continental Fossil-Bearing Sediment Record in Terms of the Genesis Flood: Insights from Numerical Modeling of Erosion, Sediment Transport, and Deposition Processes on a Global Scale." In *Proceedings of the Seventh International Conference on Creationism*. Edited by Mark Horstemeyer. Pittsburgh, Pennsylvania: Creation Science Fellowship

Baumgardner, John R. 2018a. "Numerical Modeling of the Large-Scale Erosion, Sediment Transport, and Deposition Processes of the Genesis Flood." *Answers Research Journal* 11 (June 27): 149–170.

Baumgardner, John R. 2018b. "Understanding How the Flood Sediment Record was Formed: The Role of Large Tsunamis." In *Proceedings of the Eighth International Conference on Creationism*. Edited by John H. Whitmore, 287–305. Pittsburgh, Pennsylvania: Creation Science Fellowship.

Billingsley, George H., and Donald P. Elston. 1989. "Geologic Log of the Colorado River from Lees Ferry to Temple Bar, Lake Mead, Arizona." In: *Geology of Grand Canyon, Northern Arizona (with Colorado River Guides)*. Edited by Donald P. Elston, George H. Billingsley, and Richard A. Young, 1–36. Washington, D.C.: American Geophysical Union.

Blakey, Ronald C., and Larry T. Middleton. 2012. "Geologic History and Paleogeography of Paleozoic and Early Mesozoic Sedimentary Rocks, Eastern Grand Canyon, Arizona." In *Grand Canyon Geology: Two Billion Years of Earth's History*. Edited by J. Michael Timmons and Karl E. Karlstrom, 81–92. Boulder, Colorado: Geological Society of America, *Special Paper 489*.

Boggs, Samuel, Jr. 1995. *Principles of Sedimentology and Stratigraphy*. 2nd ed., 79–107. Upper Saddle River, New Jersey: Prentice-Hall.

Borsch, K., John H. Whitmore, Raymond Strom, and George Hartree. 2018. "The Significance of Micas in Ancient Cross-Bedded Sandstones." In *Proceedings of the Eighth International Conference on Creationism*. Edited by John H. Whitmore, 306–326. Pittsburgh, Pennsylvania: Creation Science Fellowship.

Brand, Leonard R., and James Florence. 1982. "Stratigraphic Distribution of Vertebrate Fossil Footprints Compared with Body Fossils." *Origins* 9 (June 1): 67–74.

Brand, Leonard R. 1997. *Faith, Reason and Earth History*. Berrien Springs, Michigan: Andrews University Press.

Brand, Leonard R, Mingmin Wang, and Arthur V. Chadwick. 2015. "Global Database of Paleocurrent Trends Through the Phanerozoic and Precambrian." *Scientific Data* 2, no. 1: 150025. doi: 10.1038/sdata.2015.25.

Bromley, Richard G., and Ulla Asgaard. 1991. "Ichnofacies: A Mixture of Taphofacies and Biofacies." *Lethaia* 24, no. 2 (October): 153–163.

Burgert, B.L. 1972. "Petrology of the Cambrian Tapeats Sandstone, Grand Canyon, Arizona." M.S. Thesis (unpublished). Flagstaff, Arizona: Northern Arizona University.

Chadwick, Arthur V. 1978. "Megabreccias: Evidence for Catastrophism." *Origins* 5 (January 1): 39–46.

Chadwick, Arthur V., and Elaine G. Kennedy. 1998. "Depositional Environment of the Tapeats Sandstone in the Region of Grand Canyon, Arizona, USA." In *15th International Sedimentological Congress* 15: 247–248. Ghent, Belgium: International Association of Sedimentologists.

Chandler, Francis W. 1988. "Quartz Arenites: Review and Interpretation." *Sedimentary Geology* 58, no. 2–4 (August): 105–126.

Clarey, Timothy L., and Davis J. Werner. 2018. "Global Stratigraphy and the Fossil Record Validate a Flood Origin for the Geologic Column." In *Proceedings of the Eighth International Conference on Creationism*. Edited by John H. Whitmore, 327–350. Pittsburgh, Pennsylvania: Creation Science Fellowship.

DeCelles, Peter G., and William Cavazza. 1992. "Constraints on the Formation of Pliocene Hummocky Cross-Stratification in Calabria (southern Italy) from Consideration of hydraulic and Dispersive Equivalence, Grain-flow Theory, and Suspended-load Fallout Rate." *Journal of Sedimentary Petrology* 62, no. 4 (1 July): 555–568.

Dehler, Carol M., George E. Gehrels, Susannah M. Porter, Matt Heizler, Karl E. Karlstrom, Grant Cox, Laura J. Crossey, and J. Michael Timmons. 2017. "Synthesis of the 780–740 Ma Chuar, Uinta Mountain, and Pahrump (ChUMP) Groups, Western USA: Implications for Laurentia-wide Cratonic Marine Basins." *Geological Society of America Bulletin* 129, no. 5 (May 1): 607–624.

Dott, Robert H. 1964. "Wacke, Graywacke and Matrix—What Approach to Immature Sandstone Classification?" *Journal of Sedimentary Petrology* 34, no. 3 (September): 625–632.

Dott, Robert H. Jr., and Joanne Bourgeois. 1982. "Hummocky Stratification: Significance of its Variable Bedding Sequences." *Geological Society of America Bulletin* 93, no. 8 (August): 663–680.

Dott, Robert H. 2003. "The Importance of Eolian Abrasion in Supermature Quartz Sandstones and the Paradox of Weathering on Vegetation-Free Landscapes." *The Journal of Geology* 111, no. 4 (July): 387–405.

Droser, Mary L., and David J. Bottjer. 1989. "Ichnofabric of Sandstones Deposited in High-Energy Nearshore Environments: Measurement and Utilization." *Palaios* 4, no. 6 (December): 598–604.

Duke, William L. 1985. "Hummocky Cross-Stratification, Tropical Hurricanes, and Intense Winter Storms." *Sedimentology* 32, no. 2 (April): 167–194.

Duke, William L., R. William C. Arnott, and Richard J. Cheel. 1991. "Shelf Sandstones and Hummocky Cross-Stratification: New Insights on a Stormy Debate." *Geology* 19, no. 6 (Jone 1): 625–628.

Elliott, David K., and Daryl L. Martin. 1987. "A New Trace Fossil from the Cambrian Bright Angel Shale, Grand Canyon, Arizona." *Journal of Paleontology* 61, no. 4 (July): 641–648.

Elston, Donald P. 1979. "Late Precambrian Sixtymile Formation and Orogeny at Top of the Grand Canyon Supergroup, Northern Arizona." *Professional Paper 1092*, 1–17. Washington, D.C.: U.S. Geological Survey.

Elston, Donald P., and Stephan L. Bressler. 1977. "Paleomagnetic Poles and Polarity Zonation from Cambrian and Devonian Strata of Arizona." *Earth and Planetary Science Letters* 36, no. 3 (October): 423–433.

Elston, Donald P., and Edwin H. McKee. 1982. "Age and Correlation of the Late Proterozoic Grand Canyon Disturbance, Northern Arizona." *Geological Society of America Bulletin* 93, no. 8 (August 1): 681–699.

Elston, Donald P. 1989. "Correlations and Facies Changes in Lower and Middle Cambrian Tonto Group, Grand Canyon, Arizona." In *Geology of Grand Canyon, Northern Arizona (with Colorado River Guides)*. Edited by Donald P. Elston, George H. Billingsley, and Richard A. Young, 131–136. Washington, D.C.: American Geophysical Union.

Fedo, Christopher M., and Anthony R. Prave. 1991. "Extensive Cambrian Braidplain Sedimentation: Insights from the Southwestern Cordillera U.S.A." In *Paleozoic Paleogeography of the Western United States-II*, vol. 1, Book 67. Edited by J.D. Cooper and Cal H. Stevens, 227–236. Los Angeles, California: The Pacific Section, Society of Economic Paleontologists and Mineralogists.

Folk, Robert Louis. 1955. "Student Operator Error in Determination of Roundness, Sphericity, and Grain Size." *Journal of Sedimentary Petrology* 25, no. 4 (1 December): 297–301.

Folk, Robert L., and William C. Ward. 1957. "Brazos River Bar: A Study in the Significance of Grain Size Parameters." *Journal of Sedimentary Petrology* 27, no. 1 (March): 3–26.

Folk, Robert L. 1966. "A Review of Grain-Size Parameters." *Sedimentology* 6, no. 2 (March): 73–93.

Folk, Robert L. 1978. "Angularity and Silica Coatings of Simpson Desert Sand Grains, Northern Territory, Australia." *Journal of Sedimentary Petrology* 48, no. 2 (June 1): 611–624.

Folk, Robert L. 1980. *Petrology of Sedimentary Rocks*. Austin, Texas: Hemphill Publishing Co.

Foster, John R. 2011. "Trilobites and Other Fauna from Two Quarries in the Bright Angel Shale (Middle Cambrian, Series 3; Delamaran), Grand Canyon National Park, Arizona." In *Cambrian Stratigraphy and Paleontology of Northern Arizona and Southern Nevada, The 16th Field Conference of the Cambrian Stage Subdivision Working Group, International Subcommission on Cambrian Stratigraphy*. Edited by J. Stewart Hollingsworth, Frederick A. Sundberg, and John R. Foster, 99–120. Flagstaff, Arizona: Museum of Northern Arizona, *Bulletin 67*.

Garzanti, Eduardo, Sergio Andò, Giovanni Vezzoli, Michele Lustrino, Maria Boni, and Pieter Vermeesch. 2012. "Petrology of the Namib Sand Sea: Long-Distance Transport and Compositional Variability in the Wind-Displaced Orange Delta." *Earth-Science Reviews* 112, nos. 3–4 (May): 173–189.

Garzanti, Eduardo, Alberto Resentini, Sergio Andò, Giovanni Vezzoli, Alcides Pereira, and Pieter Vermeesch. 2015. "Physical Controls on Sand Composition and Relative Durability of Detrital Minerals during Ultra-Long Distance Littoral and Aeolian Transport (Namibia and Southern Angola)." *Sedimentology* 62, no. 4 (June): 971–996.

Garzanti, Eduardo. 2017. "The Maturity Myth in Sedimentology and Provenance Analysis." *Journal of Sedimentary Research* 87, no. 4 (April): 353–365.

Gehrels, George E., Ronald C. Blakey, Karl E. Karlstrom, J. Michael Timmons, William Dickinson, and Mark Pecha. 2011. "Detrital Zircon U-Pb Geochronology of Paleozoic Strata in the Grand Canyon, Arizona." *Lithosphere* 3, no. 3 (June 1): 183–200.

Gilbert, George K. 1874. "On the Age of the Tonto Sandstone." *Philosophical Society of Washington Bulletin* 1: 109.

Gilbert, George K. 1875. "Report Upon the Geology of Portions of Nevada, Utah, California, and Arizona." In *Report on the Geographical and Geological Explorations and Surveys West of the One Hundredth Meridian, vol. 3*. Edited by George M. Wheeler, 17–187. Washington D.C.: U.S. Geological and Geographical Surveys, Engineers Department, United States Army.

Gilmore, Charles W. 1928. "Fossil Footprints from the Grand Canyon: Third Contribution." *Smithsonian Miscellaneous Collections* 80, no. 8 (January 28): 1–16.

Goudie, Andrew S., and A. Watson. 1981. "The Shape of Desert Sand Dune Grains." *Journal of Arid Environments* 4, no. 3 (September): 185–190.

Hagadorn, James W., Joseph L. Kirschvink, Timothy D. Raub, and Eben C. Rose. 2011. "Above the Great Unconformity: A Fresh Look at the Tapeats Sandstone, Arizona-Nevada, U.S.A." In *Cambrian Stratigraphy and Paleontology of Northern Arizona and Southern Nevada, The 16th Field Conference of the Cambrian Stage Subdivision Working Group, International Subcommission on Cambrian Stratigraphy*. Edited by J. Stewart Hollingsworth, Frederick A. Sundberg, and John R. Foster, 63–76. Flagstaff, Arizona: Museum of Northern Arizona, *Bulletin 67*.

Hallam, Anthony. 1981. *Facies Interpretation and the Stratigraphic Record*. Oxford, United Kingdom: W. H. Freeman and Company.

Harianto, Tri, Shigenori Hayashi, Yan-Jun Du, and Daisuke Suetsugu. 2008. "Effects of Fiber Additives on the Desiccation Crack Behavior of the Compacted Akaboku Soil as a Material for Landfill Cover Barrier." *Water, Air, and Soil Pollution* 194, no. 1 (October): 141–149.

Harms, John C., John B. Southard, D. R. Spearing, and Roger G. Walker. 1975. "Depositional Environments as Interpreted from Primary Sedimentary Structures and Stratification Sequences." *Society of Economic Paleontologists and Mineralogists, Short Course 2*. Broken Arrow, Oklahoma: SEPM, the Society for Sedimentary Geology.

Hayes, Philip Thayer, and George C. Cone. 1975. "Cambrian and Ordovician Rocks of Southern Arizona and New Mexico and Westernmost Texas." *Professional Paper 873*. Washington D.C.: U.S. Geological Survey.

Hereford, Richard. 1975. "Chino Valley Formation (Cambrian?) in Northwestern Arizona." *Geological Society of America Bulletin* 86, no. 5 (May): 677–682.

Hereford, Richard. 1977. "Deposition of the Tapeats Sandstone (Cambrian) in Central Arizona." *Geological Society of America Bulletin* 88, no. 2 (February): 199–211.

Hill, Carol A., and Stephen O. Moshier. 2009. "Flood Geology and the Grand Canyon: A Critique." *Perspectives in Science and Christian Faith* 61, no. 2 (June): 99–115.

Hill, Carol A. and Stephen O. Moshier. 2016. "Sedimentary Structures: Clues from the Scene of the Crime." In *The Grand Canyon, Monument to an Ancient Earth: Can Noah's Flood Explain the Grand Canyon?* Edited by Carol A. Hill, Gregg Davidson, Tim Helble, and Wayne Ranney, 66–71. Grand Rapids, Michigan: Kregel Publications.

Houbolt, Jacob J. H. C. 1968. "Recent Sediments in the Southern Bight of the North Sea." *Geologie en Mijnbouw* 47, no. 4: 245–273.

Huntoon, Peter W. 1989. "Cambrian Stratigraphic Nomenclature, Grand Canyon, Arizona—Mappers Nightmare." In *Geology of Grand Canyon, Northern Arizona (with Colorado River Guides)*. Edited by Donald P. Elston, George H. Billingsley, and Richard A. Young, 128–129. Washington, D.C.: American Geophysical Union.

Huntoon, Peter W. 2003. "Post-Precambrian Tectonism in the Grand Canyon Region." In *Grand Canyon Geology*. 2nd ed. Edited by Stanley S. Beus and Michael Morales, 222–259. New York: Oxford University Press.

International Commission on Stratigraphy. 2020. *International Chronostratigraphic Chart* v.2020/03. https://stratigraphy.org/icschart/ChronostratChart2020-03.pdf.

Jade 2010. "Software for X-Ray Diffraction Analyses." JADE for XRD (materialsdata.com). Livermore, California: Materials Data, Inc.

Karlstrom, Karl E., Samuel A. Bowring, Carol M. Dehler, Andrew H. Kroll, Susannah M. Porter, David J. Des Marais, Arlo B Weil, Zachary D. Sharp, John W. Geissman, Maya B. Elrick, J. Michael Timmons, Laura J. Crossey, and Kathleen L. Davidek. 2000. "Chuar Group of the Grand

Canyon: Record of Breakup of Rodinia, Associated Change in the Global Carbon Cycle, and Ecosystem Expansion by 740 Ma." *Geology* 28, no. 7 (July): 619–622.

Karlstrom, Karl E., Bradley R. Ilg, Michael L. Williams, David P. Hawkins, Samuel A. Bowring, and S.J. Seaman. 2003. "Paleoproterozoic Rocks of the Granite Gorges." In *Grand Canyon Geology*. 2nd ed. Edited by Stanley S. Beus, and Michael Morales, 9–38. New York: Oxford University Press.

Karlstrom, Karl E., and J. Michael Timmons. 2012. "Faulting and Uplift in the Grand Canyon Region." In *Grand Canyon Geology: Two Billion Years of Earth's History*. Edited by J. Michael Timmons and Karl E. Karlstrom, 93–107. Boulder, Colorado: Geological Society of America, *Special Paper 489*.

Karlstrom, Karl E., James W. Hagadorn, George E. Gehrels, William Matthews, Mark D. Schmitz, Lauren Madronich, Jacob Mulder, Mark Pecha, Dominique Giesler, and Laura J. Crossey. 2018. "Cambrian Sauk Transgression in the Grand Canyon Region Redefined by Detrital Zircons." *Nature Geoscience* 11 (28 May): 438–443.

Karlstrom, Karl E., M.T. Mohr, Mark D. Schmitz, Frederick A. Sundberg, S.M. Rowland, Ronald C. Blakey, John R. Foster, Laura J. Crossey, Carol M. Dehler and James W. Hagadorn. 2020. "Redefining the Tonto Group of Grand Canyon and Recalibrating the Cambrian Time Scale." *Geology* 48, no. 5 (1 May): 425–430.

Kennedy, Elaine G., Ray Kablanow, and Arthur V. Chadwick. 1996. "A Reassessment of the Shallow Water Depositional Model for the Tapeats Sandstone, Grand Canyon, Arizona: Evidence for Deep Water Deposition." *Geological Society of America Abstracts with Programs* 28: A407.

Kennedy, Elaine G., Ray Kablanow, and Arthur V. Chadwick. 1997. "Evidence for Deep Water Deposition of the Tapeats Sandstone, Grand Canyon, Arizona." In *Proceedings of the Third Biennial Conference of Research on the Colorado Plateau*. Edited by C. van Riper III, and E.T. Deschler, 215–228. Washington, D.C.: U.S. Department of the Interior, National Park Service, Transactions and Proceedings Series NPS/NRNAU/NRTP-97/12.

Krumbein, William C. 1934. "Size Frequency Distributions in Sediments." *Journal of Sedimentary Petrology* 4, no. 2 (August): 65–77.

Krumbein, William C. 1938. "Size Frequency Distributions of Sediments and the Normal Phi Curve." *Journal of Sedimentary Petrology* 8, no. 3 (December): 84–90.

Krynine, Paul D. 1946 "Microscopic Morphology of Quartz Types." *Annals of 2nd Pan-American Congress of Mining and Geological Engineers*, 35–49.

Kuenen, Philip H. 1960. "Experimental Abrasion 4: Eolian Action." *The Journal of Geology* 68, no. 4 (July): 427–449.

Landing, Ed, Gerd Geyer, Robert Buchwaldt, and Samuel A. Bowring. 2015. "Geochronology of the Cambrian: A Precise Middle Cambrian U-Pb Zircon Date for the German Margin of West Gondwana." *Geological Magazine* 152, no. 1 (15 April): 28–40.

Larson, Edwin E., Penny E. Patterson, and Felix E. Mutschler. 1994. "Lithology, Chemistry, Age, and Origin of the Proterozoic Cardenas Basalt, Grand Canyon, Arizona." *Precambrian Research* 65, nos. 1–4 (January): 255–276.

Lochman-Balk, Christina. 1970. "Upper Cambrian Faunal Patterns on the Craton." *Geological Society of America Bulletin* 81, no. 11 (November): 3197–3224.

Lochman-Balk, Christina. 1971. "The Cambrian of the Craton of the United States." In *Cambrian of the New World*. Edited by Charles H. Holland, 79–169. New York: John Wiley and Sons.

Lowe, Donald R. 1975. "Water Escape Structures in Coarse-Grained Sediments." *Sedimentology* 22, no. 2 (May): 157–204.

Maithel, Sarah A., Paul A. Garner, and John H. Whitmore. 2015. "Preliminary Assessment of the Petrology of the Hopeman Sandstone (Permo-Triassic), Moray Firth Basin, Scotland." *Scottish Journal of Geology* 51 (23 September): 177–184.

Marsland, Paul S., and John G. Woodruff. 1937. "A Study of the Effects of Wind Transportation on Grains of Several Minerals." *Journal of Sedimentary Petrology* 7, no. 1 (1 April): 18–30.

Martin, Daryl L. 1985. "Depositional Systems and Ichnology of the Bright Angel Shale (Cambrian), Eastern Grand Canyon, Arizona." M.S. Thesis (unpublished). Flagstaff, Arizona: Northern Arizona University.

Matthews, William, Bernard Guest, and Lauren Madronich. 2018. "Latest Neoproterozoic to Cambrian Detrital Zircon Facies of Western Laurentia." *Geosphere* 14, no. 1: 243–264.

McBride, Earle F. 1963. "A Classification of Common Sandstones." *Journal of Sedimentary Petrology* 33, no. 3 (1 September): 664–669.

McBride, Earle F. 1985. "Diagenetic Processes that Affect Provenance Determinations in Sandstone." In *Provenance of Arenites*. Edited by Gian G. Zuffa, 97–113. Dordrecht, The Netherlands: D. Reidel Publishing Company.

McKee, Edwin D. 1932. "Some Fucoids from the Grand Canyon." *Grand Canyon Study Notes* 8: 58–161.

McKee, Edwin D. 1940. "Three Types of Cross-Lamination in Paleozoic Rocks of Northern Arizona." *American Journal of Science* 238, no. 11 (November 1): 811–824.

McKee, Edwin D. 1945. "Stratigraphy and Ecology of the Grand Canyon Cambrian: Part 1. Cambrian History of the Grand Canyon Region." *Carnegie Institute of Washington Publication* 563, 1–168. Washington, D.C.: Carnegie Institute of Washington.

McRae, Stuart G. 1972. "Glauconite." *Earth-Science Reviews* 8, no. 4 (December): 397–440.

Middleton, Larry T., and Richard Hereford. 1981. "Nature and Controls on Early Paleozoic Fluvial Sedimentation Along a Passive Continental Margin: Examples from the Middle Cambrian Flathead Sandstone (Wyoming) and Tapeats Sandstone (Arizona)." In *Modern and Ancient Fluvial Systems: Sedimentology and Processes*. Edited by John D. Collerson and John Lewin, 83. Keele, United Kingdom: Special Congress, International Association of Sedimentologists.

Middleton, Larry T. 1989. "Cambrian and Ordovician Depositional Systems in Arizona." In: *Geologic Evolution of Arizona*. Edited by J.P. Jenney, and S.J. Reynolds, 273–286. Tucson, Arizona: Arizona Geological Society, *Digest vol. 17*.

Middleton, Larry T., and David K. Elliott. 2003. "Tonto Group." In *Grand Canyon Geology*. 2nd ed. Edited by Stanley S. Beus, and Michael Morales, 90–106. New York: Oxford University Press.

Moorhouse, Walter W. 1959. *The Study of Rocks in Thin Section*. New York: Harper and Row.

Morris, William J. 1957. "Effects of Sphericity, Roundness, and Velocity on Traction Transportation of Sand Grains." *Journal of Sedimentary Petrology* 27, no. 1 (March 1): 27–31.

Naeser, Chris W., Ian R. Duddy, Donald P. Elston, Terry A. Dumitru and Paul F. Green. 1989. "Fission-Track Dating: Ages for Cambrian Strata and Laramide and Post-Middle Eocene Cooling Events from the Grand Canyon, Arizona." In *Geology of Grand Canyon, Northern Arizona (with Colorado River Guides)*. Edited by Donald P. Elston, George H. Billingsley, and Richard A. Young, 139–144. Washington, D.C.: American Geophysical Union.

Noble, Levi F. 1914. "The Shinumo Quadrangle, Grand Canyon District, Arizona." *U.S. Geological Survey Bulletin* 549.

Noble, Levi F. 1922. "A Section of the Paleozoic Formations of the Grand Canyon at the Bass Trail." *U.S. Geological Survey Professional Paper* 131-B: 23–73.

Nummedal, Dag. 1991. "Shallow Marine Storm Sedimentation—The Oceanographic Perspective." In *Cycles and Events in Stratigraphy*. Edited by Gerhard Einsele, Werner Ricken, and Adolf Seilacher, 227–248. Berlin, Germany: Springer-Verlag.

Odom, I. Edgar. 1975. "Feldspar-Grain Size Relations in Cambrian Arenites, Upper Mississippi Valley." *Journal of Sedimentary Research* 45, no. 3 (1 September): 636–650.

Odom, I. Edgar, Thomas W. Doe, and Robert H. Dott. 1976. "Nature of Feldspar-Grain Size Relations in Some Quartz-Rich Sandstones." *Journal of Sedimentary Petrology* 46, no. 4 (1 December): 862–870.

Pemberton, S. George, James A. MacEachern, and Robert W. Frey. 1992. "Trace Fossil Facies Models: Environmental and Allostratigraphic Significance." In *Facies Models: Response to Sea Level Change*. Edited by Roger G. Walker and Noel P. James, 47–72. St. John's, Newfoundland, Canada: Geological Association of Canada.

Peng, Shanchi, Loren E. Babcock, and Roger A. Cooper. 2012. "The Cambrian Period." In *The Geologic Time Scale 2012*, vol. 2. Edited by Felix M. Gradstein, James G. Ogg, Mark D. Schmitz, and Gabi M. Ogg, 437–488. Amsterdam, The Netherlands: Elsevier.

Peters, Richard A., and Leonard R. Brand. 1999. "Origin of Polygonal Compaction Cracks in Permian Coconino Sandstone, Arizona." *Geological Society of America Abstracts with Programs* 31, no. 7: 160.

Peters, Shanan E., and Robert R. Gaines. 2012. "Formation of the 'Great Unconformity' as a Trigger for the Cambrian Explosion." *Nature* 484, no. 7394 (18 April): 363–366.

Pettijohn, Francis J. 1954. "Classification of Sandstones." *The Journal of Geology* 62, no. 4 (July): 360–365.

Pettijohn, Francis J. 1957. *Sedimentary Rocks*. New York: Harper.

Pettijohn, Francis J., Paul E. Potter, and Raymond Siever. 1973. *Sand and Sandstone*. Berlin, Germany: Springer.

Poppe, Larry .J., Mary L. DiGiacomo-Cohen, Stephen M. Smith, Harold F. Stewart, and Nicholas A. Forfinski. 2006. "Seafloor Character and Sedimentary Processes in Eastern Long Island Sound and Western Block Island Sound." *Geo-Marine Letters* 26, no. 2 (June): 59–68.

Powell, John W. 1876. *Report on the Geology of the Eastern Portion of the Uinta Mountains and a Region of Country Adjacent Thereto*. Washington D.C.: U.S. Geologic and Geographic Survey of the Territories.

Powell, John W., 1891. *Grand Canyon of the Colorado*. New York: Flood and Vincent.

Powers, Maurice C. 1953. "A New Roundness Scale for Sedimentary Particles." *Journal of Sedimentary Petrology* 23, no. 2 (1 June): 117–119.

Prave, Anthony R., and William L. Duke. 1990. "Small-scale Hummocky Cross-Stratification in Turbidites: A Form of Antidune Stratification?" *Sedimentology* 37, no. 3 (June): 531–539.

Prave, Anthony R. 1991. "Depositional and Sequence Stratigraphic Framework of the Lower Cambrian Zabriskie Quartzite: Implications for Regional Correlations and the Early Cambrian Paleogeography of the Death Valley Region of California and Nevada." *Geological Society of America Bulletin* 104, no. 5 (May 1): 505–515.

Pye, Kenneth, and Haim Tsoar. 2009. *Aeolian Sand and Sand Dunes*. Berlin, Germany: Springer-Verlag.

Ramsay, John G. 1967. *Folding Fracturing of Rocks*. New York: McGraw-Hill.

Resser, Charles E., 1945. "Cambrian Fossils of the Grand Canyon: Part II. Cambrian History of the Grand Canyon Region." *Carnegie Institute of Washington Publication* 563, 168–232. Washington, D.C.: Carnegie Institute of Washington.

Rooney, Alan D., Jacqueline Austermann, Emily F. Smith, Yang Li, David Selby, Carol M. Dehler, Mark D. Schmitz, Karl E. Karlstrom, and Francis A. Macdonald. 2018. "Coupled Re-Os and U-Pb Geochronology of the Tonian Chuar Group, Grand Canyon." *Geological Society of America Bulletin* 130, nos. 7–8 (1 July): 1085–1098.

Rose, Eben C. 2003. "Depositional Environment and History of the Cambrian Tonto Group, Grand Canyon, Arizona." M.S. Thesis (unpublished). Flagstaff, Arizona: Northern Arizona University.

Rose, Eben C. 2006. "Nonmarine Aspects of the Cambrian Tonto Group of the Grand Canyon, USA, and Broader Implications." *Palaeoworld* 15, nos. 3–4 (August–November): 223–241.

Rose, Eben C. 2011. "Proposed Modification of the Nomenclature and Revised Depositional Model for the Cambrian Tonto Group of the Grand Canyon, Arizona." In *Cambrian Stratigraphy and Paleontology of Northern Arizona and Southern Nevada, The 16th Field Conference of the Cambrian Stage Subdivision Working Group, International Subcommission on Cambrian Stratigraphy*. Edited by J. Stewart Hollingsworth, Frederick A. Sundberg, and John R. Foster, 77–98. Flagstaff, Arizona: Museum of Northern Arizona, *Bulletin 67*.

Russell, R. Dana, and Ralph E. Taylor. 1937. "Roundness and Shape of Mississippi River Sands." *The Journal of Geology* 45, no. 3 (April–May): 225–267.

Schmitz, Mark D. 2012. "Radiometric Ages Used in GTS2012." In *The Geologic Time Scale 2012*, vol. 2. Edited by Felix M. Gradstein, James G. Ogg, Mark D. Schmitz, and Gabi M. Ogg, 1045–1082. Amsterdam, The Netherlands: Elsevier.

Scholle, Peter A. 1979. *A Color Illustrated Guide to Constituents, Textures, Cements, and Porosities of Sandstones and Associated Rocks*. Tulsa, Oklahoma: The American Association of Petroleum Geologists, *Memoir 28*.

Schuchert, Charles. 1918. "The Cambrian of the Grand Canyon of Arizona." *American Journal of Science, 4th Series* 45: 362–369.

Seilacher, Adolf. 1970. "*Cruziana* Stratigraphy of Non-Fossiliferous Paleozoic Sandstones." In *Trace Fossils*. Edited by Thomas P. Crimes, and J.C. Harper, 447–476. London, United Kingdom: Geological Society of London, *Geological Journal Special Issue 3*.

Seilacher, Adolf, and Thomas Aigner. 1991. "Storm Deposition at the Bed, Facies, and Basin Scale: The Geologic Perspective." In *Cycles and Events in Stratigraphy*. Edited by Gerhard Einsele, Werner Ricken, and Adolf Seilacher, 249–267. Berlin, Germany: Springer-Verlag.

Sharp, Robert P. 1940. "Ep-Archean and Ep-Algonkian Erosion Surfaces, Grand Canyon, Arizona." *Geological Society of America Bulletin* 51, no. 8 (1 August): 1235–1270.

Sloss, Laurence L. 1963. "Sequences in the Cratonic Interior of North America." *Geological Society of America Bulletin* 74, no. 2 (February): 93–114.

Snelling, Andrew A. 2000. "Geochemical Processes in the Mantle and Crust." In *Radioisotopes and the Age of the Earth: A Young-Earth Creationist Research Initiative*. Edited by Larry Vardiman, Andrew A. Snelling, and Eugene F. Chaffin, 123–304. El Cajon, California: Institute for Creation Research, and St. Joseph, Missouri: Creation Research Society.

Snelling, Andrew A. 2005a. "Radiohalos in Granites: Evidence of Accelerated Nuclear Decay." In *Radioisotopes and the Age of the Earth: Results of a Young-Earth Creationist Research Initiative*. Edited by Larry Vardiman, Andrew A. Snelling, and Eugene F. Chaffin, 101–207. El Cajon, California: Institute for Creation Research, and Chino Valley, Arizona: Creation Research Society.

Snelling, Andrew A. 2005b. "Fission Tracks in Zircons: Evidence for Abundant Nuclear Decay." In *Radioisotopes and the Age of the Earth: Results of a Young-earth Creationist Research Initiative*. Edited by Larry Vardiman, Andrew A. Snelling, and Eugene F. Chaffin, 209–324. El Cajon, California: Institute for Creation Research, and Chino Valley, Arizona: Creation Research Society.

Snelling, Andrew A. 2005c. "Isochron Discordances and the Role of Mixing and Inheritance of Radioisotopes in the Mantle and Crust." In *Radioisotopes and the Age of the Earth: Results of a Young-Earth Creationist Research Initiative*. Edited by Larry Vardiman, Andrew A. Snelling, and Eugene F. Chaffin, 393–524. El Cajon, California: Institute for Creation Research, and Chino Valley, Arizona: Creation Research Society.

Snelling, Andrew A. 2009. *Earth's Catastrophic Past: Geology Creation and the Flood*. Dallas, Texas: Institute for Creation Research.

Snelling, Andrew A. 2017a. "Determination of the Decay Constants and Half-Lives of Uranium-238 (^{238}U) and Uranium-235 (^{235}U), and the Implications for U-Pb and Pb-Pb Radioisotope Dating Methodologies." *Answers Research Journal* 10 (January 18): 1–38.

Snelling, Andrew A. 2017b. "Problems with the U-Pb Radioisotope Dating Methods—1. Common Pb." *Answers Research Journal* 10 (July 26): 121–167.

Snelling, Andrew A. 2018. "Problems with the U-Pb Radioisotope Dating Methods—2. U and Pb Mobility." *Answers Research Journal* 11 (June 13): 85–140.

Snelling, Andrew A. 2019. "Problems with the U-Pb Radioisotope Dating Methods—3. Mass Fractionation." *Answers Research Journal* 12 (November 13): 355–392.

Southard, John B., John M. Lambie, Dennis C. Federico, Harold T. Pile, and Christopher R. Weidman. 1990. "Experiments on Bed Configurations in Fine Sands Under Bidirectional Purely Oscillatory Flow, and the Origin of Hummocky Cross-Stratification." *Journal of Sedimentary Petrology* 60, no. 1 (1 January): 1–17.

Stewart, John H. 1972. "Initial Deposits in the Cordilleran Geosyncline: Evidence of a Late Precambrian (<850 m.y.) Continental Separation." *Geological Society of America Bulletin* 83, no. 5 (May): 1345–1360.

Stewart, John H., and Christopher A. Suczek. 1977. "Cambrian and Latest Precambrian Paleogeography and Tectonics in the Western United States." In *Paleozoic Paleogeography of the Western United States*. Edited by John H. Stewart, Calvin H. Stevens, and A. Eugene Fritsche, 1-18. Society of Economic Paleontologists and Mineralogists, Pacific Section, *Paleogeography Symposium 1*.

Stewart, John H., George E. Gehrels, Andrew P. Barth, Paul K. Link, Nicholas Christie-Blick, and Chester T. Wrucke. 2001. "Detrital Zircon Provenance of Mesoproterozoic to Cambrian Arenites in the Western United States and Northwestern Mexico." *Geological Society of America Bulletin* 113, no. 10 (October): 1343–1356.

Sundberg, Frederick A. 1999. "Redescription of *Alokistocare subcoronatum* (Hall and Whitfield, 1877), the Type Species of *Alokistocare*, and the Status of Alokistocaridae Resser, 1939B (Ptychopariida: Trilobita, Middle Cambrian)." *Journal of Paleontology* 73, no. 6 (November): 1126–1143.

Sundberg, Frederick A. 2011. "Cambrian of Peach Springs Canyon, Hualapai Indian Reservation, Arizona." In *Cambrian Stratigraphy and Paleontology of Northern Arizona and Southern Nevada, The 16th Field Conference of the Cambrian Stage Subdivision Working Group, International Subcommission on Cambrian Stratigraphy*. Edited by J Stewart Hollingsworth, Frederick A. Sundberg, and John R. Foster, 186–190. Flagstaff, Arizona: Museum of Northern Arizona, *Bulletin 67*.

Sundberg, Frederick A., Gerd Geyer, Peter D. Kruse, Linda B. McCollum, Tatyana V. Pegel', Anna Żylińska, and Andrey Y. Zhuravlev. 2016. "International Correlation of the Cambrian Series 2–3, Stages 4–5 Boundary Interval." *Australasian Palaeontological Memoirs* 49 (June): 83–124.

Sundberg, Frederick A., Karl E. Karlstrom, Gerd Geyer, John R. Foster, James W. Hagadorn, M.T. Mohr, Mark D. Schmitz, Carol M. Dehler, and Laura J. Crossey. 2020. "Asynchronous Trilobite Extinctions at the Early to Middle Cambrian Transition." *Geology* 48, no. 5 (February 14): 441–445.

Swift, Donald J. P., Albert G. Figueiredo, Jr., G. L. Freeland, and George F. Oertel. 1983. "Hummocky Cross-Stratification and Megaripples: A Geological Double Standard?" *Journal of Sedimentary Petrology* 53, no. 4 (December 1): 1295–1317.

Swift, Donald J.P., and Julian A. Thorne. 1991. "Sedimentation on Continental Margins, I: A General Model for Shelf Sedimentation." In *Shelf Sand and Sandstone Bodies: Geometry, Facies, and Sequence Stratigraphy*. Edited by Donald J.P. Swift, George F. Oertel, Roderick W. Tillman, and Julian A. Thorne, *International Association of Sedimentologists, Special Publication Number 14*, 3–31. Oxford, United Kingdom: Blackwell Scientific Publications.

Tapp, Bryan, and Ken Wolgemuth. 2016. "Broken and Bent Rock: Fractures, Faults, and Folds". In *The Grand Canyon, Monument to an Ancient Earth; Can Noah's Flood Explain the Grand Canyon?*. Edited by Carol A. Hill, Gregg Davidson, Tim Helble, and Wayne Ranney, 116–127. Grand Rapids, Michigan: Kregel Publications.

Thorne, Julian A., E. Grace, Donald J.P. Swift, and A. Niedoroda. 1991. "Sedimentation on Continental Margins, III: The Depositional Fabric—An Analytical Approach to

Stratification and Facies Identification." In S*helf Sand and Sandstone Bodies: Geometry, Facies, and Sequence Stratigraphy*. Edited by Donald J.P. Swift, George F. Oertel, Roderick W. Tillman, and Julian A. Thorne, *International Association of Sedimentologists, Special Publication Number 14*, 59–87. Oxford, United Kingdom: Blackwell Scientific Publications.

Trask, Parker D. 1930. "Mechanical Analysis of Sediments by Centrifuge." *Economic Geology* 25, no. 6 (1 September): 581–599.

Tucker, Maurice E., 1981. *Sedimentary Petrology: An Introduction*. Oxford, United Kingdom: Blackwell Scientific Publications.

Twenhofel, William H. 1945. "The Rounding of Sand Grains." *Journal of Sedimentary Petrology* 15, no. 2 (1 August): 59–71.

Udden, Johan A. 1914 "Mechanical Composition of Clastic Sediments." *Bulletin of the Geological Society of America* 25, no. 1 (January): 655–744.

Ulmer-Scholle, Dana S., Peter A. Scholle, Juergen Schieber, and Robert J. Raine. 2015. *A Color Guide to the Petrography of Sandstones, Siltstones, Shales and Associated Rocks*. Tulsa, Oklahoma: The American Association of Petroleum Geologists, *Memoir 109*.

Vannier, Jean, Ivan Calandra, Christian Gaillard, and Anna Żylińska. 2010. "Priapulid Worms: Pioneer Horizontal Burrowers at the Precambrian-Cambrian Boundary." *Geology* 38, no. 8 (August): 711–714.

Vardiman, Larry, Andrew A. Snelling, and Eugene F. Chaffin, Editors. 2005. *Radioisotopes and the Age of the Earth: Results of a Young-Earth Creationist Research Initiative*. El Cajon, California: Institute for Creation Research, and Chino Valley, Arizona: Creation Research Society.

Walcott, Charles D. 1880. "The Permian and Other Paleozoic Groups of the Kanab Valley, Arizona." *American Journal of Science, 3rd Series* 20: 221–225.

Walcott, Charles D. 1883. "Pre-Carboniferous Strata in the Grand Canyon of the Colorado, Arizona." *American Journal of Science, 3rd Series* 26: 437–442.

Walcott, Charles D. 1890. "The Fauna of the Lower Cambrian or *Olenellus* Zone." *U.S. Geological Survey 10th Annual Report*, 509–760.

Walcott, Charles D. 1895. "Algonkian Rocks of the Grand Canyon of the Colorado." *The Journal of Geology* 3, no. 3 (May): 312–330.

Walcott, Charles D. 1910. "Cambrian Geology and Paleontology II: Abrupt Appearance of the Cambrian Fauna on the North American Continent." *Smithsonian Miscellaneous Collections* 57, no. 1: 1–16.

Walcott, Charles D. 1918. "Cambrian Geology and Paleontology IV: Appendages of Trilobites." *Smithsonian Miscellaneous Collections* 67, no. 4: 115–216.

Walker, Roger G., and A. Guy Plint. 1992. "Wave- and Storm-Dominated Shallow Marine Systems." In *Facies Models: Response to Sea Level Change*. Edited by Roger G. Walker, and Noel P. James, 219–238. St. John's, Newfoundland, Canada: Geological Association of Canada.

Wanless, Harold R., Jr. 1973a. "Cambrian of the Grand Canyon—A Reevaluation of the Depositional Environment." Ph.D. Thesis (unpublished). Baltimore, Maryland: Johns Hopkins University.

Wanless, Harold R., Jr. 1973b. "Cambrian of the Grand Canyon—A Reevaluation." *American Association of Petroleum Geologists Bulletin* 57, no. 4 (April): 810–811.

Wanless, Harold R., Jr. 1975. "Carbonate Tidal Flats of the Grand Canyon Cambrian." In: *Tidal Flats-A Casebook of Recent Examples and Fossil Counterparts*. Edited by R.N. Ginsburg, 269–277. New York: Springer-Verlag.

Wanless, Harold R., Jr. 1981. "Environments and Dynamics of Clastic Sediment Dispersal Across Cambrian of Grand Canyon." *American Association of Petroleum Geologists Bulletin* 65, no. (May): 1004–1005.

Wentworth, Chester K. 1922. "A Scale of Grade and Class Terms for Clastic Sediments." *The Journal of Geology* 30, no. 5 (July–August): 377–392.

Wheeler, Russell B., and Albert R. Kerr. 1936. "Preliminary Report on the Tonto Group of the Grand Canyon, Arizona." *Grand Canyon Natural History Association Bulletin* 5 (May): 1–16.

Whitmore, John H., Raymond Strom, Stephen Cheung, and Paul A. Garner. 2014. "The Petrology of the Coconino Sandstone (Permian), Arizona, USA." *Answers Research Journal* 7 (December 10): 499–532.

Whitmore, John H., 2017. "Rapid Rounding of K-feldspar Sand Grains from Beach to Dune Environments and its Significance for Ancient Sandstones." *Journal of Creation Theology and Science Series C: Earth Sciences* 7, no. 2: 2–3.

Whitmore, John H., and Raymond Strom. 2017a. "Rounding of K-feldspar and Quartz Sand Grains from Beach to Dune Environments: Implications for Ancient Sandstones." *Geological Society of America Abstracts with Programs* 49, no. 6: 295-5.

Whitmore, John H., and Raymond Strom. 2017b. "Rounding of Quartz and K-Feldspar Sand from Beach to Dune Settings Along the California and Oregon Coastlines: Implications for Ancient Sandstones." *Answers Research Journal* 10: (November 15) 259–270.

Whitmore, John H., and Paul A. Garner. 2018. "The Coconino Sandstone (Permian, Arizona, USA): Implications for the Origin of Ancient Cross-Bedded Sandstones." In *Proceedings of the Eighth International Conference on Creationism*. Edited by John H. Whitmore, 581–627. Pittsburgh, Pennsylvania: Creation Science Fellowship.

Whitmore, John H., and Raymond Strom. 2018. "The Significance of Angular K-Feldspar Grains in Ancient Sandstones." In *Proceedings of the Eighth International Conference on Creationism*. Edited by John H. Whitmore, 628-651. Pittsburgh, Pennsylvania: Creation Science Fellowship.

Wiens, Roger. 2016. "So Just How Old is That Rock?" In *The Grand Canyon, Monument to an Ancient Earth: Can Noah's Flood Explain the Grand Canyon?* Edited by Carol A. Hill, Gregg Davidson, Tim Helble, and Wayne Ranney, 88–97. Grand Rapids, Michigan: Kregel Publications.

Wise, Kurt P. 2003. "The Hydrothermal Biome: A Pre-Flood Environment." In *Proceedings of the Fifth International Conference on Creationism*. Edited by Robert L. Ivey, Jr., 359–370. Pittsburgh, Pennsylvania: Creation Science Fellowship.

Wise, Kurt P., and Andrew A. Snelling. 2005. "A Note on the Pre-Flood/Flood Boundary in the Grand Canyon." *Origins* 58 (June 1): 7–29.

Yassoglou, N., Costas S. Kosmas, Nikolaos Moustakas, E. Tzianis, and Nikolaos G. Danalatos. 1994. "Cracking in Recent Alluvial Soils as Related to Easily Determined Soil Properties." *Geoderma* 63, nos. 3–4 (November): 289–298.

Yesiller, Nazli, C.J. Miller, G. Inci, and K. Yaldo. 2000. "Desiccation and Cracking Behavior of Three Compacted Landfill Liner Soils." *Engineering Geology* 57, nos. 1–2 (June): 105–121.

Young, Davis A., and Ralph F. Stearley. 2008. *The Bible, Rocks and Time: Geological Evidence for the Age of the Earth*. Downers Grove, Illinois: InterVarsity Press.

Supplementary Material

Appendix A—Graphic Stratigraphic Log of the Tonto Group in the Unkar Creek Area (River Mile 73).

Appendix B—Graphic Stratigraphitc Log of the Tonto Group in the Blacktail Canyon Area (River Mile 120.5).

Appendix C—Graphic Stratigraphic Log of the Tonto Group in the Diamond Creek Area (River Mile 226).

Appendix D—Locations and Petrographic Descriptions of Tapeats Sandstone Samples.

Available in a single pdf file at https://assets.answersingenesis.org/doc/articles/arj/v14/tapeats-sandstone-supplement.pdf.